

# **An Investigation into the Pharmacology and Regulation of the M<sub>1</sub>, M<sub>3</sub> and M<sub>4</sub> Muscarinic Acetylcholine Receptors**

Thesis Submitted for the Degree of Doctor of Philosophy  
at the  
University of Leicester



**By Rudi Prihandoko**

Department of Cell Physiology and Pharmacology  
University of Leicester

April 2013

## Abstract

Functional selectivity, which highlights the ability of ligands to differentially activate the signalling pathways linked to G protein-coupled receptors (GPCRs) has provided an avenue for developing ligands with greater safety profiles. Pilocarpine (Pilo), a non-selective muscarinic acetylcholine receptor (mAChR) agonist has been shown to differentially activate G protein subtypes linked to the M<sub>3</sub> mAChR. In this study the pharmacology of Pilo was further investigated using a number of readouts. When compared to methacholine (MCh), a reference agonist, Pilo appeared to preferentially stimulate inositol phosphates production than global receptor phosphorylation. The ligand also appeared to preferentially promote phosphorylation of Ser412 at the third intracellular loop of the receptor than Ser577 at the C-terminal tail. This differential phosphorylation may be linked to the fact that these residues are phosphorylated by distinct protein kinases. However, such preferential phosphorylation was not evident at the mutant M<sub>3</sub> RASSL receptor that was engineered to respond to Clozapine-N-oxide (CNO). This mutant receptor was phosphorylated in response to CNO stimulation in a similar manner as the wild-type M<sub>3</sub> mAChR responding to ACh.

Allosteric modulation has been considered an attractive approach to selectively target GPCR subtypes for multiple disease indications. BQCA and LY2033298 have been shown to act allosterically at the M<sub>1</sub> and M<sub>4</sub> mAChR, respectively. In this study, we provided evidence that BQCA is probe dependent and the compound is more potent as an affinity modulator of ACh than Pilo. However BQCA did not significantly potentiate the phosphorylation state of the M<sub>1</sub> mAChR following stimulation with a sub-maximal concentration of ACh. Similar results were obtained for LY2033298 at the M<sub>4</sub> mAChR which suggest that allosteric modulators do not promote a receptor conformation that increases the accessibility of phosphorylation sites to protein kinases.

## Publication

### Papers

- **\*Butcher AJ, \*Prihandoko R**, Kong KC, McWilliams P, Edwards JM, Bottrill A, Mistry S, Tobin AB. Differential G protein-coupled receptor phosphorylation provides evidence for a signaling bar code (2011). *Journal of Biological Chemistry*. 286(13):11506-18. *\*Joint first author.*
- Alvarez-Curto E, **Prihandoko R**, Tautermann CS, Zwier JM, Padiani JD, Lohse MJ, Hoffmann C, Tobin AB, Milligan G. Developing chemical genetic approaches to explore G protein-coupled receptor function: validation of the use of a receptor activated solely by synthetic ligand (RASSL) (2011). *Molecular Pharmacology*. 80(6):1033-46.

### Chapters

- Butcher AJ, Kong KC, **Prihandoko R**, Tobin AB. Physiological role of G protein coupled receptor phosphorylation (2012). *Handbook of Experimental Pharmacology*. 208:79-94.

### Abstracts

- **Prihandoko R**, Alvarez Curto E, Milligan G, Tobin AB. Regulation of M<sub>3</sub> RASSL by Phosphorylation. *Molecular Pharmacology Gordon Research Conference*, Ventura, California, January 9-14, 2011
- **Rudi Prihandoko**, Adrian J. Butcher, Greg J. Osborne, Christopher J. Langmead, Fiona Marshall, R. A John Challiss and Andrew B. Tobin. Signalling and phosphorylation of the M<sub>1</sub> receptor is dynamically regulated by allosteric modulators. *4th BPS Focused Meeting on Cell Signalling*. Leicester, April 23-24, 2012

## Acknowledgements

There are many people to whom I wish to thank. First and foremost, my supervisor Prof. Andrew Tobin, for giving me the opportunity to carry out this research project in his laboratory and providing me with encouragement and guidance throughout my studies. Thank you to my colleagues in Hodgkin Lab 202 and fellow students both past and present for constant support and inspiration. Special thanks to Kok Choi Kong for technical assistance in phosphopeptide mapping and Adrian Butcher for expert advice on mass spectrometry and antibody generation.

I would also like to acknowledge my committee members, Prof John Challiss and Dr Gary Willars for their contributions towards this project.

As part of my studies, I spent three months at Heptares Therapeutics, an experience which was both very productive and enjoyable. I thank my industrial supervisors, Ali Jazayeri and Fiona Marshall for their supports. Also thanks to Chris Langmead for expert advice on allosterism and data analysis.

I am also very grateful for the financial support provided by the BBSRC and Heptares Therapeutics.

Last but not least, to my wife, family and friends who have been very supportive throughout my studies! I would like to dedicate this thesis to my son, Xavier Russell Prihandoko who was born in the first year of my studies and has been a great company, especially during the late night write ups!!

## **Author's declaration**

The author declares that the work presented in this thesis was conducted by the author (except where otherwise acknowledged) and has not previously been submitted for a degree or diploma at this University or any other institution. Antibodies for the M<sub>1</sub> and M<sub>3</sub> mAChRs were either developed previously in the laboratory or a kind gift from Adrian Butcher. Immunisation for the generation of antibodies for the M<sub>4</sub> mAChR was conducted by Eurogentec.

## Abbreviations

2D	Two dimensional
77-LH-28-1	(1-[3-(4-butyl-1-piperidinyl)propyl]-3,4-dihydro-2(1H)-quinolinone)
AC	Adenylate cyclase
AC-42	4- <i>n</i> -butyl-1-[4-(2-methylphenyl)-4-oxo-1-butyl] piperidine hydrogen chloride
ANOVA	Analysis of variance
AP2	Adaptor protein 2
Arec	Arecoline
ATP	Adenosine triphosphate
BCA	Bicinchoninic acid
Bis I	Bisindolylmaleimide
BSA	Bovine serum albumin
BQCA	Benzylquinolone carboxylic acid
CAMP	Cyclic adenosine 3', 5'- monophosphate
CCh	Carbachol
CHO	Chinese hamster ovary cells
CNO	Clozapine-N-oxide
CNS	Central nervous system
CK	Casein kinase
DAG	Diacylglycerol
DPM	Disintegration per minute
DREADD	Designer receptor exclusively activated by designer drugs
DTT	Dithiothreitol
EDTA	Ethylenediaminetetraacetic acid
ECL	Enhanced chemiluminescence

ECL	Extracellular loop
ERK	Extracellular signal regulated kinases
FBS	Fetal bovine serum
G-418	Geneticin
GPCR	G protein-coupled receptor
GRK	G protein-coupled receptor kinase
HEK	Human embryonic kidney
HRP	Horse radish peroxidase
ICL	Intracellular loop
IP	Inositol phosphate
IP3	Inositol 1,4,5-trisphosphate
mAChR	Muscarinic acetylcholine receptors
MAPK	Mitogen activated protein kinase
MCh	Methacholine
MEM	Minimum Eagle's medium
MPEP	2-Methyl-6-(phenylethynyl)-pyridine
Oxo	Oxotremorine
Oxo-M	Oxotremorine-M
PBS	Phosphate buffered saline
PCR	Polymerase chain reaction
PEI	Polyethylenimine
Pilo	Pilocarpine
PIP <sub>2</sub>	Phosphatidylinositol-4, 5-bisphosphate
PKA	Protein kinase A
PKC	Protein kinase C

PLA	Phospholipase A
PLC	Phospholipase C
PMA	Phorbol 12-myristate 13-acetate
RASSL	Receptor activated solely by synthetic ligand
RGS	Regulators of G protein signalling
RIPA	Radioimmunoprecipitation assay buffer
SDS	Sodium dodecyl sulphate
SDS-PAGE	Sodium dodecyl sulphate polyacrylamide gel electrophoresis
S.E.M	Standard error of the mean
siRNA	Small interfering ribonucleic acid
TAE	Tris acetate-EDTA
TBS	Tris-buffered saline
TBST	Tris-buffered saline/tween
TCA	Trichloroacetic acid
TE	Tris-EDTA
TM	Transmembrane
VIP	Vasoactive intestinal peptide
VSV-G	Vesicular stomatitis virus glycoprotein
VU0357017	4-[[2-[(2-Methylbenzoyl)amino]ethyl]amino]-1-piperidinecarboxylic acid ethyl ester hydrochloride
WT	Wild-type

# Contents

<b>Abstract</b> .....	<b>2</b>
<b>Publication</b> .....	<b>3</b>
Papers .....	3
Chapters.....	3
Abstracts.....	3
<b>Acknowledgements</b> .....	<b>4</b>
<b>Author's declaration</b> .....	<b>5</b>
<b>Abbreviations</b> .....	<b>6</b>
<b>Contents</b> .....	<b>9</b>
<b>Chapter 1: General introduction</b> .....	<b>14</b>
1.1 The superfamily of G protein-coupled receptors .....	14
1.2. Classification of GPCRs.....	14
1.3. Crystal structure of GPCRs .....	17
1.4. Signalling mechanisms of GPCRs .....	20
1.4.1. G protein dependent signalling .....	21
1.4.2. Arrestin dependent signalling .....	27
1.5. Functional selectivity of GPCRs .....	31
1.6. Allosterism at GPCRs .....	33
1.7. Regulation of GPCRs by phosphorylation .....	40
1.8. Muscarinic acetylcholine receptors .....	44
1.9. Dissecting mAChR functions using a chemical genetic approach.....	52
<b>Aims and objectives</b> .....	<b>54</b>
<b>Chapter 2: Materials and methods</b> .....	<b>55</b>
2.1. Materials.....	55
2.1.1. Standard reagents, chemicals and consumables.....	55
2.1.2. Specific reagents and assay kits .....	55
2.1.3. Bacterial strains.....	56
2.1.4. DNA plasmids and receptor constructs.....	56

2.1.5.	Mammalian cell lines .....	57
2.1.6.	Pharmacological agents .....	57
2.1.7.	Primers and siRNAs.....	58
2.1.8.	Radioisotopes and reagents for scintillation counting .....	58
2.1.9.	Antibodies .....	58
2.1.10.	Specialised equipments .....	59
2.2.	Methods.....	59
2.2.1.	Bacterial cell culture .....	59
2.2.2.	Plasmid DNA preparation.....	60
2.2.3.	Minipreps .....	61
2.2.4.	Maxipreps .....	61
2.2.5.	Plasmid DNA quantification.....	62
2.2.6.	Polymerase chain reactions.....	62
2.2.7.	Plasmids and DNA fragments restriction digestion.....	63
2.2.8.	Agarose gel electrophoresis of DNA .....	63
2.2.9.	DNA purification from solution and agarose gel.....	64
2.2.10.	DNA ligation.....	65
2.2.11.	DNA sequencing.....	65
2.2.12.	Cloning of M <sub>4</sub> mAChR sequence .....	65
2.2.13.	Mammalian cell culture .....	67
2.2.14.	Biochemical assays .....	67
2.2.15.	Radioligand binding assays.....	69
2.2.16.	Receptor phosphorylation assays.....	70
2.2.17.	Identification of protein kinases involved in receptor phosphorylation .....	74
2.2.18.	Cell signalling assay .....	75
2.2.19.	Data analysis .....	76

**Chapter 3: A study into the signalling and regulation of the M<sub>3</sub> mAChR in search for functional selectivity .....** **82**

3.1.	Introduction .....	82
3.2.	Results .....	86
3.2.1	Expression levels of the M <sub>3</sub> mAChR.....	86
3.2.2.	Agonist affinity determination.....	88

3.2.3.	Relative intrinsic efficacy of agonists in [ <sup>3</sup> H]-inositol phosphates accumulation assay.....	91
3.2.4.	Relative agonist intrinsic efficacy in ERK1/2 phosphorylation assay.....	94
3.2.5.	Constitutive and agonist dependent phosphorylation of M <sub>3</sub> mAChR.....	97
3.2.6.	Concentration dependency of M <sub>3</sub> mAChR phosphorylation following stimulation with MCh, Pilo and Arec. ....	99
3.2.7.	Use of operational model of agonism to define bias agonism. ....	102
3.2.8.	Phosphorylation profile of the M <sub>3</sub> mAChR following treatment with maximally effective concentration of MCh, Pilo and Arec. ....	104
3.2.9.	Phosphopeptide mapping to detect the patterns of M <sub>3</sub> mAChR phosphorylation. ....	106
3.2.10.	Immunoblotting with phosphosite specific antibodies to reveal differences in phosphorylation at specific residues. ....	108
3.2.11.	Kinetics of phosphorylation of M <sub>3</sub> mAChR at Ser412 and Ser577.....	114
3.2.12.	Ser412 and Ser577 are phosphorylated by different protein kinases.....	116
3.3.	Discussion .....	120
<b>Chapter 4: Phosphorylation of mutant M<sub>3</sub> mAChR solely activated by synthetic ligand (M<sub>3</sub>-RASSL).....</b>		<b>126</b>
4.1.	Introduction .....	126
	Figure 4.1.1: Topography of human M <sub>3</sub> mAChR amino acid sequence containing the RASSL mutations. ....	128
4.2.	Results .....	130
4.2.1.	Induction of receptor expression.....	130
4.2.2.	In vivo labelling and immunoprecipitation.....	132
4.2.3.	Phosphopeptide mapping .....	134
4.2.4.	Western blotting using phosphoserine specific antibodies .....	136
4.3.	Discussion .....	138
<b>Chapter 5: Pharmacological characterisation of novel allosteric ligands at the M<sub>1</sub> mAChR and their effects on receptor phosphorylation .....</b>		<b>141</b>
5.1.	Introduction .....	141
5.2.	Results .....	145
5.2.1.	Generation of stable cell line expressing human M <sub>1</sub> mAChR.....	145

5.2.2.	Characterisation of M <sub>1</sub> mAChR expressing CHO cell line .....	145
5.2.3.	BQCA increases the affinity of ACh at human M <sub>1</sub> mAChR whilst having minimal effects on the binding of antagonist, N-methylscopolamine .....	147
5.2.4.	BQCA displays probe dependency. ....	150
5.2.5.	BQCA potentiates the effect of ACh in mediating [ <sup>3</sup> H]-InsPx accumulation through the M <sub>1</sub> mAChR. ....	153
5.2.6.	BQCA displays allosteric agonism and enhances the potency of ACh in mediating phosphorylation of ERK 1/2. ....	155
5.2.7.	M <sub>1</sub> mediated phosphorylation of ERK 1/2 occurs mainly through G protein pathway and is sensitive to PKC inhibition. ....	159
5.2.8.	BQCA partially enhances ACh-mediated global phosphorylation of M <sub>1</sub> mAChR .....	161
5.2.9.	BQCA caused similar phosphorylation patterns of the M <sub>1</sub> mAChR as ACh when tested as a positive allosteric modulator. ....	164
5.2.10.	BQCA partially enhances ACh-mediated phosphorylation of M <sub>1</sub> mAChR at serine 228. ....	166
5.1.11.	BQCA as an agonist preferentially promotes phosphorylation of serine 228. ....	169
5.2.12.	VU0357017 displays a weak affinity at the M <sub>1</sub> mAChR but does not potentiate the affinity of ACh .....	171
5.2.13.	VU0357017 does not cause InsPx accumulation but negatively affect the potency of ACh .....	173
5.2.14.	VU0357017 behaved as a partial agonist in promoting ERK1/2 phosphorylation but negatively affected the potency of ACh .....	175
5.2.15.	VU0357017 causes minimal M <sub>1</sub> mAChR phosphorylation.....	177
5.3.	Discussion .....	180

**Chapter 6: Phosphorylation and allosteric modulation of the M<sub>4</sub> mAChR .....185**

6.2.	Introduction .....	185
6.3.	Results .....	188
6.3.1.	Molecular cloning of the M <sub>4</sub> mAChR.....	188
6.3.2.	Generation and characterisation of M <sub>4</sub> mAChR expressing CHO-cell line ....	190
6.3.3.	<sup>32</sup> P-labelling and intact cells phosphorylation .....	192
6.3.4.	Mass spectrometric analysis and identification of phosphorylation sites .....	194
6.3.5.	Generation and characterisation of phosphorylation specific antibodies .....	198

6.3.6.	Characterisation of HepM <sub>4</sub> cell line .....	201
6.3.7.	Ser379 is entirely phosphorylated in an agonist dependent manner for membrane bound M <sub>4</sub> mAChR. ....	204
6.3.8.	Phosphorylation of Ser379 is modestly enhanced by the ago-allosteric modulator LY2033298.....	206
6.4.	Discussion .....	208
	Figure 6.4.1: Topography of M <sub>4</sub> mAChR amino acid sequence indicating the putative phosphorylation sites. ....	211
	<b>Chapter 7: General discussion.....</b>	<b>214</b>
	<b>Chapter 8: Critical evaluation and future directions .....</b>	<b>221</b>
	<b>References.....</b>	<b>223</b>

# Chapter 1: General introduction

## 1.1 The superfamily of G protein-coupled receptors

The ability to sense extracellular signals and transduce the information into various intracellular signalling molecules is paramount to cells in living organisms. G protein-coupled receptors (GPCRs) are a class of cell surface proteins that mediate such signal transduction process. These receptors recognise a diverse array of stimuli and play key roles in a wide range of physiological processes including memory formation, muscle contraction, glandular secretion and cellular growth and differentiation (Lefkowitz, 2004; Lefkowitz, 2000). More than 1% of the human genome is known to code for GPCRs which makes these receptors one of the largest and most ubiquitous cell surface proteins found in nature (Pierce *et al.*, 2002; Venter *et al.*, 2001). Additionally, mutations that result in a loss or gain of function have been linked with diseased states and as such GPCRs represent an important drug target for the pharmaceutical industry (Rana *et al.*, 2001).

## 1.2. Classification of GPCRs

All GPCRs share a common architecture of seven transmembrane (TM) domains connected by intracellular (ICL) and extracellular (ECL) loops, a cytoplasmic C-terminus and an exoplasmic N-terminus (Kristiansen, 2004; Lagerstrom *et al.*, 2008; Pierce *et al.*, 2002). The ECL1 and ECL2 are connected by a disulphide bond between two conserved cysteine residues which helps to fold the protein in a correct conformation (Bockaert *et al.*, 1999; Lamah *et al.*, 1990). The transmembrane domains among many GPCRs are relatively similar, but the loop regions and terminal domains are highly diverse (Bockaert *et al.*, 1999). These differences allow GPCRs to be grouped into families and classes.

Initial GPCR classification was based on primary sequence analysis and via this method GPCRs were grouped into three families (Family A-C) (Pierce *et al.*, 2002). However this

classification has been expanded into five families (Family A, B, C, adhesion and frizzled\taste2) owing to the discovery of novel GPCRs and differences in ligand binding sites, (Bockaert *et al.*, 1999; Lagerstrom *et al.*, 2008; Rosenbaum *et al.*, 2009). Family A is the largest group and can be further divided into  $\alpha$ ,  $\beta$ ,  $\gamma$  and  $\delta$  subfamilies. The  $\alpha$  subfamily include receptors for light, odorants, small molecule biogenic amines, hormones and neurotransmitters. These receptors have a ligand binding site located deep within the transmembrane helical bundle (Bockaert *et al.*, 1999). The  $\beta$ -subgroup consists of receptors for peptide hormones such as endothelin, neurotensin and gonadotropin-releasing hormone which have a shallow binding pocket formed mainly by the ECLs and N-terminal domain (Lagerstrom *et al.*, 2008). The  $\gamma$  subfamily includes receptors for peptides and lipid like molecules such as chemokines, opioid and somatostatin which also utilise the ECLs and N-terminal domain to engage the endogenous ligands (Lagerstrom *et al.*, 2008). The  $\delta$  family consists of receptors for odorant and proteases (Lagerstrom *et al.*, 2008). Interestingly, the protease activated receptors (PARs) have a large N-terminal domain which undergoes a proteolytic cleavage either by thrombin (PAR1, 3 and 4) or trypsin (PAR2) to reveal a tethered ligand. This ligand then activates the receptor by interacting with the ECL2 (Kristiansen, 2004).

A characteristic feature of family A GPCRs is that most of them contain highly conserved structural motifs such as the E/DRY sequence at the interface of TM3 and ICL2 and NPxxY motif in TM7 (Fredriksson *et al.*, 2003; Kristiansen, 2004). These motifs are known to be important for receptor activation.

Family B GPCRs has about 25 members and include receptors for peptide hormones such as glucagon, secretin, calcitonin and parathyroid hormone (Pierce *et al.*, 2002). These receptors share very little sequence homology but usually have a large N-terminal domain that is rich in cysteine residues (Gether, 2000; Lagerstrom *et al.*, 2008). These cysteine residues form a

network of disulphide bonds which are important for the endogenous ligand binding (Pal *et al.*, 2012).

Family C is also relatively small and include the  $\gamma$ -aminobutyric acid (GABA<sub>B</sub>) receptor, calcium sensing receptor (CASR) and metabotropic glutamate receptors (mGluRs). These receptors have a large N-terminal domain that is critical for ligand binding (Bockaert *et al.*, 1999; Fredriksson *et al.*, 2003; Gether, 2000; Lagerstrom *et al.*, 2008; Pierce *et al.*, 2002).

The N-terminal domain of metabotropic glutamate receptor forms two lobes separated by a hinge region, a globular arrangement known as the Venus fly trap (VFT) (Bessis *et al.*, 2002; Kunishima *et al.*, 2000). Structural analysis of this region showed that the VFT motif shares a low but significant homology to the bacterial periplasmic binding protein, LIVBP (Bockaert *et al.*, 1999; O'Hara *et al.*, 1993). In addition to the VFT motif, most family C GPCRs also have a cysteine rich domain that is thought to be important for receptor activation. This domain is proposed to transmit the conformational change at the VFT motif to the transmembrane domain and facilitates receptor activation (Bockaert *et al.*, 1999; Lagerstrom *et al.*, 2008).

Most family C GPCRs exist as a dimer and in some cases this dimerisation is required for proper functionality. For instance, the GABA<sub>B</sub> receptor has two subtypes which play distinct roles in signal transduction. The GABA<sub>B1</sub> subtype binds to the ligand and the GABA<sub>B2</sub> interacts with G protein. The two subunits must form a heterodimer with each other in order to form a fully functional GABA<sub>B</sub> receptor (Bockaert *et al.*, 1999).

The adhesion family include receptors for lectomedin and CD97 antigen which bind to the extracellular matrix (Fredriksson *et al.*, 2003; Lagerstrom *et al.*, 2008). These receptors have an excessively long N-terminal domain that forms a mucin-like stalk. This N-terminal domain also contains several functional domains including a proteolytic cleavage site and a

cadherin-like motif that is important for ligand binding (Fredriksson *et al.*, 2003; Lagerstrom *et al.*, 2008).

The frizzled receptors are activated by the glycoprotein ligand, Wnt which plays an important role in cell proliferation and embryonic development (Fredriksson *et al.*, 2003). The taste2 receptors are expressed predominantly in the taste buds and mediate bitter taste sensation. These receptors have several features including short N-and C-terminal domains and the presence of highly conserved IFL, SFLL and SxKTL motifs in TM2, TM5 and TM7 respectively (Fredriksson *et al.*, 2003). The N-terminal domain of frizzled receptors is also rich in cysteine residues that are necessary for ligand binding (Schulte, 2010).

### **1.3. Crystal structure of GPCRs**

In order to understand the structural basis of GPCR functions, it has been necessary to obtain high resolution crystal structures of GPCRs bound to antagonist or agonist and to downstream signalling molecules. Because GPCRs are expressed at low levels in native tissues and are highly unstable when purified out of the membranes, rhodopsin has served as an important model system for crystallography due to its high expression levels in rod outer segments and stability in the dark (Palczewski, 2000). However great progress in protein engineering and crystallographic methods has been made which enabled other GPCRs to be crystallised. Such methods include mutagenesis, removal of flexible regions and fusion with an antibody fragment or T4 lysozyme which proved to be thermostabilising and extremely helpful for crystals formation (Zhao *et al.*, 2012). More than sixteen different GPCRs have now been crystallised to high resolution in various different conformations (antagonist bound, agonist bound and G protein coupled) (Katritch *et al.*, 2013). These structures revealed interesting differences and similarities between receptors from different subfamilies and

receptors within subfamilies. Most of these common and distinct structural features were found at the ligand binding pocket and the loop regions of the receptor.

The binding pocket of the aminergic receptor family is known to contain a highly conserved aspartate residue (Asp<sup>3.32</sup>) which plays an important role in ligand binding and receptor activation (superscript represents Ballesteros Weinstein numbering, (Ballesteros *et al.*, 1995). In the structure of the dopamine D<sub>3</sub> receptor (Chien *et al.*, 2010), M<sub>2</sub> and M<sub>3</sub> mAChRs (Haga *et al.*, 2012; Kruse *et al.*, 2012) and  $\beta_1$  and  $\beta_2$  adrenergic receptors (Rasmussen *et al.*, 2007; Warne *et al.*, 2008), this residue was found to interact with the amine group of the bound ligand. Asp<sup>3.32</sup> was also found in the opioid receptors, though it did not participate in ligand binding. Instead, the ECL2 which forms a highly conserved  $\beta$ -hairpin arrangement served as the ligand binding motif (Granier *et al.*, 2012; Katritch *et al.*, 2013; Manglik *et al.*, 2012; Thompson *et al.*, 2012; Wu *et al.*, 2012).

In the inactive structure of rhodopsin, the ligand, 11-*cis*-retinal was bound covalently to a lysine residue in TM7 (Lys<sup>7.43</sup>) via a protonated Schiff's base linkage (Palczewski, 2000). This interaction was further stabilised by a counterion of Glu<sup>3.28</sup> and protected from the extracellular environment by ECL2 which forms a lid over the binding pocket. A similarly restricted binding pocket was also observed in the crystal structure of sphingosine-1-phosphate 1 (S1P<sub>1</sub>) receptor (Hanson *et al.*, 2012). The closely packed arrangement of the residues at the top of the binding pocket may suggest that the endogenous ligand enters the pocket via the membrane bilayer (Hanson *et al.*, 2012; Katritch *et al.*, 2013).

An additional layer of complexity in the ligand binding pocket was revealed in the crystal structure of the M<sub>2</sub> and M<sub>3</sub> mAChRs. In these structures, the binding pocket was highly hydrophilic and the bound antagonist (QNB in M<sub>2</sub> mAChR and tiotropium in M<sub>3</sub> mAChR) was protected from the extracellular milieu by an aromatic cage formed by three tyrosine

residues (Tyr<sup>3.33</sup>, Tyr<sup>6.51</sup> and Tyr<sup>7.39</sup>). A second binding pocket was found at the top of the cage which is thought to be a site for allosteric modulators (Haga *et al.*, 2012; Kruse *et al.*, 2012). The binding pocket in the two structures was highly similar which highlights the difficulty in developing selective pharmacological agents at the orthosteric binding pocket of this receptor family.

In contrast, the binding pocket for the adenosine A<sub>2A</sub> receptor, histamine H<sub>1</sub> and  $\beta_1$ - and  $\beta_2$ -adrenergic receptors was accessible to the extracellular environment. The ECL2 of these receptors was disordered and lacked the rigid  $\beta$ -sheet arrangement (Jaakola *et al.*, 2008; Jaakola *et al.*, 2010; Rasmussen *et al.*, 2007; Rosenbaum *et al.*, 2007; Rosenbaum *et al.*, 2009; Warne *et al.*, 2008). The binding pocket in the  $\beta_1$ - and  $\beta_2$ - adrenergic receptors overlaps with the binding pocket of rhodopsin, but the binding pocket of the histamine H<sub>1</sub> and adenosine A<sub>2A</sub> receptors was much deeper (Doré *et al.*, 2011; Jaakola *et al.*, 2008; Shimamura *et al.*, 2011). This allowed the antagonist (ZM241385 in adenosine A<sub>2A</sub> and doxepin in histamine H<sub>1</sub> receptor) to bind in an extended conformation.

At the intracellular regions, rhodopsin has an additional helix (helix 8) and an ionic lock formed by Arg<sup>3.50</sup> in the E/DRY motif of TM3 and Glu<sup>6.30</sup> in TM6. This interaction is thought to stabilise the receptor in the inactive conformation (Palczewski, 2000; Rosenbaum *et al.*, 2009). Interestingly, helix 8 and ionic lock interaction were absent in many of the non-visual GPCR structures. The functional significance of the lack of helix 8 in these structures is unknown but the absence of ionic lock interaction is thought to be related to constitutive activity of the receptor (Katritch *et al.*, 2012; Katritch *et al.*, 2013).

In addition to inactive structures, several GPCRs including rhodopsin, adenosine A<sub>2A</sub> and  $\beta_2$  adrenergic receptors have also been crystallised in the active conformation, which provided insights into the mechanisms of receptor activation (Choe *et al.*, 2011; Park *et al.*, 2008;

Rasmussen *et al.*, 2011a; Rosenbaum *et al.*, 2011; Scheerer *et al.*, 2008; Warne *et al.*, 2012; Warne *et al.*, 2011; Xu *et al.*, 2011). Overall, the structural changes at the ligand binding pocket were very small (between 0.8 – 1.2 Å) but changes at the intracellular regions were much more pronounced (Ahuja *et al.*, 2009; Katritch *et al.*, 2012; Katritch *et al.*, 2013; Lebon *et al.*, 2012). These include an outward rotation of the intracellular portion of TM6 and the breaking of the ionic lock (in rhodopsin). This movement, often referred to as the rotamer toggle, also resulted in TM6 moving closer to TM5. A rigid body movement was observed at the TM3 which resulted in the helix moving up and in some cases along its axis (Katritch *et al.*, 2012; Katritch *et al.*, 2013). The intracellular portion of TM7 moved inward toward the centre of the 7TM bundle and created a distortion in the region of the conserved NPxxY motif. These global structural changes resulted in the opening of a binding crevice for G protein at the intracellular region between TM3, TM5 and TM6 (Rosenbaum *et al.*, 2009).

Structural insights into how GPCRs interact with and activate G protein were obtained from the crystal structure of opsin (an active form of rhodopsin) bound to the C-terminal tail of *Gat* (transducin) and the  $\beta_2$  adrenergic receptor bound to heterotrimeric G protein. In these structures, the TM5 and TM6 of the receptors were found to make significant interactions with the  $\alpha 5$  helix of the C-terminal portion of  $G\alpha$  subunit (Rasmussen *et al.*, 2011b; Scheerer *et al.*, 2008). The  $\alpha$ -helical domain of the G proteins also rotated from the GTPase domain by  $\sim 125^\circ$  which may facilitate GDP release and nucleotide exchange (Lebon *et al.*, 2012; Rasmussen *et al.*, 2011b).

#### **1.4. Signalling mechanisms of GPCRs**

The ability of GPCRs to mediate a diverse array of cellular responses is centred on the fact that these receptors are able to interact with multiple transducer proteins and activate a

complex signalling network (Marinissen *et al.*, 2001). Among cellular targets of GPCRs are the heterotrimeric G proteins and arrestins.

#### **1.4.1. G protein dependent signalling**

Heterotrimeric G proteins form the major signalling pathway by which GPCRs function. Four families of G protein have been identified based on the  $G\alpha$  subunit;  $G\alpha_s$ ,  $G\alpha_i$ ,  $G\alpha_{q/11}$  and  $G\alpha_{12/13}$  (Cabrera-Vera *et al.*, 2003; Johnston *et al.*, 2007; Oldham *et al.*, 2008). The heterotrimeric G protein consists of  $\alpha$ ,  $\beta$  and  $\gamma$  subunits. Based on cloning and homology analysis of the human genome, 35 genes have been proposed to code for G proteins; 16 for the  $\alpha$  subunit, 5 for the  $\beta$  subunit and 14 for the  $\gamma$  subunit (Milligan *et al.*, 2006). Because the  $\beta$  and  $\gamma$  subunits are tightly bound together (via an N terminal domain coil-coiled interaction), these subunits are considered as one functional unit (Oldham *et al.*, 2008). GPCRs interact with the G protein and promote the exchange of GTP for GDP at the  $G\alpha$  subunit. Thus, GPCRs act as a guanine nucleotide exchange factor (GEF) upon stimulation by an agonist (McCudden *et al.*, 2005; Oldham *et al.*, 2008; Oldham *et al.*, 2006; Willars, 2006). This nucleotide exchange leads to the dissociation of G protein into the  $\alpha$  and  $\beta\gamma$  functional units. Termination of G protein mediated signalling involves the hydrolysis of GTP and the re-association of  $G\alpha$  subunit with the  $G\beta\gamma$  dimer (**Figure 1.4.1.1**) (Cabrera-Vera *et al.*, 2003; Johnston *et al.*, 2007; McCudden *et al.*, 2005). In vivo, this rate of GTP hydrolysis is greatly enhanced by a family of proteins known as regulators of G protein signalling (RGS) proteins (Willars, 2006).

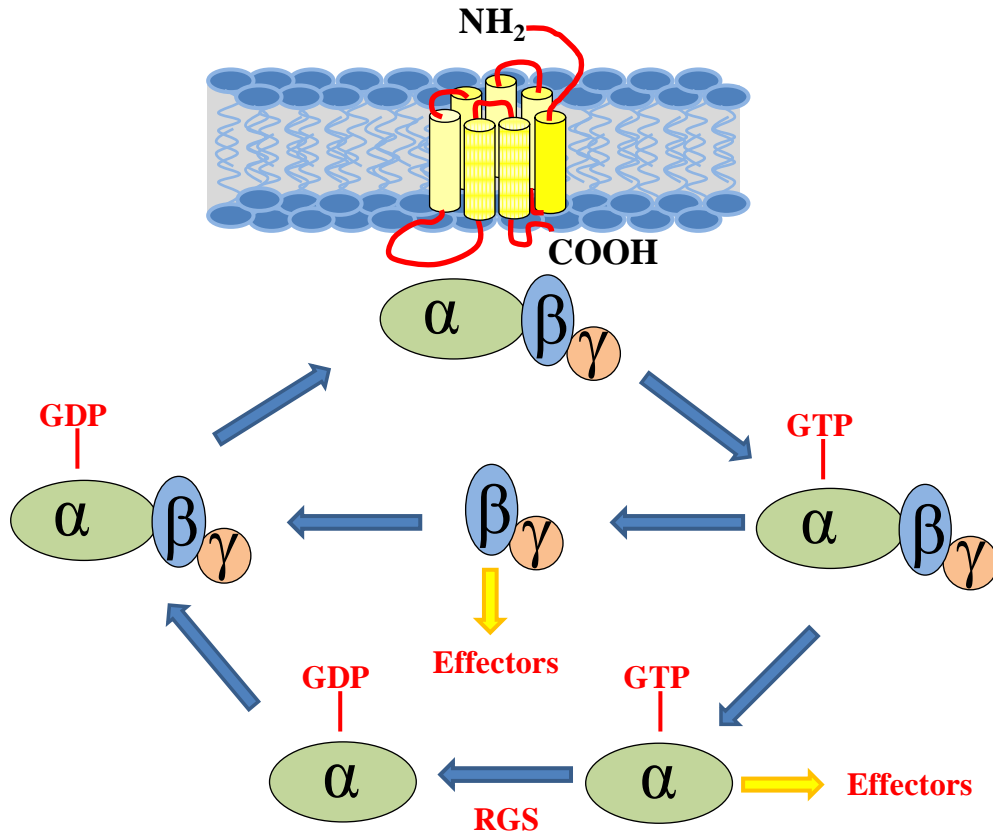


**Figure 1.4.1.1: G protein activation cycle.** Activation of a GPCR by an agonist results in the binding of the receptor to the heterotrimeric G protein. This coupling causes the release of GDP at the  $G\alpha$  subunit and the subsequent binding of GTP which exists at a much higher concentration in cells. This nucleotide exchange resulted in the release of  $G\alpha$  subunit from the  $G\beta\gamma$  dimer. Both  $G\alpha$  and  $G\beta\gamma$  subunits are active signalling molecules which then regulate the activity of downstream effector molecules. Termination of receptor signals is mediated by GTP hydrolysis and the re-association of the  $G\alpha$  subunit with the  $G\beta\gamma$  subunits. In vivo, the rate of this hydrolysis is greatly enhanced by the regulators of G protein signalling (RGS) proteins.

The  $G\alpha$  subunit is thought to play the predominant role in transmitting the GPCR signal (See **Figure 1.4.1.2 and table 1.4.1.1** for downstream effectors of  $G\alpha$  subunit). However the  $\beta\gamma$  subunits have also been shown to be able to activate downstream effector targets such as  $PI3K\gamma$  and G protein inward rectifying  $K^+$  channels (GIRKs) (Clapham *et al.*, 1997; Pierce *et al.*, 2002).

Structurally the  $G\alpha$  subunit contains of a GTPase domain and an  $\alpha$ -helical domain (Lambright *et al.*, 1996; Oldham *et al.*, 2008; Sondek *et al.*, 1996; Sondek *et al.*, 1994). The GTPase domain is conserved across all four families of G proteins as well as in small monomeric G proteins. The GTPase domain contains helical regions that act as a molecular switch (helix I, II, III). These helices adopt different conformations when bound to GDP or GTP, suggesting that they are important for G protein activation (Oldham *et al.*, 2008). The helical domain is unique to the  $G\alpha$  subunit and consists of six  $\alpha$ -helical bundles that form a lid over the nucleotide-binding pocket (Oldham *et al.*, 2008). All  $G\alpha$  subunits with the exception of  $G\alpha_t$  (transducin) are post translationally modified by palmitoylation at the N-terminus which allows the heterotrimeric G protein to anchor to the plasma membrane (McCudden *et al.*, 2005; Oldham *et al.*, 2008).

The  $G\beta$  subunit is made up of seven bladed antiparallel  $\beta$ -strands that bind tightly to the  $G\gamma$  subunit via the N-terminal domain. The  $G\gamma$  subunit is in turn anchored to the plasma membrane by isoprenylation of their C-terminal domain with either a farnesyl or geranylgeranyl moiety (Oldham *et al.*, 2008).

Critical domains that allow G proteins to interact with GPCRs and effector targets have also been determined. It was shown that the  $G\alpha$  subunit plays the predominant role for both processes. For GPCR binding, these domains were mapped to the  $\alpha_5$  helix,  $\alpha_4/\beta_6$  loop and certain residues at the N terminal domain (Johnston *et al.*, 2007; Oldham *et al.*, 2006). The

binding site for downstream effectors such as adenylate cyclase (AC) was mapped to the switch II and  $\alpha 3$  helix of the  $G\alpha$  subunit. The extreme C terminal domain of  $G\alpha$  subunit was found to be important for conferring effector selectivity. For instance replacement of the last 3 C-tail residues of  $G\alpha i$  with the corresponding peptide for  $G\alpha q$  resulted in a chimeric G protein that is responsive to activation by a  $G\alpha i$  coupled receptor but activate phospholipase C (Cabrera-Vera *et al.*, 2003; Conklin *et al.*, 1993; Oldham *et al.*, 2008).

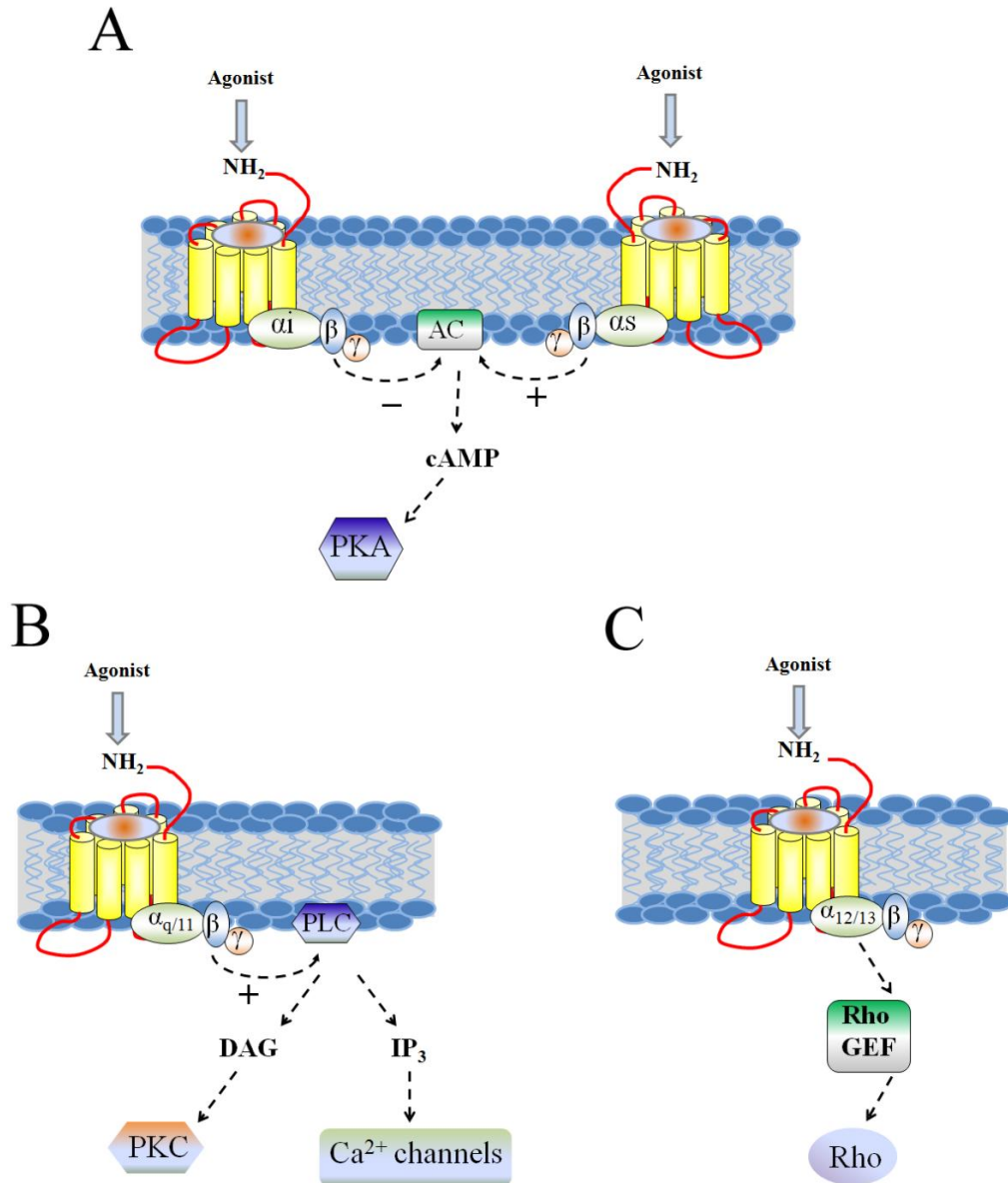


**Figure 1.4.1.2: GPCR signalling via heterotrimeric G proteins.** Activation of heterotrimeric G proteins of the *G<sub>as</sub>* and *G<sub>ai</sub>* families resulted in the activation and inhibition of adenylylate cyclase (AC) leading to changes in cyclic AMP (cAMP) formation (A). Activation of *G<sub>αq</sub>* (B) and *G<sub>α12/13</sub>* (C) proteins resulted in the activation of phospholipase C and Rho-GEF, respectively. Other known effector targets of GPCRs are listed in **Table 1.4.1.1.**

**Table 1.4.1.1: Examples of effector targets of heterotrimeric G proteins.** AC, adenylate cyclase; cGMP, cyclic GMP; PDE, phosphodiesterase; PLC, phospholipase C; PKC, protein kinase C; PKD, protein kinase D; PI3K, phosphatidylinositol-3-kinase; GRKs, G protein-coupled receptor kinases; ERK1/2, extracellular signal regulated protein kinase 1 and 2; GEF, guanine nucleotide exchange factor. ↑ Represents activation and ↓ indicates inhibition. Table adapted from (Gudermann *et al.*, 1996; Gudermann *et al.*, 1997; Hermans, 2003; Offermanns, 2003; Pierce *et al.*, 2002)

G protein family	Main subunits	Effectors
<b>G<sub>s</sub></b>	<b>G<math>\alpha</math><sub>s</sub>, G<math>\alpha</math><sub>olf</sub></b>	↑ AC, Ca <sup>2+</sup> channels, Cl <sup>-</sup> channels, Na <sup>+</sup> Channels
<b>G<math>\alpha</math><sub>i/o</sub></b>	<b>G<math>\alpha</math><sub>i1-3</sub></b>	↓ AC, Cl <sup>-</sup> channels, Na <sup>+</sup> Channels ↑ K <sup>+</sup> channels, C-Src
	<b>G<math>\alpha</math><sub>oA-B</sub></b>	↓ AC, Cl <sup>-</sup> channels ↑ K <sup>+</sup> channels
	<b>G<math>\alpha</math><sub>i1-2</sub></b>	↑ cGMP-PDE ↓ Na <sup>+</sup> Channels
	<b>G<math>\alpha</math><sub>z</sub></b>	↑ cGMP-PDE
<b>G<math>\alpha</math><sub>q/11</sub></b>	<b>G<math>\alpha</math><sub>q</sub>, G<math>\alpha</math><sub>11,14-15</sub></b>	↑ PLC
<b>G<math>\alpha</math><sub>12</sub></b>	<b>G<math>\alpha</math><sub>12</sub>, G<math>\alpha</math><sub>13</sub></b>	↑ ERK1/2, JNK, p115RhoGEF Na <sup>+</sup> /H <sup>+</sup> exchanger
<b>G<math>\beta\gamma</math></b>	Combinations of different $\beta$ and $\gamma$ subunits	↑ AC (II and IV) ↑ GRKs, PKC, PKD, PI3K, PLC Ca <sup>2+</sup> channels, K <sup>+</sup> channels, Na <sup>+</sup> Channels

#### **1.4.2. Arrestin dependent signalling**

In addition to activating heterotrimeric G proteins, many GPCRs have also been discovered to interact with arrestins (DeWire *et al.*, 2007; Kendall *et al.*, 2009; Reiter *et al.*, 2006; Shenoy *et al.*, 2005). Arrestins are cytosolic proteins that become recruited to the plasma membrane as a result of receptor activation. Two mechanisms of arrestin binding to GPCRs have been proposed; 1, arrestins have a polar core which attracts the phosphorylated or negatively charged residues on the receptor, and 2, arrestin molecules have an activation sensor which recognises the active conformation of the receptor (Gurevich *et al.*, 2006; Kendall *et al.*, 2009). Hence the recruitment of arrestins to the plasma membrane is greatly enhanced by phosphorylation and the active conformation of GPCRs.

In vertebrates, arrestins are encoded by large genes (15-30 kb) containing 14-17 exons (Gurevich *et al.*, 2006). Four arrestin subtypes have been cloned in mammals which have distinct expression profiles; arrestin 1 and arrestin 4 are predominantly expressed in the retina and preferentially bind to rhodopsin and the cone opsin, respectively. Arrestin 2 and 3 are expressed virtually in every cells of the body and have been shown to be able to interact with a plethora of different GPCRs (Reiter *et al.*, 2006).

The nature of the interactions between GPCRs and arrestins generally fall into two categories depending on the stability of the interactions and the affinity of the receptor for arrestin 3 over arrestin 2 (Oakley *et al.*, 2000). Receptors that bind transiently to arrestins and do not translocate into the perinuclear compartments are categorised as Class A receptors (Gurevich *et al.*, 2006; Kendall *et al.*, 2009; Luttrell *et al.*, 2010). These receptors often have greater preference for binding to arrestin 3 than arrestin 2. Conversely, GPCRs that bind equally well to both arrestin subtypes and form a stable complex that traffics into the cytosol are categorised as Class B receptors (Gurevich *et al.*, 2006; Kendall *et al.*, 2009; Luttrell *et al.*, 2010; Oakley *et al.*, 2000).

The crystal structure of all four arrestins has been obtained which provided insights into the mechanisms of arrestin activation. Overall, the tertiary structure of the protein is highly conserved and composed of two elongated domains (N-terminal and C-terminal domains) connected by a short linker (Granzin *et al.*, 1998; Gurevich *et al.*, 2006; Han *et al.*, 2001; Hirsch *et al.*, 1999; Sutton *et al.*, 2005; Zhan *et al.*, 2011). The two domains form a “clamp” like structure held in an inactive conformation by three main intramolecular interactions. One of these interactions involves the C-terminal domain extension folding back into the centre of the protein and making contacts with the polar core. The other interaction is a network of ionic bonds between specific residues along the concave of the protein, including the highly conserved lysine (Lys175 in arrestin1) and aspartate (Asp296) residues (Gurevich *et al.*, 2006). It is thought that receptor binding disrupts these interactions and causes structural changes in the two domains that allow arrestins to bind to downstream target(s).

Arrestin dependent and G protein dependent signalling pathways have been shown to be spatially segregated. Although arrestins 2 and 3 have nuclear localisation signal, the proteins often remain and sequester their downstream targets in the cytosol (Gurevich *et al.*, 2006). In contrast, G protein targets are free to translocate to the nucleus. One example of such target is I $\kappa$ B $\alpha$ , a protein that binds to the nuclear transcription factor, NF $\kappa$ B. Interaction of I $\kappa$ B $\alpha$  with either arrestin 2 or arrestin 3 resulted in the sequestration of NF $\kappa$ B in the cytoplasm (Witherow *et al.*, 2004). This prevents the translocation of the I $\kappa$ B $\alpha$ :NF $\kappa$ B complex to the nucleus and inhibits the transcription of genes involved in inflammatory and autoimmune responses (Karin *et al.*, 2005).

Studies using siRNA have also shown that arrestin dependent signalling is temporally distinct from G protein mediated signalling (Ahn *et al.*, 2004; Ren *et al.*, 2005). Whereas G protein dependent phosphorylation of extracellular signal regulated protein kinases 1/2 (ERK 1/2)

occurs very rapidly and reached maximal level after 5 minutes of receptor stimulation, arrestin dependent ERK 1/2 phosphorylation typically occurs much later (10 min post receptor stimulation) and can persist for many hours (Ahn *et al.*, 2004; Ren *et al.*, 2005).

Many cellular proteins have been identified as arrestin targets including the non-receptor tyrosine kinases C-Src, Hck, Fgr and Yes (DeWire *et al.*, 2007; Lefkowitz *et al.*, 2005; Lefkowitz *et al.*, 2004; Shukla *et al.*, 2011). Arrestins have also been shown to scaffold Akt and protein kinase cascade modules consisting of ASK1, MKK4 and JNK3 (Coffa *et al.*, 2011; Kendall *et al.*, 2009; Shukla *et al.*, 2011). Since these protein kinases play a key role in various mammalian physiological processes including learning and memory, cell proliferation, chemotaxis and anti-apoptosis, suggests that arrestin dependent signalling may provide a novel mechanism for therapeutic intervention (Berkeley *et al.*, 2001; DeWire *et al.*, 2007; Kendall *et al.*, 2009).

In addition to transmitting GPCR signals, arrestins have also been shown to interact with cellular proteins that are involved in receptor internalisation (see **Section 1.7** for further information). These proteins include clathrin, associated protein 2 (AP2) and the ubiquitin ligase mdm2 (**Figure 1.4.2.1**) (Pierce *et al.*, 2001; Pierce *et al.*, 2002).

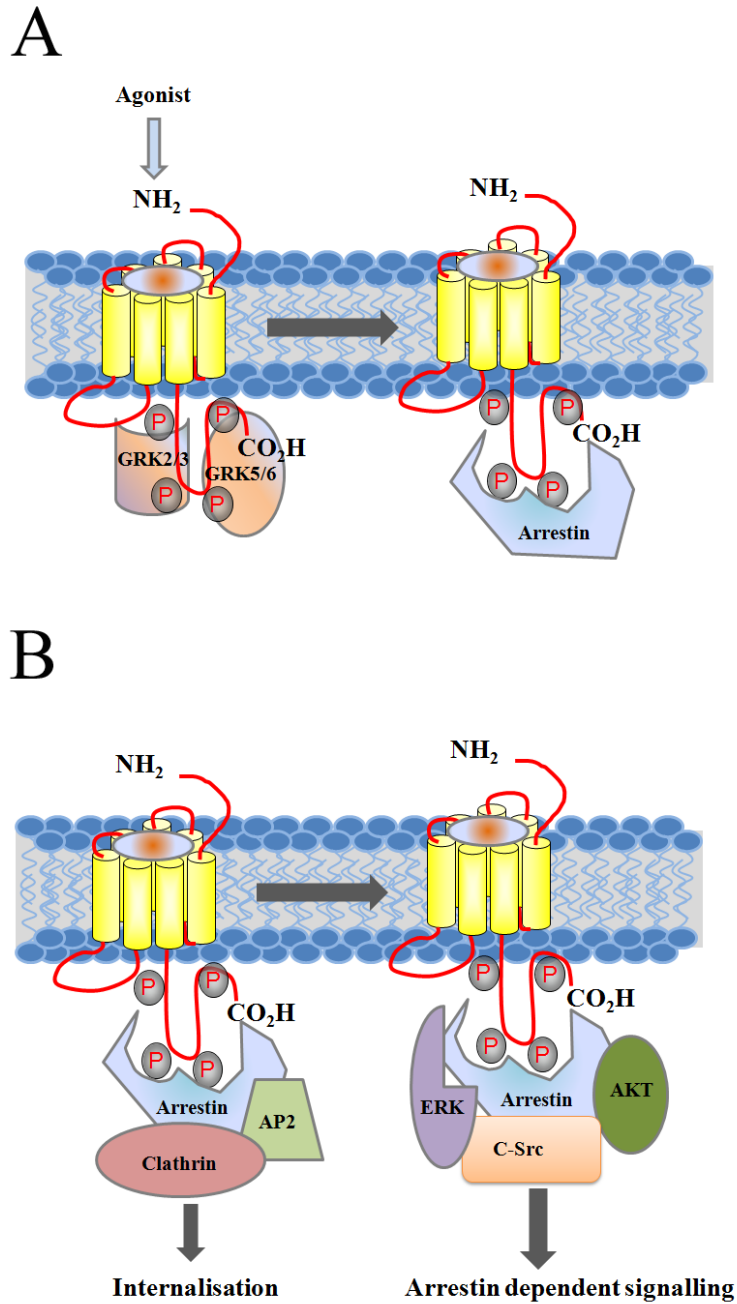


**Figure 1.4.2.1: GPCR signal transduction and regulation by arrestins.** Activation of a receptor by an agonist results in the phosphorylation of ICL regions and C-tail of the receptor by protein kinases such as GRKs (A). This leads to the recruitment of arrestins to the activated receptor. Arrestins scaffold endocytic machinery and facilitate receptor internalisation or recruit signalling molecules such as ERK or the non receptor tyrosine kinase C-Src (B) to initiate alternative signalling cascades.

## 1.5. Functional selectivity of GPCRs

Classical concepts in receptor pharmacology propose that GPCRs exist in an equilibrium between active ( $R^*$ ) and inactive ( $R$ ) states. Accordingly, ligands that preferentially stabilise the  $R^*$  state are classed as agonists whereas ligands that preferentially bind to the  $R$  state are referred to as inverse agonists. Neutral antagonists do not differentiate between the two states but block the actions of other ligands at the receptor. In this view, the propensity of ligands to cause receptor activation (i.e. intrinsic efficacy) is considered linear and can range from partial to full agonists across multiple signalling pathways. However, it has become apparent that GPCRs are structurally flexible and able to adopt multiple active conformations (Caramellini *et al.*, 1998; Kobilka *et al.*, 2007; Swaminath *et al.*, 2004). These conformations can be differentially stabilised by agonists and give rise to functional selectivity or biased agonism (Luttrell *et al.*, 2011; Rajagopal *et al.*, 2010; Urban *et al.*, 2007; Violin *et al.*, 2007). An early example of functional selectivity was reported at the 5-HT<sub>2A</sub> and 5-HT<sub>2C</sub> receptors which showed that synthetic ligands TFMPP (3-fluoromethylphenyl-piperazine) and DOI ((+)-1-(2, 5-dimethoxy-4-iodophenyl)-2-aminopropane) were more efficacious at promoting arachidonic release than inositol phosphate accumulation when compared to the endogenous ligand 5-HT (Berg *et al.*, 1998). Subsequently, studies at other GPCRs including the  $\beta_2$  adrenergic receptor have also revealed the pleiotropic behaviour of a number of GPCR agonists (Azzi *et al.*, 2003; Galandrin *et al.*, 2007; May *et al.*, 2010). This behaviour was characterised by the reversal in potency of the agonists for two distinct signalling pathways linked to the same receptor.

In addition to reversed potency, agonists (such as JNJ7777120) also display dual efficacy, acting as an antagonist in one signalling pathway and an agonist in another pathway (Rosethorne *et al.*, 2011). However, such an “extreme” ligand bias is very rare (Kenakin,

2011) and in most cases, agonists display only weakly or partial bias for one signalling pathway over another. As such bias agonism can be difficult to detect.

Several methods for detecting and quantifying ligand bias have been developed to overcome this difficulty, which include the comparison of maximal receptor responses evoked by the same concentrations of agonists (Gregory *et al.*, 2010) and comparison of agonist concentrations that result in equal receptor responses (Figuroa *et al.*, 2007; Figuroa *et al.*, 2009). Other methods include the use of the operational model of agonism to determine the intrinsic efficacy ( $\tau$ ) of the agonists (Black, 1996; Black *et al.*, 1983; Strange, 2008; Strange, 2007) and then comparing the values to the intrinsic efficacy of a reference agonist (often the endogenous ligand) to obtain an effective signalling bias and a bias factor (a quantitative measure of ligand bias) (Rajagopal *et al.*, 2011). The operational model of agonism requires a known affinity value for the agonists and as such, a separate radioligand binding experiment needs to be performed in addition to signalling assays. Because agonist affinity can vary depending on the state of the receptor (G protein coupled/uncoupled, arrestin bound etc.) an extension of the operational model of agonism was also proposed which compares the agonist efficacy and affinity ( $\tau/K_A$ ) ratios (Evans *et al.*, 2011; Kenakin, 2009).

Using these various approaches, many ligands acting at various different GPCRs have been shown to display biased agonism (Kenakin, 2011; Rajagopal *et al.*, 2010; Reiter *et al.*, 2012; Violin *et al.*, 2007). The nature of the bias varies from G protein bias, arrestin bias and differential G protein subtypes coupling. Since these divergent signalling profiles have the potential to cause different cellular responses, functional selectivity may provide an avenue for developing more effective therapeutic agents (i.e. by selectively activating a therapeutically beneficial signalling pathway while negating the pathway linked to unwanted side effects) (Kenakin, 2012; Whalen *et al.*, 2011). Indeed a number of biased ligands have been developed that showed efficacy in preclinical and early clinical studies in heart failure

and acute pain (Boerrigter *et al.*, 2011; Boerrigter *et al.*, 2012; Ibrahim *et al.*, 2012; Kim *et al.*, 2012).

## 1.6. Allostereism at GPCRs

Allostereism is an important property of proteins as it allows the effects of binding of a molecule at one site of the protein to be transmitted to another site (Kenakin, 2009). This concept was first described by Changeux, Monod, and co-workers in their prominent work on feedback inhibition of enzymes involved in bacterial biosynthetic pathways (Monod *et al.*, 1963; Monod *et al.*, 1965). This concept was then extended to GPCRs to describe the pharmacological effects of ligands which interact with the receptor at a site distinct from the binding site used by the endogenous ligand (Ehlert, 2005; Ehlert, 1988).

It is known that GPCRs contain multiple binding sites that can accommodate the binding of two distinct ligands. The orthosteric binding site, which is used by the endogenous ligand, is highly conserved across GPCR subtypes, while the other site, termed the allosteric site is less evolutionarily conserved (Christopoulos, 2002; Christopoulos *et al.*, 2002). Although the two sites are spatially distinct they are conformationally linked such that the binding of an allosteric modulator at its site will result in a conformational change that alters the reactivity of the receptor for the orthosteric ligand and vice versa (Christopoulos *et al.*, 2004).

The allosteric binding site on GPCRs represents an attractive target for drug development as compounds that interact with this site are likely to be more selective. This site has been extensively probed, particularly for family A and family C GPCRs. For instance, studies on the mAChR, a prototypical family A GPCR have uncovered regions at the extracellular domains that are important for the binding and signalling of allosteric modulators. These include residues in the ECL2 (172-EDGE-175 motif and Y177 at the M<sub>2</sub> mAChR, Y179 at the M<sub>1</sub> mAChR and F186 at the M<sub>4</sub> mAChR), residues in the ECL3 (N419 at the M<sub>2</sub> mAChR

and D432 at the M<sub>4</sub> mAChR) and regions at the top of TM7 (W422 at the M<sub>2</sub> mAChR and W400 at the M<sub>1</sub> mAChR) which are distinct from the residues that form the orthosteric binding pocket (Gregory *et al.*, 2010; Huang *et al.*, 2005; Jager *et al.*, 2007; Leppik *et al.*, 1994; May *et al.*, 2007a; May *et al.*, 2007b; Nawaratne *et al.*, 2010; Prilla *et al.*, 2006). Furthermore, the crystal structures of the M<sub>2</sub> and M<sub>3</sub> mAChRs also revealed that the allosteric site is located at the extracellular region near the top of the main orthosteric binding pocket, which confirmed the spatial differences between the two sites (Haga *et al.*, 2012; Kruse *et al.*, 2012). Several ligands acting at family A GPCRs have now been shown to interact allosterically, including brucine, AC-42 and BQCA at M<sub>1</sub> mAChR and Org27569 and Org27759 at the cannabinoid CB<sub>1</sub> receptor (Lazareno *et al.*, 1997; Ma *et al.*, 2009; Price *et al.*, 2005; Spalding *et al.*, 2002).

Unlike class A GPCRs, the allosteric binding site of family B and family C GPCRs is located within the 7TM helical bundle (Soudijn *et al.*, 2004). Studies on the metabotropic glutamate receptor subtype 5 (mGluR5), a member of family C GPCRs have indicated that residues in TM3 (I651, P655 and S658), and TM7 (A810) to be critical for the binding of the allosteric inhibitor MPEP (May *et al.*, 2007b; Pagano *et al.*, 2000). Additionally, removal of the N-terminal domain containing the orthosteric binding site did not affect the binding of another allosteric compound, 3,3'-difluorobenzaldazine, highlighting that the allosteric site is spatially distinct from the orthosteric binding site (Goudet *et al.*, 2004; Soudijn *et al.*, 2004). Interestingly, analogous allosteric binding site was found at the mGluR1 indicating that some allosteric modulators may occupy overlapping positions within the 7TM domain of different receptor subtypes (May *et al.*, 2007b; Pagano *et al.*, 2000)

Allosteric modulators acting at GPCRs can exhibit a number of pharmacological properties (**Figure 1.6.1**) (Conn *et al.*, 2009a; May *et al.*, 2007b). Allosteric modulators that bind to GPCRs and affect only the affinity of the receptor for the orthosteric ligands are classed as

affinity modulators (Christopoulos *et al.*, 2002; May *et al.*, 2007b). The magnitude and direction of the effects can vary from negative (i.e. negative allosteric modulator or NAM) to positive (positive allosteric modulator or PAM). Allosteric modulators can also affect the efficacy of the orthosteric ligand at the receptor (i.e. efficacy modulators) by altering the stability of the ligand/receptor/G protein complex (Christopoulos *et al.*, 2002). Some allosteric modulators are also able to perturb receptor functions in the absence of the orthosteric ligand and hence classed as allosteric agonists (Langmead *et al.*, 2008a; Langmead *et al.*, 2006a; Langmead *et al.*, 2006b). Such allosteric agonists often possess bimodal/bitopic interactions that involve both the allosteric and orthosteric binding pockets (Lane *et al.*, 2013; Valant *et al.*, 2012b; Valant *et al.*, 2009).

Allosteric modulators often display more than one of the properties described above and as such a combination of radioligand binding and functional signalling assays is required to detect and characterise their full behaviours (Burford *et al.*, 2011; Ehlert, 2005; Ehlert, 1988; Langmead, 2011). Similarly, some allosteric modulators may “modulate” certain signalling pathways more strongly than others and as such, a quantitative analysis of allosteric interactions is paramount to gain full understanding of their pharmacology.

Several models have been developed to quantify allosteric interactions at GPCRs (Christopoulos *et al.*, 2002; Conn *et al.*, 2009a; Ehlert, 2005; Ehlert, 1988; May *et al.*, 2007b). The first model was named the simple allosteric ternary complex model (ATCM) which describes the effect of allosteric modulators on the affinity of the orthosteric ligand (and vice versa) (**Figure 1.6.2**). In this model, the orthosteric and allosteric ligands bind to their respective binding sites with an apparent dissociation constant,  $K_A$  and  $K_B$  respectively (Christopoulos *et al.*, 2002; Conn *et al.*, 2009a; May *et al.*, 2007b). The magnitude and direction of the affinity modulation is governed by the cooperativity factor  $\alpha$ . An allosteric modulator that enhances the affinity of the orthosteric ligand will have  $\alpha$  value greater than 1,

whereas allosteric modulators that decrease the affinity of the orthosteric ligand will have  $\alpha$  value less than 1. This model has also been extended to accommodate the binding of a second orthosteric ligand **Figure 1.6.2** (Langmead, 2011). In this scenario, the apparent dissociation constant of the second orthosteric ligand is denoted by  $K_I$  and the effect of the allosteric modulator on the affinity of the second orthosteric ligand is governed by the cooperativity factor  $\alpha'$  (Langmead, 2011). Because the ATCM does not take into account the effects of the allosteric modulators on the signalling efficacy of the receptor in response to an orthosteric agonist, a final model was proposed. This model was based on a combination of the simple ATCM and the operational model of agonism which allows the quantification of the modulator effect on the efficacy of the orthosteric agonist (denoted  $\beta$ ) as well as determination of the orthosteric ( $\tau_A$ ) and allosteric ( $\tau_B$ ) ligand intrinsic efficacies (Langmead, 2011; Leach *et al.*, 2007).

Allosteric modulators possess a number of theoretical advantages over orthosterically acting compounds as therapeutic agents. First, they are likely to be more selective due to the allosteric binding site being diverse among receptor subtypes (Christopoulos *et al.*, 2004; Conn *et al.*, 2009a; Kenakin, 2012; May *et al.*, 2007b). Secondly, some allosteric modulators that do not perturb receptor functions in the absence of the endogenous ligand will preserve the temporal and spatial properties of cellular signalling processes *in vivo* (Christopoulos *et al.*, 2004; Conn *et al.*, 2009a; Kenakin, 2012; May *et al.*, 2007b). Finally, allosteric modulators that have limited cooperativity will have a saturable effect and so less likely to produce toxic effects associated with an overdose (Christopoulos *et al.*, 2004; Conn *et al.*, 2009a; Kenakin, 2012; May *et al.*, 2007b).

Developing allosterically acting therapeutics however, present novel challenges (Christopoulos *et al.*, 2004). First, some allosteric modulators are probe-dependent and they may not be detected if an incorrect orthosteric ligand is used (Valant *et al.*, 2012a). This

situation may occur if the endogenous ligand for the receptor is unavailable or that it is too weak to be used in drug discovery programs. Second, allosteric modulators may exhibit mixed pharmacology and deciding which parameters to use for guiding structure activity relationship is difficult. Additionally, some allosteric modulators are species dependent and the magnitude of modulation on GPCRs obtained from different species orthologs (i.e. mouse vs. human) is different (Suratman *et al.*, 2011). This will complicate preclinical studies during which animal models are used to test the allosteric compounds.

Despite these challenges, two allosteric compounds have now entered the clinic for the treatment of HIV infections (maraviroc, a negative allosteric modulator of the chemokine CCR5 receptor) and hyperparathyroidism (cinacalcet, a positive allosteric modulator of the calcium sensing receptor), highlighting the feasibility of developing novel therapeutics acting at an allosteric site of GPCRs (Cavanaugh *et al.*, 2012; Conn *et al.*, 2009a; Dentone *et al.*, 2012; Henrich *et al.*, 2013; Marcocci *et al.*, 2012; Mora-Peris *et al.*, 2012; Nozza *et al.*, 2012; Patterson *et al.*, 2012; Portsmouth *et al.*, 2012; Urwyler, 2011; Ward *et al.*, 2012).

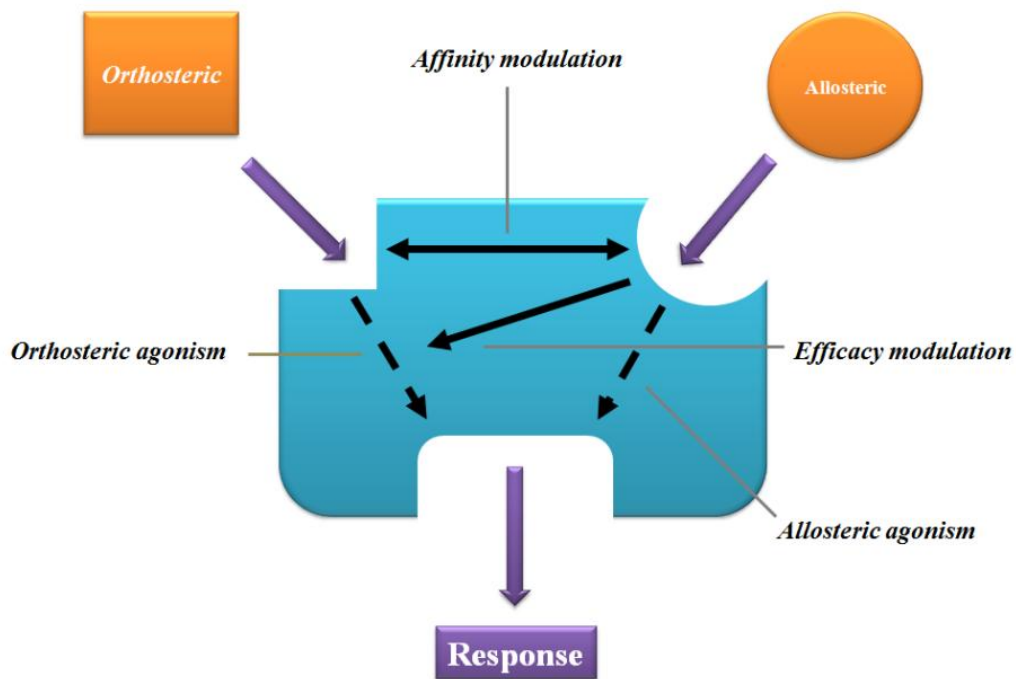


**Figure 1.6.1: Mode of action and pharmacological properties of allosteric modulators.**

Allosteric modulators bind to a site on the receptor that is spatially distinct from the binding site used by the endogenous ligand and affect the affinity and efficacy (or both) of the endogenous ligand. Some allosteric ligands have intrinsic activity in their own right and as such behave as ago-allosteric modulators. Adapted from Conn P, J *et al* 2009a.

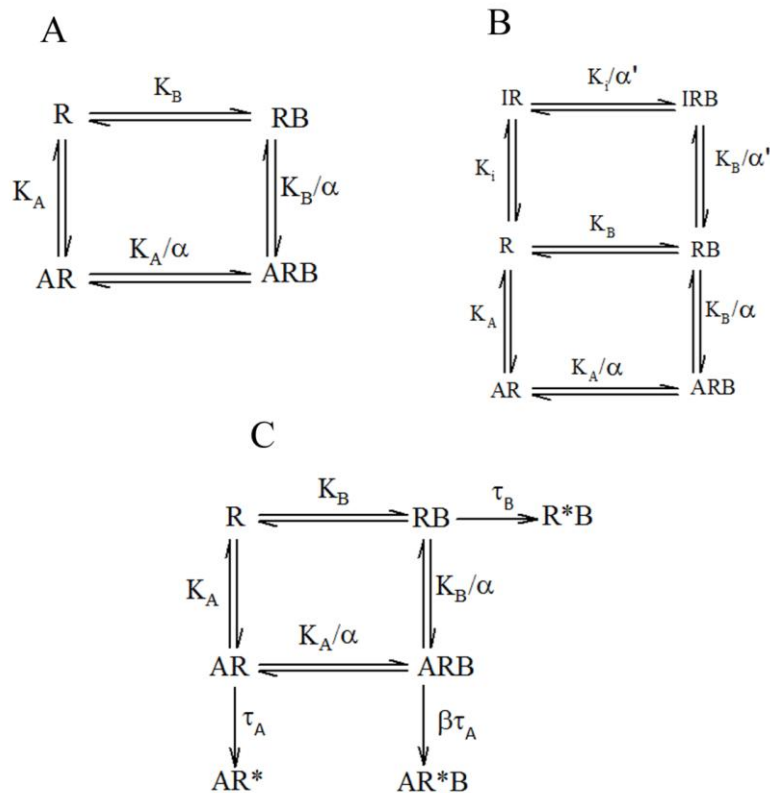


**Figure 1.6.2: Allosteric models at GPCRs.** (A) The simple allosteric ternary complex model (ATCM) describes the binding of orthosteric ligand A and allosteric modulator B, with an equilibrium dissociation constant  $K_A$  and  $K_B$  respectively. The cooperativity factor  $\alpha$  describes the magnitude by which the affinity of each ligand is altered by the simultaneous binding of the other. An  $\alpha$  value  $> 1$  denotes positive affinity modulation and an  $\alpha$  value  $< 1$  indicates negative modulation. (B) The extended ATCM incorporates the binding of a second orthosteric ligand which has an equilibrium dissociation constant,  $K_i$ . The magnitude of affinity modulation by the allosteric modulator is described by the  $\alpha'$  value. (C) The operational model of allosterism and agonism describes the intrinsic efficacy of the orthosteric ( $\tau_A$ ) and allosteric ( $\tau_B$ ) ligands and the magnitude of allosteric modulation when both ligands are interacting with the receptor ( $\beta\tau_A$ ). Adapted from Langmead *et al* 2011.

## 1.7. Regulation of GPCRs by phosphorylation

GPCRs are highly regulated receptor proteins. In response to a continuous stimulation by an agonist, most GPCRs undergo phosphorylation (Pierce *et al.*, 2002; Tobin *et al.*, 2008). This post-translational modification is very rapid and leads to uncoupling of the receptor from G proteins (Pierce *et al.*, 2002). Studies over the years have established that a diverse family of protein kinases are able to phosphorylate GPCRs including the second messenger activated protein kinases (PKA and PKC) and receptor specific protein kinases such as the serine/threonine casein kinase (CK) and G protein-coupled receptor kinase (GRK) families (Benovic *et al.*, 1989; Benovic *et al.*, 1987; Kuhn *et al.*, 1972; Pitcher *et al.*, 1998; Tobin, 2008; Tobin *et al.*, 2008).

Receptor phosphorylation by second messenger activated protein kinases directly uncouples the receptor from G proteins and can occur in the presence or absence of an agonist (Lefkowitz, 1993; Pierce *et al.*, 2002). Therefore these kinases are involved in both homologous desensitisation (by a negative feedback mechanism) and heterologous desensitisation (via phosphorylation of other receptor types). Interestingly, PKA mediated phosphorylation has been shown to cause G protein switching from  $G_{\alpha s}$  to  $G_{\alpha i}$ , indicating that PKA plays an important role in defining the signalling outcome of some GPCRs (Daaka *et al.*, 1997; Martin *et al.*, 2004).

The CK family consists of two members, CK1 and CK2 (Tobin, 2002). CK1 consists of five subtypes (CK1  $\alpha$ ,  $\beta$ ,  $\gamma$ 1-3,  $\delta$  and  $\epsilon$ ) and is ubiquitously expressed (Tobin, 2002). CK1 $\alpha$  is the smallest member of the family (~40 kDa) and the protein has been shown phosphorylate the  $M_3$  mAChR in an agonist dependent manner (Budd *et al.*, 2000; Luo *et al.*, 2008; Tobin, 2002). CK2 is a heterotetramer holoenzyme consisting of two regulatory  $\beta$ -subunits and two catalytic subunits ( $\alpha'$  and  $\alpha$ ). CK2 has been shown to phosphorylate a number of GPCRs

including the D<sub>2</sub> (dopamine) receptor and the M<sub>3</sub> mAChR (Rebholz *et al.*, 2009; Torrecilla *et al.*, 2007).

The G protein-coupled receptor kinase family (GRK) consists of seven members (GRK1-7) which has been functionally grouped into three subfamilies: GRK1-like, GRK2-like and GRK3-like (Moore *et al.*, 2007; Pitcher *et al.*, 1998; Premont *et al.*, 2007). Each member has a catalytic domain comprising of an ATP binding site and a conserved DL/MG sequence motif in the middle of the polypeptide chain (Maeda *et al.*, 2003; Pitcher *et al.*, 1998). The C-terminal domain is highly variable and contains residues critical for interactions with the plasma membrane whereas the N-terminal domain appears to be important for receptor recognition (Maeda *et al.*, 2003; Pitcher *et al.*, 1998).

The GRK1-like subfamily consists of GRK1 and GRK7 which are predominantly expressed in the rod and cone cells (Premont *et al.*, 2007). These kinases mainly phosphorylate rhodopsin and regulate visual signalling. GRK2-like subfamily includes GRK2 and GRK3 which contain a pleckstrin homology domain that interacts with the  $\beta\gamma$  subunits of G proteins and PIP<sub>2</sub> (Lefkowitz, 1993; Pitcher *et al.*, 1998; Premont *et al.*, 2007). These interactions are thought to bring the kinases close to the target receptor and enable them to mediate phosphorylation. The GRK4-like subfamily includes GRK4, GRK5 and GRK6 which are constitutively associated with the plasma membrane (Pitcher *et al.*, 1998; Premont *et al.*, 2007). Of these non visual GRKs, GRK2, 3, 5 and 6 are ubiquitously expressed and have been shown to phosphorylate a wide range of different GPCRs (Pierce *et al.*, 2002). In contrast, GRK4 has a limited tissue distribution and is mainly expressed in the testis (Lefkowitz, 1993; Pitcher *et al.*, 1998; Premont *et al.*, 2007).

All GRKs share a common mechanism in that they phosphorylate receptors only in the presence of an agonist (Lefkowitz, 1993; Pitcher *et al.*, 1998; Willets *et al.*, 2003). This is

because the phospho-acceptor sites for these kinases are concealed when the receptors are unoccupied and the conformational change resulting from agonist binding uncovers these sites. Although there are currently no known GRK specific sequence motifs, GRK2/3 have been shown to prefer acidic residues N terminal of the phosphorylation sites, while GRK5/6 prefer basic residues (Pitcher *et al.*, 1998).

In addition to desensitisation and G protein subtype switching, phosphorylation has also been shown to cause receptor internalisation (Hanyaloglu *et al.*, 2008; Puthenveedu *et al.*, 2007). This process leads to reduction in total number of receptors expressed at the cell surface and hence reduction in cellular responsiveness to circulating agonist(s). It has been shown that receptor internalisation can occur via at least two distinct mechanisms; clathrin dependent internalisation and caveolae dependent internalisation (Pierce *et al.*, 2002; Sorkin *et al.*, 2009). Whilst clathrin dependent internalisation requires the recruitment of arrestins and clathrin associated protein 2 (AP2) to the receptor (**Figure 1.4.2.1**), caveolae dependent internalisation requires the activity of caveolin and cholesterol (Pierce *et al.*, 2002). Clathrin mediated internalisation also requires the GTPase activity of membrane bound dynamin. Dynamin is thought to pinch the clathrin coated pits containing the receptor from the plasma membrane and facilitates the formation of vesicles (Pierce *et al.*, 2002). The vesicles are then transported to the endosomes where they undergo cell sorting.

Receptors in the endosomes are sorted either by being recycled back to the cell surface or transported to the lysosomes for degradation (Sorkin *et al.*, 2009). Receptor recycling involves dephosphorylation of the internalised receptor by protein phosphatase A2 and also requires the activity of small GTPase, Rab7 which targets the receptor to the plasma membrane (Sorkin *et al.*, 2009). Once at the plasma membrane, the re-sensitised receptors are fully functional and able to mediate subsequent rounds of signal transduction.

Receptor degradation leads to reduction in total receptor populations in the cell, a process also known as receptor down regulation. Receptor ubiquitination (i.e. the addition of 8.5 kDa ubiquitin moiety) plays an important role in this process as it signals the proteosomes to degrade the internalised receptor (Hanyaloglu *et al.*, 2008; Puthenveedu *et al.*, 2007).

Receptor phosphorylation has also been shown to regulate the activity of certain protein kinases such as ERK 1/2 and C-Jun N-terminal kinase 3 (JNK3) (Budd *et al.*, 2001; Torrecilla *et al.*, 2007). In many cases, these processes require arrestin binding (**Section 1.4.2, Figure 1.4.2.1**) but for some receptors the role of arrestin in the regulation of ERK1/2 and JNK3 activity is unknown. SiRNA knockdown experiments have shown that activation of ERK1/2 requires receptor phosphorylation by GRK5/6 whereas receptor internalisation requires the actions of GRK2 and GRK3 (Kim *et al.*, 2005; Pierce *et al.*, 2001; Ren *et al.*, 2005).

The diversity of cellular processes that are regulated through GPCR phosphorylation has been attributed to the fact that phosphorylation is highly flexible and dynamic process (Tobin, 2008; Tobin *et al.*, 2008). Traditionally, receptor phosphorylation has been studied through metabolic labelling of cells with radioactive phosphates to reveal phosphorylation at all sites. However, there has been a significant shift in the use of more sophisticated non-radioactive approaches such as mass spectrometry, site directed mutagenesis and phosphorylation sensitive antibodies which revealed site specific information of receptor phosphorylation. These approaches have shown that different protein kinases are able to phosphorylate distinct as well as overlapping sites on GPCRs (Busillo *et al.*, 2010; Liu *et al.*, 2009; Tobin, 2008). The functional outcome of this differential phosphorylation has been highlighted in a study on CXCR<sub>4</sub> which showed that phosphorylation of Ser 324/5 and Ser339 by GRK6 resulted in enhanced ERK activation whereas phosphorylation of the receptor by GRK2 at distinct sites resulted in negative regulation of ERK activation (Busillo *et al.*, 2010)

Studies have also shown that the same receptor subtype expressed in different tissue/cell types are differentially phosphorylated (Butcher *et al.*, 2011; Liu *et al.*, 2009; Tobin *et al.*, 2008; Torrecilla *et al.*, 2007). This suggests that different tissues may express different complements of protein kinases that are necessary for proper regulation of GPCR functions. Additionally, studies have also revealed that the same receptor subtype expressed in the same cell is differentially phosphorylated in response to different agonists (Butcher *et al.*, 2011; Kao *et al.*, 2011; Nobles *et al.*, 2011; Oppermann *et al.*, 1999; Poll *et al.*, 2010; Zidar *et al.*, 2009). The patterns of phosphorylation in these receptors may form barcodes which code for the regulation of certain receptor mediated signalling pathways (Liggett, 2011). In this scenario, the mechanism by which GPCRs regulate downstream signalling proteins may be governed by the phosphorylation state of the receptor (Zidar *et al.*, 2009).

## **1.8. Muscarinic acetylcholine receptors**

The muscarinic acetylcholine receptor family (mAChR) represents a prototypical family A GPCRs and an important receptor system for the study of GPCR functions. Early pharmacological studies using selective antagonists and toxins have indicated the existence of multiple receptor subtypes (Bradley, 2000; Carsi *et al.*, 1999; Hammer *et al.*, 1980; Jolkkonen *et al.*, 1994; Max *et al.*, 1993; Melchiorre *et al.*, 1987). These observations were confirmed by molecular cloning which revealed the existence of five subtypes of mAChR (termed M<sub>1</sub>-M<sub>5</sub>) (Hulme *et al.*, 1990; Kubo, 1993). The M<sub>1</sub> subtype, the first receptor to be cloned (Kubo *et al.*, 1986) was shown to be expressed in many areas of the brain including the hippocampus, cortex and striatum (Brann *et al.*, 1993; Wess, 2004; Wess *et al.*, 2003b). The receptor plays an important role in controlling body movement and high order central nervous system (CNS) functions such as working memory and memory consolidation (Wess, 2004). Since these CNS functions are disrupted in patients suffering from Alzheimer's

disease, the M<sub>1</sub> mAChR has been considered an attractive drug target for the pharmaceutical industry (Eglen *et al.*, 2001; Felder *et al.*, 2000; Langmead *et al.*, 2008b).

The M<sub>2</sub> mAChR, which was cloned immediately after the M<sub>1</sub> mAChR (Kubo *et al.*, 1986) has been shown to have a widespread tissue distribution. In the CNS, the receptor is mainly expressed in the thalamus and brainstem, though it is also found in the cortex and hippocampus (Wess, 2004). Studies using knockout mice have indicated that the receptor plays an important role in regulating body temperature, tremor and pain (Wess, 2004). In the peripheral nervous system the receptor is expressed mainly in the heart and mediates the parasympathetic control of heart rate through modulation of voltage gated K<sup>+</sup> channels (Wess, 2004).

The M<sub>3</sub> and M<sub>4</sub> mAChRs were cloned based on homology sequence analysis of the TM2 domain. By designing oligonucleotide probes for this region, the rat M<sub>3</sub> and M<sub>4</sub> mAChR genes were identified (Bonner *et al.*, 1987). Expression profiling by northern blot analysis and in situ hybridization have shown that the M<sub>3</sub> mAChR is expressed predominantly in exocrine glands and the smooth muscles of the gastrointestinal and urinary tracts (Hulme *et al.*, 1990; Wess, 2004). These receptors play an important role in regulating glucose homeostasis and smooth muscle contraction (Duttaroy *et al.*, 2004; Gautam *et al.*, 2007; Gautam *et al.*, 2006; Kong *et al.*, 2010; Wess, 2004). The M<sub>3</sub> mAChR is also expressed at low levels in the thalamus, cortex and hippocampus where it was suggested to play a key role regulating food intake and mediating learning and memory processes (Poulin *et al.*, 2010; Yamada *et al.*, 2001).

The M<sub>4</sub> mAChR is predominantly expressed in the striatum and has been implicated in the regulation of locomotor activity and dopaminergic neurotransmission (Chapman *et al.*, 2011; Tzavara *et al.*, 2004; Tzavara *et al.*, 2003). The dopaminergic system is thought to play a key

role in psychosis and antagonists for the dopamine receptors have been shown to alleviate the psychotic symptoms of patients suffering from schizophrenia (Atzori *et al.*, 2007; Corrigan *et al.*, 2004; Grinshpoon *et al.*, 1998; Remington, 2008; Schmidt *et al.*, 2012). As such, the M<sub>4</sub> mAChR is considered an attractive target for the treatment of the psychotic symptoms associated with schizophrenia (Eglen *et al.*, 2001; Felder *et al.*, 2000; Langmead *et al.*, 2008b).

The M<sub>5</sub> mAChR was cloned by screening genomic library for genes that have intronless coding regions (Bonner *et al.*, 1988). The identity of the receptor was confirmed by measuring its ability to bind to the mAChR antagonist QNB and respond to stimulation by carbachol (CCh). The M<sub>5</sub> mAChR has a restricted tissue distribution and is expressed predominantly in the midbrain area (Hulme *et al.*, 1990; Langmead *et al.*, 2008b). Studies using knockout mice have indicated that the receptor is involved in the regulation of cerebral blood flow and may also be associated with drug addiction and reward mechanisms (Wess, 2004; Wess *et al.*, 2003a; Yamada *et al.*, 2003).

The M<sub>1</sub>, M<sub>3</sub> and M<sub>5</sub> mAChRs generally couple to the G $\alpha_{q/11}$  family of G proteins and activate phospholipase enzymes (PLC), whereas the M<sub>2</sub> and M<sub>4</sub> mAChR subtypes preferentially couple to G $\beta_{i/o}$  family of G proteins to inhibit adenylate cyclase enzymes (AC) (Caulfield *et al.*, 1998; Wess, 2004). Activation of phospholipase C- $\beta$  (PLC- $\beta$ ) by the M<sub>1</sub>, M<sub>3</sub> and M<sub>5</sub> mAChRs leads to the breakdown of membrane bound PIP<sub>2</sub> and the release of second messengers IP<sub>3</sub> and DAG. IP<sub>3</sub> and DAG then modulate downstream signalling targets such as protein kinase C, extracellular signal regulated protein kinases 1 and 2 (ERK 1 and 2) and IP<sub>3</sub> sensitive Ca<sup>2+</sup> channels (Christopoulos, 2007; Nahorski *et al.*, 1997). Enhanced activity of PLC has also been linked with the modulation of M currents through inhibition of electrically evoked K<sup>+</sup> channels (Christopoulos, 2007; Delmas *et al.*, 2005). Other phospholipase enzymes activated by the M<sub>1</sub>, M<sub>3</sub> and M<sub>5</sub> mAChRs include phospholipase A<sub>2</sub> (PLA<sub>2</sub>) which

hydrolyses phospholipids to release arachidonic acid and lysophospholipid (Conklin *et al.*, 1988) and phospholipase D (PLD) which breaks down phosphatidylcholine to yield phosphatidic acid and choline (Rumenapp *et al.*, 2001; Schmidt *et al.*, 1994).

Adenylate cyclases are enzymes that catalyse the formation of cAMP from ATP. Inhibition of these enzymes by the M<sub>2</sub> and M<sub>4</sub> mAChRs results in a decrease in the formation of cAMP and the activity of subsequent downstream targets such as protein kinase A (PKA). The M<sub>2</sub> and M<sub>4</sub> mAChRs have also been shown to modulate the activity of G protein inward rectifying K<sup>+</sup> channels (GIRKs) through direct interaction with the βγ dimer, independent of AC activity (Christopoulos, 2007; Clapham *et al.*, 1997; Pierce *et al.*, 2002; Slesinger *et al.*, 1995)

Intense studies over the years have shown that these signalling pathways are highly regulated (van Koppen *et al.*, 2003). The mechanisms for this regulation have been extensively studied and it has been established that phosphorylation plays a key part, at least at the receptor level (Tobin, 2008; van Koppen *et al.*, 2003; Wu *et al.*, 1997; Yang *et al.*, 1995) (see **Table 1.8.1** for locations of phosphorylation). For instance, the M<sub>2</sub> mAChR has been shown to be phosphorylated at a cluster of serine and threonine residues within the third intracellular loop of the receptor and this phosphorylation event led to desensitisation of G protein dependent signalling and receptor internalisation (Hosey *et al.*, 1999; Pals-Rylaarsdam *et al.*, 1997a; Pals-Rylaarsdam *et al.*, 1997b). Similarly phosphorylation of the M<sub>1</sub> mAChR has also been shown to cause desensitisation and receptor internalisation (Lameh *et al.*, 1992; Maeda *et al.*, 1990; Moro *et al.*, 1993; Shockley *et al.*, 1999; Waugh *et al.*, 1999). The regulation of the M<sub>3</sub> mAChR by phosphorylation appeared to be more complex. Phosphorylation of the receptor by CK1α and CK2 has been shown to regulate the coupling of the receptor to the ERK1/2 and JNK pathways, respectively (Budd *et al.*, 2000; Budd *et al.*, 2001; Torrecilla *et al.*, 2007), whereas phosphorylation by GRK6 results in desensitisation (Willets *et al.*, 2001; Willets *et*

*al.*, 2002). In contrast, less is known about the role of phosphorylation in the regulation of the M<sub>4</sub> and M<sub>5</sub> mAChRs although both receptors have been implicated to be a target for GRKs and the M<sub>4</sub> mAChR a target for CaM kinase II (Guo *et al.*, 2010; Tsuga *et al.*, 1998).

**Table 1.8.1: Putative Phosphorylation Sites in M<sub>1</sub>-M<sub>4</sub> mACh Receptors.** Putative phosphorylation sites for PKC, GRK2 and casein kinase Ia (CK1a) in M<sub>1</sub>-M<sub>4</sub> mACh receptors. ND not determined. Table adapted from van Koppen and Kaiser, 2003.

mAChR subtype	Kinase	Amino acid sequence	Reference
hM <sub>1</sub>	PKC	Thr354, Ser356 and Ser451, Thr455, Ser457 (putative)	Haga <i>et al.</i> , 1996
	GRK2	284SerMetGluSerLeuThrSerSerGlu292 (putative)	Lameh <i>et al.</i> , 1992 Moro <i>et al.</i> , 1993
hM <sub>2</sub>	GRK2	286SerThrSerValSer290 and 307ThrValSerThrSer311	Pals-Rylaarsdam and Hosey, 1997; Moro <i>et al.</i> , 1993
		Val385, Thr386, Ile389, Leu390, Ala438	Schlador <i>et al.</i> , 2000
hM <sub>3</sub>	GRK2	332SerSerSer334 and 349SerAlaSerSer352	Moro <i>et al.</i> , 1993; Wu <i>et al.</i> , 2000
	CK1 $\alpha$	370Lys-Ser425	Budd <i>et al.</i> , 2000; 2001
	ND	Thr550, Thr553; Thr554	Yang <i>et al.</i> , 1995
mM <sub>3</sub>	ND	Ser384, Ser412, Ser577	Butcher <i>et al.</i> , 2011
rM <sub>4</sub>	CAMKII	Thr145	Guo <i>et al.</i> , 2012

The mAChRs, particularly the M<sub>1</sub>, M<sub>3</sub> and M<sub>4</sub> subtypes represent therapeutically significant targets for CNS and smooth muscle disorders and as such a large number of pharmacological agents have been developed to target these receptors (Eglen *et al.*, 1999; Eglen *et al.*, 2001; Felder *et al.*, 2000; Langmead *et al.*, 2008b). Ligands that act at the mAChRs range from orthosteric antagonists and agonists to allosteric modulators (**Figure 1.8.1**). Orthosteric

ligands interact with the same binding site as ACh and generally show very little subtype selectivity (Conn *et al.*, 2009a). Examples of orthosteric ligands include N-methylscopolamine (NMS), 3-quinuclidinyl benzilate (QNB), methacholine (MCh), pilocarpine (Pilo) and arecoline (Arec). In contrast, allosteric modulators exert their effects on receptors by interacting with sites that are topographically distinct from the binding site used by ACh (Christopoulos *et al.*, 2002; Leach *et al.*, 2007; May *et al.*, 2003; Melancon *et al.*, 2012). Since the allosteric site is less evolutionarily conserved, allosteric modulators have the potential to be more subtype selective and more effective as therapeutic agents. Indeed several allosteric modulators have been demonstrated to possess greater selectivity for one mAChR subtype over another and these include benzyl quinolone carboxylic acid (BQCA), 77-LH-28-1 and VU0357017 at the M<sub>1</sub> mAChR and LY2033298 at the M<sub>4</sub> mAChR (Conn *et al.*, 2009b). BQCA was shown to potentiate the affinity and potency of ACh in vitro (Ma *et al.*, 2009; Shirey *et al.*, 2009). The compound has also been shown to rescue scopolamine induced memory deficit in mice suggesting that it is able to penetrate the blood brain barrier and reach the target receptor (Digby *et al.*, 2010; Ma *et al.*, 2009). VU0357017 was shown to activate the M<sub>1</sub> mAChR in the absence of ACh, indicating that it is an allosteric agonist (Lebois *et al.*, 2010).

LY2033298 has diverse pharmacological properties. The compound has been shown to potentiate the affinity and potency of ACh at the M<sub>4</sub> mAChR in vitro and in vivo (Chan *et al.*, 2008; Leach *et al.*, 2010). The allosteric property of the compound is species dependent such that the degree of affinity and potency enhancement is greater at the human M<sub>4</sub> mAChR compared to the mouse M<sub>4</sub> mAChR (Suratman *et al.*, 2011; Valant *et al.*, 2012a). LY2033298 is also able to induce receptor response in the absence of ACh in certain signalling readouts (Nawaratne *et al.*, 2008). As such LY2033298 also behaves as an ago-allosteric modulator.

Like orthosterically acting agonists, allosteric modulators also have the potential to engender functional selectivity (Leach *et al.*, 2007). However, allosteric modulators that display such behaviour at the mAChRs are limited (Challiss *et al.*, 2009). Currently, AC-42 and 77-LH-28-1 are the only allosteric agonists that have been shown to promote differential receptor signalling. In Chinese hamster ovary (CHO) cells expressing the human M<sub>1</sub> mAChR, AC-42 and 77-LH-28-1 promoted receptor coupling to both G $\alpha_s$  and G $\alpha_{q/11}$  G proteins (Thomas *et al.*, 2008). However, unlike the orthosteric ligands, oxotremorine-M (Oxo-M) and arecoline (Arec), the compounds did not promote receptor coupling to the G $\alpha_{i1/2}$  G protein (Thomas *et al.*, 2008).

Similarly, evidence for orthosteric ligands that display functional selectivity at the mAChR is limited (Challiss *et al.*, 2009). Pilocarpine (Pilo) appears to be the only compound that has been shown to display distinct pharmacological properties. The compound preferentially activates G $\alpha_i$  G protein via the M<sub>3</sub> mAChR over G $\alpha_{q/11}$  G protein (Akam *et al.*, 2001). The compound has also been shown to promote ERK activation via a different pathway compared to ERK activation mediated CCh (Lin *et al.*, 2008), although the significance of this pathway specific ERK activation is unknown.

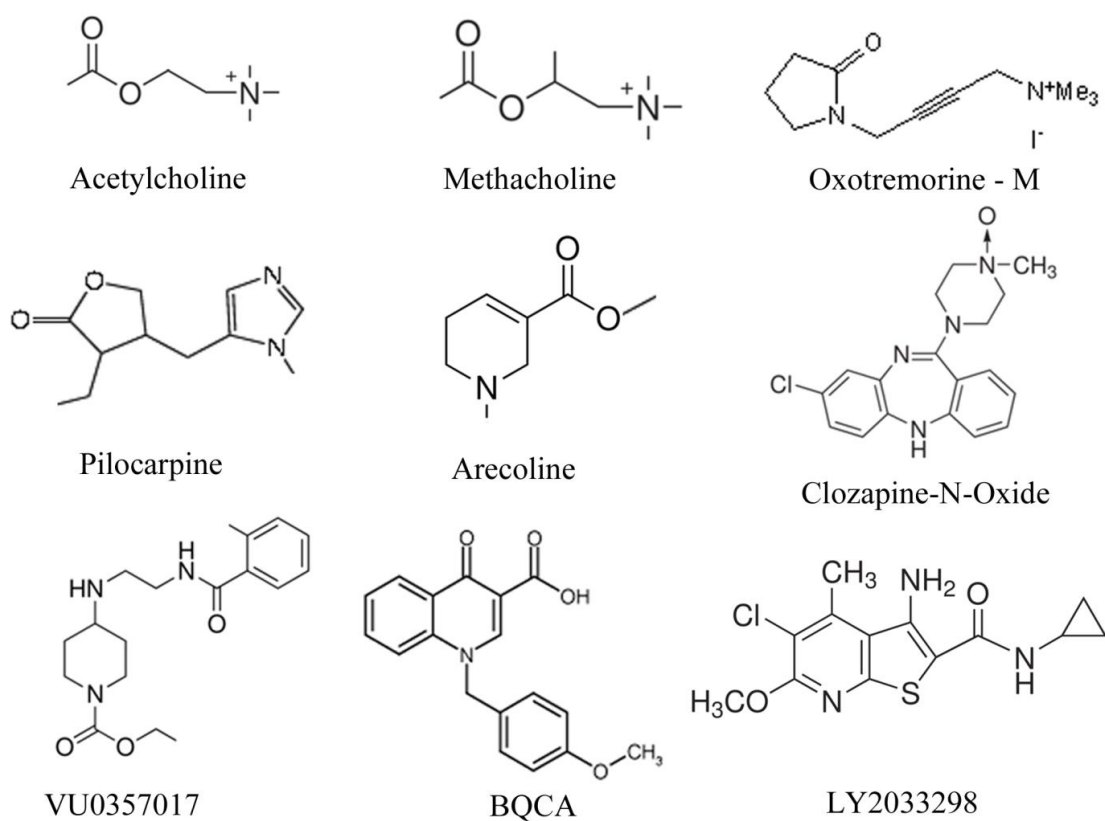


**Figure 1.8.1: Structures of pharmacological agents that interact with the mAChRs.**

Acetylcholine is the endogenous ligand; oxotremorine-M, methacholine, pilocarpine and arecoline are non-selective orthosteric agonists. VU0357017 and BQCA are allosteric modulators of the M<sub>1</sub> mAChR whereas LY2033298 is a selective allosteric modulator of the M<sub>4</sub> mAChR. Clozapine N-Oxide (CNO) is a potent agonist of the RASSL/DREADD mAChRs.

## 1.9. Dissecting mAChR functions using a chemical genetic approach

Much knowledge of the physiological roles of the mAChRs has been gained through studies using mutant mice lacking each of the five mAChR subtypes and pharmacological characterisation with relatively selective agonists and antagonists (Wess, 2004; Wess *et al.*, 2003b). Another powerful approach to study GPCR functions in vivo is the generation of mutant receptors that do not respond to the endogenous ligand but can be activated potently and efficaciously by synthetic ligands (Armbruster *et al.*, 2007; Conklin, 2007; Conklin *et al.*, 2008; Dong *et al.*, 2010a; Pei *et al.*, 2008; Scearce-Levie *et al.*, 2002). These receptors have been named receptors activated solely by synthetic ligands (RASSL) or designer receptors exclusively activated by designer drugs (DREADD) (Conklin *et al.*, 2008; Dong *et al.*, 2010b; Scearce-Levie *et al.*, 2001). When expressed in animals these receptors would remain functionally silent until the application of the exogenous ligand(s). Since the exogenous ligands are otherwise inert, the method enables specific activation of the relevant receptor in vivo.

Several RASSL receptors have now been created including the  $\kappa$ -opioid receptor, serotonin 4 receptor (5-HT<sub>4</sub>), melanocortin 4 receptor (MC<sub>4</sub>) and muscarinic M<sub>1</sub>-M<sub>5</sub> mAChRs (Pei *et al.*, 2008). These mutant receptors have proven to be valuable research tools for dissecting the signalling pathways linked to the receptor both in vitro and in vivo.

The RASSL for the  $\kappa$ -opioid receptor was developed by substituting the second extracellular loop of the receptor with that of the  $\delta$ -opioid receptor. This chimeric receptor, also called Ro1, had significantly reduced affinity for dynorphin but retained its ability to bind to the exogenous agonist, spiradoline (Coward *et al.*, 1998). The receptor was subsequently expressed in a number of tissues including the heart and taste buds (Redfern *et al.*, 1999;

Zhao *et al.*, 2003) where it was shown to cause reduction in heart rate and mediates taste sensation, respectively.

The RASSL for the mAChRs was developed through a yeast mutagenesis approach to identify mutations that would significantly reduce ACh binding but create binding to clozapine-N-oxide (CNO) (Armbruster *et al.*, 2007). CNO was chosen because the compound has good bioavailability and is biologically inert, making it ideal for in vivo studies. In all of the 5 mAChR subtypes, two residues within the transmembrane domains (Y106C and A196G in the M<sub>1</sub> mAChR, Y149C and A239G in the M<sub>3</sub> mAChR and Y113C and A203G in the M<sub>4</sub> mAChR) were found to be important for conferring CNO affinity but significantly reducing ACh binding (Abdul-Ridha *et al.*, 2013; Armbruster *et al.*, 2007; Nawaratne *et al.*, 2008). Pharmacological characterisation of the M<sub>3</sub> RASSL receptor in vitro has shown that the receptor couples to the PLC and ERK 1/2 phosphorylation pathways in response to CNO stimulation (Armbruster *et al.*, 2007). When expressed in the hippocampus and pancreatic  $\beta$  cells, the receptor was shown to cause neuronal firing and insulin secretion, respectively (Alexander *et al.*, 2009; Guettier *et al.*, 2009). Hence, the mutant receptor appeared to be able to replicate the WT M<sub>3</sub> mAChR functionality in native tissues.

The M<sub>4</sub> RASSL receptor has also been shown to function in a similar manner as the WT receptor when stimulated with CNO. For instance, the receptor caused neuronal silencing when transiently expressed in hippocampal neurons and activated GIRK when co-transfected in HEK cells with the K<sup>+</sup> channels (Armbruster *et al.*, 2007). The receptor was also shown to cause c-fos expression in striatal neurons indicating modulation of neuronal activity in whole animals (Ferguson *et al.*, 2011). Interestingly, ACh could stimulate a functional response at the M<sub>4</sub> RASSL in the presence of the allosteric modulator LY2033298, highlighting that the allosteric site is unaffected by the RASSL mutations (Nawaratne *et al.*, 2008).

## Aims and objectives

1. To investigate the signalling and regulation of the WT M<sub>3</sub> mAChR in response to full and partial orthosteric agonists to determine if these compounds display functional selectivity. This will then be extended to the study of the regulation of the M<sub>3</sub> RASSL receptor since this mutant receptor is considered a valuable research tool for dissecting the physiological roles of the M<sub>3</sub> mAChR in vivo.
2. To characterise the pharmacology of two novel allosteric ligands at the M<sub>1</sub> mAChR and the effects of these compounds on receptor phosphorylation.
3. To determine the phosphorylation state of the M<sub>4</sub> mAChR and identify the sites of phosphorylation using mass spectrometry. The effects of the allosteric modulator LY2033298 on site specific phosphorylation of the M<sub>4</sub> mAChR will also be investigated.

## **Chapter 2: Materials and methods**

### **2.1. Materials**

#### **2.1.1. Standard reagents, chemicals and consumables**

General laboratory chemicals and reagents were purchased from either Sigma Aldrich (Poole, U.K.) or Fisher Scientific (Loughborough, U.K.). Water used for preparing solutions was of ultra pure quality obtained from ELGA Filtration System (ELGA Labwater, Marlow, U.K.). Water used for bacterial cell culture and molecular biology was filter sterilised and autoclaved at 121°C for 15min. All mammalian cell culture reagents including various culture media, phosphate buffered saline (PBS), foetal bovine serum (FBS), penicillin/streptomycin mix, geneticin (G-418) and hygromycin B were purchased from Invitrogen (Paisley, U.K.). Glass coverslips (diameter 25mm, or 18×18mm), thin layer chromatography (TLC) plates and cell culture plastic consumables were purchased from VWR International (Lutterworth, U.K.). Agarose powder was purchased from Geneflow Ltd (Fradley, U.K.). Sterile plastic inoculation loops (diameter 5mm), petri dishes (diameter, 10cm; single vent), syringe filters (0.2µm) and RNase-, DNase-, DNA-, pyrogens- and PCR (polymerase chain reaction) inhibitor-free microcentrifuge tubes (1.5mL or 2.0mL) were supplied by Appleton Woods (Birmingham, U.K.).

#### **2.1.2. Specific reagents and assay kits**

Complete EDTA-free protease inhibitor tablets, PhosStop phosphatase inhibitor tablets, octyl glucoside, calf intestinal alkaline phosphatase, T<sub>4</sub> DNA ligase, Fugene HD transfection reagent, mini plasmid isolation kit, Genopure maxi plasmid isolation kit and PCR product purification kit were provided by Roche Applied Science (Burgess Hill, UK). PfuUltra DNA polymerase and dNTPs for polymerase chain reaction (PCR) were provided by Stratagene (Cheshire, UK). SiPortamine transfection reagent was obtained from Ambion (Cambridge,

UK). Restriction enzymes and DNA ladder (1kb plus, 100bp-12kp range) were purchased from New England Biolabs (Hitchin, UK). Blasticidin, ethidium bromide for staining agarose gels and guanosine triphosphate (GTP) for radioligand binding assays were purchased from Sigma Aldrich (Poole, U.K.). SDS-PAGE reagents, Bradford reagent for protein determination and pre-stained protein molecular size markers for immunoblotting (10-250kDa range) were from Bio-Rad (Hemel Hempstead, UK). SureFire ERK1/2 phosphorylation kits were obtained from PerkinElmer (Waltham, Massachusetts, USA). Sequencing grade trypsin (lyophilised, 100 µg) was obtained from Promega (Southampton, UK). Protein A-Sepharose beads (1.5 g) and enhanced chemiluminescence (ECL) films were purchased from GE Healthcare (Little Chalfont, U.K.). Bicinchoninic acid (BCA) assay kits for protein determination were obtained from Thermo Scientific (Rockford, IL, USA). Nitrocellulose membranes and immobilon horse radish peroxidase (HRP) substrates for immunoblotting were obtained from Millipore (Watford, UK). Vectashield containing DAPI for immunocytochemistry was obtained from Vector laboratories (Peterborough, UK).

### **2.1.3. Bacterial strains**

Commercially available  $\alpha$ -select chemically competent cells (Bioline, London, UK) were used for DNA transformation in routine cloning and sub-cloning procedures. These cells have been optimised to reduce recombination and hence improve the quality of transformed DNA.

### **2.1.4. DNA plasmids and receptor constructs**

All mAChR gene sequences were cloned into pcDNA3.1 (+) vector from Invitrogen (Paisley, U.K.). This vector contains an ampicillin resistance gene for selection in *Escherichia (E.) coli* and a neomycin resistance gene for selection in mammalian cell lines. The construct for the M<sub>1</sub> mAChR was obtained from Dr Ali Jazayeri (Heptares Therapeutics, Welwyn Garden City, U.K.) and this construct has a myc and His10 tags at the C-terminus. The M<sub>1</sub> mAChR sequence was inserted at the NheI (5') and NotI (3') cloning sites. The construct for the M<sub>4</sub>

mAChR was purchased from Missouri University of Science and Technology (Rolla, Missouri, USA, [www.cdna.org](http://www.cdna.org)). The sequence was cloned at the KpnI (5') and XhoI (3') sites.

#### **2.1.5. Mammalian cell lines**

WT Chinese hamster ovary cells (CHO-K1) were purchased from American Type Culture Collection (ATCC) – LGC standards (Teddington, Middlesex, UK). CHO cells stably expressing human M<sub>3</sub> mAChR (CHO-hM<sub>3</sub>R) were a kind gift from Dr. N. J. Buckley (then at the Department of Pharmacology, University College London, U.K.). CHO cells stably expressing the human M<sub>1</sub> mAChR (CHO-hM<sub>1</sub>R) was generated in house using a cDNA construct obtained from Heptares Therapeutics (BioPark, Welwyn Garden City, Herts, UK). CHO cells stably expressing the human M<sub>4</sub> mAChR (CHO-hM<sub>4</sub>R) was generated in house using a cDNA clone purchased from Missouri University of Science and Technology (Rolla, Missouri, USA, [www.cdna.org](http://www.cdna.org)) or a gift from Heptares Therapeutics. Flip-In inducible HEK cells expressing the human M<sub>3</sub> mAChR and the RASSL variant were a gift from Prof. Graeme Milligan (Glasgow, UK)

#### **2.1.6. Pharmacological agents**

Protein kinase (PK) C activator, Phorbol 12-myristate 13-acetate (PMA) and the broad spectrum PKC inhibitor bisindolylmaleimide I (Bis I) were obtained from Sigma Aldrich (Dorset, UK). Non selective mAChR orthosteric ligands, acetylcholine, methacholine, pilocarpine, arecoline and atropine were also provided by Sigma Aldrich (Dorset, UK). M<sub>4</sub> mAChR selective allosteric modulator LY2033298 was a kind gift from Heptares Therapeutics (Welwyn Garden City, UK). M<sub>1</sub> mAChR selective allosteric modulator BQCA was obtained either from Insight Biotechnology (Middlesex, UK) or a gift from Prof. Jeff Conn (Vanderbilt University, Tennessee, USA) and VU0357017 was purchased from Sigma Aldrich (Dorset, UK).

### 2.1.7. Primers and siRNAs

Annealed silencing RNA against mouse GRK2 (sense: 5'-GAAAUAUGAGAAGCUGGAGtt-3', antisense: 5'-CUCCAGCUUCUCAUAUUUCtt-3') and GRK 6 (sense: 5'-GCAAGCUGUAGAACAUGUCtt-3', antisense: 5'-GACAUGUUCUACAGCUUGCtt-3') were purchased from Ambion (Cambridge, UK). PCR primers for the cloning of the M<sub>4</sub> mAChR (5'cccggatccgccaccatggatgccaacttcacacctgtcaatggc and 3'gggtctagaactaagcgtaatctggaacatcgtatgggtaagcgtaatctggaacatcgtatgggtacctggcagtgccgatgttccgatactggcacagcagcag) were obtained from Eurogentec (Southampton, UK).

### 2.1.8. Radioisotopes and reagents for scintillation counting

<sup>3</sup>H-Myo inositol (10-25 Ci/mmol), [<sup>3</sup>H] *N*-methyl scopolamine ([<sup>3</sup>H]-NMS; 70 mCi/mmol), [<sup>32</sup>P]-orthophosphate (0.900-1.100 Ci/mmol), Ultima Gold XR liquid scintillation fluid, GF/B plates and scintillation vials (6mL and 20mL) were obtained from PerkinElmer (Waltham, Massachusetts, USA).

### 2.1.9. Antibodies

Antibodies against mAChRs were raised in house. Structural antibody for M<sub>3</sub> mAChR was developed previously (Tobin *et al.*, 1993) and phosphorylation specific antibodies were a generous gift from Dr Adrian J. Butcher. Both structural and phosphorylation specific antibodies for the M<sub>1</sub> mAChR were also a gift from Dr Adrian J. Butcher whereas the phosphorylation specific antibody for the M<sub>4</sub> mAChR was developed during this project. Rat IgG monoclonal anti-HA antibody (affinity matrix and lyophilised) was obtained from Roche Applied Science (Burgess Hill, UK). Rabbit IgG polyclonal anti-myc antibody and anti GRK2 and GRK6 antibodies were purchased from Insight Biotechnology (Middlesex, UK). Goat anti-rabbit and goat anti-mouse IgG, HRP-linked antibodies were purchased from Bio-Rad Laboratories (Hemel Hempstead, UK). Goat anti-rabbit and goat anti-mouse IgG alexa-

488 fluor-linked antibodies for immunocytochemistry was obtained from Vector laboratories (Peterborough, UK).

### **2.1.10. Specialised equipments**

PheraStar and PolarStar microplate readers were obtained from BMG Labtech (Aylesbury, UK). TomTec 96-well harvester was obtained from TomTec Inc (Hamden, Connecticut, USA). MicroBeta liquid scintillation counter was obtained from PerkinElmer (Waltham, Massachusetts, USA). Automated cell counter was provided by Nexcelome Bioscience (Sarisbury Green, UK). Polytron homogenizer was purchased from Kinematica (Basel, Switzerland) and Beckman Coulter centrifuge from Beckman Coulter Inc (High Wycombe, UK). PCR thermal cycler and SpeedVac concentrator centrifuge were obtained from Eppendorf (Cambridge, UK). HTLE 7002 electrophoresis system was purchased from CBS Scientific (San Diego, CA, USA). STORM phosphoimager were obtained from GE Healthcare (Little Chalfont, UK) and confocal microscope was obtained from Leica Microsystems (Milton Keynes, UK)

## **2.2. Methods**

### **2.2.1. Bacterial cell culture**

#### **2.2.1.1 Growth and maintenance**

*Escherichia coli* (*E. coli*) cells were grown at 37°C either in Luria-Bertani (LB) broth (1% w:v tryptone, 0.5% w:v yeast extract, and 1% w:v NaCl) with shaking at 220-230rpm or on LB agar (1% w:v tryptone , 0.5% w:v yeast extract, 1% w:v NaCl and 1.5% w:v agar) plates. Ampicillin (100µg/mL) was used as appropriate.

### **2.2.1.2. *E. coli* stock**

Glycerol stocks of *E. coli* cells were prepared by mixing 400 $\mu$ L of fresh overnight culture and 400 $\mu$ L of 40% (v:v) glycerol in sterile 2mL cryo-vials. Vials were then stored at -80°C until required. To grow cells from a glycerol stock, the frozen cells were scraped with a sterile plastic inoculating loop and streaked onto a fresh LB agar plate containing the appropriate antibiotics. The plate was then incubated inverted at 37°C overnight and stored at 4°C until required.

### **2.2.1.3. Bacterial transformation**

Plasmid DNA containing receptor sequences were transformed into  $\alpha$ -select chemically competent (*E. coli*) cells. A 50-100 $\mu$ L aliquot of the competent cells was thawed on ice for 10 min. A 0.5-1.0  $\mu$ g aliquot of plasmid DNA or 5 $\mu$ L of ligation reaction (**Section 2.2.10**) was added and the mixture incubated on ice for a further 30min. The DNA/cell mixture was then heat-shocked at 42°C for 45s and immediately placed on ice for 2min. The reaction mixture was adjusted to 1mL with SOC medium (0.5% w:v yeast extract, 2% w:v tryptone, 10mM NaCl, 2.5mM KCl, 10mM MgCl<sub>2</sub>, 10mM MgSO<sub>4</sub>, 20mM glucose). The cells were incubated at 37°C for 1hr and then 10-100 $\mu$ L aliquots were spread onto a 10cm LB agar plate containing the appropriate antibiotics and incubated at 37°C overnight. The plates were then sealed with Saran film and stored inverted at 4°C.

### **2.2.2. Plasmid DNA preparation**

Transformation is often followed by antibiotic selection to enable bacterial cells that have taken up the plasmid DNA to be propagated. The plasmid DNA that has been expanded was isolated either in miniprep or maxiprep scales using commercially available kits. Minipreps were conducted for a small amount of DNA for diagnostic purposes such as selecting DNA

clones that contains an insert and confirming a potential construct. Maxipreps were carried out to prepare larger scale DNA samples for transfection in mammalian cells.

### **2.2.3. Minipreps**

Plasmid DNA was purified using the high pure plasmid isolation kit provided by Roche. 2mL of bacterial culture was pelleted by centrifugation (6,000 x g; 5 min) and resuspended in 250 $\mu$ L of re-suspension buffer (50 mM Tris-HCl, 10 mM EDTA; pH8.0) supplemented with 100  $\mu$ g/mL RNase A by gentle pipetting. Cells were lysed by addition of 250 $\mu$ L of lysis buffer (200 mM NaOH, 1% (w/v) SDS). Lysis was terminated after 5 min by the addition of 350 $\mu$ L of binding buffer (4.0M guanidine hydrochloride, 0.5 M potassium acetate; pH 4.2). The cell lysates were centrifuged (12,000 x g; 10 min) and the supernatant loaded onto miniprep filter tubes. The tubes were centrifuged (12,000 x g; 1 min) and washed twice with 700 $\mu$ L wash buffer (20 mM sodium chloride, 2 mM Tris-HCl, 80% (v/v) ethanol; pH 7.5). After washing, bound DNA was eluted from the column by addition of 50-100 $\mu$ L sterile water by centrifugation (12,000 x g; 5min) into sterile 1.5 mL Eppendorf tubes.

### **2.2.4. Maxipreps**

The Genopure plasmid maxi kit was used to produce larger scale DNA samples. A 200mL of overnight culture was pelleted by centrifugation (3000g, 10 min). Media was carefully decanted and the cell pellet resuspended in 12mL of suspension buffer supplemented with 100  $\mu$ g/ $\mu$ L RNase A. Cells were lysed for 10min at room temperature by the addition of 12mL lysis buffer. Lysis was stopped by the addition of 12mL neutralisation buffer. The bacterial lysates were cleared by centrifugation (3000g, 10 min) and filtration through a membrane. Meanwhile, a NucleoBond AX 500 column was equilibrated by the addition of 6 ml Equilibration Buffer. The cell lysates were added onto the equilibrated tip and allowed to drain by gravity flow. The column was washed twice with 16mL of wash buffer. The DNA was then eluted by the addition of 15mL of elution buffer. The DNA was precipitated by the

addition of 11mL isopropanol and pelleted by centrifugation (3,750g; 90 min; 4 °C). The DNA pellet was washed with 5mL of room temperature 70% (v/v) ethanol and then centrifuged (3750g; 60 min; 4°C). The supernatant was carefully removed and the pellet allowed to dry prior to re-suspension in 0.5mL of ultra pure H<sub>2</sub>O.

#### **2.2.5. Plasmid DNA quantification**

The yield of isolated plasmid DNA was determined by measuring absorbance at 260nm. An absorbance of 1 at 260nm corresponds to a concentration of 50µg/mL pure double-stranded DNA (dsDNA). The purity of DNA was determined by measuring absorbance at 280nm; a DNA solution with A<sub>260</sub>/A<sub>280</sub> ratio of 1.7-2.0 indicated relatively pure DNA. Samples were first diluted 1:100 in ultrapure H<sub>2</sub>O and then measured.

#### **2.2.6. Polymerase chain reactions**

PCR reactions were performed in a sterile environment with total volume of 50µL. The reaction mixture contained 1µL of the thermostable DNA polymerase PfuUltra (2,500unit/mL), 5µL of 10× PfuUltra reaction buffer, 1µL (0.2µg/µL) of each 5'- and 3'- primers, 0.4µL of 25mM dNTPs (0.2 mM), 0.25µg plasmid DNA template and an appropriate volume of H<sub>2</sub>O. The reactions were carried out in the Eppendorf thermal cycler with a heated lid. Unless otherwise stated, the standard PCR protocols listed in **Table 2.2.6.1** is followed. After the reactions, the PCR products were separated from the template DNA by agarose gel electrophoresis (**Section 2.2.8**) and purified using a commercially available kit (**Section 2.2.9**).

**Table 2.2.6.1: Standard PCR cycling parameters for amplifying receptor sequences.**

Step	Number of cycles	Temperature	Duration
Denaturation	1	92°C	2 min
Denaturation	30	92°C	30 sec
Annealing		50-60°C	30 sec
Extension		72°C	3 min
Extension	1	72°C	10 min
Termination	1	4°C	Forever

### **2.2.7. Plasmids and DNA fragments restriction digestion**

In order to introduce cohesive ends for ligation, plasmid DNA and purified PCR products were digested with appropriate restriction enzymes. The reactions were carried out in a 50µL reaction volume containing 2µg of purified DNA, 5µL 10× enzyme-specific buffer, 10U enzyme (10U/µL) and an appropriate volume of H<sub>2</sub>O. The mixture was incubated at 37°C for 3hr. After digestion, the target fragments were separated by agarose gel electrophoresis (**Section 2.2.8** followed by DNA purification (**Section 2.2.9**). Restriction digests were also performed for diagnostic purposes such as confirming a construct with an appropriate insert. In this case the reaction was performed in a reduced volume (20µL), containing 0.5µg DNA, 2µL 10× appropriate enzyme buffer, 3U enzyme (10U/µL or 20U/µL) and an appropriate amount of H<sub>2</sub>O. The digested DNA was also resolved by agarose gel electrophoresis (**Section 2.2.8**).

### **2.2.8. Agarose gel electrophoresis of DNA**

DNA fragments, including intact PCR products, digested PCR products and digested plasmids were resolved by agarose gel electrophoresis. Depending on the length of the fragments, different percentages of agarose gels were prepared by dissolving agarose powder in 50mL TAE buffer (Tris/Acetate/EDTA: 40 mM Tris acetate, 1 mM EDTA, pH 8.0). The powder was heated in a microwave oven to ensure it is completely dissolved. The gel was

then poured into a casting tray containing a comb to form the sample wells. The gel was allowed to solidify at RT. The gel was inserted horizontally into an electrophoresis tank and covered with TAE buffer. The comb was removed and DNA samples mixed with 10× loading buffer (50% v:v glycerol, 2% v:v Ficoll (hydrophilic polysaccharide), 50mM EDTA and 5% w:v bromophenol blue prepared in sterile water) were applied into the sample wells. A 1.0 kb DNA ladder (0.5µg/lane) was used to estimate the size of the DNA fragments. The gel was run at 100 volts for 60-80 min, removed from the tank and incubated with ethidium bromide for 30 min at RT. Gels were placed on the UV trans-illuminator and photographed using a digital camera.

### **2.2.9. DNA purification from solution and agarose gel**

High Pure PCR Product Purification Kits were used to purify DNA fragments from agarose gels and solutions to remove dNTPs, primers, enzymes, salts, agarose, and other impurities.

To extract DNA from an agarose gel, the band of interest was excised using a clean scalpel under the UV trans-illuminator and weighed in a 1.5mL microfuge tube of known weight. The gel band was incubated in a volume of Binding Buffer (µL) equivalent to three times the gel weight (mg) at 56°C with occasional mixing for 10 min or until the gel fragment has dissolved. Isopropanol was then added at a volume (µL) 1.5 times to the gel weight (mg). The sample mixed and applied to a High Pure Filter Tube which has been assembled on the Collection Tube. This was centrifuged for 1 min at 15,000g, the flow-through discarded and 0.5mL of Wash Buffer added to the column, which was then centrifuged (1min, 15,000g). The column was washed by the addition of 0.2mL of Wash Buffer and further centrifuged (1min, 15,000g). The flow-through was discarded and the Filter Tube column centrifuged (1min, 15,000g) again to remove residual ethanol. DNA was then eluted with 100 µL of TE buffer (10mM Tris, pH 8.0, 1mM EDTA) and collected by centrifugation (1min, 15, 000g).

To extract DNA fragments from a restriction digest or PCR mixture, 500 $\mu$ L of Binding Buffer was added and the mixture was applied to the Filter Tube. The fragments were washed and processed as above.

#### **2.2.10. DNA ligation**

Digested DNA fragments containing sticky ends were ligated into plasmid vector using T4 DNA ligase. A ratio of 1:7 vector to DNA insert was incubated (overnight at 4°C) with 1 unit of ligase and 1 $\mu$ L 10 x ligase buffer in a final volume of 10 $\mu$ L. A 5 $\mu$ L aliquot of the reaction was then transformed directly into 50 $\mu$ L of  $\alpha$ -select chemically competent cells as described in **Section 2.2.1.3**.

#### **2.2.11. DNA sequencing**

DNA sequencing was performed by the ‘Protein and Nucleic Acid Chemistry Laboratory’ (Centre for Core Biotechnology Services, University of Leicester, UK) using an Applied Biosystems 3730 automated capillary DNA sequencer. In all cases the following primers were used: forward primer (T7) 5’-AATACGACTCACTATAGGG-3’ and reverse primer (BGH) 5’-TAGAAGGCACAGTCGAGG-3’. Sequences obtained were compared the the sequence available in the public domain (M<sub>1</sub> mAChR accession number P11229, M<sub>3</sub> mAChR accession number P20309 and M<sub>4</sub> mAChR accession number P08173).

#### **2.2.12. Cloning of M<sub>4</sub> mAChR sequence**

The M<sub>4</sub> mAChR cDNA purchased from University of Missouri-Rolla contains the sequence that codes for 3xHA tag at the N-terminus of the receptor. To avoid the possibility that this N-terminal tag might interfere with expression, the tag sequence was removed and replaced to the C-terminus of the receptor using PCR. Furthermore, the new C-terminal tag contains only 2xHA. The 5’ end primer for the PCR cloning of the receptor contains a BamHI restriction site, a kozak sequence (to increase translation efficiency) and a portion of the M<sub>4</sub>



### **2.2.13. Mammalian cell culture**

#### **2.2.13.1. Cell counting and viability test**

Cells numbers were determined using a haemocytometer observed under a light microscope or automatic cell counter provided by Nexcelome Bioscience (Sarisbury Green). Live cells were determined by staining cells with 0.4% Trypan Blue.

#### **2.2.13.2. Generation of stable cell line and cell culture maintenance**

CHO-K1 cells were seeded at 250 000 cells/well in 6-well plate and allowed to adhere overnight at 37°C. Cells were serum starved for 2 hrs and then transfected with appropriate mAChR cDNA using Fugene HD transfection reagent according to the manufacturer's instructions. Twenty four hours later, the media were replaced with complete media in the presence of 500 µg/ml of G-418. Cells were continuously selected until total cellular death was observed in non-transfected controls. Successful transfectants were plated in 10 cm dishes at high dilutions to allow the formation single colonies. Single colonies were picked, grown and screened for receptor expression using intact cells radioligand binding assay (**Section 2.2.15.1**). Where appropriate, selected clones were further subcloned to ensure homogeneous cell populations were obtained. All stable cell lines were grown in  $\alpha$ -minimum Eagle's medium ( $\alpha$ -MEM) supplemented with 10% foetal bovine serum, 100 U/ml penicillin, 100 µg/ml streptomycin, 2.5 µg/ml fungizone and 250 µg/ml geneticin. CHO-K1 cells were grown in the same buffer but without the addition of G-418. Cells were maintained in a 5% CO<sub>2</sub>, 95% air, humidified incubator at 37°C.

### **2.2.14. Biochemical assays**

#### **2.2.14.1. Membrane preparations**

Cells expressing the receptor of interest were grown until approximately 90% confluence and harvested using 1 mM EDTA in PBS (137 mM NaCl, 2.7 mM KCl, 4.3 mM Na<sub>2</sub>HPO<sub>4</sub>, and

1.5 mM  $\text{KH}_2\text{PO}_4$ ) at pH 7.4. Cells were collected in tubes and centrifuged at 1200g for 5 min to form pellets. The cell pellets were resuspended in 20 ml of buffer containing 20 mM HEPES, 10 mM EDTA and Complete EDTA-free protease inhibitors (pH 7.4). All subsequent steps were performed at 4°C. The cell suspension was homogenized using a Polytron homogenizer with two 10 second bursts separated by cooling on ice. The cell homogenate was centrifuged for 5 min at 1200g, and the supernatant was transferred to new tubes. Where appropriate the remaining pellets were resuspended as before and re-homogenised to increase membrane yield. Pooled homogenates were centrifuged at high speed (45 min, 40,000g) in a Beckman Coulter centrifuge. The pellet was resuspended in 10 ml of storage buffer (20 mM HEPES and 0.1 mM EDTA, pH 7.4) and briefly homogenized to ensure uniform consistency. The protein concentration was determined by the method of Bradford or BCA assay using bovine serum albumin as a standard (Bradford, 1976; Noble and Bailey, 2009). Membranes were aliquoted and stored at -80°C until required.

#### **2.2.14.2. Quantification of proteins using Bradford and BCA assays**

Protein concentrations in lysates and membrane preparations were determined by measuring the absorbance at 595nm in a spectrophotometer or plate reader. The spectrophotometer was blanked with 1:1000 dilutions of lysis buffer or storage buffer (1mL volume) and 1mL of Bradford Reagent. BSA standards (2000µg/mL - 25µg/mL) were prepared and mixed with 1mL Bradford reagent. Protein samples were diluted 1:1000 in lysis buffer or storage reagent (1 mL volume) and 1mL of Bradford Reagent was added to each sample. The absorbance of the BSA standards and samples was measured and the protein concentrations in the samples were determined by interpolating their absorbance with the absorbance of BSA standards. For BCA assay, working reagent solution was prepared by mixing 19.6mL of Reagent A and 0.4mL of Reagent B. 25µL of samples/blank/BSA standards were added to 96-well plate. BCA reagent mixture (200µL) was added to the wells. The plate was incubated at 37°C for 30

min and then read on a PolarStar plate reader. Protein concentrations in the samples were determined as described for the Bradford assay.

## **2.2.15. Radioligand binding assays**

### **2.2.15.1. Intact cells binding**

Cells grown in 6, 12 or 24-well plates were washed three times in 1 ml Krebs/HEPES buffer (10 mM HEPES, 118 mM NaCl, 4.69 mM KCl, 1.18 mM MgSO<sub>4</sub>·7H<sub>2</sub>O, 1.3 mM CaCl<sub>2</sub>, 25.0 mM NaHCO<sub>3</sub>, 11.7 mM glucose, pH 7.4). Cells were incubated with ~5 nM [<sup>3</sup>H]-NMS for 1 hr at 37°C. Nonspecific binding was determined by the inclusion of 10 μM Atropine. Cells were washed three times with 1 ml ice-cold Krebs/HEPES buffer and then lysed with 200 μL of RIPA buffer (10 mM Tris, 2 mM EDTA, 20 mM Glycerol-2-phosphate, 160 mM NaCl, 1% Nonidet P-40, 0.5% deoxycholate, pH 7.4) for 10 min on ice. Bound [<sup>3</sup>H]-NMS in cell extracts was determined by liquid scintillation counting.

### **2.2.15.2. Membrane binding assay**

For protein linearity experiments, 5 μg – 30 μg of membranes were incubated with ~0.5 nM of [<sup>3</sup>H]-NMS in 0.4 ml Krebs / HEPES buffer for 2 hr at room temperature. Atropine at 10 μM was included in the assay to determine nonspecific binding. Reaction was terminated by rapid filtration onto 0.1% polyethylenimine (PEI) soaked GF/B plate using a TomTec harvester, followed by four 2 ml washes with water. Plates were dried extensively in a 60°C incubator and 50 μl of scintillation fluid was added to each well. The plates were sealed and radioactivity was determined using a MicroBeta scintillation counter. For saturation binding, membranes were incubated with ~ 0.03 nM - 5 nM [<sup>3</sup>H]-NMS in 1 ml Krebs/HEPES buffer for 2 hr at room temperature before termination of the assay by rapid filtration onto GF/B plate. Nonspecific binding was defined in the presence of 10 μM atropine. Plates were washed with 4 x 2 ml water and dried extensively in 60°C incubator. Scintillation fluid (50

μl) was added to each well and radioactivity was counted as described above. For inhibition binding assays, membranes were incubated with ~0.5 nM [<sup>3</sup>H]-NMS in 0.4 ml Krebs/HEPES buffer containing 200 μM GTP and increasing concentrations of the cold ligand for 2 h at room temperature. For allosteric interaction studies, competition of [<sup>3</sup>H]-NMS binding by ACh was performed in the presence of increasing concentration of BQCA for CHO-hM<sub>1</sub>R membranes and LY2033298 for CHO-hM<sub>4</sub>R membranes. For both experiments, nonspecific binding was defined by 10 μM atropine. The reaction was terminated by rapid filtration and radioactivity was counted as described previously.

## **2.2.16. Receptor phosphorylation assays**

### **2.2.16.1. In vivo labelling and receptor purification**

Cells seeded at 250 000/well in 6-well plates were grown for 48 hrs and washed three times in 1 ml phosphate free Krebs/HEPES buffer (10 mM HEPES, 118 mM NaCl, 4.69 mM KCl, 1.18 mM MgSO<sub>4</sub>·7H<sub>2</sub>O, 1.3 mM CaCl<sub>2</sub>, 25.0 mM NaHCO<sub>3</sub>, 11.7 mM glucose, pH 7.4). Cells were incubated with 50 μCi/ml of [<sup>32</sup>P]-orthophosphate for 1 h at 37°C. Cells were stimulated with an agonist for an appropriate time at 37°C. The reactions were terminated by rapid aspiration of the buffer followed by addition of 1 ml ice-cold RIPA buffer for 10 min on ice. Cell lysates were cleared by centrifugation (20 000g for 5 min) and receptors were immunoprecipitated from pre-cleared lysates using 1 μg/sample of the appropriate antibody for 2 hr or overnight at 4°C. Immunocomplexes were isolated on protein A-Sepharose beads and the beads were washed three times with ice-cold TEG buffer (10 mM Tris, 2 mM EDTA, 20 mM Glycerol-2-phosphate, pH 7.4). Immunocomplexes were resuspended in 2x SDS-PAGE sample buffer (125 mM Tris, 200 mM dithiothreitol, 4% SDS, 20% glycerol and 0.05% bromophenol blue, pH 6.8) and placed in a 60°C water bath for 3-5 min. Receptor proteins were resolved on 8% SDS-PAGE gels and electroblotted onto nitrocellulose membranes using the wet transfer method and Tris-Glycine transfer buffer (25 mM Tris, 190

mM Glycine, 20% methanol). Receptor phosphorylation was detected by autoradiography. The membranes were also analysed by western blot to check for consistency in sample loading.

#### **2.2.16.2. Phosphopeptide Mapping**

Metabolic labelling of cells with [<sup>32</sup>P]-orthophosphate and receptor purification was carried out as above except cells were labelled with 100 µCi/well of [<sup>32</sup>P]-orthophosphate and receptor immunocomplexes from one entire 6-well plate were pooled and resolved on an 8% SDS-PAGE gel. Resolved receptor proteins were transferred to nitrocellulose membrane and subjected to autoradiography to detect receptor phosphorylation. The autoradiogram was superimposed on the nitrocellulose membrane and the band of interest was excised into small pieces. The membrane pieces were incubated with 200 µl of blocking solution (0.5% PVP containing 0.6% acetic acid) for 30 min at 37°C and then washed three times with distilled water and one time with 50 mM ammonium bicarbonate. Proteins on the membrane pieces were digested with 2 µg/sample trypsin diluted in 50 mM ammonium bicarbonate solution overnight at 37°C (60 µl final volume). The supernatant from the tryptic digest was recovered and transferred to a fresh tube. The membrane pieces were washed three times with 50-100 µl distilled water shaking at 1500g for 15 min, the supernatant from each wash was pooled and dried using a SpeedVac centrifuge at room temperature for 2-6 hrs. The pellet was dissolved in 25-50 µl of pH 1.9 buffer (88% formic acid: acetic acid: water, 25:78:897 (v/v/v)) and dried again using the speedVac centrifuge. The pellet was resuspended in 5 – 10 µl of pH 1.9 buffer, vortex mixed intensely and applied to a cellulose thin layer chromatography plate in small volumes (1 µl). Samples were dried with a fan without heating and separated in two dimensions. The first dimension was electrophoresis in pH 1.9 buffer for 30-40 min at 2000 V using the HTLE 7002 electrophoresis system. The second dimension was ascending thin layer chromatography using isobutyric acid chromatography buffer (isobutyric acid:n-

butanol:pyridine:acetic acid:water, 1250:38:96:58:558 (v/v/v/v/v). The plates were dried extensively in a fume hood, wrapped in cling film and exposed to a phosphoimager. Resolved phosphopeptides were visualised using the STORM phosphoimager instrument. Where appropriate parallel radioligand binding was performed to ensure that equal number of cells between experimental replicates was used.

### **2.2.16.3. Mass spectrometry and identification of phosphorylation sites**

Cells were grown in roller bottles until ~90% confluence and harvested using 1 mM EDTA in PBS (pH 7.4). Membranes were prepared as described previously and receptors in the membranes were solubilised in 1% NP-40 in PBS supplemented with protease and phosphatase inhibitors for 4 hrs at 4°C. The receptors were separated from other cellular components by centrifugation (20 000g, 20 min). The supernatants were transferred to fresh 15 ml tubes and diluted 1:1 with PBS before 200 µl of anti HA antibody coupled to agarose beads was added to each tube. The samples were incubated at 4°C for 4 hr or overnight to allow immunocomplexes to form. The immunocomplexes were washed 4 x 10 ml with PBS and eluted with 1 volume of 2x SDS-PAGE sample buffer. Purified receptors were resolved on 8% SDS-PAGE gel and the gel was stained with colloidal coomassie blue to reveal receptor band(s). The bands were excised and cut into 1-2 mm squares. Gel squares were washed 3 x 15 min with 100 mM ammonium bicarbonate and then resuspended in 10 mM DTT (dissolved in 50 mM ammonium bicarbonate) and incubated for 30 min at 65°C. The DTT solution was discarded and the gel pieces were incubated with 100 mM iodoacetamide (dissolved in 50 mM ammonium bicarbonate) for 30 min at room temperature in the dark. The gel pieces was washed 3 x 15 min with 50% acetonitrile in 50 mM ammonium bicarbonate and 1 x 15 min 100% acetonitrile. The acetonitrile was removed and the gel pieces dried in a speedvac centrifuge. The gel pieces were incubated with 1 µg sequencing grade trypsin (in 50 mM ammonium bicarbonate) overnight at 37°C. The supernatant was

transferred to fresh tubes and the gel pieces were washed twice with 0.1% trifluoroacetic acid (TFA) dissolved in 50% acetonitrile. The supernatants were pooled and submitted to Protein and Nucleic Acid Chemistry Laboratory (PNAACL) for analysis in QTRAP LC MS/MS.

#### **2.2.16.4. Generation of phosphorylation specific antibodies**

Antibodies against putative phosphorylation sites on the receptor were raised using a three months programme provided by Eurogentec. The antibodies were then purified with same phosphopeptides used to immunise the animals before being characterised and applied in western blot experiments.

#### **2.2.16.5. Antibody characterisation using phosphatase treatment**

To characterise the phosphorylation specific antibodies, phosphatase treatment experiments were performed. Cells seeded at 250 000/well in 6-well plates were grown for 48hr at 37°C. Cells were washed three times in 1mL Krebs/HEPES buffer (10 mM HEPES, 118 mM NaCl, 4.69 mM KCl, 1.18 mM MgSO<sub>4</sub>.7H<sub>2</sub>O, 1.3 mM CaCl<sub>2</sub>, 25.0 mM NaHCO<sub>3</sub>, 11.7 mM glucose, pH 7.4) and incubated in the same buffer for 1hr at 37°C. Cells were stimulated with an agonist and receptors were purified by immunoprecipitation as described above (**Section 2.2.16.1**). The immunoprecipitated receptors were washed 3 x 150 µl with calf intestinal alkaline phosphatase (CIAP) buffer supplemented with protease inhibitors and 0.2% octyl glucoside. The beads were resuspended in 50 µL CIAP buffer in the presence of 40 U CIAP and incubated overnight at 37°C. Positive controls which consist of immunoprecipitated receptors incubated in buffer were included. The CIAP buffer was aspirated and the beads resuspended in SDS-PAGE sample buffer. Samples were run on 8% SDS-PAGE and analysed by western blot (**Section 2.2.17.3**)

## **2.2.17. Identification of protein kinases involved in receptor phosphorylation**

### **2.2.17.1. Pharmacological inhibition of protein kinases**

To determine the role of PKC in receptor phosphorylation, cells expressing the receptor of interest were treated with 10  $\mu$ M Bisindolylmaleimide I for 10 min before stimulated with an agonist or PKC activator PMA for 5 min at 37°C. Cells were lysed using CHAPS lysis buffer (20 mM Tris, 150 mM NaCl, 3 mM EDTA, 1% CHAPS, 0.5% sodium deoxycholate, pH7.4) supplemented with protease and phosphatase inhibitors and lysates were cleared by centrifugation (20 000g for 5 min). The supernatant was transferred to new tubes and the protein concentrations in the supernatant were determined by Bradford assay (**Section 2.2.14.2**). Samples were mixed with 2x SDS-PAGE sample buffer and resolved on 8% gels. Resolved proteins were analysed by western blot (**Section 2.2.17.3**).

### **2.2.17.2. Depletion of protein kinase levels by siRNA knock-down.**

Due to the lack of specific inhibitors for GRK subtypes, siRNA approach was employed to deplete the cellular GRK levels. Cells were seeded at in 12 well plates and allowed to adhere overnight at 37°C. Transfection mixture was prepared in 100  $\mu$ L final volume as follows: 3 $\mu$ L of SiPortamine transfection reagent was added to 47  $\mu$ L of OPTI-MEM I media and the mixture was incubated at RT for 10 min. 50 nM GRK specific siRNA or control siRNA were prepared in OPTI-MEM I media (50  $\mu$ L volume). The two mixtures were combined and added to cells in drop-wise. Cells were incubated for 48 hr and then harvested for western blot analysis (**Section 2.2.17.3**).

### **2.2.17.3. Immunoblotting**

Receptors that have been resolved on SDS-PAGE gels were transferred to nitrocellulose membranes using the semi-dry or wet transfer methods. Membranes were incubated in blocking solution (20 mM Tris, 150 mM NaCl, 0.1% Tween-20 (TBST), 5% non-fat dried

milk, pH 7.5) for 1 h at room temperature or overnight at 4°C. Membranes were probed with the appropriate primary antibody (diluted in blocking solution) for 1hr at room temperature. Membranes were washed 3 x 15 min in TBST and then incubated with a secondary antibody (diluted in blocking solution) for 1h at room temperature. Following 3 x 15 min washes in TBST the membranes were dried by blotting the edge onto a piece of tissue paper. The membranes were placed on glass plates and HRP substrate was added for 5 min. Immunoreactivity was visualized by ECL.

## **2.2.18. Cell signalling assay**

### **2.2.18.1. Extracellular-signal regulated protein kinase 1/2 phosphorylation assay.**

Cells were seeded into transparent 96-well plates at 35 000 cells/well and grown overnight at 37°C. Cells were washed with PBS and incubated in serum-free  $\alpha$ -MEM at 37°C for at least 4 h to allow FBS-stimulated pERK1/2 levels to subside. For initial assay optimisation, time course experiments were performed in which cells were stimulated with agonist for 5 min to 2 hr at 37°C. Where appropriate, a broad spectrum PKC inhibitor was included in the assay to assess the contribution of PKC in receptor mediated ERK1/2 phosphorylation. For functional allosteric interaction studies, cells were incubated with varying concentrations of agonist in the presence and absence of increasing concentrations of an allosteric compound. 10% FBS was used as a positive control, and vehicle controls were also included in the assay. The reaction was terminated by the removal of compounds and addition of 50  $\mu$ L of SureFire lysis buffer. The lysates were agitated for 30 min at room temperature and 4  $\mu$ L of each lysate was transferred into a 384-well opaque Optiplate. SureFire detection mix (7  $\mu$ L/well) consisting of detection reagent; activation reagent; donor beads and acceptor beads (660:110:11:11 v/v) were added to the plate. Plates were incubated in the dark at room temperature for 2 h with gentle agitation before fluorescence signal was measured using a PheraStar plate reader.

### **2.2.18.2. Total [<sup>3</sup>H]-Inositol phosphate accumulation assay.**

Cells were seeded at 100 000 cells/well in 12-well plates and incubated with 0.5 ml of fresh media containing 2.5  $\mu$ Ci/ml [<sup>3</sup>H]-inositol (9.25 MBq) for 24 hr. Cells were washed twice in Krebs/HEPES buffer (pH7.4) and incubated with 10 mM LiCl for 20 min at 37°C.

Appropriate concentrations of compounds were added for 5 min to stimulate [<sup>3</sup>H]-InsPx production. Reactions were terminated by rapid aspiration of the buffer and addition of 1 M ice-cold trichloroacetic acid (500  $\mu$ L). Cell lysates were transferred to centrifuge tubes and incubated with 10 mM EDTA (50  $\mu$ L) and 1,1,2-trichlorofluoroethane:tri-n-octylamine (1:1, v/v, 500  $\mu$ l) for 15 min at RT. Samples were centrifuged at 14000 rpm for 4 min. ~ 400  $\mu$ l aliquot from the top layer was recovered and transferred to fresh tubes. 60 mM of NaHCO<sub>3</sub> was added to each tube. The [H] inositol mono-, bis-, and trisphosphate ([<sup>3</sup>H]InsPx) was recovered by anion exchange chromatography. Dowex-1 (formate form) columns were regenerated with 10 mL of ammonium formate (2M)/formic acid (0.1M) and washed thoroughly with distilled water. Samples were applied to the columns and the columns washed with 10 ml distilled water. Columns were then washed with ammonium formate (60 mM)/sodium tetraborate (10 mM). ([<sup>3</sup>H]-InsPx) fraction was eluted in 10 ml of ammonium formate (0.75 M)/formic acid (0.1M). A 5 ml aliquot from the eluate was mixed with 10 ml of SafeFluor scintillation cocktail and radioactivity was detected by liquid scintillation counting.

### **2.2.19. Data analysis**

Quantification of immunoblots and autoradiograms was performed using ImageQuant and AlphaEase FC softwares. Data from radioligand binding and cellular signalling assays were analysed using PRISM 5 software with built-in or user defined equations. For saturation binding experiments the total and nonspecific binding were fitted to one site saturation

binding equations to estimate the total receptor numbers (Bmax) and equilibrium dissociation constant ( $K_A$ ) of the radioligand (**Equation 1**).

$$Y = \frac{B_{max} \times [A]}{[A] + K_A} + NS \times [A] \quad \text{Equation 1}$$

Where Y is the specific radioligand binding, [A] is the radioligand concentration and NS is the nonspecific binding.

Competition binding experiments were fitted to one site binding equations to initially estimate the logarithmic inhibitory constants ( $\log IC_{50}$ ) of the competing ligands (**Equation 2**). The equilibrium dissociation constant ( $K_I$ ) of each ligand was then determined using the Cheng and Prusoff equation (**Equation 3**)

$$Y = \frac{E_{max} - Basal}{1 + 10^{(\log[A] - \log_{IC_{50}})}} + Basal \quad \text{Equation 2}$$

Where

$$IC_{50} = K_I(1 + [A]/K_A) \quad \text{Equation 3}$$

Where Y is the specific radioligand binding, [A] is the concentration of the radioligand,  $E_{max}$  is the total binding and basal is the nonspecific binding.

Competition binding experiments between an orthosteric radioligand and allosteric modulator were fitted to the simple allosteric ternary complex model as described by (**Equation 4**):

$$Y = \frac{B_{\max} \times [A]}{[A] + K_{\text{APP}}} + \text{NS} \times [A] \quad \text{Where} \quad K_{\text{APP}} = K_A \left( \frac{1 + [B]/K_B}{1 + (\alpha \times [B])/K_B} \right) \quad \text{Equation 4}$$

where  $Y$  is the specific radioligand binding,  $B_{\max}$  is the total number of receptors,  $[A]$  and  $[B]$  are the concentrations of radioligand and allosteric modulator respectively,  $K_A$  and  $K_B$  are the equilibrium dissociation constants of the radioligand and allosteric modulator respectively and  $\alpha$  is the binding cooperativity between the allosteric modulator and the radioligand.

Three way competition binding experiments between an orthosteric radioligand, an unlabelled orthosteric compound and an allosteric modulator were fitted to the extended allosteric ternary complex model as described by Langmead (Langmead, 2011) and Nawaratne *et al* (Nawaratne *et al.*, 2010) and is shown in **Equation 5**.

$$Y = \frac{B_{\max}[A]}{\left( \frac{K_A K_B}{\alpha' [B] + K_B} \right) \left( 1 + \frac{[I]}{K_I} + \frac{[B]}{K_B} + \frac{\alpha [I][B]}{K_I K_B} \right)} \quad \text{Equation 5}$$

where  $Y$  is the specific radioligand binding,  $B_{\max}$  is the total number of receptors,  $[A]$ ,  $[B]$ , and  $[I]$  are the concentrations of radioligand, allosteric modulator, and unlabeled orthosteric ligand, respectively,  $K_A$ ,  $K_B$ , and  $K_I$  are the equilibrium dissociation constants of the radioligand, allosteric modulator, and unlabeled orthosteric ligand, respectively, and  $\alpha'$  and  $\alpha$  are the cooperativity factors between allosteric modulator and the radioligand or unlabeled orthosteric ligand, respectively

Agonist concentration response curves were fitted to four parameter logistics equation (**Equation 6**) and the operational model of agonism (**Equation 7**) (Black *et al.*, 1983):

$$Y = \text{Basal} + \frac{\text{Emax} - \text{Basal}}{1 + 10 (\text{Log}_{\text{EC}_{50}} - \text{Log}[A])^n} \quad \text{Equation 6}$$

$$E = \frac{\text{Emax} \tau [A]}{\tau [A] (A + K_A)} \quad \text{Equation 7}$$

Where Y is the specific agonist response, Emax is the maximal possible response of the system (not the agonist), Basal is the basal level of response in the absence of agonist, [A] is the concentration of the agonist and EC<sub>50</sub> represents the agonist concentration that elicits half-maximal response. K<sub>A</sub> denotes the functional equilibrium dissociation constant of the agonist (A) and τ is an index of the coupling efficiency (or efficacy) of the agonist. In the operational model of agonism, it is assumed that the affinity (K<sub>A</sub>) of the agonists remains the same in the different assay readouts and the profile of the agonist response is in accordance of the law of mass action (i.e. hyperbolic or sigmoidal when agonist concentrations are expressed in logarithmic scale).

Quantitative analysis of functional selectivity was performed according to the method of Rajagopal *et al* (Rajagopal *et al.*, 2011). First, the ability of an agonist to signal to downstream signalling pathways was compared to a reference agonist to yield effective signalling ( $\sigma_{\text{lig}}$ ; **Equation 8**)

$$\sigma_{\text{lig}} = \left( \frac{\tau_{\text{lig}}}{\tau_{\text{ref}}} \right) = \left( \frac{\varepsilon_{\text{lig}}}{\varepsilon_{\text{ref}}} \right) \quad \text{Equation 8}$$

Then a bias factor,  $\beta_{\text{lig}}$ , for test compounds was determined from the effective signalling factors using **Equation 9**:

$$\beta_{\text{lig}} = \left( \frac{\sigma_{\text{lig}}^{\text{path1}} - \sigma_{\text{lig}}^{\text{path2}}}{\sqrt{2}} \right) \quad \text{Equation 9}$$

Functional allosteric interaction studies such as [<sup>3</sup>H]-InsPx accumulation and ERK1/2 phosphorylation were analyzed using a simplified operational model of allosterism as described previously (**Equation 10**) (Langmead, 2011; Leach *et al.*, 2007).

$$Y = \frac{E_m (\tau_A[A](K_B + \alpha\beta[B]) + \tau_B[B]K_A)^n}{([A]K_B + K_A K_B + K_A[B] + \alpha[A][B])^n + (\tau_A[A](K_B + \alpha\beta[B]) + \tau_B[B]K_A)^n} \quad \text{Equation 10}$$

where  $E_m$  is the maximum possible tissue response, [A] and [B] are the concentrations of orthosteric and allosteric ligands, respectively,  $K_A$  and  $K_B$  are the equilibrium dissociation constant of the orthosteric and allosteric ligands, respectively,  $\tau_A$  and  $\tau_B$  are operational measures of orthosteric and allosteric ligand efficacy, respectively,  $\alpha$  is the binding cooperativity parameter between the orthosteric and allosteric ligand, and  $\beta$  denotes the allosteric effect of the modulator on the efficacy of the orthosteric agonist. The binding cooperativity  $\alpha$  was fixed to that determined separately in radioligand binding assays. In all instances,  $\alpha$ ,  $K_A$  and  $K_B$  values were fixed to the values determined from the radioligand binding assays. The simplified operational model of allosterism assumes that receptor has minimal constitutive activity and that the orthosteric ligand used in the assay is a full agonist.

The Hill-Langmuir binding isotherms were used for receptor phosphorylation experiments that require equal percentage of receptor occupancy to be achieved (**Equation 11**)

$$\% \text{ Receptor occupancy} = [A] / ([A] + K_A) \quad \text{Equation 11}$$

Where [A] is the agonist concentration and  $K_A$  is the affinity of the agonist.

All data are expressed as mean  $\pm$  SEM for the indicated number of experiments with statistical significance determined using a one-way analysis of variance (ANOVA) followed by Bonferroni post hoc.

## **Chapter 3: A study into the signalling and regulation of the M<sub>3</sub> mAChR in search for functional selectivity**

### **3.1. Introduction**

The M<sub>3</sub> mAChR is a member of the muscarinic acetylcholine receptor (mAChR) family and represents a prototypical family A GPCRs (Caulfield *et al.*, 1998). The receptor was first discovered in 1987 and was shown to be encoded by a single intronless gene (Bonner *et al.*, 1987). Based on the primary sequence analysis, the receptor is predicted to form a seven transmembrane helical domain connected together by intracellular and extracellular loops and flanked by an extracellular N-terminus and an intracellular C-terminus (Hulme *et al.*, 1990). The recently solved crystal structure of the receptor provided detailed information on the arrangement of the seven transmembrane domains and the ligand binding pocket (Kruse *et al.*, 2012).

The M<sub>3</sub> mAChR is expressed in many areas of the brain including the hippocampus and cortex and in the peripheral tissues such as the pancreas and salivary glands where they mediate the metabotropic actions of the neurotransmitter, ACh (Wess, 2004). The development of mutant mice lacking the M<sub>3</sub> mAChR gene has enabled the elucidation of the physiological roles of the receptor in vivo. It was shown that the receptor plays an important role in smooth muscle contraction, glandular secretion and learning and memory processes (Duttaroy *et al.*, 2004; Gautam *et al.*, 2006; Kong *et al.*, 2010; Poulin *et al.*, 2010). Studies have also indicated that the receptor is an important drug target for smooth muscle disorders such as chronic obstructive pulmonary disease and urinary incontinence (Eglen *et al.*, 1999; Eglen *et al.*, 2001; Wess, 2004). As such, a number of pharmacological agents have been developed to treat these debilitating conditions (Eglen *et al.*, 1999).

The M<sub>3</sub> mAChR predominantly couples to G<sub>q/11</sub> family of G protein to evoke cellular responses. This coupling leads to the regulation of a variety of cellular targets including phospholipase C-β, phospholipase A<sub>2</sub>, protein kinase (PK) C, Ca<sup>2+</sup> channels, extracellular signal regulated protein kinase 1 and 2 (ERK1/2) and C-jun N-terminal kinase 3 (JNK3) (Christopoulos, 2007; Luo *et al.*, 2008). The M<sub>3</sub> mAChR also couples to the ubiquitous multifunctional adaptor proteins, arrestins to mediate distinct but sometime overlapping cellular targets as those mediated by G<sub>q/11</sub> G proteins (Kong *et al.*, 2010; Poulin *et al.*, 2010).

The regulation of the M<sub>3</sub> mAChR functions has been the subject of intense research in recent years. Using a wide variety of techniques including <sup>32</sup>P-labelling, mass spectrometry, phosphopeptide mapping and antibodies against specific residues, it has been shown that the receptor is regulated by phosphorylation in response to agonist stimulation (Butcher *et al.*, 2011; Tobin, 2002; Tobin, 2008; Tobin *et al.*, 2008). This post translational modification leads to the dampening or enhancement of downstream signalling pathways such as phosphorylation of ERK 1/2 and JNK and activation of phospholipase enzymes (Budd *et al.*, 2000; Budd *et al.*, 2001; Luo *et al.*, 2008; Torrecilla *et al.*, 2007; Willets *et al.*, 2001; Willets *et al.*, 2002). Phosphorylation has also been shown to cause receptor internalisation and down-regulation (Tsuga *et al.*, 1998).

The pharmacology of the M<sub>3</sub> mAChR has also been extensively explored and there are numerous agonists and antagonists available as tools to study the signalling and regulation of the receptor. Methacholine (MCh), carbachol (CCh), oxotremorine-M (Oxo-M) and arecoline (Arec) are among the full agonists that cause maximal receptor activation and pilocarpine (Pilo) and oxotremorine (Oxo) are partial agonists that do not fully activate the receptor even at saturating concentrations. Interestingly, Pilo has been shown to cause ERK phosphorylation by a different mechanism compared to ERK phosphorylation mediated by CCh (Lin *et al.*, 2008). This study indicates that different agonists have the potential to

activate different signalling pathways that converge to the same cellular process (i.e. ERK phosphorylation).

Additionally, increasing number of agonists acting at other GPCRs has been reported to be able to activate a subset of signalling pathways available to the receptors. This phenomenon which has been referred to as functional selectivity or biased agonism has important implications in GPCR pharmacology and may provide an avenue for developing novel therapeutics with greater safety profiles (Rajagopal *et al.*, 2010; Urban *et al.*, 2007; Violin *et al.*, 2007; Whalen *et al.*, 2011; Zidar *et al.*, 2009). Interestingly, some of these biased agonists have been reported to promote different patterns of receptor phosphorylation such that they produce a 'barcode' that encode specific signalling pathways (Cescato *et al.*, 2010; Kao *et al.*, 2011; Nobles *et al.*, 2011; Poll *et al.*, 2010; Tobin, 2008; Tobin *et al.*, 2008; Zidar *et al.*, 2009). In the case of the somatostatin subtype 2A (sst2A) receptor, activation of the receptor by octreotide resulted in the phosphorylation four threonine residues (Thr353, Thr354, Thr356 and Thr359). This phosphorylation event was shown to be mediated by GRK2/3 and resulted in  $\beta$ -arrestin recruitment and receptor internalisation (Poll *et al.*, 2010). However, stimulation of the receptor by pasireotide was shown to cause phosphorylation of only two of these threonine residues (Thr356 and Thr359) and this resulted in only  $\beta$ -arrestin recruitment. Since evidence for functional selectivity at the M<sub>3</sub> mAChR is very limited (Challiss *et al.*, 2009), the aim of this chapter is to investigate the effects of a number of agonists (MCh, Pilo and Arec) on the signalling and phosphorylation of the M<sub>3</sub> mAChR to determine if these agonists display functional selectivity.

Using a number of assay readouts such as total inositol phosphates accumulation, ERK1/2 phosphorylation and M<sub>3</sub> mAChR phosphorylation at the global, peptide and individual amino acid levels, we show that the rank order of agonist intrinsic efficacy was maintained across

the majority of these readouts. However, Pilo appeared to be more efficacious in promoting inositol phosphates accumulation than global M<sub>3</sub> mAChR phosphorylation when compared to MCh suggesting that this compound may be biased. Additionally, a preferential phosphorylation of Ser412 was observed relative to Ser577 whereby Pilo, an otherwise weak partial agonist caused equivalent phosphorylation as MCh, a full agonist. Time course and siRNA knockdown experiments showed that phosphorylation of Ser412 occurred very rapidly and can be mediated by a number of protein kinases including GRK2 and GRK6, whereas phosphorylation of Ser577 appeared to be largely mediated by PKC.

## 3.2. Results

### 3.2.1 Expression levels of the M<sub>3</sub> mAChR

CHO cells expressing human M<sub>3</sub> mAChR were used as a model system to study the effects of full and partial agonists on the signalling and phosphorylation profiles of the receptor. The expression level of the receptor was estimated from the Bmax in <sup>3</sup>H-NMS saturation binding experiments and determined to be  $1.70 \pm 0.16$  pmol/mg proteins (n = 3). The binding of <sup>3</sup>H-NMS to the receptor was saturable with an equilibrium dissociation constant (K<sub>D</sub>) of  $0.11 \pm 0.01$  nM (n=3). No specific binding was observed in the parental CHO cells indicating that the M<sub>3</sub> mAChR is not endogenously expressed in this cell line (**Figure 3.2.1.1**).

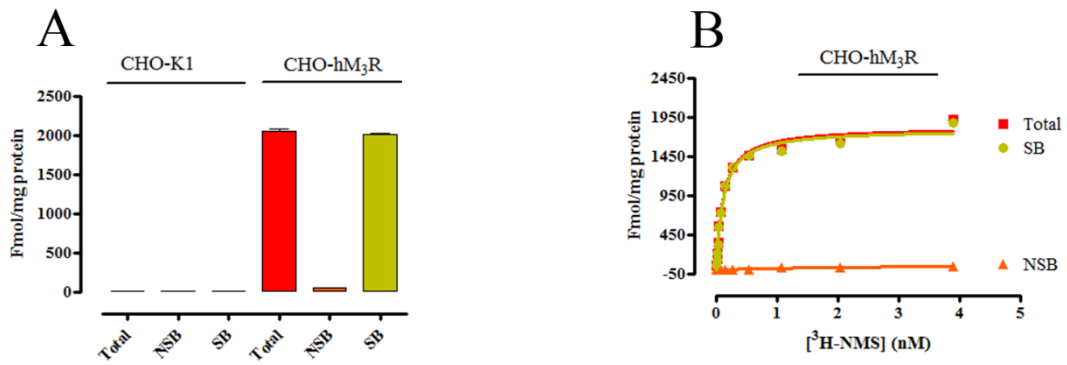


**Figure 3.2.1.1: Detection of M<sub>3</sub> mAChR expression in whole cell binding (A) and membrane saturation binding (B).** Cells grown on 6 well plates were incubated with ~ 1 nM <sup>3</sup>H-NMS and then lysed with RIPA buffer. Non specific binding was determined using 10 μM atropine. Non transfected cells were used as negative controls. Lysates were mixed with scintillation fluid and radioactivity was determined using a Beckmann scintillation counter (A). Membranes (15 μg/well) were incubated with ~5 pM to ~ 4 nM <sup>3</sup>H-NMS in 96-well plate for 2 hrs at RT (final assay volume, 1 ml). Non-specific binding was determined in the presence of 10 μM atropine. Samples were transferred onto PEI (0.1%) pre-soaked GF/B plates using a TomTec harvester. Plates were dried extensively and 50 μl scintillation fluids were added to each well. Radioactivity was determined using a MicroBeta scintillation counter. Data represent the mean ± SEM of three independent experiments performed in duplicate.

### 3.2.2. Agonist affinity determination

Affinity estimates for MCh, Pilo and Arec at CHO-M<sub>3</sub>R membranes were determined in radioligand binding assays in the presence of 200  $\mu$ M GTP. This ensures that the ligands bind to the G protein uncoupled state of the M<sub>3</sub> mAChR. As shown in **Figure 3.2.1.2**, all three ligands caused concentration-dependent decreases in the specific binding of <sup>3</sup>H-NMS. The Hill slope for the three ligands did not differ significantly from unity indicating that the receptor exists in a single affinity state. MCh and Arec bind to the receptor with similar affinity whereas Pilo binds to the receptor with a slightly higher affinity (**Table 3.2.1.1**). These affinity values are comparable to the previously reported data (Sykes *et al.*, 2009).

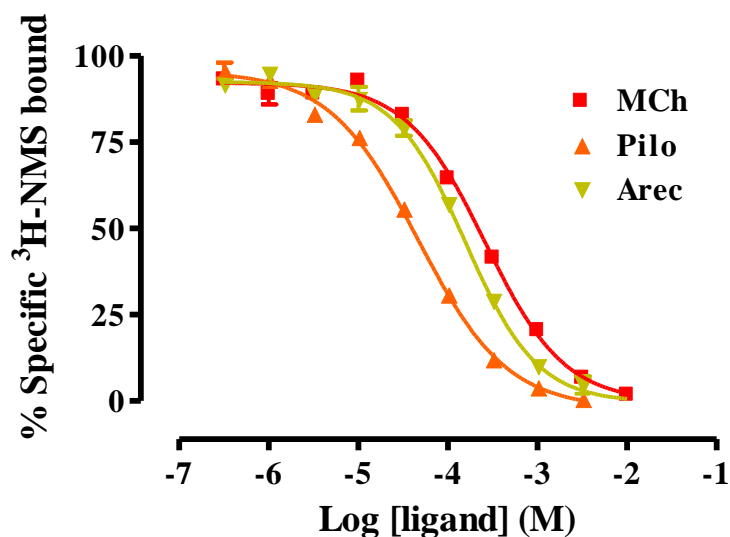


**Figure 3.2.1.2: Agonist affinity estimation using membrane competition binding.**

Membranes (15  $\mu\text{g}/\text{well}$ ) were incubated with  $\sim 0.5 \text{ nM}$   $^3\text{H-NMS}$  in 96-well plate in the presence of increasing concentration of competing ligand and  $200 \mu\text{M}$  GTP for 2 hours at room temperature (final assay volume,  $400 \mu\text{l}$ ). Non-specific binding was determined in the presence of  $10 \mu\text{M}$  atropine. Reaction was terminated by rapid filtration through GF/B plates (pre-soaked in 0.1% PEI); washed three times with 1 mL distilled water and dried before addition of  $50 \mu\text{L}$  scintillation fluid. Plates were sealed and radioactivity was determined using a MicroBeta scintillation counter. Data represent the mean  $\pm$  SEM of three independent experiments performed in duplicate.

**Table 3.2.1.1: Affinity estimates of agonists.** Affinity (pKi) values for agonists were determined from competition binding with <sup>3</sup>H-NMS.

Agonist	pKi	Hill Slope	n
MCh	4.40 ± 0.03	0.98 ± 0.06	3
Pilo	5.14 ± 0.02	0.87 ± 0.04	3
Arec	4.62 ± 0.03	1.08 ± 0.07	3

### 3.2.3. Relative intrinsic efficacy of agonists in [<sup>3</sup>H]-inositol phosphates accumulation assay

Stimulation of the M<sub>3</sub> mAChR by agonists leads to the activation of phospholipase C, which in turn causes the breakdown of PIP<sub>2</sub> into IP<sub>3</sub> and DAG second messenger molecules. To assess the potency of the agonists in mediating this process, experiments measuring total [<sup>3</sup>H]-inositol phosphates accumulation in the presence of lithium were carried out. As shown in **Figure 3.2.3.1** MCh stimulated inositol phosphates accumulation with a pEC<sub>50</sub> of 6.23 ± 0.11 (n = 5). Both Pilo and Arec stimulated inositol phosphate accumulation with lower potency than MCh (**Table 3.2.3.1**). Application of the operational model of agonism to the data resulted in the rank order of agonist intrinsic efficacy: MCh > Arec > Pilo. MCh and Arec behaved as a full agonist with a log τ value >1 (**Table 3.2.3.1**) whereas Pilo was a partial agonist with log τ < 1 and maximum response less than 50% of MCh response.

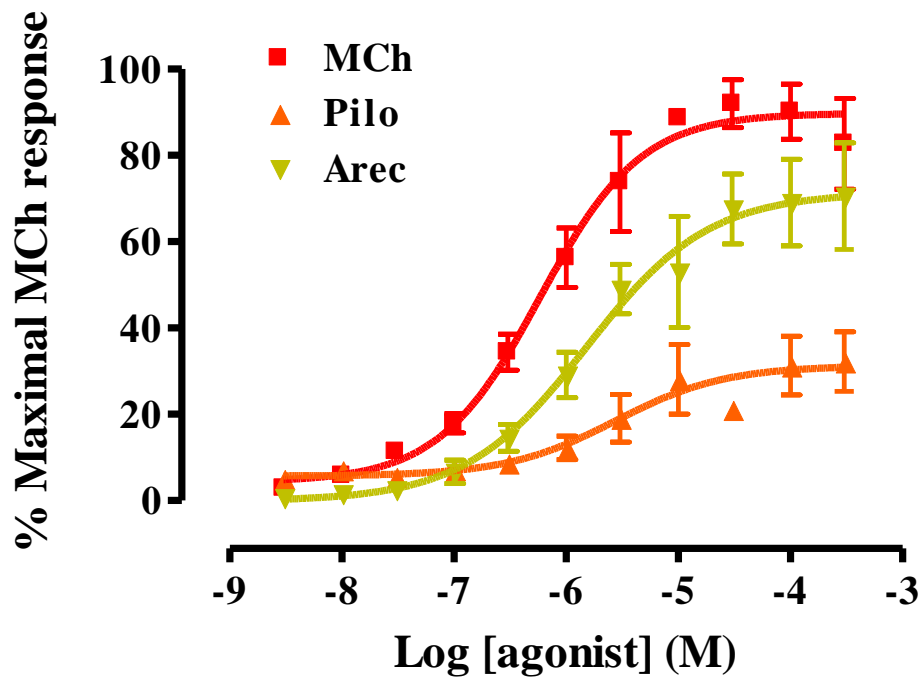


**Figure 3.2.3.1: Agonist efficacy profiles in [<sup>3</sup>H]-inositol phosphates accumulation assay.**

Cells were incubated with 2.5  $\mu\text{Ci/ml}$  [<sup>3</sup>H] myo-inositol overnight at 37°C and then washed twice with 1 ml Krebs buffer. Cells were incubated in Krebs buffer containing 10 mM lithium for 20 min and then stimulated with agonist for 10 min at 37°C. Reaction was terminated by aspiration of buffer followed by addition of 1M trichloroacetic acid for 30 min at 4°C.

Samples were extracted by separation in trichlorofluoroethane and tri-n-octylamine. Total inositol phosphates ([<sup>3</sup>H]-InsPx) were recovered by anion exchange chromatography and radioactivity was detected by liquid scintillation counting. Data represent the mean  $\pm$  S.E.M of at least three independent experiments performed in duplicate.

**Table 3.2.3.1: Relative intrinsic efficacy of agonists in [<sup>3</sup>H]-inositol phosphates**

**accumulation assay.** pEC<sub>50</sub> denotes agonist potency and Rmax represents the maximum response elicited by the agonist. Log  $\tau$  represents intrinsic efficacy as described by Black *et al* and value >1 indicates full agonism (Black, 1996; Black *et al.*, 1983).

Agonist	pEC <sub>50</sub>	Rmax	Log $\tau$	n
MCh	6.23 ± 0.11	100	1.60 ± 0.12	5
Pilo	5.56 ± 0.29	31.29 ± 3.67	0.51 ± 0.08	3
Arec	5.82 ± 0.18	71.43 ± 5.66	1.19 ± 0.02	3

### **3.2.4. Relative agonist intrinsic efficacy in ERK1/2 phosphorylation assay**

To further examine the relative intrinsic efficacy of MCh, Pilo and Arec in receptor mediated signalling pathways, phosphorylation of ERK1/2 experiments were performed. As shown in **Figure 3.2.4.1** and **Table 3.2.4.1** the potency of all the agonists for the stimulation of ERK1/2 phosphorylation was higher than for the total inositol phosphate accumulation. This indicates that there is greater signal amplification in ERK1/2 phosphorylation than in inositol phosphates accumulation as this pathway is more downstream of receptor activation. Interestingly, all of the agonists have greater intrinsic efficacy and all behaved as a full agonist in this assay ( $\log \tau \geq 1$ ).

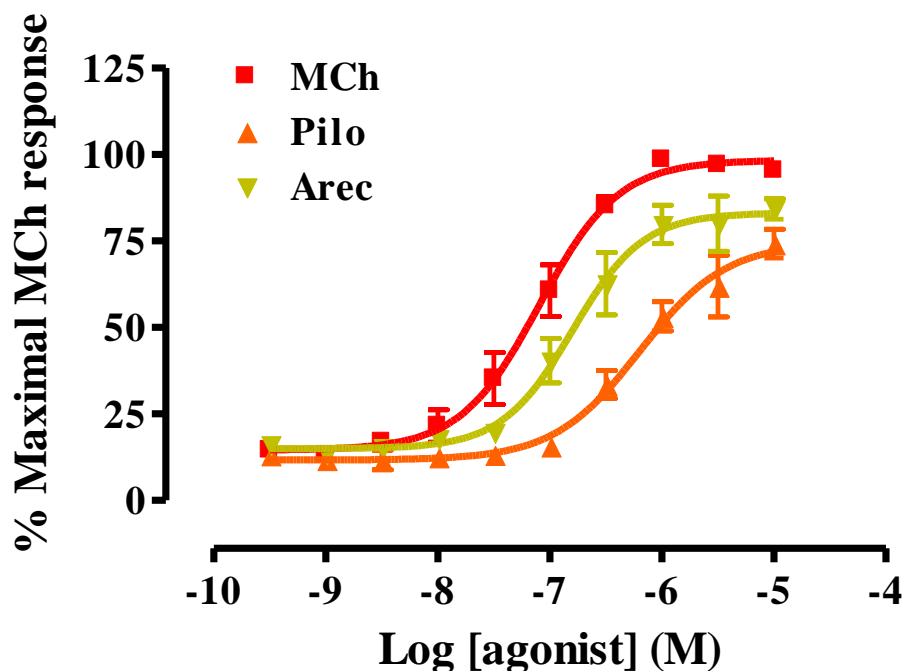


**Figure 3.2.4.1: Agonists efficacy profiles in ERK1/2 phosphorylation.** CHO-hM<sub>3</sub>R cells grown in 96-well plates were serum starved for 4 hours or overnight at 37°C. Cells were stimulated with agonists for 5 min at 37°C. Reaction was terminated by removal of buffer followed by addition of 50 µl lysis buffer for 30 min at room temperature. Each lysate (4 µL) was transferred into 384-well plates and detection mix (7 µl) consisting of detection buffer, activation buffer, donor beads and acceptor beads (60;10;1;1 v/v) were added to each well. Plates were incubated for 2 hrs at RT with gentle agitation and fluorescence signal was measured using an AlphaScreen plate reader. Data represent the mean ± SEM of three independent experiments performed in duplicate.

**Table 3.2.4.1: Relative intrinsic efficacy of agonists in ERK1/2 phosphorylation assay.**

pEC<sub>50</sub> denotes agonist potency and R<sub>max</sub> represents the maximum response elicited by the agonist. Log  $\tau$  represents logarithmic agonist intrinsic efficacy as described by Black *et al* and value >1 indicates full agonism ((Black, 1996; Black *et al.*, 1983).

Agonist	pEC <sub>50</sub>	R <sub>max</sub>	Log $\tau$	n
MCh	7.09 ± 0.06	100	2.82 ± 0.23	3
Pilo	6.20 ± 0.12	74.57 ± 5.37	0.85 ± 0.31	3
Arec	6.80 ± 0.08	83.16 ± 2.75	2.14 ± 0.78	3

### **3.2.5. Constitutive and agonist dependent phosphorylation of M<sub>3</sub> mAChR**

In this study, MCh was used as a reference agonist because the compound behaves as a full agonist. To determine the effect of MCh on the phosphorylation state of the M<sub>3</sub> mAChR, <sup>32</sup>P-labelling and immunoprecipitation experiments were performed. As shown in **Figure 3.2.5.1A**, the M<sub>3</sub> mAChR was phosphorylated in the basal states and ran at ~100 kDa. Stimulation of the CHO-hM<sub>3</sub>R cells with maximally effective concentration (100 μM) of MCh resulted in ~ 4 fold increase in receptor phosphorylation above basal levels (**Figure 3.2.5.1C**). In the WT CHO cells, this apparent ~100 kDa phosphoprotein was not detected indicating that the M<sub>3</sub> mAChR is not endogenously expressed in this cell line (**Figure 3.2.5.1A and B**).

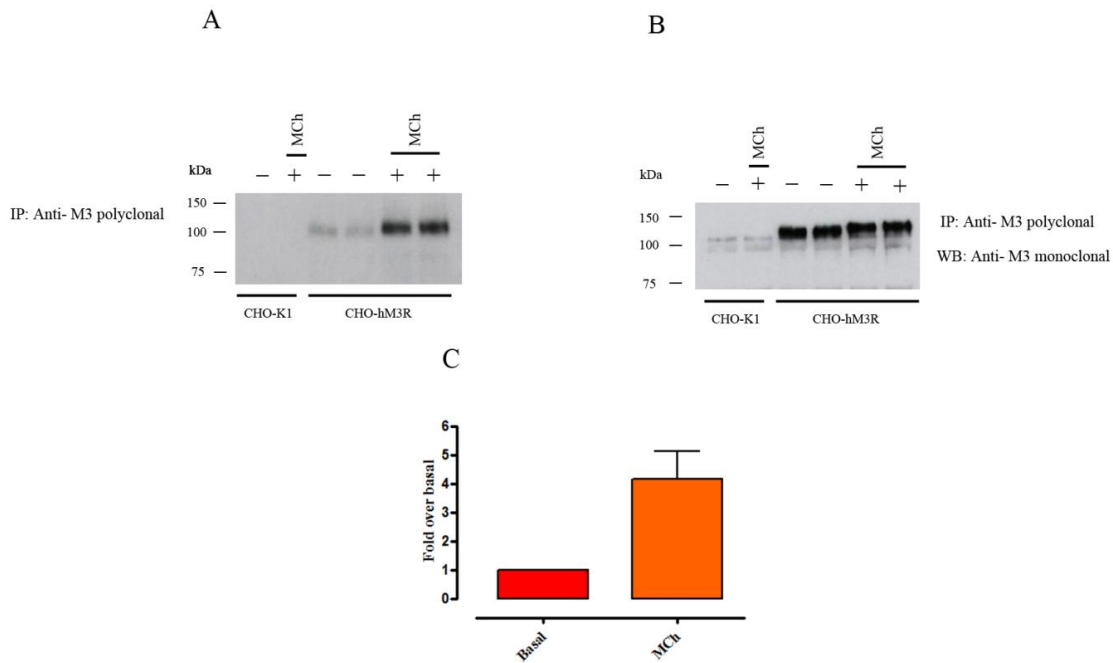


**Figure 3.2.5.1: Basal and agonist mediated phosphorylation of M<sub>3</sub> mAChR.** CHO-hM<sub>3</sub>R plated at 250,000 cells per well on 6-well plate were grown for 48hrs at 37°C. Cells were incubated with 50 µCi/well of <sup>32</sup>P-orthophosphate for 1 hr at 37°C and then stimulated with methacholine (MCh) for 5 min at 37°C. Cells were lysed and receptors were purified by immunoprecipitation with a polyclonal anti M<sub>3</sub> mAChR antibody and resolved on 8% SDS-PAGE gels. Phosphorylation was detected by autoradiography (A) and resolved receptor proteins were immunoblotted with a monoclonal M<sub>3</sub> mAChR specific antibody to detect for loading consistency (B). Autoradiograms were quantified using ImageQuant and AlphaEase FC softwares and data are presented as increase over basal phosphorylation (C). Immunoblot and autoradiogram is a representative of three independent experiments performed in singlicate. Bar graph represents the mean ± S.E.M of the phosphorylation bands.

### **3.2.6. Concentration dependency of M<sub>3</sub> mAChR phosphorylation following stimulation with MCh, Pilo and Arec.**

Although the total inositol phosphate accumulation assay indicated that 100  $\mu$ M of agonist was sufficient to produce maximal effects, concentration-response experiments were carried out to confirm that this is also the case for receptor phosphorylation. As shown in **Figure 3.2.6.1**, maximum receptor phosphorylation was achieved at 3  $\mu$ M concentration for all agonists. This level of phosphorylation was maintained up to 100  $\mu$ M and then decreased slightly at 300  $\mu$ M. The data was analysed using a three-parameter non linear regression and the operational model of agonism to estimate the potency and intrinsic efficacy of the agonists. The data showed that these agonists caused global M<sub>3</sub> mAChR phosphorylation in the same rank order of potency and efficacy as the total inositol phosphates accumulation and ERK phosphorylation (**Figure 3.2.6.1, Table 3.2.6.1**). Pilo showed the weakest activity, consistent with this ligand being a partial agonist.

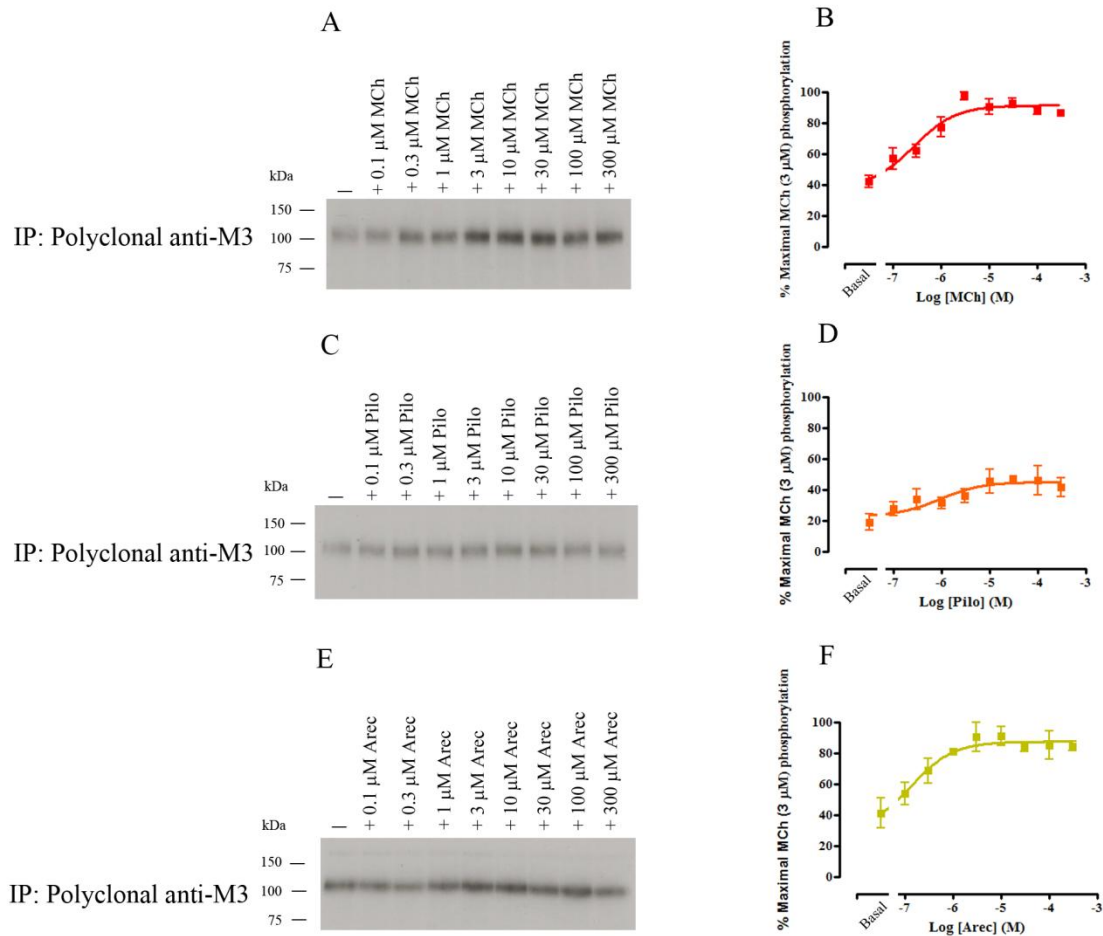


**Figure 3.2.6.1: Concentration response curve of M<sub>3</sub> mAChR phosphorylation following stimulation with MCh, Pilo and Arec.** CHO-hM<sub>3</sub>R plated at 250, 000 cells per well on 6-well plate were grown overnight at 37°C. Cells were incubated with 50 μCi/well of <sup>32</sup>P-orthophosphate for 1 hr at 37°C and then stimulated with the appropriate agonists for 5 min at 37°C. Cells were lysed and receptors were purified by immunoprecipitation with a polyclonal anti M<sub>3</sub> mAChR antibody and resolved on 8% SDS-PAGE gels. Phosphorylation was detected by autoradiography (A, C and E). Autoradiograms were quantified using ImageQuant and AlphaEase FC softwares and quantitative data were analysed using Prism 5 (B, D and F). Autoradiograms are a representative of three independent experiments performed in singlicate. Concentration response data represent the mean ± S.E.M of the phosphorylation bands.

**Table 3.2.6.1: Relative intrinsic efficacy of agonists in promoting global receptor phosphorylation.** pEC<sub>50</sub> denotes agonist potency and Rmax represents the maximum response elicited by the agonist. Log  $\tau$  represents logarithmic agonist intrinsic efficacy as described by Black *et al* and value > 1 indicates full agonism (Black, 1996; Black *et al.*, 1983).

Agonist	pEC <sub>50</sub>	Rmax	Log $\tau$	n
MCh	6.38 ± 0.30	100	2.80 ± 0.31	3
Pilo	5.62 ± 0.60	45.76 ± 3.49	0.67 ± 0.42	3
Arec	6.90 ± 0.61	88.06 ± 3.42	2.56 ± 0.27	3

### 3.2.7. Use of operational model of agonism to define bias agonism.

Although a number of analytical methods are available to quantify bias agonism, the most robust method has been the operational model of agonism initially developed by Black *et al* (Black *et al.*, 1983; Rajagopal *et al.*, 2011). This method yields tau ( $\tau$ ) which indicates the intrinsic efficacy of the agonists for the signalling pathway(s) under investigation. This value is influenced by the levels of receptor expression and cellular background. However it can be nullified by using the same cell type which expresses the same levels of receptor and by comparing the activity of test agonists to a reference ligand. By comparing the  $\tau$  value of the test agonists for the different signalling pathways against a reference agonist, effective signalling and bias factor can be obtained (Rajagopal *et al.*, 2011). Here we used this approach to determine if MCh, Pilo and Arec display bias agonism at the M<sub>3</sub> mAChR. MCh was used as a reference agonist because the compound is structurally similar to the endogenous ligand, ACh. The data suggests that Pilo is biased toward inositol phosphates accumulation relative to global M<sub>3</sub> mAChR phosphorylation (**Figure 3.2.7.1**). There was also a trend that Pilo might be bias towards ERK1/2 phosphorylation compared to global M<sub>3</sub> mAChR phosphorylation, however this was not statistically significant. No apparent bias was observed between ERK1/2 phosphorylation and inositol phosphates accumulation.

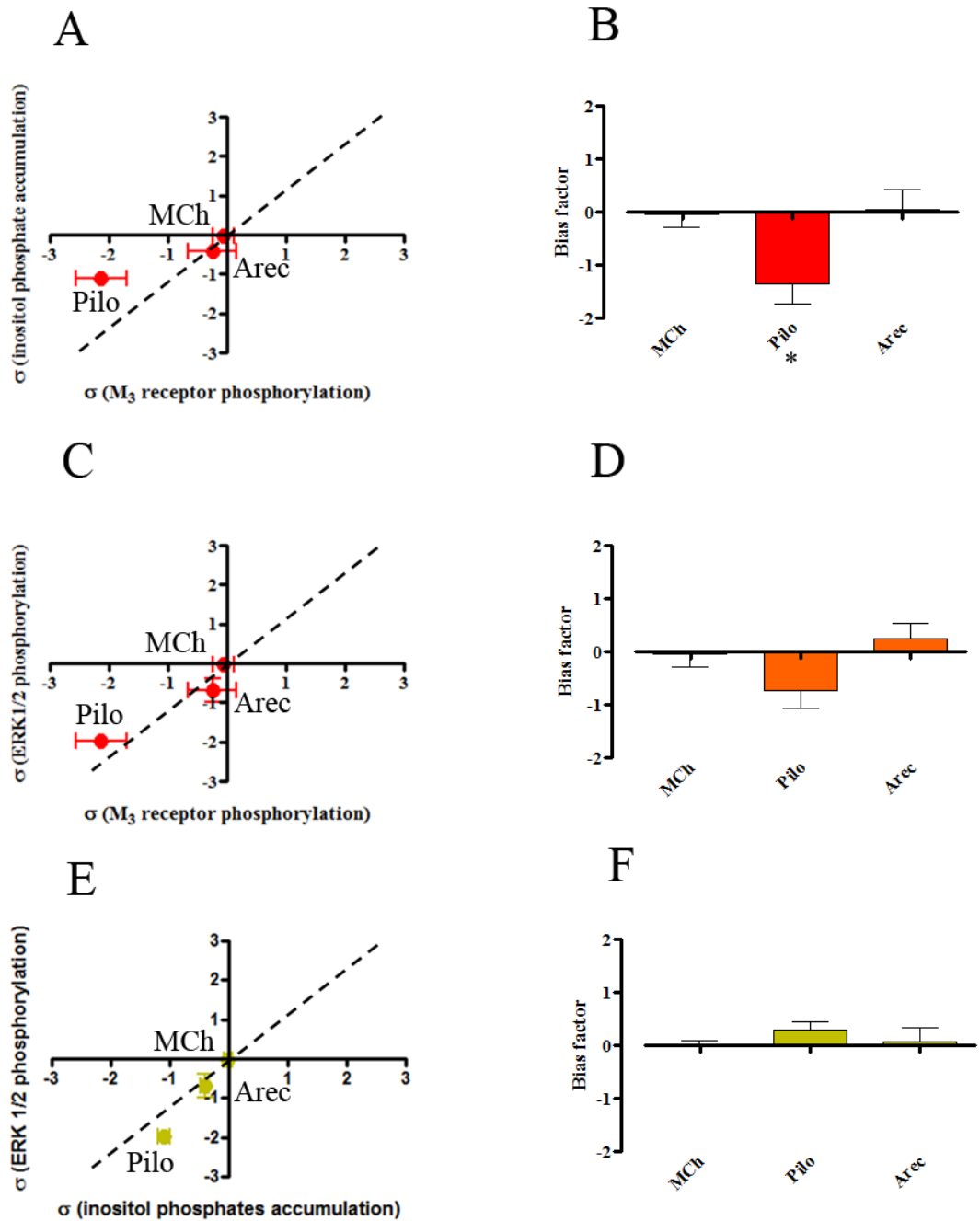


**Figure 3.2.7.1: Identification of bias agonism at the  $M_3$  mAChR using the operational model of agonism.** Effective signalling ( $\sigma$ ) was calculated using  $\tau$  values obtained from an operational model fit of combined datasets. Error bars represent S.E.M values. Bias factor was calculated from the effective signalling as described previously (Rajagopal *et al.*, 2011). \* $P < 0.05$ ; as measured using a one-way ANOVA with Bonferonni's post-hoc test.

### **3.2.8. Phosphorylation profile of the M<sub>3</sub> mAChR following treatment with maximally effective concentration of MCh, Pilo and Arec.**

We wish to fully examine the effects of MCh, Pilo and Arec on the phosphorylation state of the M<sub>3</sub> mAChR. Therefore we performed <sup>32</sup>P-labelling and immunoprecipitation experiments using maximally effective (100 μM) concentration of each agonist in the first instance. As shown in **Figure 3.2.8.1**, all of the agonists caused an increase in the phosphorylation state of the receptor above basal levels. The extent of phosphorylation correlated well with the intrinsic efficacy of the agonists for the activation of downstream signalling pathways such as inositol phosphates accumulation and ERK 1/2 phosphorylation.

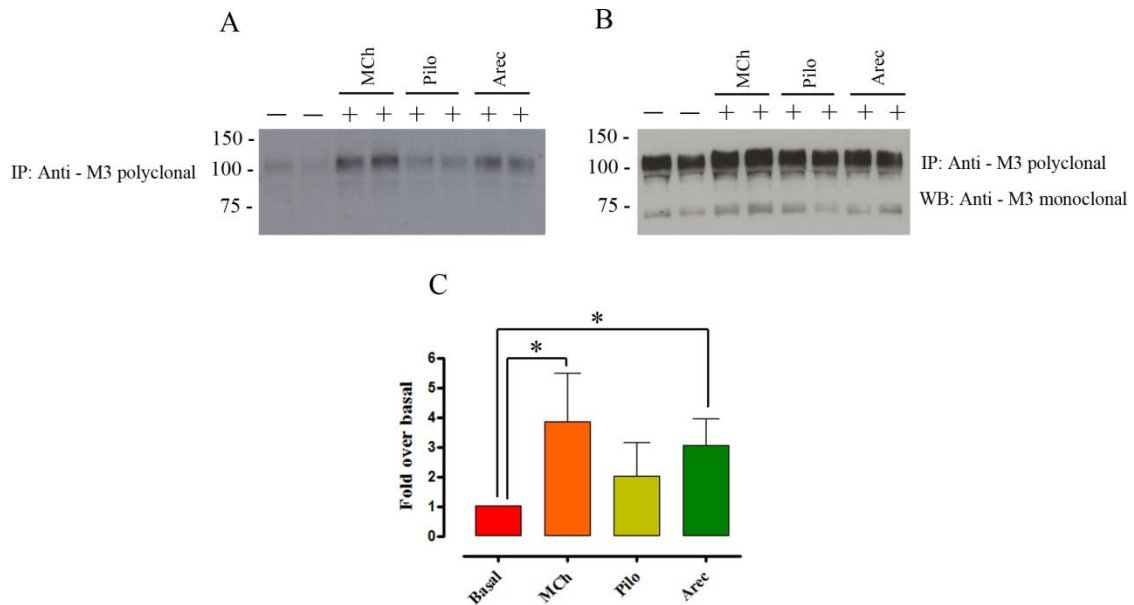


**Figure 3.2.8.1: Phosphorylation profile of M<sub>3</sub> mAChR following stimulation with maximally effective concentration of agonist.** CHO-hM<sub>3</sub>R plated at 250,000 cells per well on 6-well plate were grown overnight at 37°C. Cells were incubated with 50 µCi/well of <sup>32</sup>P-orthophosphate for 1 hr at 37°C and then stimulated with the appropriate agonists for 5 min at 37°C. Cells were lysed with RIPA buffer and receptors were purified by immunoprecipitation and resolved on 8% SDS-PAGE gels. Phosphorylation was detected by autoradiography (A). Resolved receptors were immunoblotted with M<sub>3</sub> mAChR specific antibody (B) to detect for loading consistency. Phosphorylation data were analysed using ImageQuant and AlphaEase FC softwares and presented as increase over basal (C) and relative to MCh. Autoradiograms are a representative of three independent experiments performed in singlicate. Bar graph represents the mean ± S.E.M of the phosphorylation bands. \*P<0.05; as measured using a one-way ANOVA with Bonferonni's post-hoc test.

### **3.2.9. Phosphopeptide mapping to detect the patterns of M<sub>3</sub> mAChR phosphorylation.**

To further examine the phosphorylation state of the M<sub>3</sub> mAChR following stimulation with MCh, Pilo and Arec, phosphopeptide mapping was performed on purified, <sup>32</sup>P-labelled M<sub>3</sub> mAChR. As shown in **Figure 3.2.9.1**, the patterns of phosphorylation in these maps were very complex showing at least fourteen different peptides. Whilst the majority of these peptides were equally phosphorylated in the stimulated and non-stimulated cells at least four peptides were differentially phosphorylated (**Figure 3.2.9.1A**, labelled spots 1-4 and **Figure 3.2.9.1B**). Surprisingly, one of the peptides (“spot 1”) showed a decrease in phosphorylation in cells stimulated with MCh and Arec but not in cells treated with Pilo. “Spots 2 and 3” were phosphorylated only in cells stimulated with MCh and this is consistent with the inositol phosphate and ERK1/2 phosphorylation data (**Figure 3.2.3.1** and **Figure 3.2.4.1**) which indicate that MCh is the most potent agonist. “Spot 4” was phosphorylated equally in cells treated with all agonists and this indicates that Pilo is acting as a full agonist.

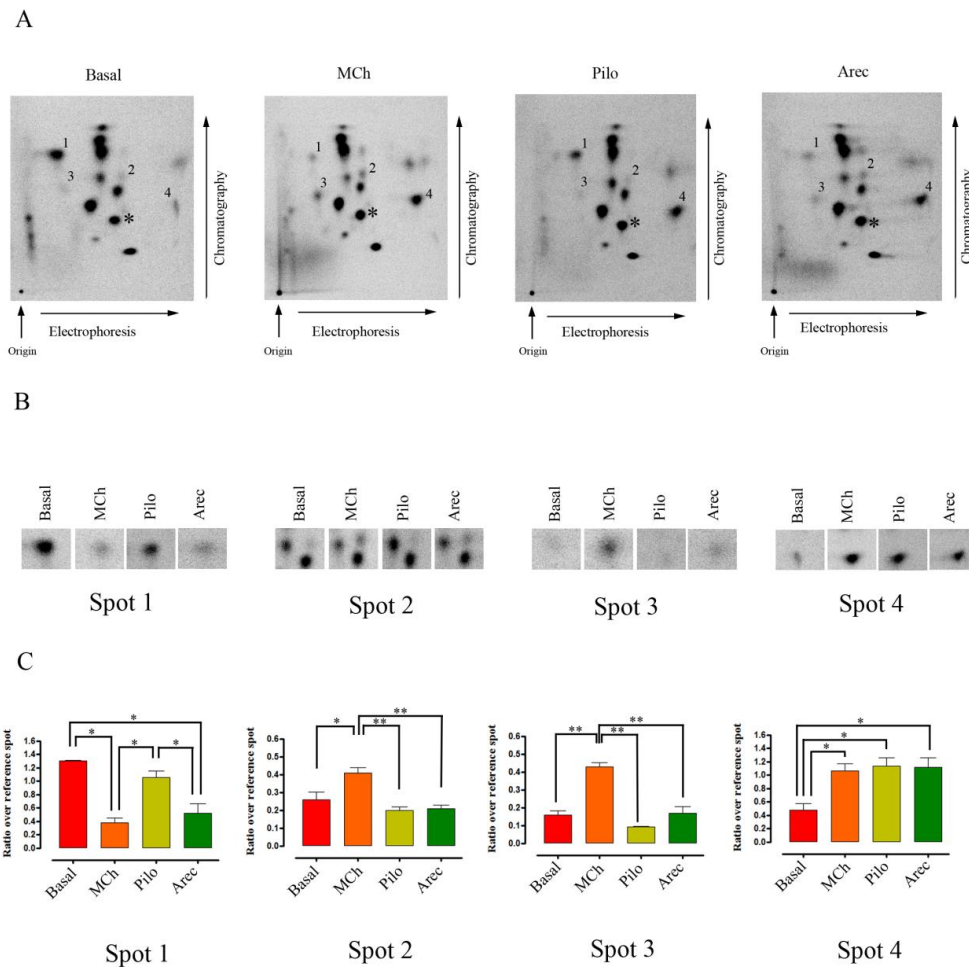


**Figure 3.2.9.1: Phosphopeptide maps of M<sub>3</sub> mAChR following stimulation with full and partial agonists.** Purified <sup>32</sup>P-labelled M<sub>3</sub> mAChR were digested with trypsin to produce fragments of various sizes. The fragments were spotted onto a nitrocellulose thin layer chromatography plate and separated according to their charge via electrophoresis and hydrophobicity via chromatography. After exposing the plate to a phosphoimager film, the resolved phospho-peptides were visualised using a STORM phosphoimager instrument. Phosphopeptides were analysed relative to a reference peptide (labelled asterisk) which was constitutively phosphorylated. Autoradiograms are a representative of three independent experiments performed in singlicate. Bar graph represents the mean ± S.E.M of the phosphorylated peptides. \*P<0.05, \*\*P<0.01; as measured using a one-way ANOVA with Bonferonni's post-hoc test.

### **3.2.10. Immunoblotting with phosphosite specific antibodies to reveal differences in phosphorylation at specific residues.**

To determine which phosphorylation sites are regulated by the three different agonists, western blotting experiments using phosphosite specific antibodies were carried out. Based on mass spectrometry studies conducted by Dr Adrian Butcher, Ser384 and Ser412 in the third intracellular loop and Ser577 at the C terminal tail of the mouse M<sub>3</sub> mAChR were phosphorylated upon stimulation with MCh (Butcher *et al.*, 2011). Polyclonal antibodies recognising these sites (pS384, pS577 and pS412) were raised (see **Figure 3.2.10.1** for locations of phosphorylation).

Since the current study uses the human M<sub>3</sub> mAChR, the phosphospecific antibodies were characterised to ensure that they would recognise the receptor. Sequence alignment of the human and mouse M<sub>3</sub> mAChRs has shown that all of the serine residues found in the mouse M<sub>3</sub> mAChR were also present in the human M<sub>3</sub> mAChR (**Figure 3.2.10.2**). So it would appear intuitive that the phosphosite specific antibodies raised against the mouse M<sub>3</sub> mAChR would cross react with the human M<sub>3</sub> mAChR. To confirm this, purified human M<sub>3</sub> mAChR from MCh-stimulated and non stimulated CHO-hM<sub>3</sub>R cells were probed with the antibodies in western blot experiments. As shown in **Figure 3.2.10.3**, all of the phosphosite specific antibodies cross reacted with the human M<sub>3</sub> mAChR (**Figure 3.2.10.3A-C**, - CIAP).

Furthermore phosphatase treatment abolished the reactivity of the antibodies for the receptor which demonstrates that they are phosphorylation sensitive (**Figure 3.2.10.3A-C**, + CIAP).

We then used these antibodies to probe for changes in M<sub>3</sub> mAChR phosphorylation following treatment with MCh, Pilo and Arec. Interestingly, Ser384 was negatively regulated by all of the agonists and Pilo was the least effective in mediating this dephosphorylation event.

Ser412 was positively regulated by all agonists and these agonists were equally effective at mediating phosphorylation at this site (**Figure 3.2.10.4**). This suggests that Pilo, although

determined to be a weak partial agonist in inositol phosphate assay, was acting as a full agonist in mediating phosphorylation of Ser412. In contrast, Ser577 was positively regulated by MCh and Arec but not by Pilo (**Figure 3.2.10.4**). Thus phosphorylation at this residue follows the same rank order of agonist efficacy as the inositol phosphates accumulation and ERK1/2 phosphorylation pathways.

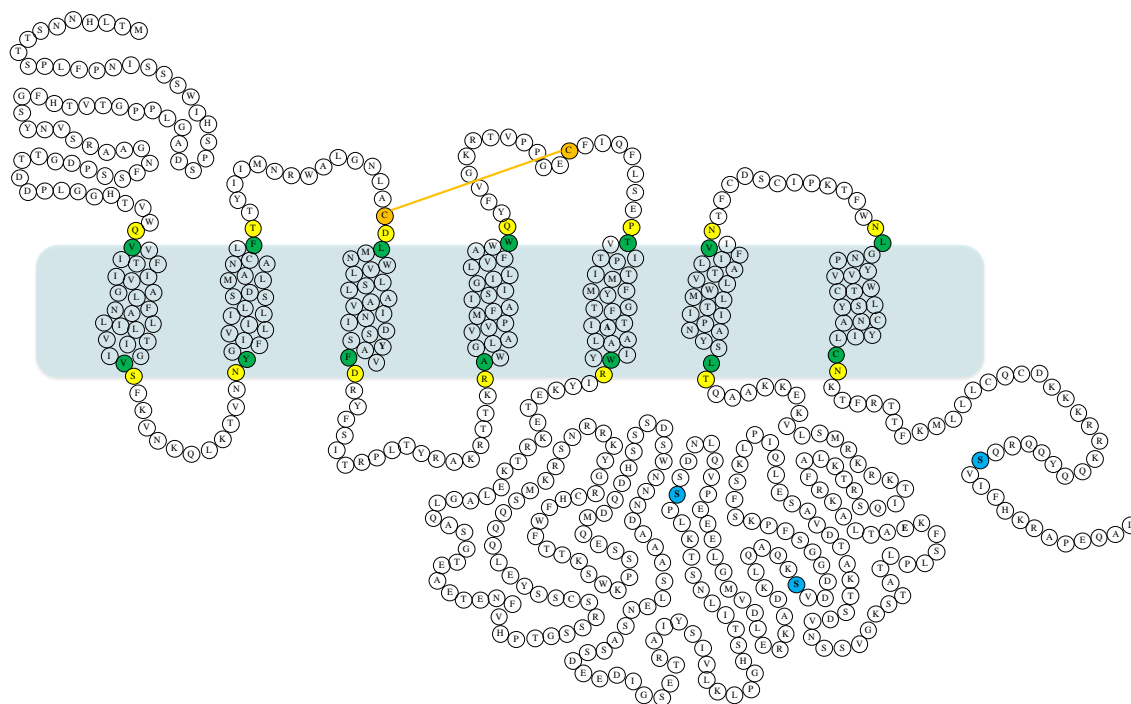


**Figure 3.2.10.1: Topography of human M3 mAChR amino acid sequence.** The junctions between the TM and loop regions as determined by protein knowledgebase sequence alignment ([www.uniprot.org](http://www.uniprot.org), chrn3, accession number: P20309) are represented by residues in green and yellow. The phospho-serines identified by Butcher *et al* (Butcher *et al.*, 2011) are shown in blue.

	A. Ser384	B. Ser412	C. Ser577
	↓	↓	↓
HUMAN	LNSTKLPSSDNLQVP	KLQAQKSVDDGGSFP	KQYQQRQSVIFHKR
MOUSE	LNSTKLPSSDNLQVP	KLQAQKSMDDRDNCQ	KQYQQRQSVIFHKR
MATCHED SEQUENCE	LNSTKLPSSDNLQVP	KLQAQKS DD	KQYQQRQSVIFHKR

**Figure 3.2.10.2: Sequence alignment of the human and mouse M<sub>3</sub> mAChRs showed conserved serine residues (highlighted in blue) that were found to be phosphorylated.**

Protein sequences were retrieved from PubMed (<http://www.ncbi.nlm.nih.gov/pubmed/>) and aligned using the Vector NTI software provided by Invitrogen.

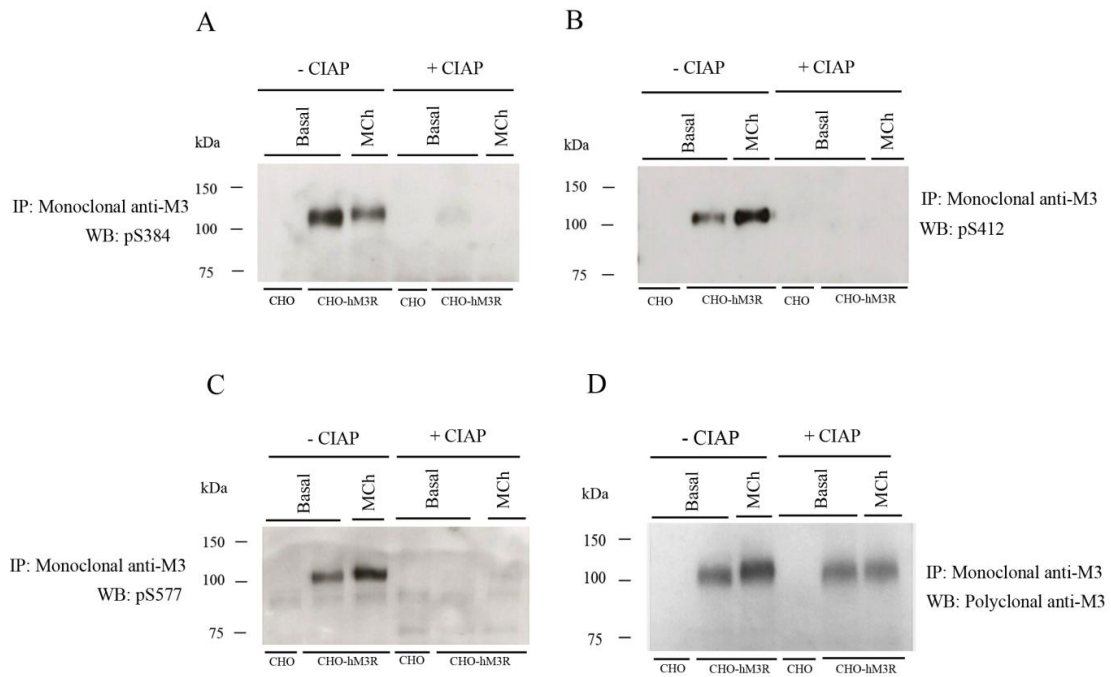


**Figure 3.2.10.3: Characterization of phosphosite-specific antibodies.** Antibodies raised against the mouse M<sub>3</sub> mAChR were tested for reactivity against the phosphorylated (- CIAP) and dephosphorylated human M<sub>3</sub> mAChR (+ CIAP). Cells grown on 6 well plates were incubated in Krebs buffer for 1 hr at 37°C and then stimulated with 100 μM MCh for 5 min at 37°C. Cells were lysed with RIPA buffer and the receptor was purified by immunoprecipitation. Immunoprecipitated receptors were treated with CIAP or buffer before being resolved on 8% SDS-PAGE gels and transferred onto nitrocellulose membrane. Membrane was subjected to western blot analysis with the phosphospecific antibodies or polyclonal anti M<sub>3</sub> mAChR antibody. Data represents single experiments performed in singlicate.

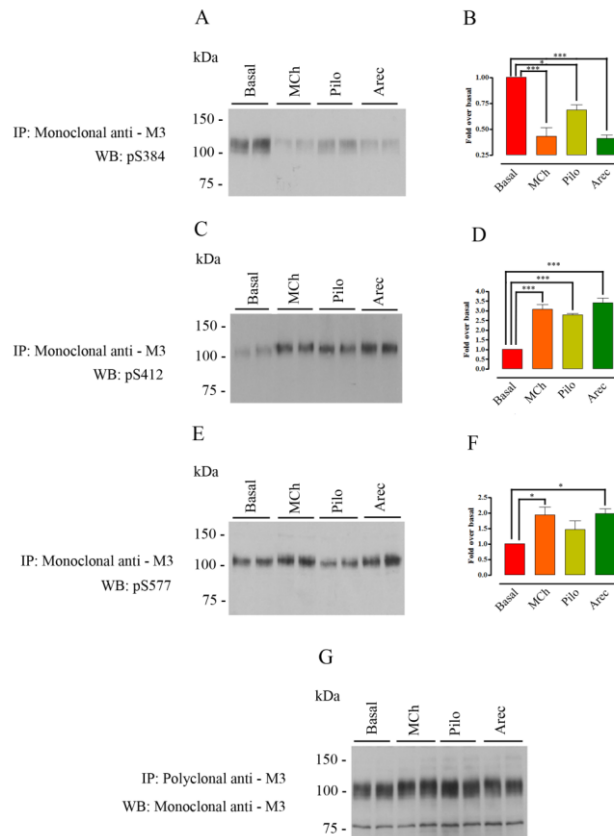


**Figure 3.2.10.4: Immunoblotting with phosphosite specific antibodies revealed**

**differential receptor phosphorylation at specific serine residues.** CHO-hM<sub>3</sub>R cells grown on 6-well plate were incubated in Krebs buffer for 1 hr at 37°C and then stimulated with 100 μM of agonist for 5 min at 37°C. Cells were lysed with RIPA buffer and receptors were purified by immunoprecipitation. Immunoprecipitated receptors were resolved on 8% SDS-PAGE gels and transferred onto nitrocellulose membrane. Membrane was subjected to western blot analysis with the phosphospecific antibodies (A, C and E) or polyclonal anti M<sub>3</sub> mAChR antibody (G). Phosphorylation data were analysed using ImageQuant and AlphaEase FC softwares and presented as increase over basal phosphorylation (B, D and F).

Autoradiograms are representative of three independent experiments performed in singlicate.

Bar graph represents the mean ± S.E.M of the phosphorylation bands. \*P<0.05, \*\*\*P<0.001; as measured using a one-way ANOVA with Bonferonni's post-hoc test.

### **3.2.11. Kinetics of phosphorylation of M<sub>3</sub> mAChR at Ser412 and Ser577.**

To examine if the difference in the pattern of phosphorylation at Ser412 and Ser577 in response to the three agonists was due to the kinetics of phosphorylation at these residues, time course experiments were carried out. As shown in **Figure 3.2.11.1** phosphorylation at both serine residues was very rapid and occurred within 30 seconds of stimulation. This agonist mediated phosphorylation was also maintained after 10 minutes of stimulation. This suggests phosphorylation at Ser412 and Ser577 occurred within similar time frame.

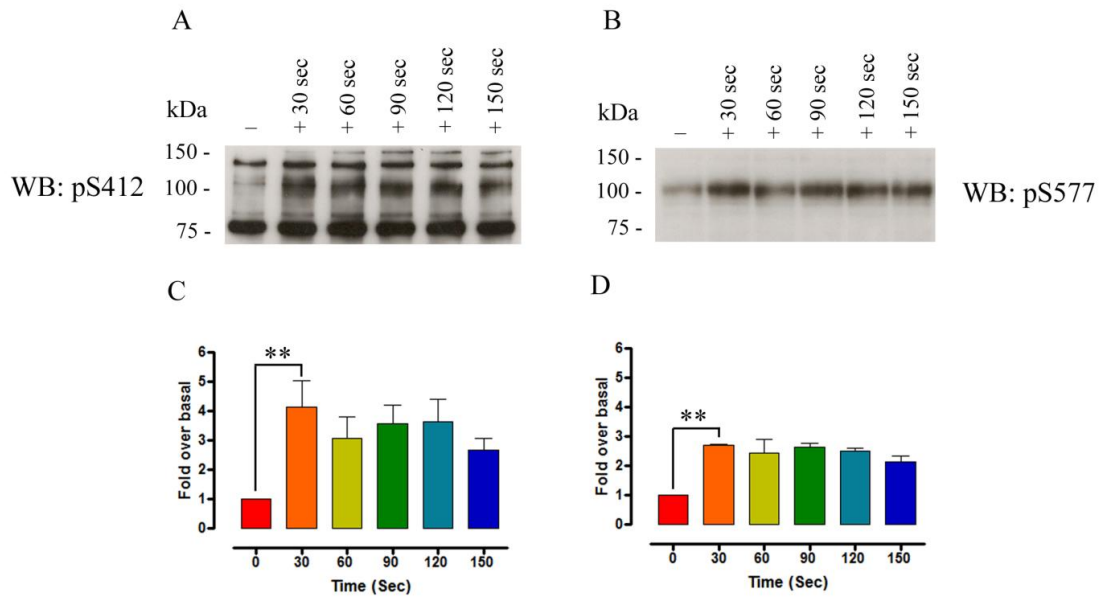


**Figure 3.2.11.1: Kinetics of phosphorylation of M<sub>3</sub> mAChR at Ser412 and Ser577.** Cells grown on 6 well plates were incubated in Krebs buffer for 1 hr at 37°C and then stimulated with 100 μM MCh for the indicated time. Cells were lysed with CHAPS lysis buffer and the lysates were cleared by centrifugation. Lysates were resolved on 8% SDS-PAGE gels and transferred onto nitrocellulose membrane. Receptor phosphorylation was identified by western blot analysis using pS412 and pS577 antibodies. Autoradiograms are a representative of three independent experiments performed in singlicate. Bar graph represents the mean ± S.E.M of the phosphorylation bands. \*\*P<0.01; as measured using a one-way ANOVA with Bonferonni's post-hoc test.

### **3.2.12. Ser412 and Ser577 are phosphorylated by different protein kinases.**

Given that the M<sub>3</sub> mAChR is known to be a substrate for many different protein kinases, identifying which kinase(s) phosphorylate which residues are important in order to understand the site specificity of these kinases. This information may also explain the observed differences between phosphorylation of Ser412 and Ser577.

Since the phosphorylation of Ser577 follows the same rank order of efficacy as the inositol phosphate pathway, suggests that phosphorylation of this residue may be dependent on second messenger generation. Therefore phosphorylation experiments were performed using PKC activator, phorbol 12-myristate 13-acetate (PMA) and a broad spectrum PKC inhibitor, bisindolylmaleimide I (Bis I) to identify if this protein kinase is responsible for mediating phosphorylation of Ser577. As shown in **Figure 3.2.12.1**, activation of PKC with PMA resulted in an increase in the phosphorylation of Ser577 compared to basal. This PKC mediated phosphorylation was completely abolished by treatment of cells with 10 μM Bis I for 10 min. Similarly, MCh mediated phosphorylation of Ser577 was also reduced to nearly basal level following treatment of cells with 10 μM Bis I. This indicates that PKC is largely responsible for mediating phosphorylation of Ser577.

The contribution of PKC in the phosphorylation of Ser412 was also assessed in parallel experiments. However the data were inconclusive and so additional experiments were performed to determine which other protein kinases are responsible for phosphorylating this residue.

Studies have indicated that GRKs are able to phosphorylate the M<sub>3</sub> mAChR in an agonist dependent manner (Torrecilla *et al.*, 2007; Willets *et al.*, 2001; Willets *et al.*, 2002). Since specific inhibitors for these kinases are currently unavailable, experiments were performed using siRNA approach. These double stranded RNA molecules will bind to the

complementary nucleotide sequence on the gene encoding the GRK and interfere with its expression. Initially, GRK2 and GRK6 were investigated as these kinases are the predominant subtypes responsible for phosphorylating GPCRs. As shown in **Figure 3.2.12.2** application of siRNA to both protein kinases reduced the agonist dependent phosphorylation of Ser412 compared to mock transfected controls. Immunoblotting experiments with an antibody specific for GRK2 or GRK6 also showed a reduction in the expression levels of these protein kinases. These data suggests that both GRK2 and GRK6 are able to phosphorylate Ser412 in an agonist dependent manner.

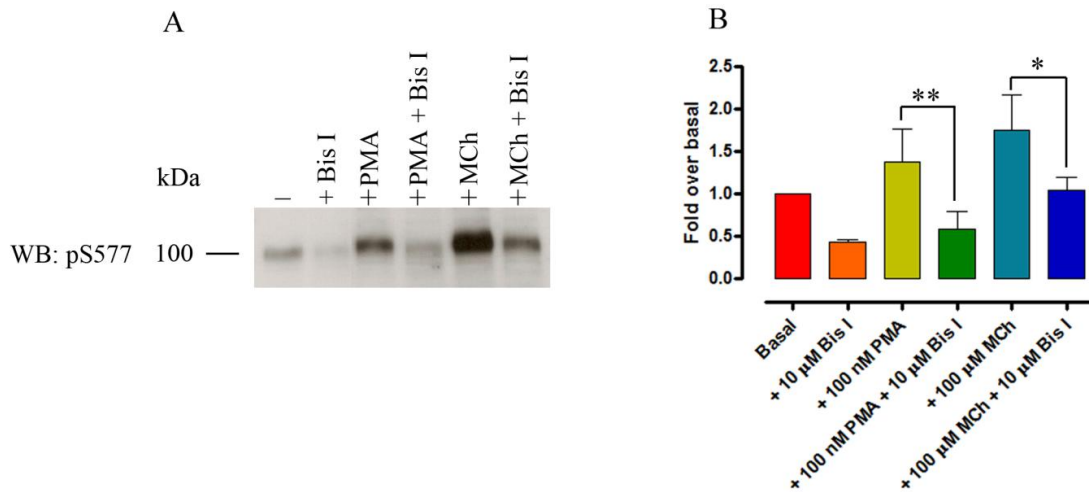


**Figure 3.2.12.1: Phosphorylation of M<sub>3</sub> mAChR at Ser577 is mediated by protein kinase C (PKC).** Cells grown on 6 well plates were incubated in Krebs buffer for 1 hr at 37°C and then stimulated with 100 μM MCh for 1 min at 37°C. Cells were lysed with CHAPS lysis buffer and the lysates were cleared by centrifugation. Lysates were resolved on 8% SDS-PAGE gels and transferred onto nitrocellulose membrane. Receptor phosphorylation was identified by western blot analysis using pS577 antibody (A). Immunoblots were quantified using ImageQuant and AlphaEase FC softwares and data are presented relative to basal phosphorylation (B). Autoradiogram is a representative of three independent experiments performed in singlicate. Bar graph represents the mean ± S.E.M of the phosphorylation bands. \*P<0.05, \*\*P<0.01; as measured using a one-way ANOVA with Bonferonni's post-hoc test.

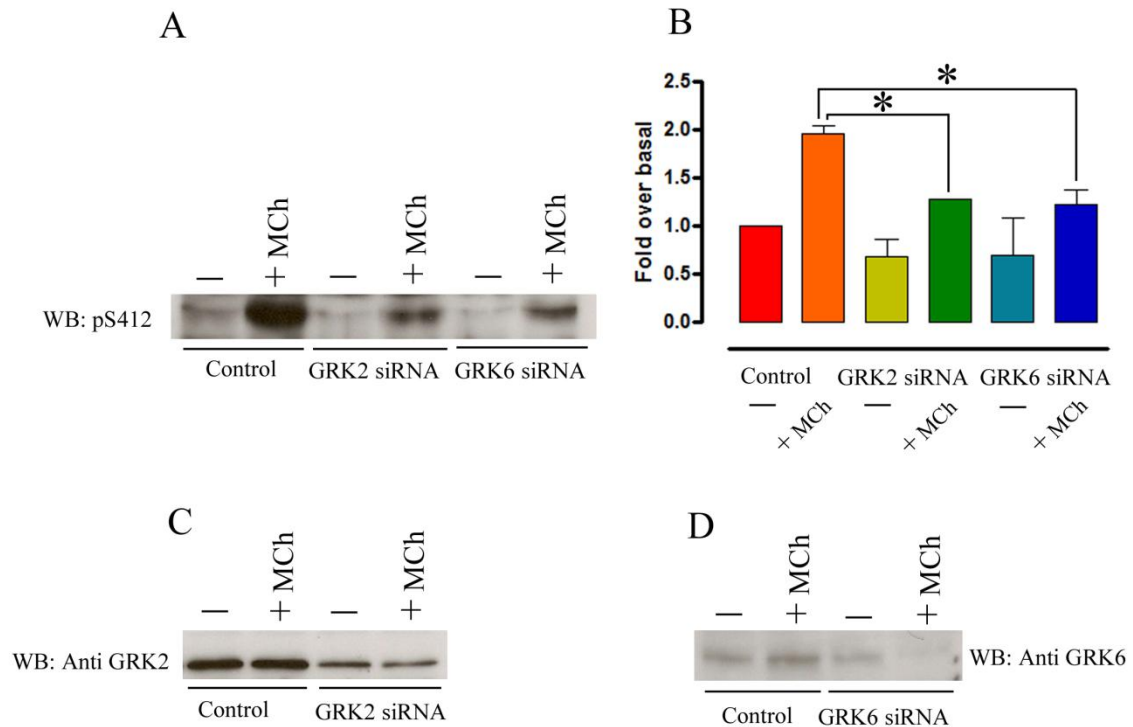


**Figure 3.2.12.2: Phosphorylation of M<sub>3</sub> mAChR at serine 412 is mediated by GRK2 and GRK6.** Cells grown on 6 well plates were incubated in Krebs buffer for 1 hr at 37°C and then stimulated with 100 μM MCh for 1 min at 37°C. Cells were lysed with CHAPS lysis buffer and the lysates were cleared by centrifugation. Lysates were resolved on 8% SDS-PAGE gels and transferred onto nitrocellulose membrane. Receptor phosphorylation was identified by western blot analysis using pS412 antibody. Immunoblots were quantified using ImageQuant and AlphaEase FC softwares and data are presented relative to basal phosphorylation (B). Reduction in GRK proteins was determined by western blotting with GRK subtype specific antibody. Autoradiogram is a representative of three independent experiments performed in singlicate. Bar graph represents the mean ± S.E.M of the phosphorylation bands. \*P<0.05; as measured using a one-way ANOVA with Bonferonni's post-hoc test.

### 3.3. Discussion

The M<sub>3</sub> mAChR represents a prototypical family A GPCR and an attractive therapeutic target for disorders associated with smooth muscle dysfunctions such urinary incontinence and overactive bladder. The receptor couples predominantly to Gq/11 family of G protein to activate PLA<sub>2</sub> and PLC-β. Activation of PLA<sub>2</sub> leads to the breakdown of phospholipids to release arachidonic acid and lysophospholipid whereas activation of PLC-β results in inositol phosphates and DAG accumulation from membrane bound PIP<sub>2</sub> (Nahorski *et al.*, 1997). Studies over the past twenty years have established that the M<sub>3</sub> mAChR is highly regulated. For instance, in response to a continuous or repeated stimulation by an agonist the receptor becomes rapidly phosphorylated (Tobin *et al.*, 1993). This process can lead to the dampening of the receptor's coupling to G protein, a phenomenon also known as desensitisation (Tobin *et al.*, 1992; Tsuga *et al.*, 1998).

The pharmacology of the M<sub>3</sub> mAChR has also been extensively explored and there are various agonists and antagonists known to interact with the receptor (Sykes *et al.*, 2009). MCh, Arec and Oxo-M are among full agonists that are able to elicit receptor response similar to the endogenous ligand, ACh whereas Pilo and oxotremorine are partial agonists. However, it is widely appreciated that ligands acting at GPCRs can have non linear efficacy which results in the activation of different subsets of signalling pathways available to the receptor (Galandrin *et al.*, 2007; Luttrell *et al.*, 2011). This phenomenon has been referred to as bias agonism or functional selectivity. The clearest example of bias agonism is the reversal in agonist potency for one receptor mediated pathway (i.e. G protein dependent signalling) relative to another (i.e. arrestin dependent signalling) (May *et al.*, 2010). This has been demonstrated for a number of GPCRs including the serotonin (5-HT<sub>2C</sub>) and β<sub>2</sub> adrenergic receptors (Azzi *et al.*, 2003; Baker *et al.*, 2003; Berg *et al.*, 1998). However such an

“absolute” bias is rare and in many cases ligands display only weakly bias for one pathway over another and a thorough data analysis is required to reveal this behaviour.

In a recent study, methods used to quantify biased agonism were presented and evaluated. It was shown that the operational model of agonism was the best approach for quantifying ligand bias (Rajagopal *et al.*, 2011). In this study we adopted this approach to determine if MCh, Pilo and Arec display biased agonism in mediating global receptor phosphorylation, inositol phosphates accumulation and ERK1/2 phosphorylation at the M<sub>3</sub> mAChR. Using MCh as the reference agonist, our data suggest that Pilo appeared to be more efficient in promoting inositol phosphates accumulation than global M<sub>3</sub> mAChR phosphorylation.

Interestingly, when the data was analysed in a “standalone” fashion, the rank order of potency of these agonists correlated well across these two receptor functions. This indicates that ranking agonists according to their potency may not be sufficient to uncover potentially weak biased agonists and that the use of the operational model of agonism and data comparison with a reference agonist is required to do so.

Other studies have shown that Pilo caused ERK activation through M<sub>3</sub> mAChR endogenously expressed in human salivary (HSY) cells via a different mechanism as CCh (Lin *et al.*, 2008). Similarly, in vitro studies employing GTP $\gamma$ S and immunoprecipitation approach have shown that pilocarpine was more efficacious in promoting G<sub>ai</sub> activation than G<sub>aq</sub> suggesting that Pilo has distinct pharmacology (Akam *et al.*, 2001). Furthermore in vivo studies have also shown that Pilo, despite being a weak partial agonist was able to cause seizure indicating that Pilo has distinct pharmacological properties in physiological setting as well (Wess *et al.*, 2003b). This may be due to the fact that Pilo is a non selective mAChR agonist and that this seizure is caused by the compound acting at the M<sub>1</sub> mAChR (Wess, 2004). The fact that the levels of expression of the M<sub>1</sub> mAChR in the brain is very high (i.e. 1 pmol/mg in the

hippocampus and 0.8 pmol/mg in the striatum) it is also possible that Pilo might act as a full agonist in vivo (Wall *et al.*, 1991).

One caveat in this study is that only a limited number of agonists were tested and that the endogenous ligand ACh was not used as the reference agonist. However, a recent review indicates that besides AC-42 and 77-LH-28-1 ( $M_1$  mAChR allosteric agonists) and Pilo there is very little evidence implicating that the currently known muscarinic agonists display bias agonism (Challiss *et al.*, 2009; Thomas *et al.*, 2008). Therefore this study was not extended to testing a wider range of agonists.

MCh is structurally similar to ACh and as such it was deemed acceptable to use this ligand as the reference agonist. However, given the (emerging) importance of probe dependency in GPCR pharmacology, ACh will be used in subsequent chapters for agonist comparator.

The regulation of GPCRs by phosphorylation is highly dynamic and can occur at multiple sites throughout the intracellular loops of the receptor (Tobin, 2008; Tobin *et al.*, 2008). Therefore we extended our study into investigating the effects of MCh, Pilo and Arec on the phosphorylation state of the  $M_3$  mAChR at the peptide and individual amino acid levels to provide a more comprehensive view of the regulatory process that operate at this receptor subtype. Our data showed that both at the peptide and individual amino acid levels, the overall patterns of phosphorylation correlated well with the intrinsic efficacy of the agonists for the stimulation of inositol phosphates and ERK1/2 phosphorylation pathways. However, there was a preferential phosphorylation of “spot 4” in the phosphopeptide maps and Ser412 in western blots whereby Pilo, a weak partial agonist was equally efficacious as MCh, a full agonist at mediating phosphorylation of these sites. These results suggest that despite the global receptor phosphorylation being in the same rank order of potency as the downstream

receptor signalling pathways, phosphorylation at specific sites is more flexible and can unmask a deviation from this rank order of potency.

These observations can be rationalised by the notion that different ligands acting at the M<sub>3</sub> mAChR are able to stabilise different receptor conformations which then regulates the accessibility of phosphorylation sites to protein kinases. In line with this concept, the conformation stabilised by MCh and Arec would unmask “spot 4”, Ser412 and Ser577, whereas the conformation stabilised by Pilo would unmask “spot 4” and Ser412 only. Such a mechanism of agonist mediated “revealing” of phosphorylation sites has been proposed to be in operation for GRK-mediated receptor phosphorylation (Lefkowitz, 2004; Lefkowitz, 2000; Pitcher *et al.*, 1998). Indeed our data from siRNA knock down experiments suggests that both GRK2 and GRK6 were able to phosphorylate Ser412.

Alternatively, the break in the relative agonist potency for the phosphorylation of Ser412 and “spot 4” could be due to these sites being more sensitive and even a weak partial agonist such as Pilo could efficiently promote phosphorylation of these sites.

It is also plausible that Pilo, purely by having higher affinity for the M<sub>3</sub> mAChR compared MCh and Arec, would occupy a greater proportion of the receptor. This would shift the dynamic equilibrium of the receptor toward an active state, resulting in a greater proportion of Ser412 being phosphorylated.

It is also interesting to note that despite kinetically similar to Ser412, phosphorylation of Ser577 was mediated by a distinct protein kinase (PKC). The pattern of phosphorylation of Ser577 was the same as the agonist efficacy profiles for the inositol phosphates pathway. These data suggest that different protein kinases may have the same kinetics or mechanism of activation but are able to phosphorylate distinct residues on receptors.

This study also revealed certain sites (i.e. “spot 1” and Ser384) undergoing dephosphorylation upon agonist stimulation. Since dephosphorylation is associated with a mechanism that enables internalised receptors to be recycled back to the cell surface after the removal of agonists, our finding that the M<sub>3</sub> mAChR become dephosphorylated upon agonist stimulation is unique and to our knowledge has only been reported for the  $\beta_2$  adrenergic receptor (Nobles *et al.*, 2011). Moreover, this dephosphorylation event was not observed in the M<sub>3</sub> mAChR expressed in the hippocampus suggesting that this is a cell type specific phenomenon (Poulin *et al.*, 2010).

The pattern of phosphorylation of spot 1 and spot 4 in the phosphopeptide maps is very similar to Ser384 and Ser412 respectively. It is therefore possible that they may represent the same phosphorylation sites. To confirm this, it would be necessary to perform site directed mutagenesis on Ser384 and Ser412 and then compare the phosphopeptide maps of the mutant receptors to the WT receptor. Alternatively, the spots could be extracted and the phosphopeptides sequenced to reveal the sites of phosphorylation. Although found to be feasible (Torrecilla *et al.*, 2007), the latter approach is technically challenging and requires a protein/peptide sequencing equipment dedicated for radioactive materials.

Many reports have indicated that different phosphorylation events can lead to the regulation of different signalling pathways. The patterns of phosphorylation have been proposed to generate a barcode that resembles a code which cells or agonists can dial to regulate cellular signalling (Tobin *et al.*, 2008; Zidar *et al.*, 2009). In the case of the somatostatin (sst)<sub>2A</sub> receptor, phosphorylation at Thr353, Thr354, Thr356 and Thr359 was shown to cause  $\beta$ -arrestin recruitment and receptor internalisation whereas phosphorylation of Thr356 and Thr359 was shown to cause  $\beta$ -arrestin recruitment only (Poll *et al.*, 2010).

To determine if the phosphorylation patterns observed in this study would affect the signalling profiles of the receptor it would be necessary to fully define which phosphorylation sites are differentially phosphorylated and then individually mutated. Given that there are 15 residues within the ICL3 and C-tail of the M<sub>3</sub> mAChR known to be phosphorylated (Butcher *et al.*, 2011), mutating these residues and raising antibodies for each mutant receptor would be very costly and impractical. Another complication would be the difficulty in interpreting the data as agonists possess intrinsic efficacy and different phosphorylation events can lead to different functional outcomes. We therefore, did not pursue with generating mutant M<sub>3</sub> mAChR that have different phosphorylation sites mutated.

In summary, this chapter provided evidence that Pilo may be bias for the stimulation of inositol phosphates pathway compared to receptor phosphorylation at the M<sub>3</sub> mAChR. The ligand also appeared to preferentially cause phosphorylation of spot 4 and Ser412 as it behaves as a full agonist in mediating phosphorylation of these sites. Phosphorylation of Ser412 was kinetically similar to Ser577 though mediated by different protein kinases. These differences may explain the preferential phosphorylation seen with Pilo.

## **Chapter 4: Phosphorylation of mutant M<sub>3</sub> mAChR solely activated by synthetic ligand (M<sub>3</sub>-RASSL)**

### **4.1. Introduction**

The development of a chemical genetic approach to produce receptors that do not respond to their endogenous ligands but can be fully activated by synthetic ligands has provided a powerful tool for studying GPCR functions in vivo (Conklin *et al.*, 2008; Dong *et al.*, 2010a; Nichols *et al.*, 2009). Such mutant receptors, also called receptors activated solely by synthetic ligands (RASSLs) or designer receptors exclusively activated by designer drugs (DREADDs) have been shown to be functionally silent when expressed in tissues and cells and can be selectively activated upon the application of the exogenous ligands (Pei *et al.*, 2008; Scearce-Levie *et al.*, 2001; Scearce-Levie *et al.*, 2002). As a consequence, the effects of the loss of receptor function and specific activation of the receptor on animal physiology and behaviour can be studied simultaneously.

The first RASSL receptor to be created was the  $\beta_2$ -adrenergic receptor (Strader *et al.*, 1991). By mutating a conserved aspartate residue in the third transmembrane domain to a serine (Asp113Ser), the  $\beta_2$ -adrenergic receptor was shown to be unresponsive to adrenaline but can be activated by catechol esters and ketones (Strader *et al.*, 1991). However, due to poor physicochemical properties and low binding affinity of these compounds, the  $\beta_2$ -RASSL receptor was not used for in vivo studies. To overcome this issue, Coward et al developed a second RASSL receptor based on the  $\kappa$ -opioid receptor (KOR) (Coward *et al.*, 1998). The KOR is known to possess two binding sites that are spatially distinct; one at the extracellular surface which binds to the endogenous peptide (e.g. dynorphin) and the other within the transmembrane region which is recognised by synthetic ligands. By substituting the second extracellular loop of the KOR with that of the  $\delta$ -opioid receptor, Coward et al. showed that

the receptor had significantly reduced affinity for dynorphin but retained its ability to bind to the exogenous agonist, spiradoline (Coward *et al.*, 1998). The mutant receptor, also called Ro1 was subsequently expressed in a number of tissues including the heart and taste buds where it was shown to control heart rate and mediate taste sensation, respectively (Redfern *et al.*, 1999; Zhao *et al.*, 2003).

A number of other RASSL receptors have also been developed which include the histamine H<sub>1</sub> receptor, serotonin (5-HT) 4 receptor, melanocortin (MC) 4 receptor and M<sub>1</sub>-M<sub>5</sub> mAChRs (Armbruster *et al.*, 2007; Bruysters *et al.*, 2005; Chang *et al.*, 2007; Pei *et al.*, 2008; Srinivasan *et al.*, 2007; Srinivasan *et al.*, 2003). In the case of the mAChRs, a yeast mutagenesis approach was used to identify mutations that would abrogate ACh binding but create binding to clozapine-N-oxide (CNO) (Armbruster *et al.*, 2007). CNO was chosen because the compound has good bioavailability and is biologically inert, making it ideal for in vivo studies ((Armbruster *et al.*, 2007; Bender *et al.*, 1994; Conklin, 2007).

In all of the 5 mAChR subtypes, two residues within transmembrane domains (Y106C and A196G in the M<sub>1</sub> mAChR, Y149C and A239G in the M<sub>3</sub> mAChR and Y113C and A203G in the M<sub>4</sub> mAChR) were found to be important for this switch in receptor pharmacology (Abdul-Ridha *et al.*, 2013; Armbruster *et al.*, 2007; Nawaratne *et al.*, 2008). **Figure 4.1.1** shows the locations of the RASSL mutations at the human M<sub>3</sub> mAChR. In vitro characterisation of this mutant M<sub>3</sub> RASSL receptor has shown that the receptor couples to the PLC and ERK 1/2 phosphorylation pathways in response to stimulation by CNO (Armbruster *et al.*, 2007). Subsequent expression of the mutant receptor in the hippocampus and pancreatic  $\beta$  cells has shown that the receptor caused neuronal cell firing and insulin secretion, respectively following CNO administration. It therefore appears that the RASSL M<sub>3</sub> receptor is able to replicate the signalling activity of the WT M<sub>3</sub> receptor in native tissue (Armbruster *et al.*, 2007; Guettier *et al.*, 2009).

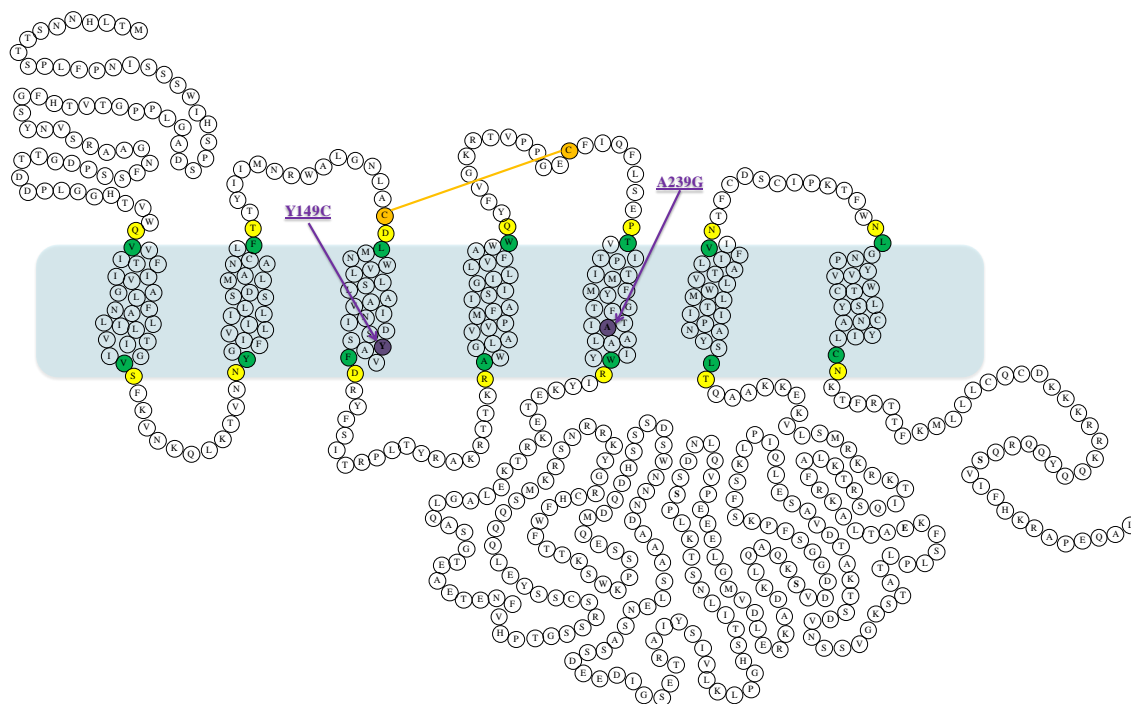


**Figure 4.1.1: Topography of human M3 mAChR amino acid sequence containing the RASSL mutations.** The junctions between the TM and loop regions as determined by protein knowledgebase sequence alignment ([www.uniprot.org](http://www.uniprot.org), chrn3, accession number: P20309) are represented by residues in green and yellow. The amino acid substitutions that resulted in the creation of the RASSL receptor are highlighted in purple.

The M<sub>4</sub> RASSL receptor has also been shown to function in a similar manner as the WT receptor when stimulated with CNO. For instance, the receptor caused neuronal silencing when transiently expressed in hippocampal neurons and activated GIRK when co-transfected in HEK cells with the K<sup>+</sup> channels (Armbruster *et al.*, 2007). The receptor was also shown to cause c-fos expression in striatal neurons indicating modulation of neuronal activity in whole animals (Ferguson *et al.*, 2011). Interestingly, the signalling efficacy of ACh at the M<sub>4</sub> RASSL was rescued by the allosteric modulator LY2033298, highlighting that the allosteric site is unaffected by the RASSL mutations (Nawaratne *et al.*, 2008).

It is widely recognised that ligands acting at the same GPCR can differentially modulate the signalling properties of the receptor (Urban *et al.*, 2007). Such receptor behaviour has been named variously as trafficking of receptor signals, bias agonism or functional selectivity (Kenakin, 2011). Given that RASSL receptors were evolved to accommodate unnatural ligands, these receptors may be regulated or signal differently in response to the exogenous compounds. As such, the aim of this chapter is to investigate the phosphorylation states of the M<sub>3</sub> RASSL receptor in response to CNO stimulation. This is a collaboration effort involving the group of Prof Graeme Milligan who is interested in establishing the pharmacology of the M<sub>3</sub> RASSL receptor. Using a combination of <sup>32</sup>P-labelling, phosphopeptide mapping and immunoblotting with phosphorylation specific antibodies, we show here that the phosphorylation profiles of the CNO-bound M<sub>3</sub> RASSL receptor were similar to those of the ACh-bound WT mAChR. Hence results obtained from *in vivo* studies employing the M<sub>3</sub> RASSL receptor would represent the physiological effects of the WT M<sub>3</sub> mAChR responding to ACh.

## 4.2. Results

### 4.2.1. Induction of receptor expression

A tetracycline inducible system was used to generate a stable cell line expressing the VSV-G-SNAP tagged WT M<sub>3</sub> and M<sub>3</sub> RASSL receptors (Alvarez-Curto *et al.*, 2010). Induction of receptor expression was achieved with 2 ng/ml of doxycycline (DOX), a potent analogue of tetracycline as shown by the presence of 125 kDa band on SDS-PAGE gels which was not detected in non induced cells (**Figure 4.2.1.1**).

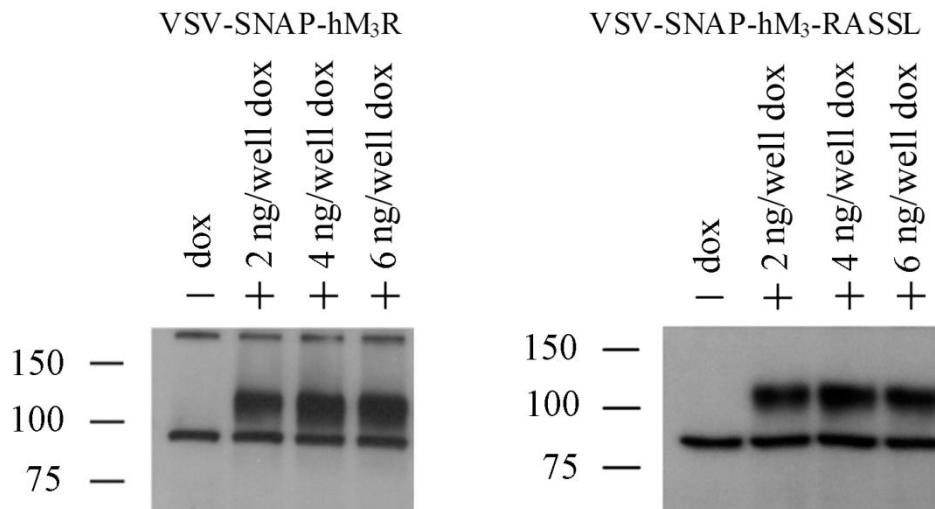


**Figure 4.2.1.1: Induction of receptor expression.** HEK-293 cells expressing the M<sub>3</sub> RASSL and the WT M<sub>3</sub> mAChR in a doxycycline inducible fashion were plated at 250000 cells per well in 6-well plates and allowed to adhere for 24 hrs at 37°C. Cells were treated with 2 to 6 ng/ml of doxycycline for 18 hrs at 37°C. Lysates derived from these cells were then probed with M<sub>3</sub> mAChR specific antibody in western blot experiment to detect receptor expression. Immunoblots represent three independent experiments performed in singlicate.

#### 4.2.2. In vivo labelling and immunoprecipitation

Initial phosphorylation experiments were performed using  $^{32}\text{P}$ -labelling and immunoprecipitation methods. To allow direct comparison, the experiments were designed such that the concentration of the ligands used would occupy similar receptor populations. It has been shown that CNO has an affinity of  $0.91\ \mu\text{M}$  at the  $\text{M}_3$  RASSL receptor and ACh has an affinity of  $4.91\ \mu\text{M}$  at the WT  $\text{M}_3$  mAChR (Guettier *et al.*, 2009). Therefore stimulation of the  $\text{M}_3$  RASSL receptor with  $100\ \mu\text{M}$  CNO and the WT  $\text{M}_3$  mAChR with  $500\ \mu\text{M}$  ACh would produce approximately ~99% receptor occupancy for both receptor types. In this assay, both the WT and  $\text{M}_3$  RASSL receptors appeared to be phosphorylated under basal conditions (**Figure 4.2.2.1**). The phosphorylation level of the RASSL receptor was increased to ~ 4 fold above basal upon stimulation with  $100\ \mu\text{M}$  CNO but remained unchanged when stimulated with ACh. These data are consistent with the  $\text{M}_3$  RASSL being insensitive to ACh but highly responsive to CNO. In contrast, the WT  $\text{M}_3$  mAChR was phosphorylated only with ACh and not CNO treatment.

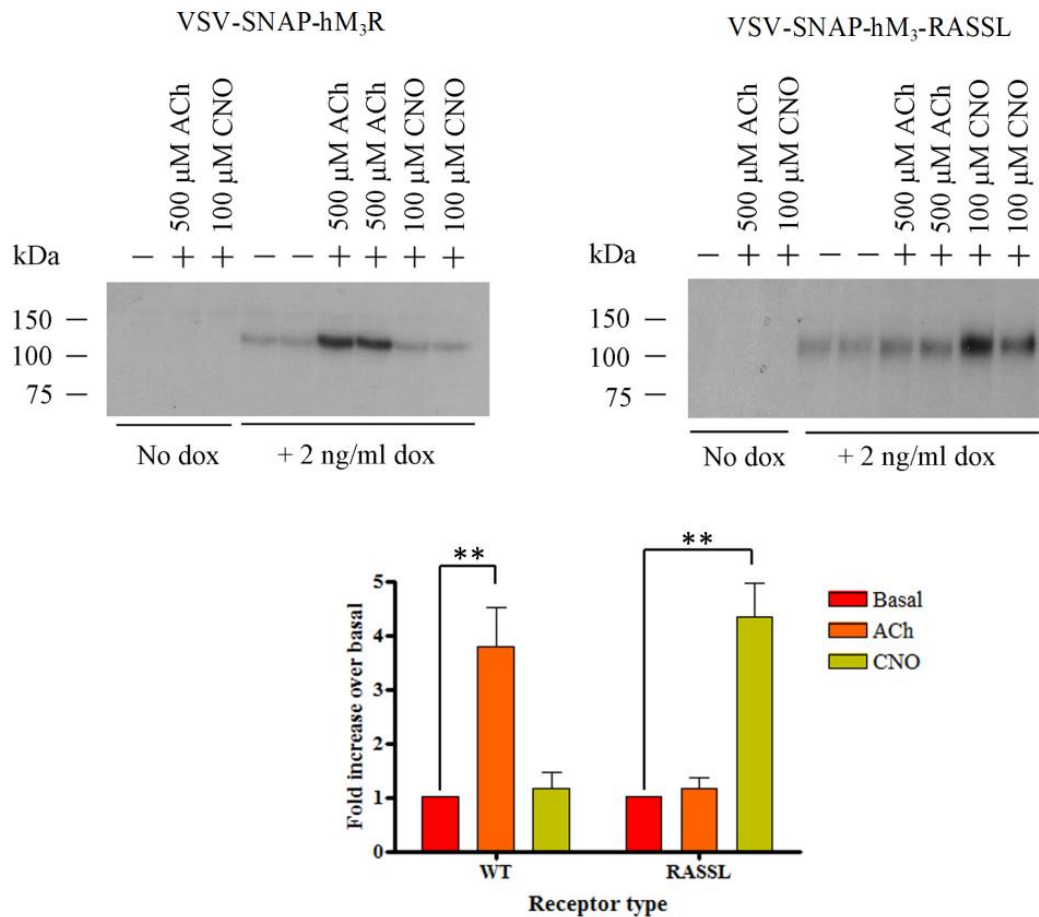


**Figure 4.2.2.1:  $^{32}\text{P}$ -labelling and intact cell phosphorylation.** HEK-293 cells expressing the  $\text{M}_3$  RASSL and the WT  $\text{M}_3$  mAChR in a doxycycline inducible fashion were plated at 250000 cells per well in 6-well plates and allowed to adhere for 24 hrs at  $37^\circ\text{C}$ . Following induction with 2 ng of doxycycline, cells were labelled with  $50 \mu\text{Ci/ml}$   $^{32}\text{P}$ -orthophosphate for 1 hr at  $37^\circ\text{C}$  and then stimulated with agonist for 5 min. Receptors were immunoprecipitated with  $\text{M}_3$  mAChR specific antibody and then resolved on 8% SDS-PAGE gel. Receptor phosphorylation was visualised by autoradiography. Immunoblots represent three independent experiments performed in singlicate and bar graphs represent the mean  $\pm$  S.E.M of the immunoblots quantified using ImageQuant and AlphaEase FC softwares.

\* $P < 0.05$ , \*\* $P < 0.01$ ; as measured using a one-way ANOVA with Bonferonni's post-hoc test.

### 4.2.3. Phosphopeptide mapping

A more detailed analysis of the phosphorylation status of the M<sub>3</sub> RASSL was performed using phosphopeptide mapping. This method utilises electrophoresis and chromatography to separate phosphopeptides derived from enzymatic digestion of receptors in two dimensions. In these experiments the CNO mediated phosphorylation profile of the M<sub>3</sub> RASSL receptor were compared with that of the WT receptor stimulated with the endogenous ligand, ACh. As shown in **Figure 4.2.3.1** the pattern of phosphorylation of the M<sub>3</sub> RASSL in response to CNO stimulation was similar to that of the WT M<sub>3</sub> mAChR responding to ACh, with both receptors exhibiting twelve phosphorylated peptides.

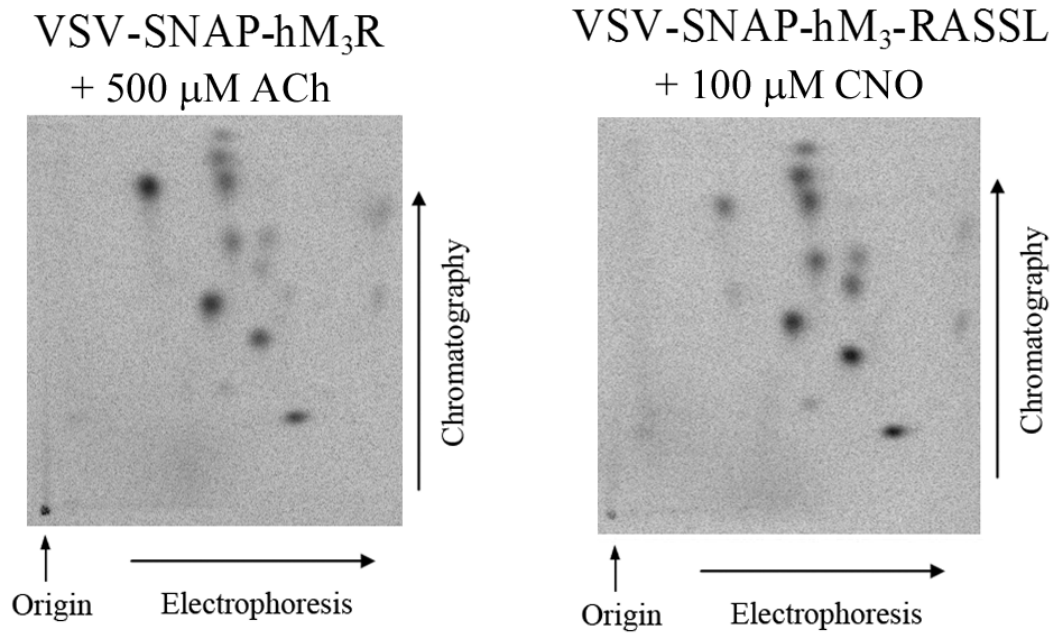
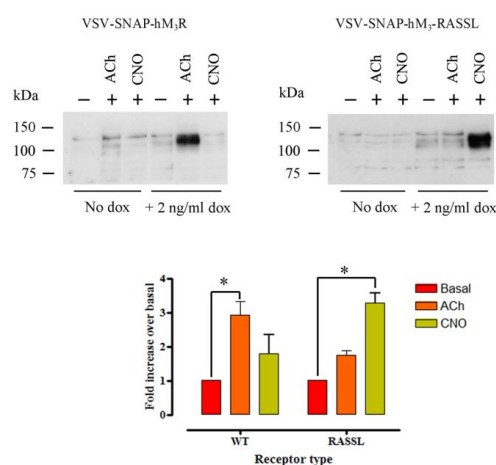


**Figure 4.2.3.1: Phosphopeptide mapping.** Receptors which had been resolved on 8% SDS-PAGE gel were digested with trypsin overnight at 37°C. Peptide fragments were spotted onto TLC plates and separated in two dimensions. The first dimension was electrophoresis to separate the fragments according to charge and the second dimension was chromatography to separate the peptides according to hydrophobicity. Resolved phosphopeptides were detected by phosphoimager. Maps are a representative of three independent experiments performed in singlicate.

#### **4.2.4. Western blotting using phosphoserine specific antibodies**

The use of phosphospecific antibodies to investigate phosphorylation has been described for a number of GPCRs (Busillo *et al.*, 2010; Liu *et al.*, 2008; Liu *et al.*, 2009; Oppermann *et al.*, 1999; Tran *et al.*, 2004). In the case of the M<sub>3</sub> mAChR, we recently developed three phosphorylation sensitive antibodies targeting Ser384 and Ser412 at the ICL3 and Ser577 at the C-tail of the receptor (Butcher *et al.*, 2011). To further investigate the phosphorylation state of the M<sub>3</sub> RASSL, we used these antibodies to probe for changes in phosphorylation at specific residues. Our results show that the M<sub>3</sub> RASSL was phosphorylated at Ser412 and Ser577 only in response to CNO stimulation and not to ACh. Similarly the WT M<sub>3</sub> mAChR was phosphorylated at these residues only in response to its cognate ligand, ACh (**Figure 4.2.4.1**). Hence at individual sites, the phosphorylation state of the M<sub>3</sub> RASSL is similar to that of the WT receptor.

A. Intracellular loop 3 Serine 412



B. C-tail Serine 577

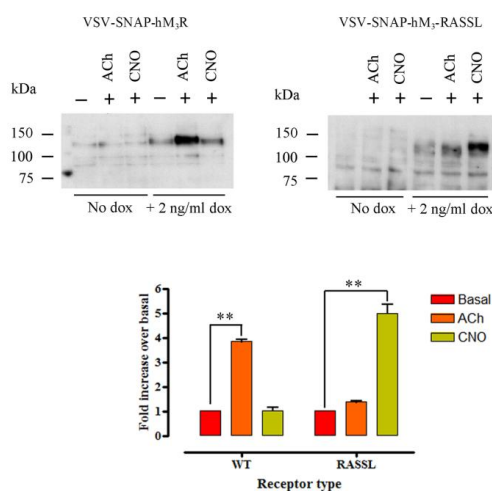


**Figure 4.2.4.1: Western Blotting.** HEK-293 cells expressing the M<sub>3</sub> RASSL and the WT M<sub>3</sub> mAChR in a doxycycline inducible fashion were plated at 250,000 cells per well in 6-well plates and allowed to adhere for 24 hrs at 37°C. Following induction with 2 ng/well of doxycycline, cells were incubated in an assay buffer for 1 hr at 37°C and then stimulated with agonist for 5 min. Cells were lysed and receptor proteins were resolved on 8% SDS-PAGE gels and subjected to western blotting using a phospho-specific antibody recognising phosphorylated serine 412 and serine 577. Immunoblots are a representative of three independent experiments performed in singlicate and graphs represent the mean ± S.E.M of the experimental replicates. \*P<0.05, \*\*P<0.01; as measured using a one-way ANOVA with Bonferonni's post-hoc test.

### 4.3. Discussion

The mAChRs represent a prototypical family A GPCRs and a therapeutically important target for multiple central nervous systems disorders (Eglen *et al.*, 2001; Felder *et al.*, 2000; Langmead *et al.*, 2008b). Due to lack of subtype selective ligands for mAChRs, much of the knowledge of the physiological roles of these receptors has been gained through the generation of knockout animals lacking each of the five subtypes of the mAChR family (Wess, 2004; Wess *et al.*, 2003b; Wess *et al.*, 2007). Hence the M<sub>3</sub> mAChR has been shown to play a role in insulin secretion and glucose homeostasis, learning and memory processes and smooth muscle contractility (Duttaroy *et al.*, 2004; Gautam *et al.*, 2007; Gautam *et al.*, 2006; Kong *et al.*, 2010; Kong *et al.*, 2011; Poulin *et al.*, 2010; Wess, 2004). Recently, an alternative method for studying receptor functions in vivo has been proposed. This method employs chemical genetics to create receptors that no longer able to respond to the endogenous ligands but can be activated by otherwise pharmacologically inert compounds (Armbruster *et al.*, 2007; Dong *et al.*, 2010a; Scarce-Levie *et al.*, 2002). Originally developed for the  $\beta_2$ -adrenergic receptor (Strader *et al.*, 1991), this approach has now been used for a variety of GPCRs including the  $\kappa$ -opioid receptor, melanocortin 4 (MC<sub>4</sub>) receptor and the M<sub>1</sub>-M<sub>5</sub> mAChRs (Pei *et al.*, 2008). These mutant receptors would remain physiologically silent when expressed in vivo and then become activated by the application of the exogenous ligand. Hence this method allows investigators to study the effects of the loss of receptor functions and specific activation of the receptor simultaneously.

In the case of the M<sub>3</sub> mAChR, two mutations at the orthosteric binding pocket (Y149C and A239G) were found to significantly reduce ACh binding but confer binding to clozapine N-oxide (Armbruster *et al.*, 2007). Initial in vitro characterisation has shown that the receptor couples to the activation of phospholipase C and ERK 1/2 phosphorylation in response to CNO stimulation (Armbruster *et al.*, 2007). However the regulation of the M<sub>3</sub> RASSL

receptor is currently unknown. Given that the M<sub>3</sub> RASSL receptor has been expressed in a number of tissues, understanding the regulation of this mutant receptor is important.

Therefore the aim of this chapter is to investigate the phosphorylation profile of the M<sub>3</sub> RASSL receptor since phosphorylation is considered as a key regulatory process that controls the signalling of many GPCRs. Using intact cell phosphorylation as an initial approach, we found that the M<sub>3</sub> RASSL was robustly phosphorylated following stimulation with CNO. In contrast, ACh had negligible effect on the phosphorylation state of the M<sub>3</sub> RASSL receptor but was able to cause a dramatic increase in the phosphorylation state of the WT M<sub>3</sub> receptor. These initial experiments provided early evidence that the M<sub>3</sub> RASSL receptor is selectively phosphorylated in response to CNO stimulation and not to ACh.

As phosphorylation can occur at multiple sites throughout the intracellular regions of GPCRs (Tobin, 2008), mapping the phosphorylation sites or peptides containing the phosphorylated residues would provide valuable information on the phosphorylation signatures of the receptor. Here, the phosphorylation signatures of the M<sub>3</sub> RASSL receptor at the peptide level using 2D mapping and individual sites using phosphorylation specific antibodies were investigated and compared with the phosphorylation profiles of the WT M<sub>3</sub> receptor. Our data showed that the agonist dependent phosphorylation signatures of the M<sub>3</sub> RASSL receptor were similar to those of the WT M<sub>3</sub> receptor responding to ACh. However, a caveat to this conclusion is that the 2D maps of the M<sub>3</sub> RASSL receptor and the WT control under basal conditions were not investigated. This was due to the technical difficulty in performing the experiments and the potential difficulty in data interpretation (i.e. comparing background phosphorylation with another background phosphorylation).

Studies have indicated that ligands acting at GPCRs can differentially modulate the signalling pathways available to the receptors, a phenomenon referred to as biased agonism or functional selectivity. To determine if the RASSL mutations would alter the pharmacology of

the receptor, our collaborators have further investigated the signalling properties of the M<sub>3</sub> RASSL receptor in response to CNO stimulation. The data showed that the receptor signals in a similar manner as the WT receptor and that it did not display functional selectivity (Alvarez-Curto *et al.*, 2011). However, studies using another RASSL receptor (M<sub>4</sub> RASSL) have shown that this mutant receptor was able to respond to ACh in the presence of an allosteric modulator. These data suggest that the binding site of ACh is still intact and the introduction of the RASSL mutations might affect the conformation of the receptor such that the receptor is no longer able to respond to ACh. To completely eliminate ACh binding, one would need to introduce further mutations on the RASSL receptor. However, given that there are currently no endogenous allosteric modulators known to act at the mAChRs, the present mutations may be sufficient to allow specific activation of the M<sub>3</sub> RASSL receptor by CNO. In light of this, several *in vivo* studies have shown that activation of the M<sub>3</sub> RASSL by CNO resulted in a number of physiological responses such as insulin secretion and neuronal firing in pancreatic islets and hippocampal neurons respectively (Alexander *et al.*, 2009; Guettier *et al.*, 2009).

To summarise our data together with those of others have indicated the M<sub>3</sub> RASSL receptor is fully functional and able to replicate the WT receptor characteristics. The M<sub>3</sub> RASSL receptor was also regulated by phosphorylation in response to CNO stimulation and that it did not display functional selectivity. These data will provide confidence that observations made from *in vivo* studies using the M<sub>3</sub> RASSL receptor will reflect the actions of the WT M<sub>3</sub> receptor responding to ACh.

# **Chapter 5: Pharmacological characterisation of novel allosteric ligands at the M<sub>1</sub> mAChR and their effects on receptor phosphorylation**

## **5.1. Introduction**

The M<sub>1</sub> mAChR represents an important drug target for the treatment of cognitive deficits associated with Alzheimer's disease (AD) and schizophrenia (Felder *et al.*, 2000; Langmead *et al.*, 2008b; Wess *et al.*, 2007). Originally cloned in 1986 the receptor is now known to be expressed in many areas of the brain including the hippocampus and cerebral cortex where it mediates key central nervous system (CNS) functions such as learning and memory (Anagnostaras *et al.*, 2003; Kubo *et al.*, 1986; Wess *et al.*, 2007). Studies also indicate that activation of the M<sub>1</sub> mAChR causes the breakdown of amyloid precursor proteins (APPs) in favour of the formation of non toxic soluble metabolites (APP $\alpha$ ), and inhibition of neurotoxic A $\beta$ -peptides (Davis *et al.*, 2010). This suggests that M<sub>1</sub> mAChR plays a key role in the pathology of AD and may provide an avenue for developing drugs with disease modifying properties.

Efforts to discover selective M<sub>1</sub> mAChR agonists have been challenging and have largely failed. This is partly due to conventional drug discovery efforts which have been directed toward discovering ligands that act at the same binding site as ACh, namely the orthosteric site (Conn *et al.*, 2009a). Since the orthosteric site is highly conserved across the five mAChR subtypes, these efforts led to the discovery of compounds that are non-selective and produce unwanted side effects mediated by other mAChR subtypes.

An alternative approach to overcoming this selectivity issue has been to discover ligands that interact with the receptor at a topographically distinct site, termed the allosteric site. This site, which is located at the extracellular domains of family A GPCRs (Soudijn *et al.*, 2004), is less evolutionarily conserved and ligands which modulate receptor activity via this site are predicted to be more selective.

In agreement with this concept several compounds have been discovered to interact allosterically at the M<sub>1</sub> mAChR and display superior selectivity for this receptor subtype compared to the other mAChR subtypes. Such allosteric modulators include AC-42, 77-LH-28-1, BQCA and VU0357017 (Conn *et al.*, 2009b; Langmead *et al.*, 2008a; Lebon *et al.*, 2009; Ma *et al.*, 2009; Spalding *et al.*, 2002). These compounds have diverse pharmacology and affect the receptor behaviour in many different ways. AC-42 and 77-LH-28-1 were initially classed as allosteric agonists and these compounds were able to elicit receptor activation in the absence of ACh (Langmead *et al.*, 2008a; Langmead *et al.*, 2006b; Spalding *et al.*, 2002). Furthermore the signalling profiles of the receptor in response to these compounds were distinct from those elicited by orthosteric agonists such as MCh or Pilo, suggesting that allosteric ligands may possess functional selectivity (Thomas *et al.*, 2009; Thomas *et al.*, 2008). However, further examinations suggest that AC-42 and 77-LH-28-1 were more likely to be bitopic ligands since they inhibited the specific binding of the orthosteric antagonist NMS down to non-specific levels and their effects on receptor signalling were blockable by scopolamine (Avlani *et al.*, 2010).

In vitro studies indicate that VU0357017 is an allosteric agonist and the compound is able to activate the M<sub>1</sub> mAChR in its own right (Digby *et al.*, 2012; Lebois *et al.*, 2010). VU0357017 has also been shown to be able modulate the M<sub>1</sub> mAChR activity in vivo, suggesting that the

compound has good bioavailability (Digby *et al.*, 2012; Lebois *et al.*, 2010; Thomsen *et al.*, 2012).

In contrast, BQCA was reported to be a positive allosteric modulator and the compound enhances the affinity and signalling efficacy of ACh at the M<sub>1</sub> mAChR (Canals *et al.*, 2012; Ma *et al.*, 2009; Shirey *et al.*, 2009). Additionally, BQCA has intrinsic efficacy on its own when tested in functional ERK1/2 phosphorylation assay (Canals *et al.*, 2012). BQCA has also been shown to be able to penetrate the blood brain barrier and activate the M<sub>1</sub> mAChR in the hippocampus, making the compound an ideal tool to study the M<sub>1</sub> mAChR functions in vivo (Ma *et al.*, 2009; Shirey *et al.*, 2009).

In addition to coupling to various downstream signalling pathways, the M<sub>1</sub> mAChR also undergoes rapid phosphorylation in response to agonist stimulation (Waugh *et al.*, 1999). It has been suggested that for a number of GPCRs the patterns of phosphorylation is important for the signalling profiles of the receptor (Butcher *et al.*, 2011; Nobles *et al.*, 2011; Tobin, 2008; Tobin *et al.*, 2008; Zidar *et al.*, 2009). Since less is known about the effects of allosteric modulators on receptor phosphorylation, the study here is focussed on investigating the effects of allosteric modulators (in particular BQCA and VU0357017) on the phosphorylation state of the M<sub>1</sub> mAChR stably expressed in CHO cells.

Additionally, increasing number of allosteric modulators has been discovered to display functional selectivity which has a significant impact on drug discovery and in vivo physiological studies (Leach *et al.*, 2007; Wang *et al.*, 2009). Hence this study is also focussed on further characterising the pharmacology of BQCA and VU0357017 to determine if these compounds possess bias agonism.

Our data suggest that BQCA is a PAM with an agonist property in its own right. The compound is probe dependent as a PAM, but appeared to preferentially promote

phosphorylation of serine 228 as an agonist. VU0357017 appeared to behave as a partial agonist. The compound has a weak activity in phospho-ERK 1/2 assay and decreases the potency of ACh in this assay.

## 5.2. Results

### 5.2.1. Generation of stable cell line expressing human M<sub>1</sub> mAChR

A stable CHO cell line expressing the human M<sub>1</sub> mAChR was generated by transfecting the WT CHO cells with c-Myc tagged M<sub>1</sub> mAChR cDNA using Fugene HD Transfection reagent. Successful transfectants were selected with 500 µg/ml of geneticin and cells that survived the selection were plated at high dilutions to allow single colonies to form. Single colonies were picked and screened using ~1 nM tritiated antagonist, N-methylscopolamine (<sup>3</sup>H-NMS) in a whole cell radioligand binding assay. From this screening, clone 66 which gave high <sup>3</sup>H-NMS binding was isolated and used throughout the project.

### 5.2.2. Characterisation of M<sub>1</sub> mAChR expressing CHO cell line

To determine the expression levels of the M<sub>1</sub> mAChR in clone 66, membrane saturation binding assays were performed. Initially the optimum membrane concentration that would produce sufficient levels of specific binding and acceptable levels of radioligand depletion was determined. As shown in **Figure 5.2.2.1**, 10 µg per reaction of membrane gave high levels of radioactivity counts but less than 10% ligand depletion. Therefore 10 µg of membrane proteins were used in the saturation binding experiments. The saturation binding studies showed that <sup>3</sup>H-NMS binds to the M<sub>1</sub> mAChR with an apparent dissociation constant of  $0.22 \pm 0.03$  nM (**Figure 5.2.2.1**, n=3). The expression level of the M<sub>1</sub> mAChR (B<sub>max</sub>) was found to be  $4.3 \pm 0.26$  pmol/mg protein.

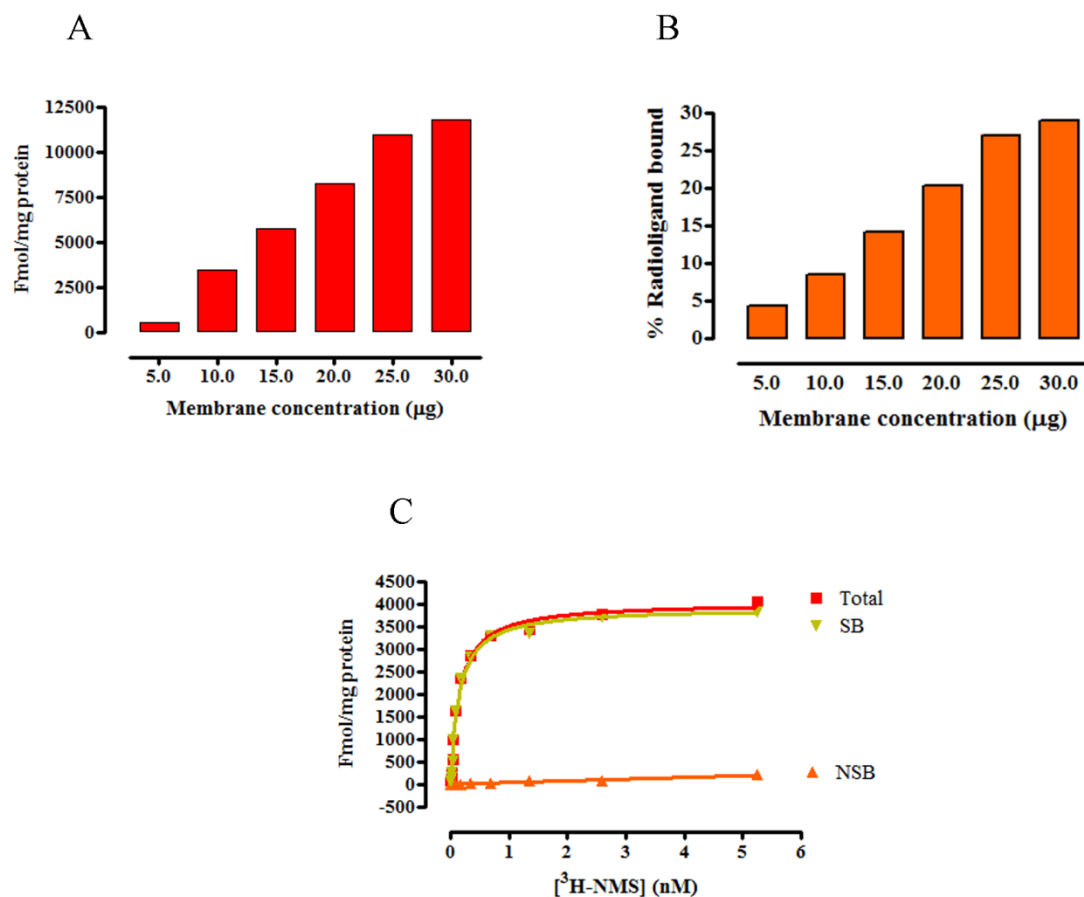


**Figure 5.2.2.1: Characterisation of M<sub>1</sub> mAChR expressing CHO cell line.** For membrane optimisation (A and B) 5 µg to 30 µg/well membranes derived from CHO-hM<sub>1</sub>R cells were incubated with ~0.5 nM tritiated NMS (<sup>3</sup>H-NMS) in 96-well plate for 2 hours at room temperature (final assay volume, 400 µl). For saturation binding 10 µg/well membrane was incubated with ~5 pM to ~5 nM <sup>3</sup>H-NMS in 96-well plate for 2 hours at room temperature (final assay volume, 1 ml). 10 µM of atropine was included in both assays to determine non-specific binding. Samples were transferred onto polyethyleneimine (PEI, 0.1%) pre-soaked GF/B plates using the TomTec 96-well harvester. Plates were dried extensively and 50 µl of scintillation fluids were added to each well. Plates were sealed and radioactivity was determined using a MicroBeta scintillation counter. Data represent a single experiment (A and B) and a representative of three independent experiments performed in duplicate (C).

### **5.2.3. BQCA increases the affinity of ACh at human M<sub>1</sub> mAChR whilst having minimal effects on the binding of antagonist, N-methylscopolamine**

BQCA has previously been reported to be a selective positive allosteric modulator at the M<sub>1</sub> mAChR as the compound enhances the affinity of the endogenous ligand, ACh at the receptor (Ma *et al.*, 2009; Shirey *et al.*, 2009). To confirm this effect in this system radioligand binding assays were carried out using membranes prepared from CHO-hM<sub>1</sub>R cells. Initially the effect of increasing concentration of BQCA on the binding of <sup>3</sup>H-NMS was assessed under equilibrium conditions (Jacobson *et al.*, 2010). As shown in **Figure 5.2.3.1**, BQCA does not significantly inhibit the binding of <sup>3</sup>H-NMS to the M<sub>1</sub> mAChR highlighting that BQCA acts allosterically. Application of the simple allosteric ternary complex model to the data showed that BQCA binds to the M<sub>1</sub> mAChR with an affinity (pK<sub>B</sub>) of  $5.25 \pm 0.63$  (n = 3) and the modulator has a weak negative binding cooperativity with <sup>3</sup>H-NMS binding ( $\alpha = 0.44 \pm 0.30$ ; n = 3) (**Figure 5.2.3.1**; **Table 5.2.3.1**). Subsequent radioligand binding studies with ACh showed that BQCA has a high positive binding cooperativity with ACh as demonstrated by an increase in the affinity of ACh to inhibit specific <sup>3</sup>H-NMS binding (**Figure 5.2.3.1**). Analysis of the data using the extended ternary complex model of allosterism resulted in  $\alpha'$  value (i.e. the binding cooperativity between BQCA and ACh) of ~128. This suggests that the affinity of ACh is increased by > 100 fold when both the orthosteric and allosteric sites are occupied (**Table 5.2.3.1**) and is in agreement with the published literature (Canals *et al.*, 2012; Ma *et al.*, 2009; Shirey *et al.*, 2009).

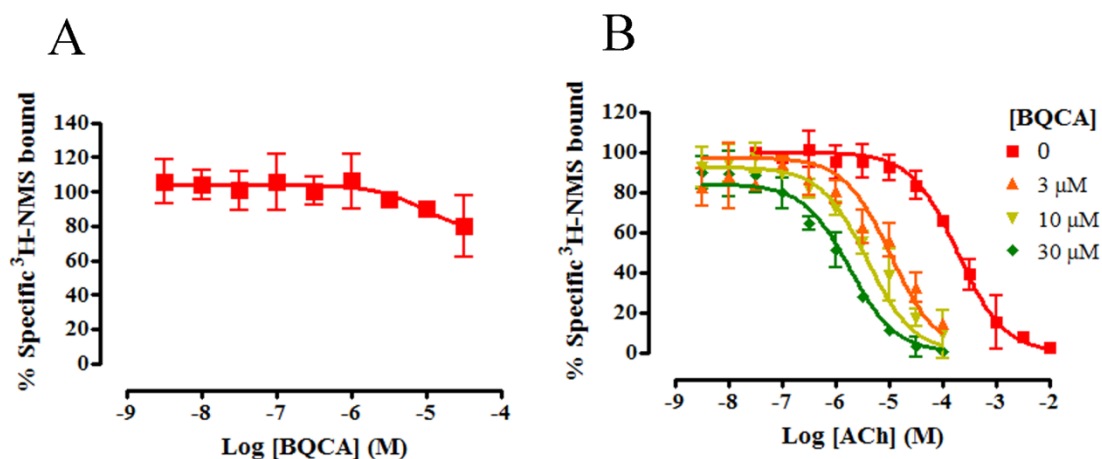


**Figure 5.2.3.1: Effects of BQCA on the binding of NMS and ACh.** Membranes (10  $\mu\text{g}/\text{well}$ ) were incubated with  $\sim 0.5$  nM tritiated NMS ( $^3\text{H-NMS}$ ) in 96-well plate in the presence of increasing concentration of BQCA for 2 hours at room temperature (final assay volume, 400  $\mu\text{l}$ ). For potentiation studies, ACh concentration response curves were prepared and the assay was carried out in the presence of 200  $\mu\text{M}$  GTP and increasing concentrations of BQCA. Non-specific binding was determined by the addition of 10  $\mu\text{M}$  atropine. Samples were transferred onto PEI (0.1%) pre-soaked GF/B plates using a TomTec filtration system. Plates were dried extensively and 50  $\mu\text{l}$  scintillation fluids were added to each well. Plates were sealed and radioactivity was determined using a MicroBeta scintillation counter. Data are expressed as a percentage of the specific binding  $^3\text{H-NMS}$ . Data points represent the mean  $\pm$  S.E.M of three independent experiments performed in triplicate.

**Table 5.2.3.1: Effects of BQCA on the binding of antagonist and agonist at the M<sub>1</sub> mAChR.**  $pK_B$  is the equilibrium dissociation constant of BQCA estimated from the ATCM,  $\alpha$  is the binding cooperativity between BQCA and <sup>3</sup>H-NMS.  $pK_I$  denotes the equilibrium dissociation constant of ACh and  $\alpha'$  is a measure of the binding cooperativity between BQCA and ACh.

Modulator	$pK_B$	$\alpha$	$pK_I$	$\alpha'$	n
BQCA	$5.25 \pm 0.63$	$0.44 \pm 0.30$	$4.24 \pm 0.06$	$128 \pm 1.35$	3

#### **5.2.4. BQCA displays probe dependency.**

Many allosteric modulators display probe dependence; the degree of binding cooperativity between the modulator with one orthosteric ligand is not the same as with another orthosteric ligand. To test whether BQCA displays probe dependence, radioligand binding assays were performed using other known orthosteric agonist probes such as MCh (MCh), oxotremorine-M (OXO-M) and pilocarpine (Pilo). As shown in **Figure 5.2.4.1**, BQCA has a positive binding cooperativity with all three orthosteric ligands tested. However, the extent of the affinity modulation was not the same for all of the agonists (**Table 5.2.4.1**), which suggests that the allosteric effect of BQCA at the M<sub>1</sub> mAChR is probe dependent.

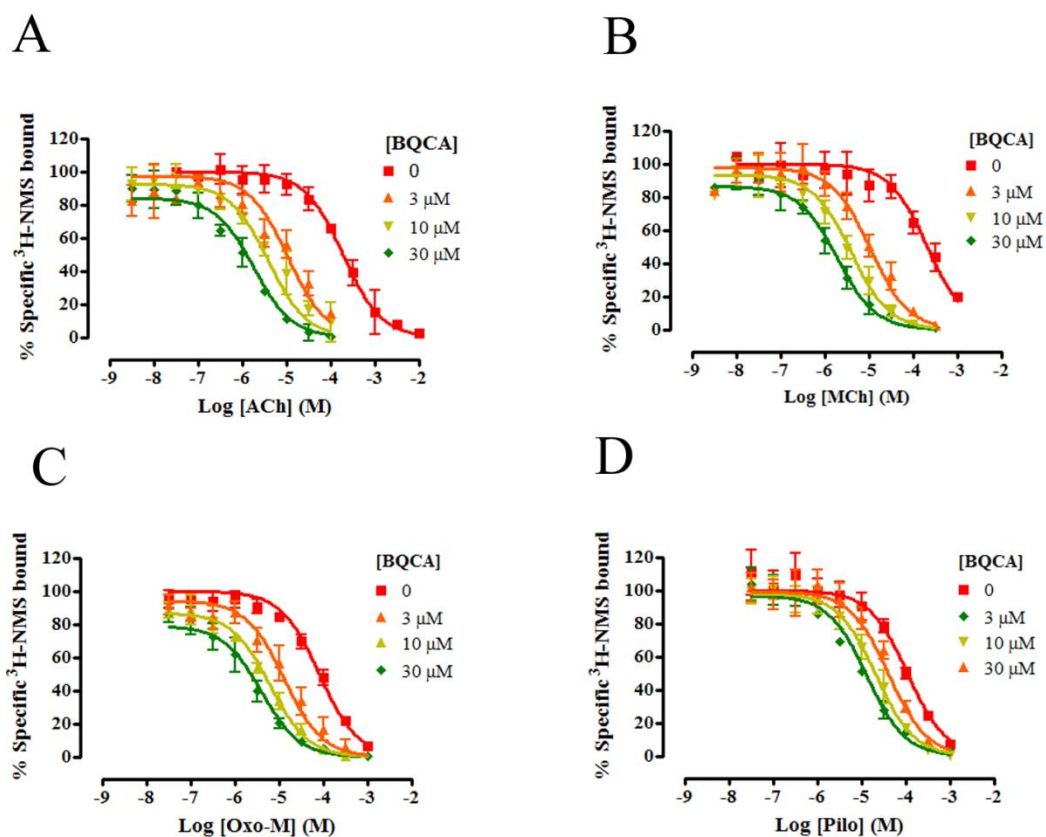


**Figure 5.2.4.1: Probe dependency of BQCA at the M<sub>1</sub> mAChR.** Membranes (10 μg/well) were incubated with ~0.5 nM tritiated NMS (<sup>3</sup>H-NMS) in 96-well plate in the presence of orthosteric agonist and increasing concentration of BQCA for 2 hours at room temperature (final assay volume, 400 μl). 200 μM GTP was included in the assay to ensure the receptor was at a low affinity state. Non-specific binding was determined in the presence of 10 μM atropine. Samples were transferred onto PEI (0.1%) pre-soaked GF/B plates using a TomTec filtration system. Plates were dried extensively and 50 μl scintillation fluids were added to each well. Plates were sealed and radioactivity was determined using a MicroBeta scintillation counter. Data are expressed as a percentage of the specific binding <sup>3</sup>H-NMS. Data points represent the mean ± S.E.M of three independent experiments performed in triplicate.

**Table 5.2.4.1: Effects of BQCA on the affinity of known mAChR orthosteric agonists.**

$pK_I$  is the equilibrium dissociation constant of the agonists and  $\alpha'$  is the binding cooperativity between BQCA and the orthosteric agonists.

Agonist	$pK_I$	$\alpha'$	n
ACh	$4.24 \pm 0.06$	$128.82 \pm 1.35$	3
MCh	$4.13 \pm 0.05$	$131.22 \pm 1.35$	3
Oxo-M	$4.55 \pm 0.03$	$118.45 \pm 1.18$	3
Pilo	$4.44 \pm 0.05$	$11.48 \pm 1.18$	3

### 5.2.5. BQCA potentiates the effect of ACh in mediating [<sup>3</sup>H]-InsPx accumulation through the M<sub>1</sub> mAChR.

The M<sub>1</sub> mAChR signals predominantly through the G<sub>q/11</sub> family of G protein and activate phospholipase C. This results in the production of inositol trisphosphate second messenger molecules. To determine the effects of BQCA on the signalling properties of the M<sub>1</sub> mAChR, a functional assay measuring total inositol phosphates accumulation (<sup>3</sup>H-InsPx) was performed in the presence of lithium. As shown in **Figure 5.2.5.1** and **Table 5.2.6.1**, BQCA has a partial agonist activity when applied alone. However upon co-administration with ACh, BQCA behaved as a positive allosteric modulator causing a concentration-dependent increase in the potency of ACh. There was no increase in the maximal response which could be due to maximum system response being reached. Analysis of the data using the operational model of allosterism and agonism yielded a maximal degree of positive cooperativity between BQCA and ACh ( $\alpha\beta$ ) of  $83.4 \pm 1.68$  (**Table 5.2.6.1**). As previously determined in the radioligand binding assay, the affinity cooperativity ( $\alpha'$ ) between ACh and BQCA at their respective binding sites was ~128, which indicates that the increase in the potency of ACh in mediating <sup>3</sup>H-InsPx accumulation is due to the increase in ACh affinity for the receptor.

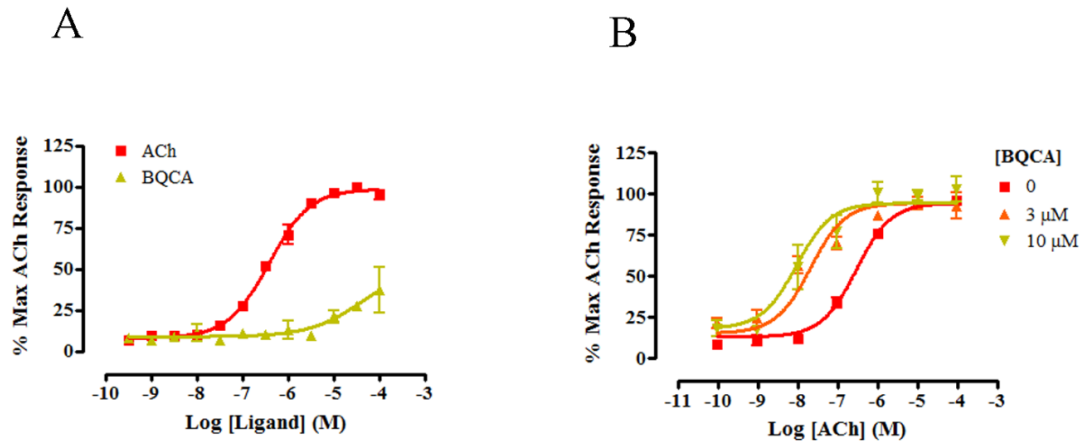


**Figure 5.2.5.1: BQCA agonism and potentiation of ACh potency in total  $^3\text{H}$ -InsPx**

**accumulation assay.** Activation of  $G_{q/11}$  G protein through the  $M_1$  mAChR was assessed by measuring total inositol phosphates accumulation in CHO-h $M_1$ R cells. Cells pre-incubated with 2.5  $\mu\text{Ci/ml}$  [ $^3\text{H}$ ] myo-inositol were treated with lithium and then stimulated with BQCA or ACh for 5 min at 37°C (A). For allosteric interaction studies, cells were pre-treated with BQCA for 1.5 min at 37°C then varying concentrations of ACh was added (B). Reaction was terminated by aspiration of buffer followed by addition of 1 M trichloroacetic acid for 30 min at 4°C. Samples were extracted by separation in trichlorofluoroethane and tri-n-octylamine. The total inositol phosphate ( $^3\text{H}$ -InsPx) was recovered by anion exchange chromatography and radioactivity was detected by liquid scintillation counting. Data are expressed as a percentage of the maximum response achieved by 100  $\mu\text{M}$  ACh. Data points represent the mean  $\pm$  S.E.M of three independent experiments performed in triplicate.

### **5.2.6. BQCA displays allosteric agonism and enhances the potency of ACh in mediating phosphorylation of ERK 1/2.**

In addition to activating phospholipase C, the M<sub>1</sub> mAChR has also been reported to activate extracellular signal regulated protein kinase 1 and 2 (ERK 1/2) in an agonist dependent manner (Berkeley et al., 2001a). As a complementary method to further examine the pharmacological properties of BQCA, functional assay employing receptor mediated ERK1/2 phosphorylation was performed. As can be seen from **Figure 5.2.6.1**, BQCA alone caused a robust phosphorylation of ERK1/2 with a pEC<sub>50</sub> of  $5.57 \pm 0.12$  (**Table 5.2.6.1**). The effects of BQCA on ERK 1/2 phosphorylation reached the same maximal level (E<sub>max</sub>) as ACh at 10 μM which indicate that the compound acts as a full agonist. In contrast to BQCA, ACh activates ERK 1/2 more potently with a pEC<sub>50</sub> of  $7.78 \pm 0.11$ . Due to agonist activity, BQCA causes an increase in the basal response at low ACh concentrations (**Figure 5.2.6.1**) as well as a progressive increase in the potency of concentration-response curves of ACh. These data suggest that BQCA behaves as an ago-allosteric agonist, a compound which enhances the effect of the endogenous ligand but also acts as an agonist in its own right. Analysis of the data using the operational model of allosterism and agonism showed that BQCA has an intrinsic efficacy ( $\tau_B$ ) of  $\sim 15.8$ ;  $\tau$  value  $>10$  indicates full agonism (Black, 1996). Interestingly also, our analysis showed that the maximal degree of positive cooperativity between BQCA and ACh ( $\alpha\beta$ ) was 5011 (**Table 5.2.6.2**). Since the allosteric enhancement of ACh binding affinity ( $\alpha'$ ) was 128, the additional positive cooperativity must be a result of allosteric enhancement of ACh signalling efficacy or the agonist property of BQCA.

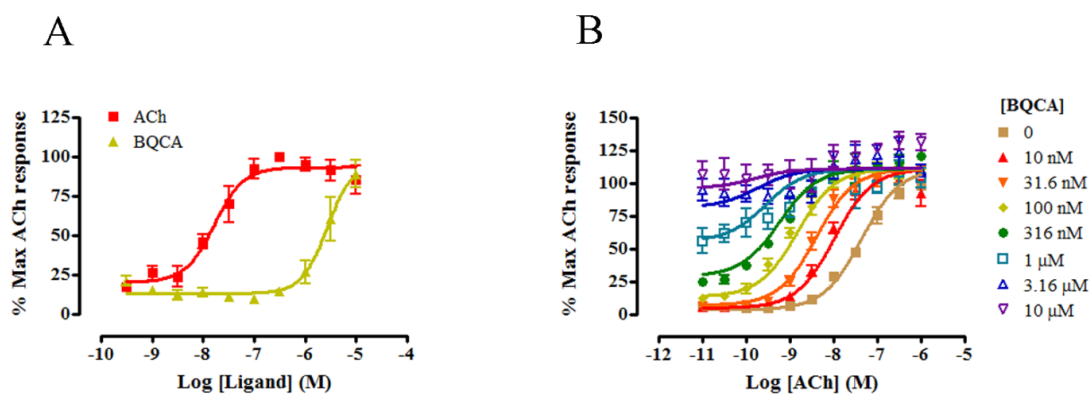


**Figure 5.2.6.1: BQCA agonism and potentiation of ACh potency in ERK 1/2**

**phosphorylation assay.** CHO-hM<sub>1</sub>R cells were seeded at 35 000 cells/well in 96-well plate and serum starved for 4 hours or overnight at 37°C. For agonist studies, cells were stimulated with BQCA or ACh for 5 min at 37°C. For allosteric potentiation studies, cells were incubated for 5 min at 37°C with varying concentrations of ACh in the absence and presence of increasing concentrations of BQCA. Reaction was terminated by removal of buffer followed by addition of 50 μl lysis buffer for 30 min at room temperature. Each lysate (4 μL) was transferred into 384-well plates and detection mix (7 μl) consisting of detection buffer, activation buffer, donor beads and acceptor beads (60;10;1;1 v/v) were added to each well. Plates were incubated for 2 hrs at RT with gentle agitation and fluorescence signal was measured using AlphaScreen plate reader. Data are expressed as a percentage of the maximum response achieved by 1 μM ACh. Data points represent the mean ± S.E.M of three independent experiments performed in triplicate.

**Table 5.2.6.1: Intrinsic activity of ACh and BQCA in <sup>3</sup>H-InsPx accumulation and ERK 1/2 phosphorylation assays.** pEC<sub>50</sub> represents agonist potency and Rmax denotes maximum response elicited by the agonists.

Agonist	<sup>3</sup> H-InsPx accumulation			ERK1/2 phosphorylation		
	pEC <sub>50</sub>	Rmax	n	pEC <sub>50</sub>	Rmax	n
ACh	6.00 ± 0.43	100	3	7.78 ± 0.11	100	3
BQCA	ND	33.56 ± 9.53	3	5.57 ± 0.12	96.46 ± 12.51	3

**Table 5.2.6.2: Potentiation of ACh mediated  $^3\text{H-InsPx}$  accumulation and ERK 1/2 phosphorylation by BQCA.**  $\alpha\beta$  is the maximal degree of cooperativity between BQCA and ACh and it describes the effects of BQCA on both the affinity and signalling efficacy of ACh.  $\tau_B$  denotes the agonist property of BQCA at the two signalling pathways.

Modulator	$^3\text{H-InsPx}$ accumulation			ERK1/2 phosphorylation		
	$\alpha\beta$	$\tau_B$	n	$\alpha\beta$	$\tau_B$	n
BQCA	$85.11 \pm 0.16$	$0.17 \pm 0.16$	3	$5011 \pm 1.23$	$15.08 \pm 1.12$	3

### **5.2.7. M<sub>1</sub> mediated phosphorylation of ERK 1/2 occurs mainly through G protein pathway and is sensitive to PKC inhibition.**

Receptor mediated phosphorylation of ERK 1/2 can occur via two distinct mechanisms; arrestin-dependent and G protein-dependent. Whereas G protein-dependent ERK 1/2 phosphorylation is rapid and transient, arrestin-dependent ERK 1/2 phosphorylation is slow in onset and is more sustained (Luttrell *et al.*, 2010). To assess the contributions of these two distinct pathways, time course experiments were performed using BQCA and ACh at a concentration that gives maximum ERK 1/2 phosphorylation. Additionally as a measure of G protein-dependent mechanism, broad spectrum protein kinase C (PKC) inhibitor, bisindolylmaleimide I (Bis I) was included in the assay. In the absence of the PKC inhibitor, both ACh and BQCA caused a rapid increase in ERK 1/2 phosphorylation that peaked after 5 minutes of stimulation (**Figure 5.2.7.1**). Very little activation was detected at later time points which suggest that phosphorylation of ERK 1/2 through M<sub>1</sub> mAChR is primarily mediated by G protein. The application of 10  $\mu$ M Bis I for 10 min dramatically reduced the early phase ERK 1/2 phosphorylation by both ligands, which confirms that G protein-dependent pathway is the predominant mechanism that mediates ERK 1/2 phosphorylation.

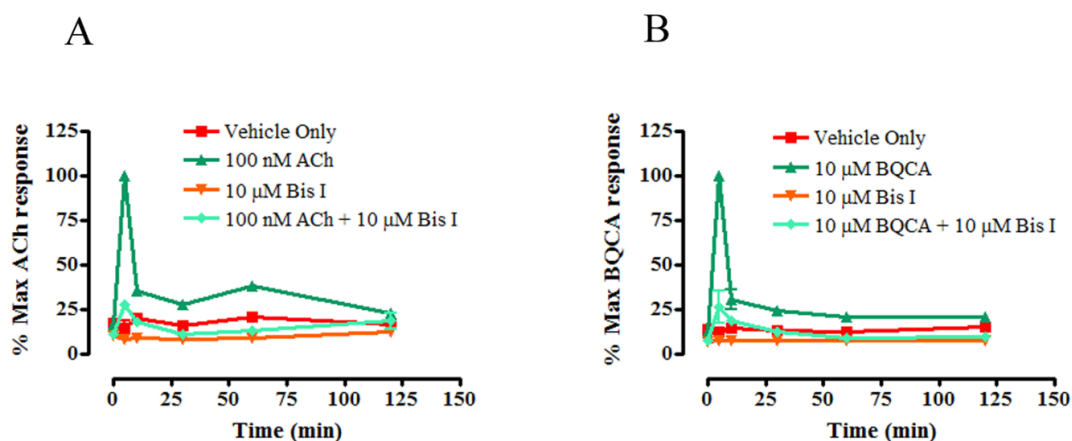


**Figure 5.2.7.1: Kinetics and PKC dependency of  $M_1$  mAChR mediated ERK1/2**

**phosphorylation.** CHO-h $M_1$ R cells seeded at 35 000 cells/well in 96-well plate were serum starved for 4 hours or overnight at 37°C and then stimulated with BQCA or ACh for the indicated times. For inhibition studies, cells were pre-incubated with 10 μM Bis I for 10 min prior to addition of ACh or BQCA. Reaction was terminated by removal of buffer followed by addition of 50 μl lysis buffer for 30 min at room temperature. Each lysate (4 μL) was transferred into 384-well plates and detection mix (7 μl) consisting of detection buffer, activation buffer, donor beads and acceptor beads (60;10;1;1 v/v) were added to each well. Plates were incubated for 2 hrs at RT with gentle agitation and fluorescence signal was measured using AlphaScreen plate reader. Data are expressed as a percentage of the maximum response achieved by 100 nM ACh or 10 μM BQCA. Data points represent the mean ± S.E.M of three independent experiments performed in triplicate.

### 5.2.8. BQCA partially enhances ACh-mediated global phosphorylation of M<sub>1</sub> mAChR

Many GPCRs, including the M<sub>1</sub> mAChR undergo rapid phosphorylation following agonist stimulation and this process is important for desensitisation and directing receptor signalling to arrestin-dependent pathways (Claing *et al.*, 2002; Pierce *et al.*, 2001; Waugh *et al.*, 1999). To determine whether BQCA could modulate the phosphorylation state of the M<sub>1</sub> mAChR, phosphorylation assays using intact cells were performed. Initially the experiment was carried out in the absence and presence of a high concentration of ACh. As shown in **Figure 5.2.8.1**, the M<sub>1</sub> mAChR is phosphorylated under basal conditions and ACh at 100 µM caused a robust increase in the phosphorylation state of the receptor. In interaction studies BQCA at 3 µM, did not cause phosphorylation on its own (**Figure 5.2.8.2**). However in the presence of a low concentration of ACh (i.e. 1 µM), BQCA enhanced the phosphorylation state of the M<sub>1</sub> mAChR. However the level of phosphorylation is less than that mediated by 100 µM ACh, an agonist concentration which occupies equivalent receptor populations. This suggests that BQCA only partially increased the levels of M<sub>1</sub> mAChR phosphorylation in response to sub maximal concentration of ACh.

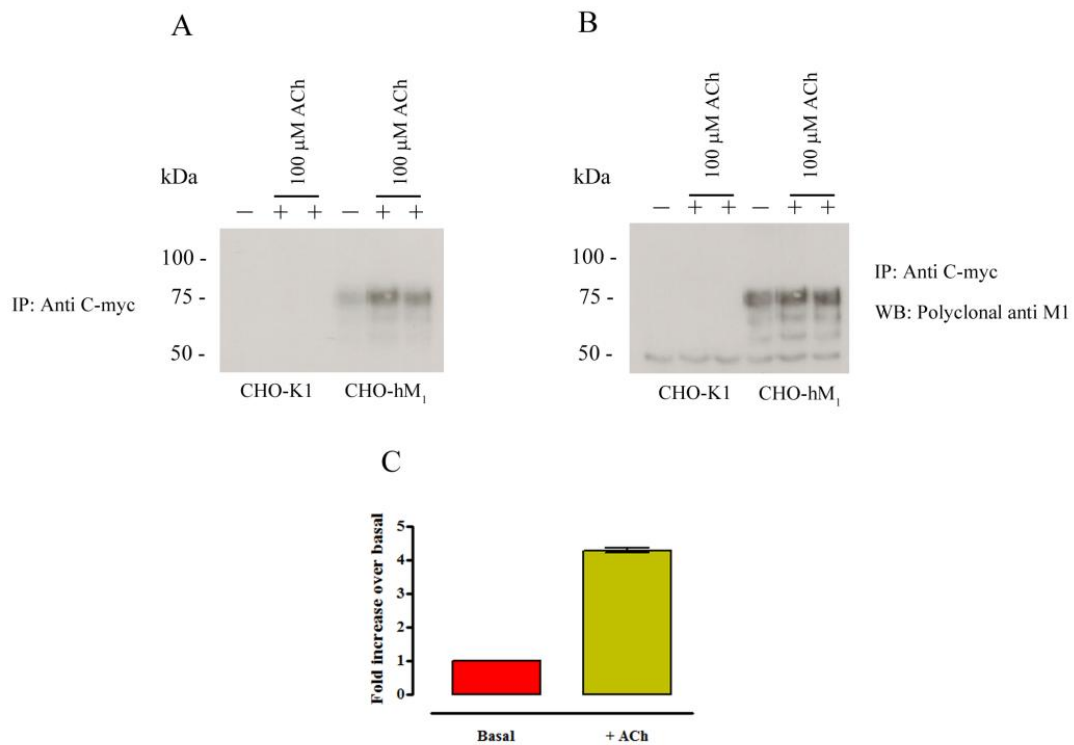


**Figure 5.2.8.1. Global phosphorylation of M<sub>1</sub> mAChR under basal conditions and in response to ACh stimulation.** CHO-hM<sub>1</sub>R cells grown on 6-well plates were incubated with 50 μCi/well <sup>32</sup>P-orthophosphate for 1 hr 37°C and then stimulated with buffer or 100 μM ACh for 5 min. Cells were lysed with RIPA buffer and receptors were purified by immunoprecipitation. Purified receptors were resolved on 8% SDS-PAGE gels and transferred onto nitrocellulose membrane. Phosphorylated receptors were visualised by autoradiography (A) and resolved receptor proteins were immunoblotted with a polyclonal M<sub>1</sub> mAChR specific antibody to detect for loading consistency (B). Quantified data are presented as increase over basal phosphorylation (C). Immunoblot and autoradiogram represents three independent experiments performed in singlicate. Bar graph represents the mean ± S.E.M of the phosphorylation bands.

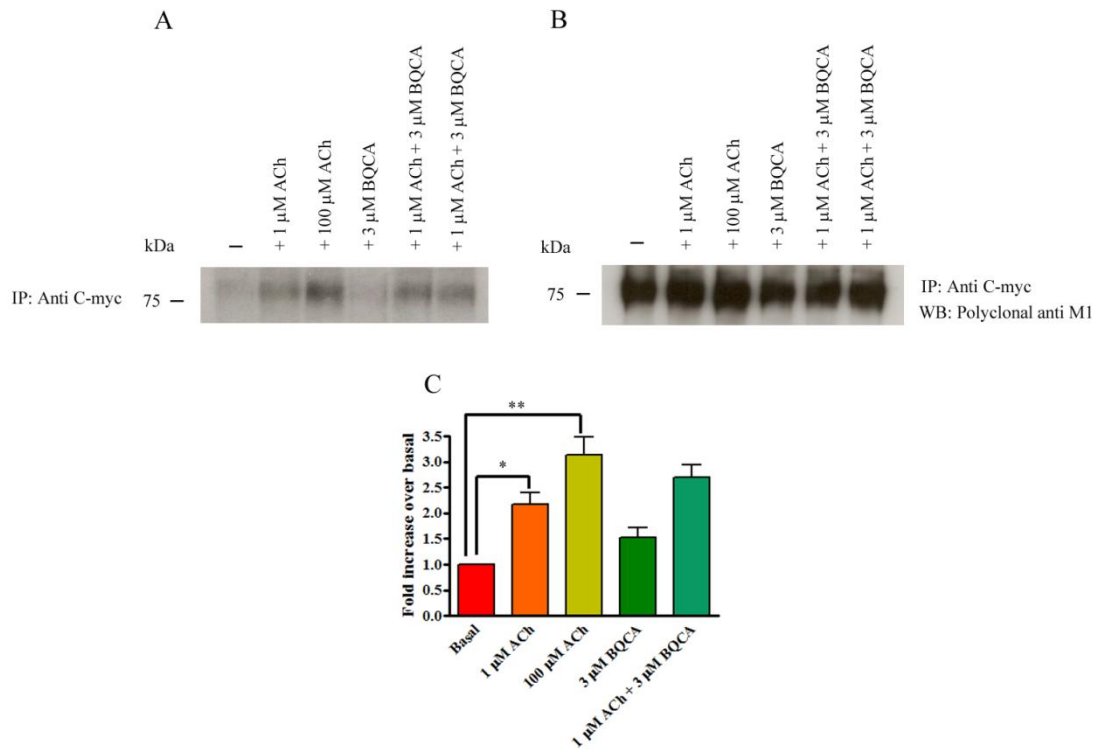


**Figure 5.2.8.2: Effects of BQCA on ACh mediated global phosphorylation of M<sub>1</sub> mAChR.** CHO-hM<sub>1</sub>R cells grown on 6-well plates were incubated in 50  $\mu$ Ci/well <sup>32</sup>P-orthophosphate for 1 hr at 37°C and then stimulated with buffer, BQCA and ACh alone or in combination for 5 min at 37°C. Cells were lysed with RIPA buffer and receptors were purified by immunoprecipitation. Purified receptors were resolved on 8% SDS-PAGE gels and then transferred onto nitrocellulose membrane. Receptor phosphorylation was detected by autoradiography (A) and resolved receptor proteins were immunoblotted with a polyclonal M<sub>1</sub> mAChR specific antibody to detect for loading consistency (B). Quantified data are presented as increase over basal phosphorylation (C). Immunoblot and autoradiogram represents three independent experiments performed in singlicate. Bar graph represents the mean  $\pm$  S.E.M of the phosphorylation bands. \*P<0.05, \*\*P<0.01; as measured using a one-way ANOVA with Bonferonni's post-hoc test.

### **5.2.9. BQCA caused similar phosphorylation patterns of the M<sub>1</sub> mAChR as ACh when tested as a positive allosteric modulator.**

It has been reported that the patterns of phosphorylation for many GPCRs are important for determining the signalling properties of the receptor (Nobles *et al.*, 2011; Rajagopal *et al.*, 2011; Tobin, 2008; Tobin *et al.*, 2008; Zidar *et al.*, 2009). To determine whether BQCA could differentially modulate the phosphorylation state of the M<sub>1</sub> mAChR, two dimensional phosphopeptide mapping experiments were performed. As shown in **Figure 5.2.9.1**, the phosphorylation patterns of the M<sub>1</sub> mAChR in response to a low concentration of ACh in the presence of BQCA is qualitatively similar to that mediated by ACh alone at equivalent receptor occupancy; this suggests that BQCA increases ACh-mediated receptor phosphorylation solely by increasing the ACh affinity for the receptor and not by engendering a novel receptor conformation. Due to the difficulty in obtaining phosphopeptide maps for low levels of basal phosphorylation, the experiments were performed in absence of basal controls.

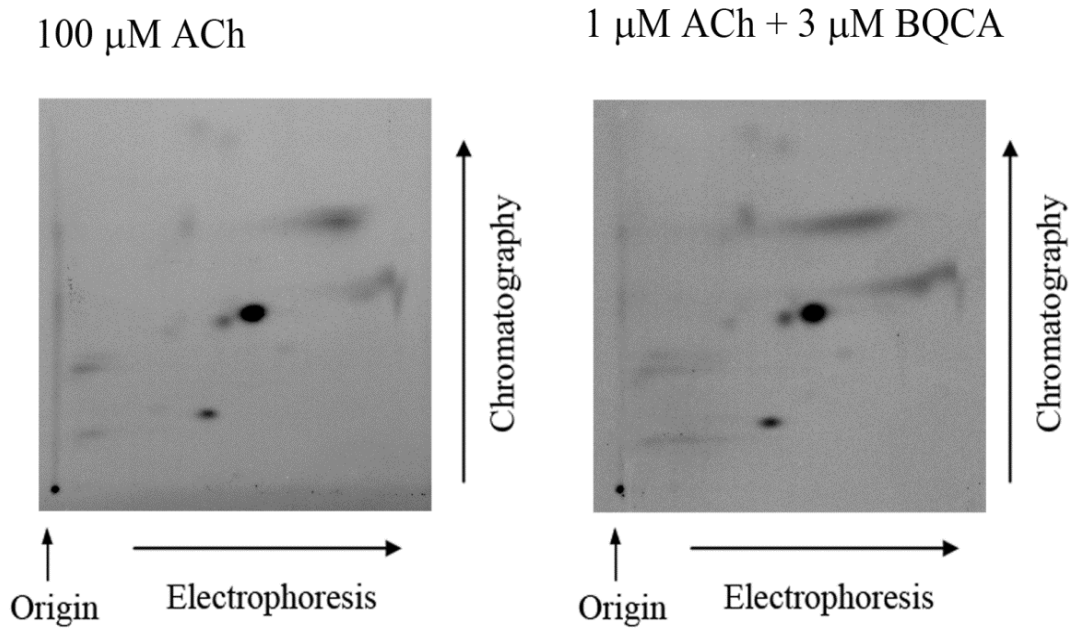


**Figure 5.2.9.1: Two dimensional analysis of the phosphorylation state of the M<sub>1</sub> mAChR in response to ACh in the presence and absence of BQCA.** Purified receptor proteins were digested with trypsin and phosphopeptides were separated on thin layer chromatography plate by electrophoresis in one dimension and chromatography in the other. Plates were exposed to phosphoimager film and resolved phosphopeptides were revealed by STORM phosphoimager. Data represents four independent experiments performed in singlicate.

### **5.2.10. BQCA partially enhances ACh-mediated phosphorylation of M<sub>1</sub> mAChR at serine 228.**

Mass spectrometric studies performed by Dr Adrian Butcher have shown that the M<sub>1</sub> mAChR is phosphorylated at 12 residues within the third intracellular loop of the receptor. Antibodies against some of these residues were raised and one of them was pS228 which recognises phosphorylation at serine 228. This antibody was then used in western blotting experiments to determine if BQCA could modulate phosphorylation of the M<sub>1</sub> mAChR specifically at serine 228. The antibody was initially characterised using receptors that had been treated with phosphatase enzyme. As shown in **Figure 5.2.10.1** the antibody recognised only the agonist stimulated receptors and that phosphatase treatment abolished the immunoreactivity. This confirms that pS228 is phosphorylation sensitive. In interaction studies, BQCA at 3 µM did not cause phosphorylation of serine 228 (**Figure 5.2.10.2**). When co-applied with a low ACh concentration, BQCA caused an enhancement of phosphorylation of serine 228 compared to ACh alone. However, the level of enhanced phosphorylation is less than that mediated by a high concentration of ACh predicted to occupy similar receptor populations. This suggests that BQCA only partially potentiates phosphorylation of serine 228.

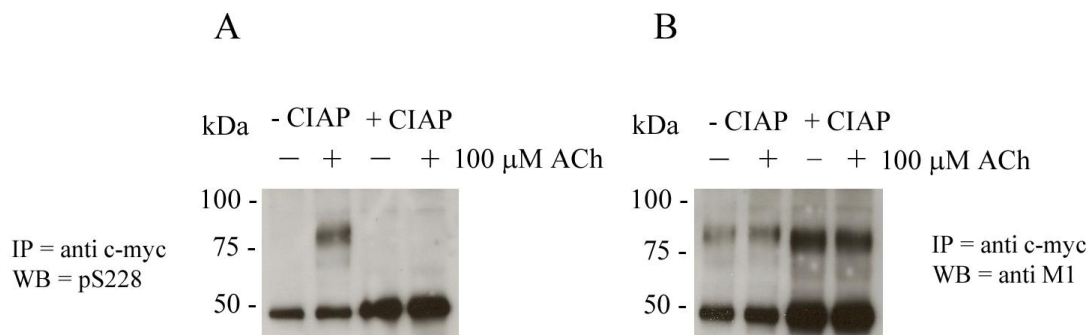


**Figure 5.2.10.1: Characterisation of pS228 antibody using phosphatase treatment.** CHO-hM<sub>1</sub>R cells grown on 6-well plate were stimulated with ACh for 5 min at 37°C. Cells were lysed with RIPA buffer and receptors were purified by immunoprecipitation. Purified receptors were treated with calf intestinal alkaline phosphatase (CIAP) or buffer before being resolved on 8% SDS-PAGE gels. Resolved receptor proteins were immunoblotted with pS228 antibody (A) or anti M<sub>1</sub> mAChR antibody (B). Data represents two experiments performed in singlicate.

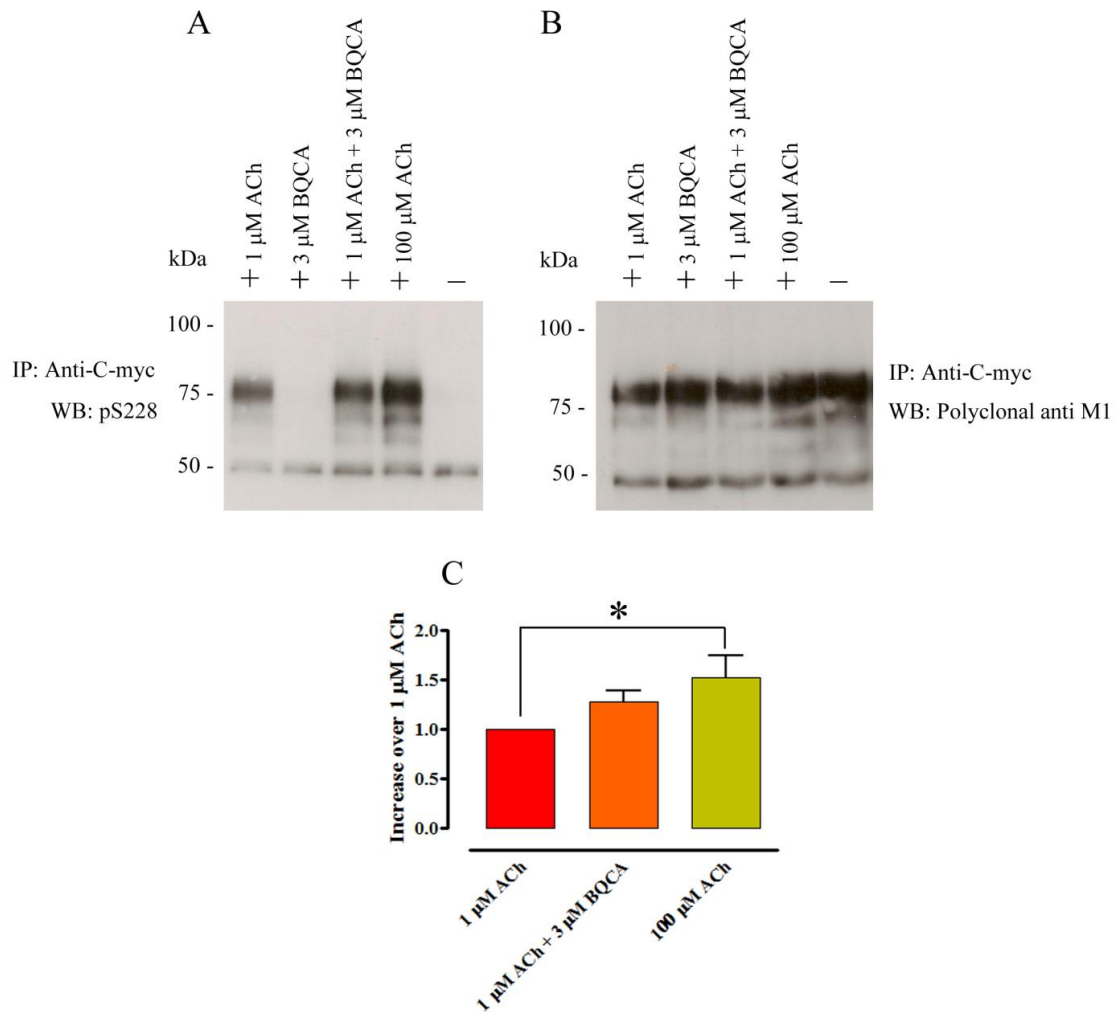


**Figure 5.2.10.2: Effects of BQCA on ACh mediated phosphorylation of M<sub>1</sub> mAChR at Ser228.** CHO-hM<sub>1</sub>R cells grown on 6-well plate were stimulated with ACh in the presence and absence of BQCA for 5 min at 37°C and the receptors were purified by immunoprecipitation. Purified receptors were resolved on 8% SDS-PAGE gels and immunoblotted with pS228 antibody (A) or anti M<sub>1</sub> mAChR antibody (B). Immunoblots represent three independent experiments performed in singlicate. Bar graph represents the mean ± S.E.M of the phosphorylation bands.\*P<0.05; as measured using a one-way ANOVA with Bonferonni's post-hoc test.

### **5.1.11. BQCA as an agonist preferentially promotes phosphorylation of serine 228.**

As previously determined in signalling assays (**Figure 5.2.5.1** and **Figure 5.2.6.1**), BQCA has intrinsic efficacy in its own right and this can be revealed in highly coupled system or if sufficiently high concentrations of the modulator is used. To test whether BQCA could drive phosphorylation of the M<sub>1</sub> mAChR in the absence of ACh, western blot experiments were performed using pS228 antibody. Consistent with previous data, BQCA at 3  $\mu$ M did not cause phosphorylation of serine 228 (**Figure 5.2.11.1**). Surprisingly at 100  $\mu$ M BQCA caused a greater phosphorylation of serine 228 compared to ACh at similar receptor occupancy. This could be interpreted as BQCA, as being biased towards phosphorylation of this residue compared to ACh or that the compound is less able to cause desensitisation.

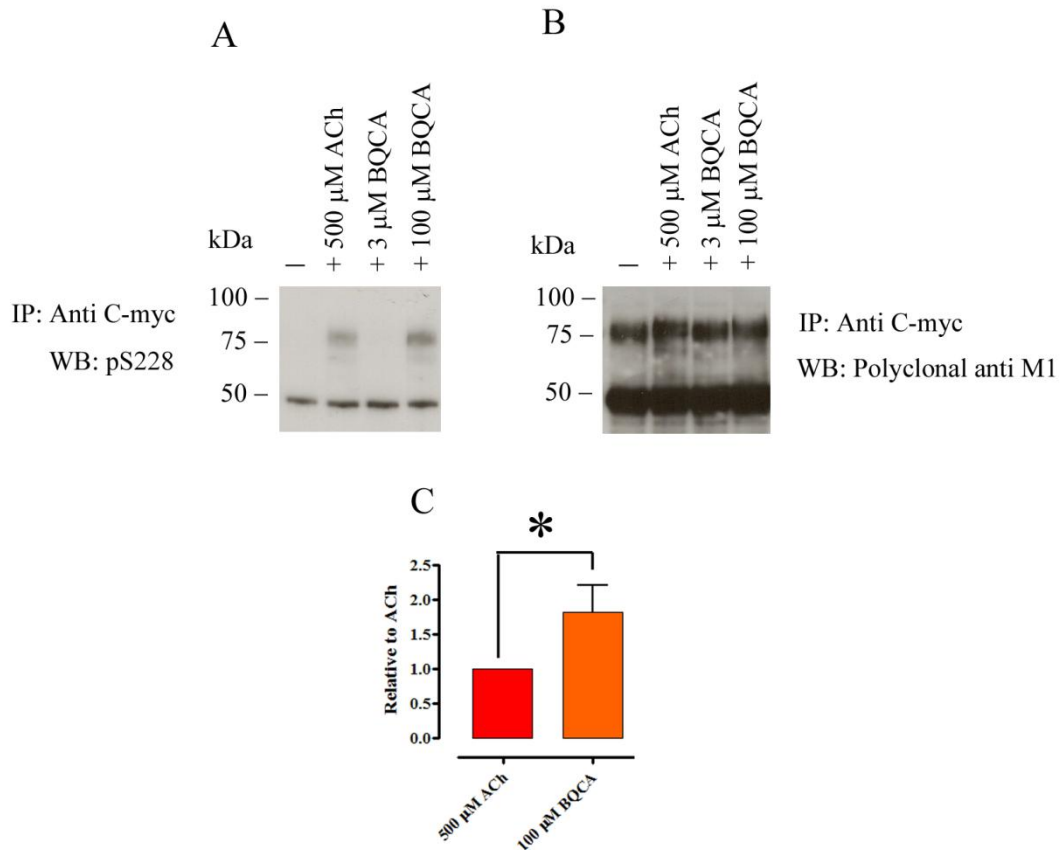


**Figure 5.2.11.1: Comparison of the phosphorylation level of M<sub>1</sub> mAChR at serine 228 following stimulation by BQCA and ACh.** CHO-hM<sub>1</sub>R cells grown on 6-well plate were stimulated with ACh or BQCA for 5 min at 37°C and the M<sub>1</sub> mAChRs were purified by immunoprecipitation. Purified receptors were resolved on 8% SDS-PAGE gels and immunoblotted with pS228 antibody (A) or M<sub>1</sub> mAChR antibody (B). Immunoblots represent three independent experiments performed in singlicate. Bar graph represents the mean  $\pm$  S.E.M of the phosphorylation bands. \*P<0.05; as measured using a one-way ANOVA with Bonferonni's post-hoc test.

### **5.2.12. VU0357017 displays a weak affinity at the M<sub>1</sub> mAChR but does not potentiate the affinity of ACh**

In addition to investigating the effects of positive allosteric modulator on the behaviour of the M<sub>1</sub> mAChR, we are also interested in investigating other allosteric ligands such as allosteric agonist/bitopic ligands. Recently a novel compound named VU0357017 was reported to be an allosteric agonist at the M<sub>1</sub> mAChR based on *in vitro* calcium signalling assays (Lebois *et al.*, 2010). To test whether this ligand affects the affinity of ACh at the M<sub>1</sub> mAChR, radioligand binding assays were performed under equilibrium conditions in the presence of 200  $\mu$ M GTP. Similar to BQCA, VU0357017 has a weak affinity at the M<sub>1</sub> mAChR and a weak negative cooperativity with <sup>3</sup>H-NMS binding ( $\alpha = 0.37 \pm 0.17$ ) (**Figure 5.2.12.1A**). However, VU0357017 did not alter the affinity of ACh at the M<sub>1</sub> mAChR, suggesting that the compound does not act as a positive allosteric modulator of ACh binding (**Figure 5.2.12.1B**).

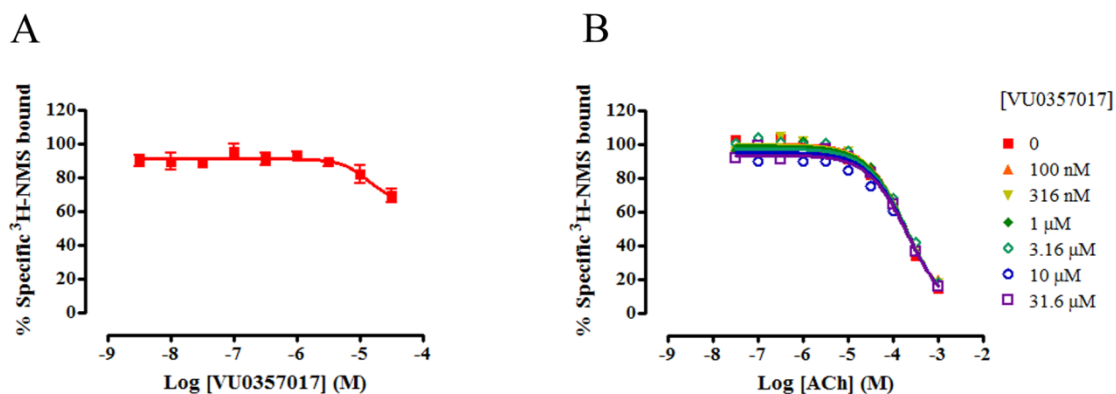


**Figure 5.2.12.1.: Effects of VU0357017 on the binding of <sup>3</sup>H-NMS and ACh.** CHO-hM<sub>1</sub>R membranes (10 μg/well) were incubated with ~0.5 nM <sup>3</sup>H-NMS in 96-well plate in the presence of increasing concentration of VU0357017 for 2 hours at room temperature (final assay volume, 400 μl). Interaction studies between ACh and VU0357017 were performed in the presence of 200 μM GTP. Non-specific binding was determined in the presence of 10 μM atropine. Samples were transferred onto PEI (0.1%) pre-soaked GF/B plates using a TomTec harvester. Plates were dried extensively and 50 μl scintillation fluids were added to each well. Plates were sealed and radioactivity was determined using a MicroBeta scintillation counter. Data are expressed as a percentage of the specific binding <sup>3</sup>H-NMS. Data points represent the mean ± S.E.M of three independent experiments performed in triplicate.

### **5.2.13. VU0357017 does not cause InsPx accumulation but negatively affect the potency of ACh**

The ability of VU0357017 to modulate the signalling of M<sub>1</sub> mAChR was tested on InsPx accumulation assay. As shown in **Figure 5.2.13.1**, VU0357017 does not cause InsPx accumulation on its own up to 10 µM, suggesting that this compound has no intrinsic efficacy in this system. Interestingly, when co-administered with ACh, VU0357017 caused a slight decrease in potency (although not statistically significant;  $P > 0.05$  as measured by one way ANOVA) in the concentration response curve of ACh, indicating that the compound could behave as a weak negative allosteric modulator. However due to insolubility, VU0357017 could not be tested beyond 30 µM which limits the extent of ACh potency modulation that can be achieved by this compound.

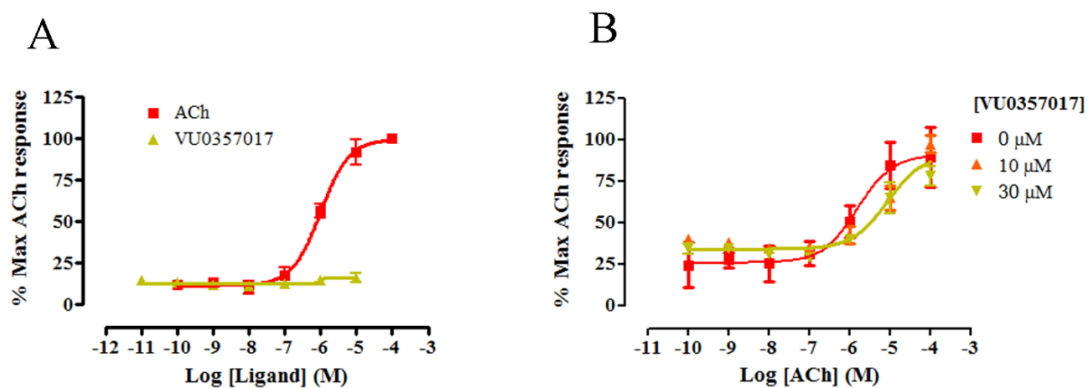


**Figure 5.2.13.1: VU0357017 agonism and potentiation of ACh potency in total  $^3\text{H}$ -InsPx accumulation assay.** CHO-hM<sub>1</sub>R cells were incubated in 2.5  $\mu\text{Ci/ml}$  [ $^3\text{H}$ ]-inositol for 24 hr at 37°C and then stimulated with VU0357017 or ACh for 5 min at 37°C (A). For interaction studies, cells were pre-incubated with VU0357017 for 1.5 min at 37°C prior to the addition of ACh. Reaction was terminated by aspiration of buffer followed by addition of 1 M trichloroacetic acid for 30 min at 4°C. Samples were extracted by separation in trichlorofluoroethane and tri-n-octylamine. The total inositol phosphate ( $^3\text{H}$ -InsPx) was recovered by anion exchange chromatography and radioactivity was detected by liquid scintillation counting. Data are expressed as a percentage of the maximum response achieved by 100  $\mu\text{M}$  ACh. Data points represent the mean  $\pm$  S.E.M of three independent experiments performed in triplicate.

#### **5.2.14. VU0357017 behaved as a partial agonist in promoting ERK1/2 phosphorylation but negatively affected the potency of ACh**

To further investigate the effects of VU0357017 on the signalling of the M<sub>1</sub> mAChR, a second assay employing ERK1/2 phosphorylation was performed. Here VU0357017 acts a weak partial agonist when tested alone and elicited a maximum response  $38 \pm 12$  % of ACh response (**Figure 5.2.14.1**). VU0357017 also has a significantly lower potency compared to ACh (pEC<sub>50</sub>  $7.63 \pm 0.10$  vs.  $6.23 \pm 0.20$ ). When investigated in interaction studies, VU0357017 caused a progressive rightward shift in the concentration response curve of ACh and a concentration dependent increase in the basal response highlighting negative cooperativity and partial agonism, respectively. However the data did not fit with the operational model of allosterism and agonism suggesting that the compound does not behave allosterically.

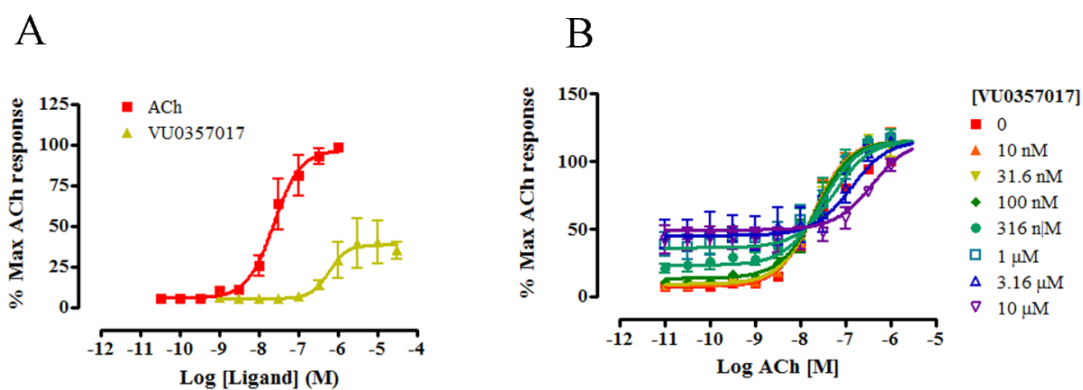


**Figure 5.2.14.1: M<sub>1</sub> mAChR mediated activation of ERK 1/2 proteins.** CHO-hM<sub>1</sub>R cells were serum starved for 4 hours or overnight at 37°C and then stimulated with VU0357017 or ACh for 5 min at 37°C. For allosteric potentiation studies, cells were incubated for 5 min at 37°C with varying concentrations of ACh in the absence and presence of increasing concentrations of VU0357017. Reaction was terminated by removal of buffer followed by addition of 50 μl lysis buffer for 30 min at room temperature. Each lysate (4 μL) was transferred into 384-well plates and detection mix (7 μl) consisting of detection buffer, activation buffer, donor beads and acceptor beads (60;10;1;1 v/v) were added to each well. Plates were incubated for 2 hrs at RT with gentle agitation and fluorescence signal was measured using AlphaScreen plate reader. Data are expressed as a percentage of the maximum response achieved by 1 μM ACh. Data points represent the mean ± S.E.M of three independent experiments performed in triplicate.

### **5.2.15. VU0357017 causes minimal M<sub>1</sub> mAChR phosphorylation**

To determine if VU0357017 could promote phosphorylation of the M<sub>1</sub> mAChR, experiments were performed using <sup>32</sup>P-labelling and western blotting using phosphorylation specific antibody (pS228). As shown in **Figure 5.2.15.1** and **Figure 5.2.15.2**, VU0357017 caused a very weak phosphorylation of the M<sub>1</sub> mAChR globally and at Ser228. These data are consistent with the ERK 1/2 phosphorylation data indicating that VU0357017 is a very weak partial agonist.

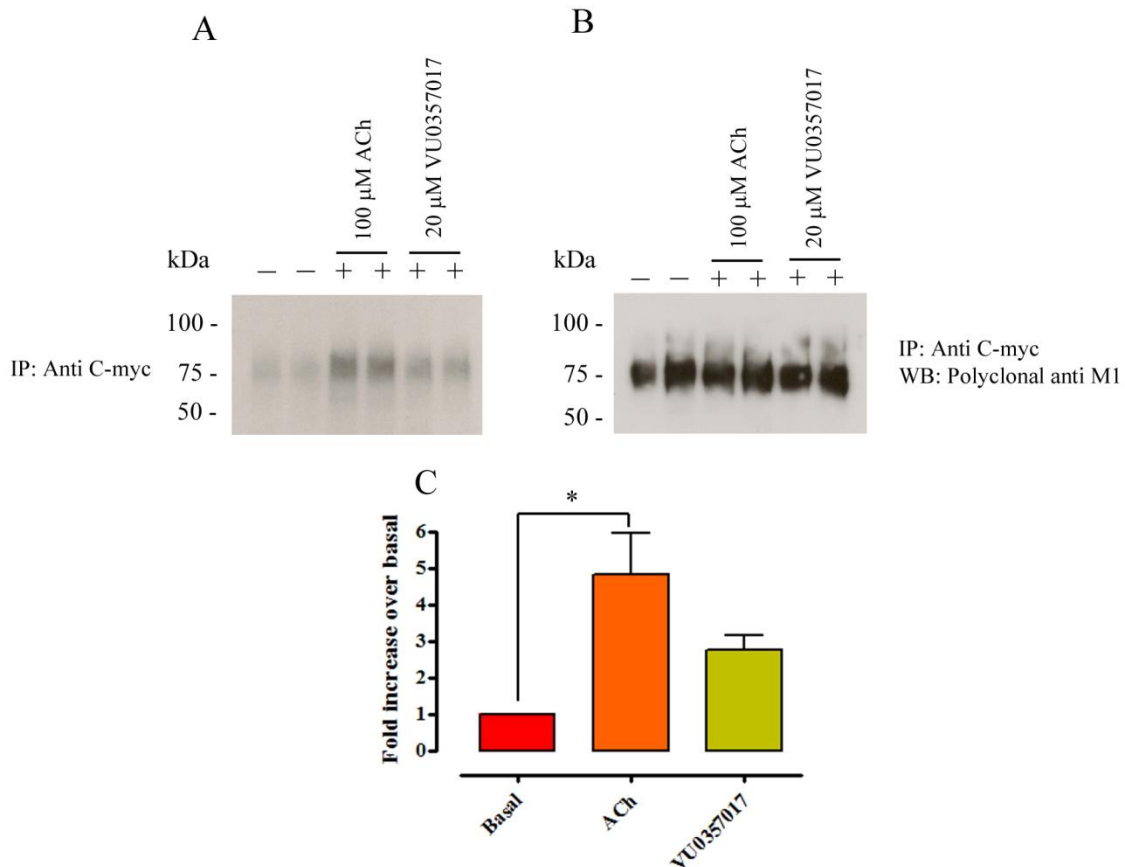


**Figure 5.2.15.1: VU0357017 caused weak phosphorylation of M<sub>1</sub> mAChR globally.**

CHO-hM<sub>1</sub>R cells grown on 6-well plates were incubated with 50 μCi/well of <sup>32</sup>P-orthophosphate for 1 hr at 37°C and then stimulated with ACh or VU0357017 for 5 min at 37°C. Receptors were purified by immunoprecipitation and resolved on 8% SDS-PAGE gels. Phosphorylation was detected by autoradiography (A) and the receptor was immunoblotted with anti M<sub>1</sub> mAChR antibody (B) to detect for loading consistency. Immunoblot and autoradiogram represents three independent experiments performed in singlicate. Bar graph represents the mean ± S.E.M of the phosphorylation bands. \*P<0.05; as measured using a one-way ANOVA with Bonferonni's post-hoc test.

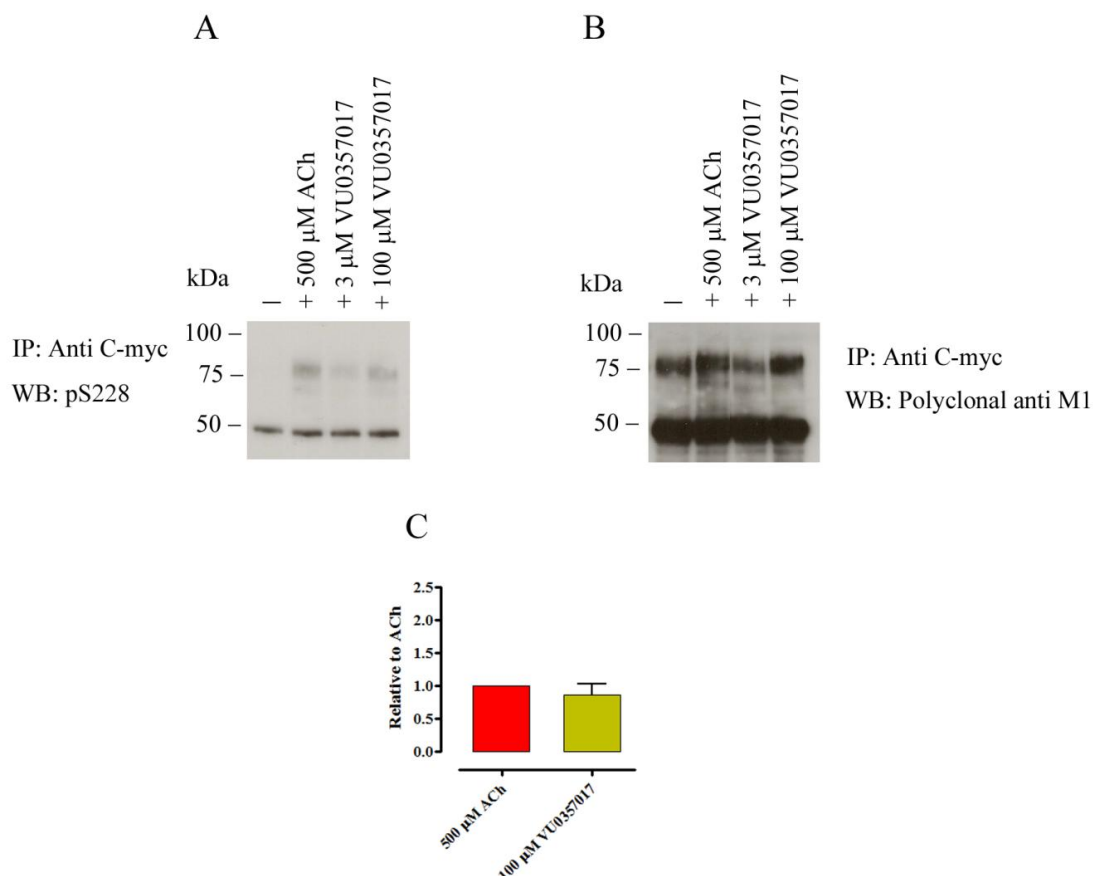


**Figure 5.2.15.2: VU0357017 caused a weak phosphorylation of M<sub>1</sub> mAChR at serine 228.** CHO-hM<sub>1</sub>R cells grown on 6-well plates were stimulated with ACh or VU0357017 for 5 min at 37°C and the receptors were purified by immunoprecipitation. Purified receptors were resolved on 8% SDS-PAGE gels and immunoblotted with pS228 antibody (A) or M<sub>1</sub> mAChR antibody (B). Data represent three independent experiments performed in singlicate. Bar graph represents the mean  $\pm$  S.E.M of the phosphorylation bands.

### 5.3. Discussion

The M<sub>1</sub> mAChR has long been considered as an important drug target for the treatment of cognitive deficits associated with Alzheimer's disease and schizophrenia (Felder *et al.*, 2000; Langmead *et al.*, 2008b; Wess *et al.*, 2007). Traditionally it has been difficult to develop drugs that selectively target the M<sub>1</sub> mAChR because the ligand binding site used by ACh is highly conserved among the five mAChR subtypes. However, the realisation that the M<sub>1</sub> mAChR also has an alternative binding site, termed the allosteric site, that is less evolutionarily conserved has resulted in the discovery of ligands that display superior selectivity for the M<sub>1</sub> mAChR compared to the other mAChR subtypes. These compounds provide important leads in drug discovery programs and valuable research tools to validate the physiological roles of the M<sub>1</sub> mAChR *in vivo*.

Ligands that interact with receptors allosterically often have complex pharmacology and can alter the receptor behaviour in many ways. As such it is necessary to profile these compounds in a wide range of assays to understand their mode of action. This study therefore focuses on the investigation of the pharmacology of two recently discovered allosteric ligands, BQCA and VU0357017 (Canals *et al.*, 2012; Digby *et al.*, 2012; Lebois *et al.*, 2010; Shirey *et al.*, 2008) at the M<sub>1</sub> mAChR heterologously expressed in CHO cells. Our data showed that BQCA has a positive binding cooperativity with ACh, increasing the affinity of ACh at the receptor. However, BQCA has a negative binding cooperativity with the antagonist NMS, which suggests that BQCA preferentially stabilises the active receptor conformation. This probe dependency was further evident in experiments performed with other known orthosteric agonists such as Pilo, MCh and Oxo-M. Whereas the binding cooperativity between BQCA and the partial agonist Pilo was weakly positive, the binding cooperativity between the modulator and the full agonists, MCh and Oxo-M was strongly positive. Studies by others also confirmed the probe dependency of BQCA and highlighted the importance of

choosing the right orthosteric agonist in characterising allosteric modulators (Canals *et al.*, 2012).

Another important property of allosteric modulators is saturability such that the degree of modulation is limited to certain level (at which no further potentiation can be achieved even with increasing concentrations of the modulator). BQCA also possesses this property as evident in competition binding with Pilo (**Figure 5.2.4.1**).

It would be interesting to define the mechanism(s) of affinity modulation by performing binding kinetics experiments to see if BQCA altered the association and dissociation rates of the agonists from the receptor. However the lack of radiolabelled agonists and the difficulty in performing binding kinetics experiments with a high affinity antagonist and low affinity allosteric modulator/orthosteric agonists has prevented us from performing these experiments.

In addition to modulating the binding affinity, allosteric modulators can also modulate the potency of the orthosteric ligand(s) in promoting receptor activation (Conn, 2009). To determine the effects of BQCA on the potency of ACh, total inositol phosphates accumulation and ERK 1/2 phosphorylation assays were performed. The data showed that BQCA also acts as a positive allosteric modulator and the compound increases the potency of ACh in activating these two signalling pathways. The degree of potentiation in inositol phosphates accumulation assay was consistent with, or can be rationalised by, the increase in ACh affinity for the receptor. However, the increase in ACh potency in promoting ERK 1/2 phosphorylation was greater than the ACh affinity modulation. This could be due to the amplification of receptor signal or that BQCA increases the signalling efficacy of ACh. Since BQCA alone caused ERK 1/2 phosphorylation it is difficult to discern which other factors (beside an increase in ACh affinity) contribute to the increase in ACh potency.

Interestingly, the agonist property of BQCA was not detected in inositol phosphates accumulation. This could be due to differences in receptor reserve between the two systems. It is also noteworthy that these two signalling pathways emanate from the same transducer protein (i.e. heterotrimeric G proteins) since PKC inhibition by bisindolylmaleimide I abrogates ERK 1/2 phosphorylation.

In response to agonist stimulation the M<sub>1</sub> mAChR undergoes rapid phosphorylation and this process has been linked to receptor desensitisation. To determine if BQCA could modulate this regulatory process, phosphorylation experiments were performed using metabolic labelling of cells with <sup>32</sup>P-orthophosphate and western blotting with phosphorylation specific antibody (pS228). In both experiments, BQCA potentiated the phosphorylation state of the receptor to a level that is less than that mediated by ACh alone at equivalent receptor occupancy. This could be that the receptor adopts a slightly less active conformation in the combined presence of low levels of ACh and BQCA compared to a high concentration of ACh. Overall the patterns of phosphorylation revealed by two dimensional phosphopeptide mapping were similar, suggesting that BQCA as a positive allosteric modulator is non-biased.

However when tested as an agonist, BQCA appears to be more efficacious at causing phosphorylation of serine 228 than ACh at equivalent receptor occupancy. It could be that BQCA is behaving as a bias agonist in promoting phosphorylation of the M<sub>1</sub> mAChR at Ser228 or that the compound has a lesser tendency to cause desensitisation of phosphorylation of this residue. To dissect this out, it would be necessary to perform concentration response experiments using ACh and BQCA.

VU0357017 was reported to be an allosteric agonist and the compound selectively activates the M<sub>1</sub> mAChR when tested against a panel of GPCRs (Digby *et al.*, 2012; Lebois *et al.*, 2010). Moreover the agonist property of the ligand was dependent upon the expression levels

or the sensitivity of the assay being used. Consistent with these observations, our study showed that VU0357017 displayed no agonist activity in inositol phosphates accumulation assay but a weak partial agonist activity in ERK 1/2 phosphorylation assay. Interestingly, when co-added with ACh, VU0357017 decreases the potency of ACh in the ERK 1/2 phosphorylation assay, suggesting that the compound may be acting as a negative allosteric modulator (NAM). However, the data did not fit with the allosteric ternary complex model of allosterism which suggests that VU0357017 might be acting orthosterically.

Consistent with the weak activity of VU0357017, the compound did not significantly promote phosphorylation of the M<sub>1</sub> mAChR globally and specifically at Ser228. As a result, phosphopeptide mapping to test the effects of the compound on the phosphorylation signatures of the M<sub>1</sub> mAChR were not performed.

At the level of receptor-ligand interactions, VU0357017 did not significantly displace <sup>3</sup>H-NMS binding or alter the affinity of ACh, suggesting that the compound has a very weak affinity and does not act as a positive allosteric modulator of ACh at the M<sub>1</sub> mAChR.

However when tested in vivo, VU0357017 was able to enhance hippocampal dependent cognitive functions, suggesting that the compound is able to activate the M<sub>1</sub> mAChR in the hippocampus. Interestingly, the compound had negligible effects on striatal and cortical functions (Digby *et al.*, 2012). Given that the M<sub>1</sub> mAChR is expressed at similar levels in these brain regions (Wall *et al.*, 1991), the tissue selectivity of VU0357017 may be related to its pharmacokinetics properties.

In summary, this study showed that BQCA is a PAM with an agonist property in its own right. The compound is probe dependent and non-biased as a PAM, but appears to preferentially promote phosphorylation of Ser228 as an agonist compared to ACh.

VU0357017 behaved as a weak affinity partial agonist and the compound does not appear to interact with the receptor allosterically.

## Chapter 6: Phosphorylation and allosteric modulation of the M<sub>4</sub> mAChR

### 6.2. Introduction

The M<sub>4</sub> mAChR plays an important role in the central nervous system functions such as regulation of locomotion and analgesia (Bymaster *et al.*, 2003; Wess, 2004). The receptor is expressed in many areas of the brain including the striatum and cerebral cortex where it resides predominantly at the pre-synaptic terminals. In certain striatal neurons, the M<sub>4</sub> mAChR is co-expressed with the D<sub>1</sub> dopamine receptor and regulates dopaminergic neurotransmission in a balanced fashion (Jeon *et al.*, 2010; Tzavara *et al.*, 2004). Disruption of this balance either by pharmacological agents or genetically “knocking” out the M<sub>4</sub> mAChR, results in enhanced dopaminergic neurotransmission and behavioural abnormalities consistent with the psychotic symptoms of patients suffering from schizophrenia (Tzavara *et al.*, 2003; Woolley *et al.*, 2009). As such the M<sub>4</sub> mAChR represents an important target for the treatment of schizophrenia.

Historically, drug discovery efforts at the M<sub>4</sub> mAChR have focused on finding agonists that interact with the same binding site as the endogenous ligand ACh. This is due to radioligand binding assay being the primary method of choice for drug discovery programs. However, such approach resulted in the discovery of orthosteric agonists that display poor subtype selectivity which caused unwanted side effects when tested in animal models (Conn *et al.*, 2009a). Recently, there has been a significant increase in the discovery of ligands that interact with a topographically distinct site as the binding site used by ACh, partly driven by the increase use of functional assays in drug discovery programs (Langmead *et al.*, 2006a). Such allosteric ligands, as exemplified by LY2033298 and VU0152100 display superior subtype

selectivity compared to orthosteric agonists and are valuable research tools for *in vivo* studies (Brady *et al.*, 2008; Chan *et al.*, 2008).

LY2033298 has been shown to increase the potency and signalling efficacy of ACh at the M<sub>4</sub> mAChR (Chan *et al.*, 2008). The compound also possesses intrinsic efficacy in its own right, suggesting that it acts as an ago-allosteric modulator (Nawaratne *et al.*, 2008). Interestingly, LY2033298 appears to enhance receptor internalisation to a much greater extent than receptor mediated signalling such as phosphorylation of ERK 1/2 suggesting that LY2033298 is bias toward receptor internalisation (Leach *et al.*, 2010). Another important property of LY2033298 is that the compound is probe and species dependent, such that the magnitude of its allosteric effect is dependent on the orthosteric ligand and the species from which the receptor is derived. In the case species dependency, LY2033298 was shown to be more potent as a positive allosteric modulator at the human M<sub>4</sub> mAChR compared to the mouse M<sub>4</sub> mAChR (Suratman *et al.*, 2011).

*In vivo* studies using a rodent model have shown that LY2033298 was active in conditioned avoidance test and prepulse inhibition of startle reflex, indicating that the compound is brain penetrant and able to engage the M<sub>4</sub> mAChR in the CNS (Chan *et al.*, 2008).

VU0152100 appeared to act solely as a positive allosteric modulator and the compound enhances the affinity and potency of ACh at the receptor (Brady *et al.*, 2008). VU0152100 was also centrally active and able to reverse amphetamine-induced hyperlocomotion, validating the role of the M<sub>4</sub> mAChR in the regulation of dopaminergic neurotransmission.

An important aspect of GPCR functions is that they are highly regulated. Post-translational modification by phosphorylation has been established as key regulatory process that controls the signalling properties of many GPCRs. This process leads to desensitisation and internalisation as well as activation of alternative G protein independent signalling pathways.

While this mechanism has been widely reported for the M<sub>1</sub>-M<sub>3</sub> mAChRs, very little is known about the regulatory process that operates at the M<sub>4</sub> mAChR. Some studies indicate that the M<sub>4</sub> mAChR undergoes rapid internalisation in response to agonist stimulation. The rate and extent of this internalisation were enhanced by over-expression of GRK2 implying that GRK2 is important for phosphorylation and subsequent internalisation of the receptor (Holroyd *et al.*, 1999; Tsuga *et al.*, 1998). However, direct evidence that the M<sub>4</sub> mAChR is phosphorylated by GRK2 is lacking. Furthermore, site directed mutagenesis studies have indicated that Thr399 and Thr145 may be important for controlling receptor internalisation (Van Koppen *et al.*, 1995), yet only T145 was confirmed to be phosphorylated (Guo *et al.*, 2010).

To better understand the phosphorylation profile of the M<sub>4</sub> mAChR we conducted intact cell phosphorylation assays, mass spectrometric analysis and western blotting using phosphorylation specific antibodies. We then extended our study by investigating if allosteric modulators such as LY2033298 could potentiate this early regulatory event.

We show here that the M<sub>4</sub> mAChR was weakly phosphorylated under basal conditions and this phosphorylation level was enhanced by stimulation of the receptor with ACh.

Application of mass spectrometric approach to purified M<sub>4</sub> mAChR showed that three serine residues (Ser247, Ser379 and Ser412) within the third intracellular loop of the receptor were phosphorylated following agonist stimulation. Interestingly one of these residues (Ser379) was phosphorylated in an agonist dependent manner in CHO-hM<sub>4</sub>R membrane preparations but basally phosphorylated in whole cell lysates. Moreover, phosphorylation of Ser379 was not significantly enhanced by LY2033298 suggesting that LY203398 does not promote a receptor conformation that increases the exposure of Ser379 to protein kinases.

## 6.3. Results

### 6.3.1. Molecular cloning of the M<sub>4</sub> mAChR

The M<sub>4</sub> mAChR cDNA used in this study was purchased from cDNA resource centre, University of Missouri-Rolla ([www.cdna.org](http://www.cdna.org)). This cDNA construct contains the sequence that codes for 3x-haemagglutinin (HA) tag at the N-terminus of the receptor. To avoid the possibility that this N-terminal tag might interfere with expression, the tag sequence was removed and replaced to the C-terminus of the receptor using PCR. The PCR also incorporates only 2xHA tag at the C-terminal tail of the receptor and Bam HI and XbaI restriction sites (**Figure 6.3.1.1A**). Analysis of the PCR products on agarose gels showed the presence of ~1500 bp fragment which correlated with the correct molecular weight of the M<sub>4</sub> receptor gene (Figure 1B). Restriction digest of transformed construct with Bam HI and XbaI restriction enzymes also showed insert of the correct size (**Figure 6.3.1.1C**). This was also confirmed by sequencing data provided by PNAACL (data not shown).

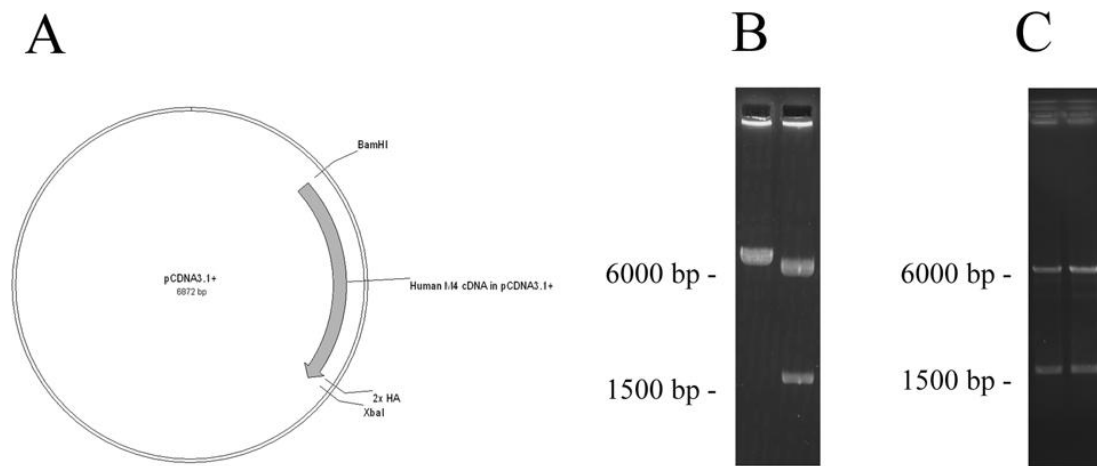


**Figure 6.3.1.1: Molecular cloning of the M<sub>4</sub> mAChR.** Construct obtained from cDNA resource centre was subjected to PCR to liberate the sequence coding for the M<sub>4</sub> mAChR. The PCR products were purified on 1 % agarose gel, extracted and digested with BamHI and XbaI restriction enzymes. The M<sub>4</sub> cDNA was then ligated into linearised pCDNA3.1 vector and transformed into competent cells. Cells that survived ampicillin selection were picked and DNA miniprep was obtained. The presence M<sub>4</sub> mAChR sequence was detected using Bam HI and XbaI restriction analysis and confirmed by DNA sequencing. (A) Vector map indicating the location of the M<sub>4</sub> mAChR, (B) products of PCR reactions (lane 1 plasmid control and lane 2 PCR products) and (C) restriction digest products of the receptor construct with Bam HI and XbaI restriction enzymes.

### **6.3.2. Generation and characterisation of M<sub>4</sub> mAChR expressing CHO-cell line**

The M<sub>4</sub> mAChR cDNA was transfected in CHO cells using the Fugene HD transfection reagent. Successful transfectants were selected using geneticin. Single colonies that survived the selection process were tested in whole cell binding assay to detect for receptor expression. From this experiment clone C2/24 which was found to have high levels of <sup>3</sup>H-NMS binding was isolated. To fully characterise the M<sub>4</sub> mAChR expression in clone C2/24, immunocytochemistry and membrane binding assays were performed. The immunocytochemistry showed that the receptors were expressed at the plasma membrane but were also present in the cytoplasm. This cytoplasmic localization may represent newly synthesized receptors that are being trafficked to the plasma membrane or internalised receptors. Membrane saturation binding assay using <sup>3</sup>H-NMS indicated that the receptor is expressed at 592 fmol/mg protein and the ligand binds to the receptor with a K<sub>D</sub> of 0.42 nM.

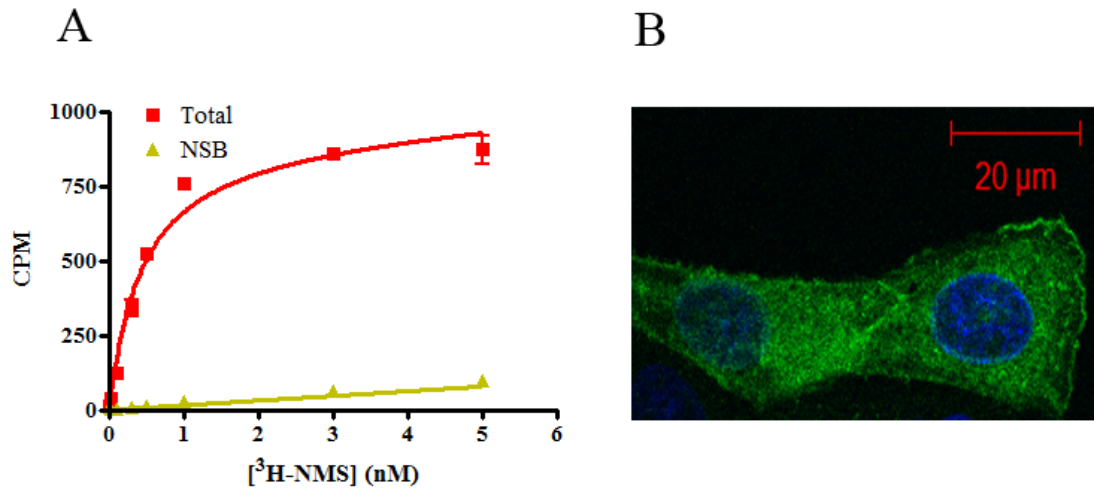


**Figure 6.3.2.1: Determination of receptor expression by membrane saturation binding and immunocytochemistry.** For saturation binding (A) 25  $\mu\text{g/well}$  membranes were incubated with  $\sim 0.05$  nM to  $\sim 5$  nM  $^3\text{H-NMS}$  in 96-well plate for 2 hours at room temperature (final assay volume, 1 ml). 10  $\mu\text{M}$  of atropine was included in the assay to determine non-specific binding. Samples were transferred onto polyethyleneimine (PEI, 0.1%) pre-soaked GF/B plates using the TomTec 96-well harvester. Plates were dried extensively and 50  $\mu\text{l}$  of scintillation fluids were added to each well. Plates were sealed and radioactivity was determined using a MicroBeta scintillation counter. For immunocytochemistry (B), cells were fixed to coverslips and permeabilised with 0.5% Triton X-100 for 30 min at RT. Cells were washed with PBS and blocked with 3% BSA for 30 min at RT. Cells were incubated with anti HA antibody for 1 hr at RT. After three quick washes with PBS, cells were incubated with goat anti mouse antibody conjugated with alexa-488 fluor. Cells were washed 3 x 5 min with PBS and the coverslips were processed for immunofluorescence. Data represents three independent experiments performed in duplicate.

### 6.3.3. <sup>32</sup>P-labelling and intact cells phosphorylation

To initially determine whether the M<sub>4</sub> mAChR was phosphorylated in an agonist dependent manner, phosphorylation experiments were carried out using <sup>32</sup>P-labelling followed by immunoprecipitation of radiolabelled receptors with anti-HA antibody. As shown in **Figure 6.3.3.1**, the receptor was modestly phosphorylated in the basal states and runs at ~75 kDa. This molecular mass is different to the nominal molecular mass of 53 kDa which suggests that the receptor may also post-translationally modified by glycosylation or palmitoylation. Application of a high concentration (100 μM) of ACh to the cells resulted in ~2 fold increase in the level of receptor phosphorylation (**Figure 6.3.3.1**). No basal or agonist mediated phosphorylation was detected in the WT CHO-K1 cells consistent with the M<sub>4</sub> mAChR not being endogenously expressed in this cell line.

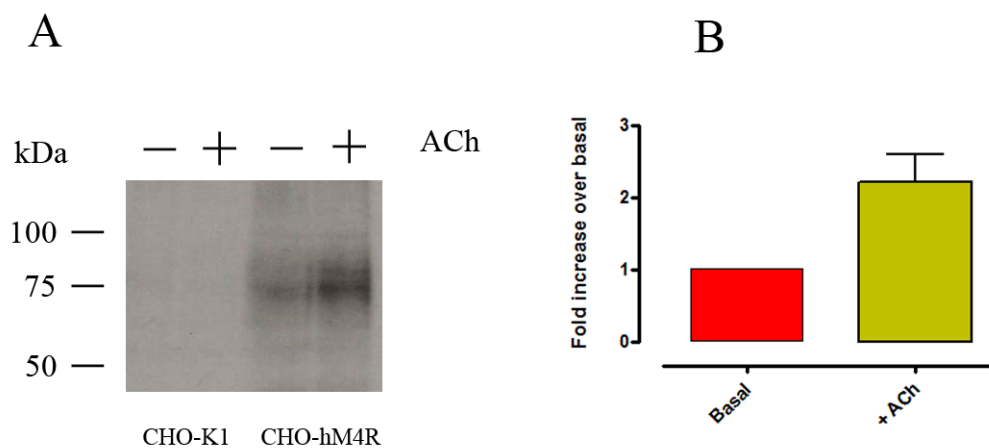


**Figure 6.3.3.1: Intact cell phosphorylation of the M<sub>4</sub> mAChR expressed in CHO cells.**

CHO-hM<sub>4</sub>R cells grown on 6-well plates were incubated in 50  $\mu$ Ci/well <sup>32</sup>P-orthophosphate for 1 hr at 37°C and then stimulated with buffer control or 100  $\mu$ M ACh for 5 min at 37°C. Cells were lysed with RIPA buffer and receptors were purified by immunoprecipitation using anti HA antibody. Purified receptors were resolved on 8% SDS-PAGE gels and transferred onto nitrocellulose membrane. Phosphorylation was detected by autoradiography (A). Phosphorylation intensity was quantified using ImageQuant and AlphaEase FC softwares and presented as increase over basal phosphorylation (B). Autoradiogram is a representative of three independent experiments performed in singlicate. Bar graph represents the mean  $\pm$  S.E.M of the phosphorylation bands.

#### **6.3.4. Mass spectrometric analysis and identification of phosphorylation sites**

We recently used a mass spectrometric approach to identify the sites of phosphorylation on the M<sub>1</sub> and M<sub>3</sub> mAChRs (**Chapter 3 and Chapter 5**). This method revealed several putative phosphorylation sites within the third intracellular loop and C-terminal tail of the receptors which we then confirmed in western blot using phosphorylation specific antibodies. Here we applied this approach on the M<sub>4</sub> mAChR to establish which residues are phosphorylated following stimulation with an agonist. Initial purification of the receptor from solubilised membranes showed an intense band running 75 kDa on 8% SDS-PAGE gels (**Figure 6.3.4.1**) which correlated well with the intact cells phosphorylation data (**Figure 6.3.3.1**). This band was extracted and subjected for LC/MS/MS study via PNACL. The band was initially treated with trypsin to allow the peptides to escape prior to injection into the mass spectrometer. The peptides were ionised via collision induced dissociation (CID) and this yielded 20% recovery of all the peptides predicted to be recovered following trypsin digestion (**Figure 6.3.4.1**). Most of these peptides were found at the loop regions of the receptor. Furthermore two peptides were consistently phosphorylated at a single residue (Ser247 and Ser379 respectively, **Figure 6.3.4.2** and **Figure 6.3.4.3A and C**). Another peptide was also phosphorylated but the location of the phosphorylation could not be ascertained due to the poor quality of the spectrum. We then reanalysed this peptide using electron transfer dissociation (ETD) as the method for ionising the peptide. This approach has a distinct advantage that it enables large peptides which contain multiple phosphorylation sites to be resolved and the phosphorylation sites determined. From this analysis, the residue being phosphorylated appears to be Ser314 located within the third intracellular loop of the receptor (**Figure 6.3.4.2B** and **Figure 6.3.4.3B**).

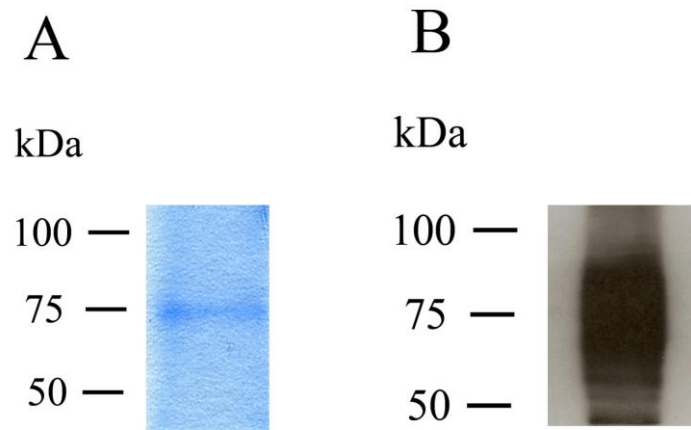


**Figure 6.3.4.1: Purification and detection of M<sub>4</sub> mAChR.** Receptors solubilised from membranes were purified by immunoprecipitation using polyclonal anti HA antibody conjugated with agarose beads. Receptors were resolved on 8% gels and stained with colloidal blue (A) and transferred onto nitrocellulose membrane for western blotting with a monoclonal anti HA antibody (B). Data represents three independent experiments performed in singlicate.

# A

MANFTPVNGSSGNQSVR **LVTSSSHNR** YETVEMVFIA TVTGSLSLVTVVGNILVMSI  
K VNRQLQTVNNYFLFSLACADLIIGAFSMNLYTVYIHKGYWPLGAVVCDLWLALDY  
VVSNASVMNLLIISFDR **YFCVTKPLTYPAR** RTTKMAGLMIAAAWVL SFVLWAPAILF  
WQFVVGKRTVPDNQCFIQFLSNPAVTFGT AIAAFYLPVVIMTVLYIHISLASRSRVHK  
**HRPEGPK** EK KAK **TLAFLKSPLMK** QSVK **KPPPGEAAR** EELRNGKLEEA **PPPALPPPPRP**  
**VADKDTSNESSSGSATQNTKERPATELSTTEATTPAMPAPPLQPR** ALNPASRWSKIQI  
VTK **QTGNECVTAIEIVPATPAGMRPAANVARKFASIAR** NQVRKKRQMAARERK VTR  
TIFAILLAFILTWTPYNVMVLVNTFCQSCIPDTVWSIGYWLCYVNSTINPACYALCNA  
TFKKTFR **HLLLCQY** RNIGTAR **YPYDVPDYAYPYDVPDYA**

# B

Phosphopeptide	Predicted mz	Observed mz
(K)TLAFLK <b>p</b> SPLMK(Q)	584.86	664.86
(R)KF <b>p</b> SIAR(N)	356.72	436.72
(K)ERPATEL <b>[STT]</b> EATTPAMPAPPLQPR(A)	888.12	968.12
* <b>(K)ERPATELpST</b> TTEATTPAMPAPPLQPR(A)	888.12	968.12

**Figure 6.3.4.2: Peptide coverage of M<sub>4</sub> mAChR and identification of phosphopeptides by MS/MS.** SDS-PAGE gel containing the receptor band was excised and incubated with DTT to denature the receptor proteins. Gel pieces were incubated with iodoacetamide and then digested with trypsin for 4 hrs at 37°C. The supernatant was transferred to fresh tubes and the gel pieces were washed twice with 0.1% trifluoroacetic acid (TFA). The supernatants were pooled and subjected to LC MS/MS analysis. (A) Overview of amino acid sequence of M<sub>4</sub> mAChR; sequences highlighted in yellow were detected by MS/MS. (B) summary of phosphopeptides identified by MS/MS. \*Phosphopeptide determined by ETD ionisation method.

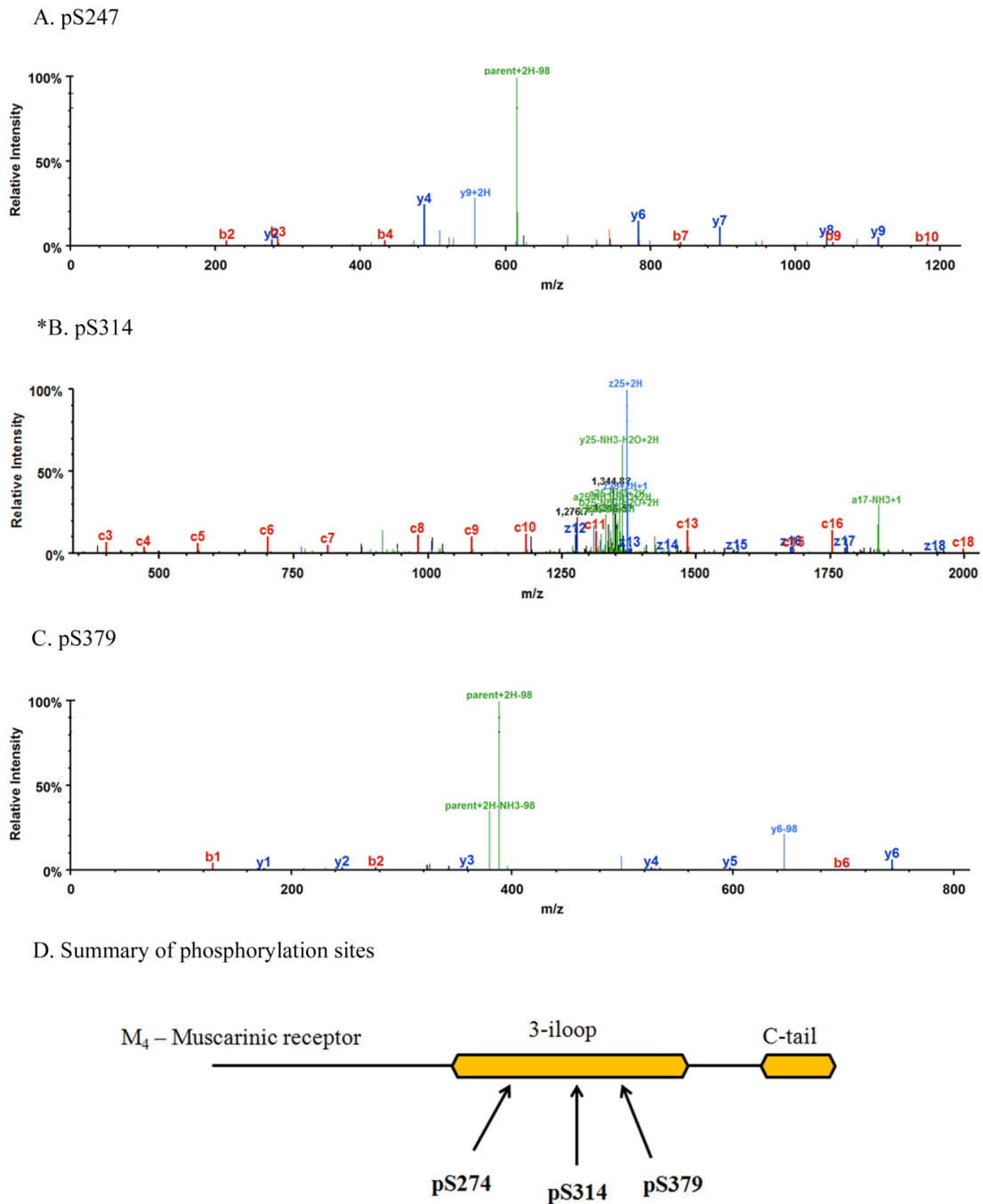


**Figure 6.3.4.3: Summary of phosphorylation sites determined by mass spectrometry using collision induced dissociation (CID) and electron transfer dissociation (ETD) methods to ionise the peptides.** The mass spectra of peptides listed in **Figure 6.3.4.2B** are shown in A, B and C. Location of phosphorylation within the third intracellular loop of the receptor is indicated in D. \*Denotes phosphopeptide determined by ETD ionisation method.

### **6.3.5. Generation and characterisation of phosphorylation specific antibodies**

The entire amino acid sequence of the M<sub>4</sub> mAChR with the phosphorylation sites indicated above was submitted to Eurogentec for immunogenicity ranking. From this analysis phosphopeptides listed in **Table 6.3.5.1** appeared to be immunogenic and was subsequently used to generate phosphospecific antibodies. These peptides were also analysed using BLAST software which showed that these peptides are unique to the M<sub>4</sub> mAChR in the mouse and rat proteome, indicating that antibodies directed against these peptides would be very specific to the M<sub>4</sub> mAChR. Thus antibodies that recognise these residues would be useful for studying the phosphorylation state of the M<sub>4</sub> mAChR in native tissues.

The antibodies were generated in rats using a three months immunisation program provided by Eurogentec.

In order to characterise these antibodies, the M<sub>4</sub> mAChR which has been immunoprecipitated with anti HA antibody was treated with CIAP and tested in western blot experiments. As shown in **Figure 6.3.5.1**, pS379 showed promising results as the antibody was highly phospho-specific as it completely loses the ability to recognise CIAP-treated receptors. This antibody was then taken forward for further studies. However, Ser379 was highly phosphorylated in the basal states of M<sub>4</sub> mAChR immunoprecipitated from whole cell lysates. This would be problematic given that we would like to test the effect of LY2033298 on the phosphorylation state of this site. To overcome this issue we sourced a different cell line, termed “HepM<sub>4</sub>” (CHO cells stably expressing M<sub>4</sub> mAChR kindly provided by Heptares Therapeutics) and used cell membranes instead of whole cell lysates for phosphorylation experiments.

**Table 6.3.5.1: Peptide sequences used to generate phosphospecific antibodies.** Amino acid residues determined to be phosphorylated are highlighted in red and addition of a cysteine residue to facilitate coupling to carrier protein is shown in blue.

<b>Antibody</b>	<b>Peptide sequence</b>
pS247	H <sub>2</sub> N - <b>C</b> LAFLK <b>S</b> (PO <sub>3</sub> H <sub>2</sub> )PLMKPS - CONH <sub>2</sub>
pS379	H <sub>2</sub> N - ARKFAS(PO <sub>3</sub> H <sub>2</sub> )IARNQ <b>V</b> <b>C</b> - CONH <sub>2</sub>
pS314	H <sub>2</sub> N - <b>C</b> ERPPT <b>E</b> L <b>S</b> (PO <sub>3</sub> H <sub>2</sub> )TTEAA - CONH <sub>2</sub>

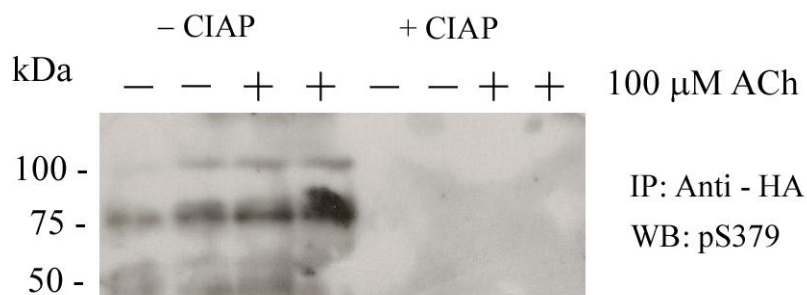


**Figure 6.3.5.1: Characterisation of pS379 antibody using phosphatase treatment.** Cells grown on 6-well plate were stimulated with buffer or ACh for 5 min at 37°C. Cells were lysed with RIPA buffer and receptors were purified by immunoprecipitation. Purified receptors were treated with calf intestinal alkaline phosphatase (CIAP) or buffer before being resolved on 8% SDS-PAGE gels. Resolved receptor proteins were immunoblotted with pS379 antibody. Data represents two experiments performed in singlicate.

### 6.3.6. Characterisation of HepM<sub>4</sub> cell line

Prior to performing phosphorylation experiments we characterised the receptor expressed in HepM<sub>4</sub> cell line and confirmed the pharmacology of LY2033298. Membrane saturation binding experiments showed that the binding of <sup>3</sup>H-NMS was saturable with a K<sub>d</sub> of  $0.17 \pm 0.02$  nM. The radioligand labels the receptor with a B<sub>max</sub> of  $4.87 \pm 0.25$  pmol/mg proteins (**Figure 6.3.6.1A**).

LY2033298 has been reported to be a potent positive allosteric modulator and the compound enhances the binding affinity of ACh for the M<sub>4</sub> mAChR. This positive binding cooperativity was confirmed in this study which showed that the LY2033298 enhanced the affinity of ACh by >100 fold (**Figure 6.3.6.1C and Table 6.3.6.1**). On its own LY2033298 partially inhibited the binding of <sup>3</sup>H-NMS indicating that LY2033298 has a high negative cooperativity with <sup>3</sup>H-NMS binding or an overlapping binding site as NMS (**Figure 6.3.6.1B and Table 6.3.6.1**). This is surprising given that previous data have shown that LY2033298 is neutral with respect to NMS binding (Chan *et al.*, 2008). This discrepancy may be due to different batches of the compound.

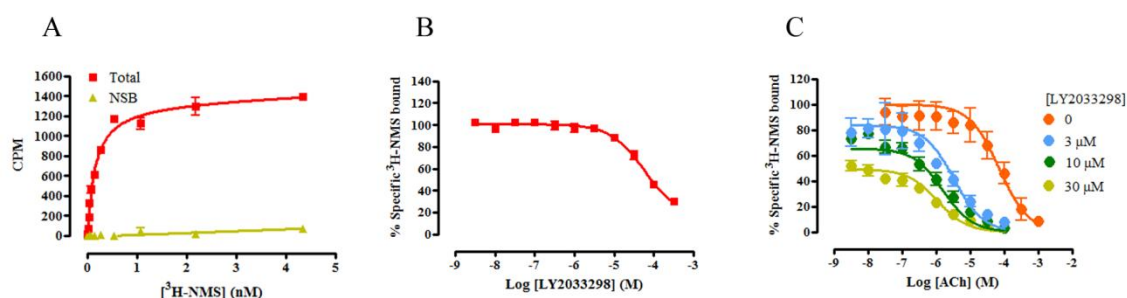


**Figure 6.3.6.1: Characterisation of HepM<sub>4</sub> cell line and the pharmacology of LY2033298**

**in radioligand binding assay.** Saturation binding experiments were performed with 5 μg/well membranes in the presence of ~5 pM - 5 nM <sup>3</sup>H-NMS in 96-well plate for 2 hours at room temperature (final assay volume, 1 ml). 10 μM of atropine was included in the assay to determine non-specific binding (A). In the competition binding experiments, 5 μg/well membranes were incubated with ~0.5 nM <sup>3</sup>H-NMS in the presence of increasing concentration of LY2033298 alone (B) or a combination of LY2033298 and ACh (C) in 96-well plate for 2 hours at room temperature (400 μl final assay volume). GTP was included in the assay to ensure the receptor was in a single affinity state. Non-specific binding was determined with 10 μM atropine. Plates were filtered onto polyethyleneimine (PEI, 0.1%) pre-soaked GF/B plates using a TomTec 96-well harvester. Plates were dried extensively and 50 μl of scintillation fluids were added to each well. Plates were sealed and radioactivity was determined using a MicroBeta scintillation counter. Data represents three independent experiments performed in duplicates.

**Table 6.3.6.1: Effects of LY2033298 on the binding of antagonist and agonist at the M<sub>4</sub> mAChR.**  $pK_B$  is the equilibrium dissociation constant of LY2033298 estimated from the ATCM,  $\alpha$  is the binding cooperativity between LY2033298 and <sup>3</sup>H-NMS.  $pK_I$  denotes the equilibrium dissociation constant of ACh and  $\alpha'$  is a measure of the binding cooperativity between LY2033298 and ACh.

Modulator	$pK_B$	$\alpha$	$pK_I$	$\alpha'$	n
LY2033298	$4.89 \pm 0.11$	$0.10 \pm 0.08$	$4.81 \pm 0.06$	$120.06 \pm 1.23$	3

### **6.3.7. Ser379 is entirely phosphorylated in an agonist dependent manner for membrane bound M<sub>4</sub> mAChR.**

To determine the suitability of the new cell line for phosphorylation studies, western blot experiments were run using membranes prepared from these cells. As can be seen in **Figure 6.3.7.1**, a low level of basal phosphorylation was detected with pS379 antibody and this phosphorylation level was increased to ~2.5 folds upon stimulation with a high concentration (100  $\mu$ M) of ACh. This suggests that the new cell line is ideal to use for in vitro membrane phosphorylation experiments.

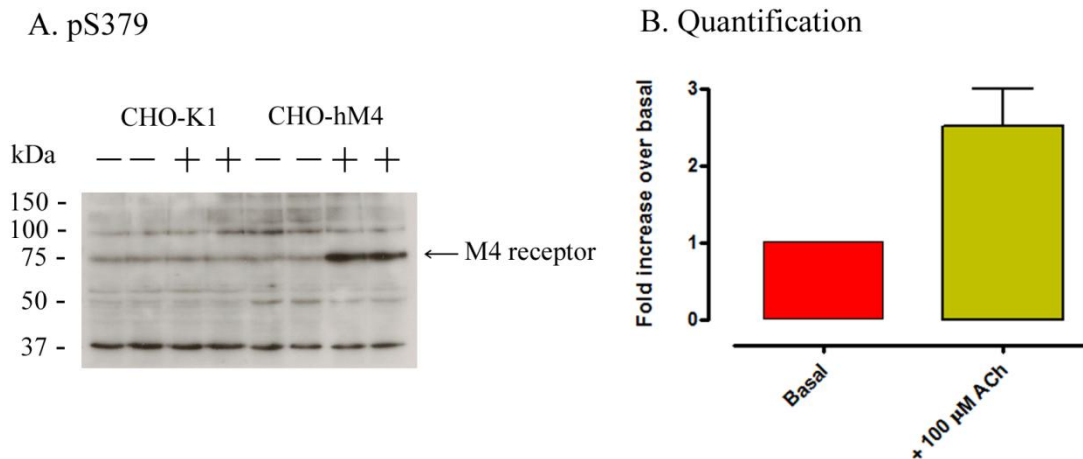


**Figure 6.3.7.1: Agonist dependency of phosphorylation of membrane bound M<sub>4</sub> mAChR**

**at Ser379.** Cells grown in flasks were stimulated with buffer control or 100 uM ACh for 10

min at 37°C. Cells were dissociated and membranes were prepared using homogeniser as

described in materials and methods. Membrane pellets were resuspended in TE buffer and

protein concentrations in the membrane were determined by Bradford reagent. Membranes

were mixed with 2x SDS-PAGE loading buffer and resolved on 8% gels. Resolved proteins

were transferred onto nitrocellulose membrane and subjected to western blot analysis using

pS379 antibody (A). Phosphorylation intensity was quantified using ImageQuant and

AlphaEase FC softwares and presented as increase over basal phosphorylation (B).

Autoradiogram is a representative of three independent experiments performed in singlicate.

Bar graph represents the mean  $\pm$  S.E.M of the phosphorylation bands.

### **6.3.8. Phosphorylation of Ser379 is modestly enhanced by the ago-allosteric modulator LY2033298.**

To determine if LY2033298 could modulate the phosphorylation profile of the M<sub>4</sub> mAChR at Ser379, membrane phosphorylation experiments were performed. As shown in **Figure 6.3.8.1**, stimulation of cells with a low concentration of ACh (3 μM), resulted in a modest phosphorylation of Ser379. The presence of LY2033298 at concentration that did not cause phosphorylation alone (3 μM) did not significantly enhance the phosphorylation of this residue, suggesting that LY2033298 did not promote a receptor conformation that increases the accessibility of Ser379 to protein kinases.

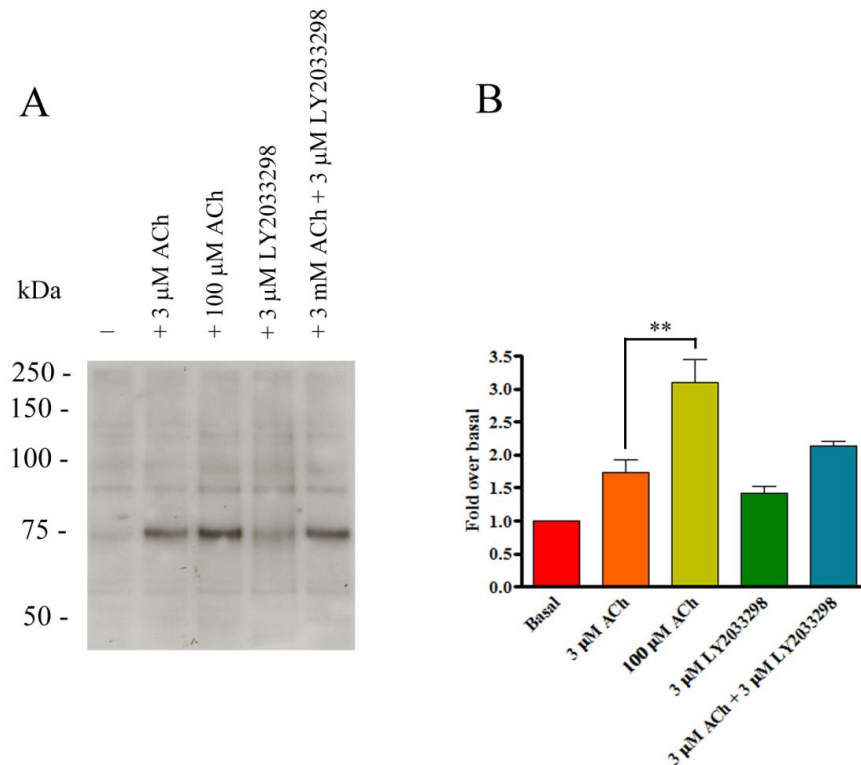


**Figure 6.3.8.1: Agonist dependency of phosphorylation of membrane bound M<sub>4</sub> mAChR at Ser379.** Cells grown in flasks were stimulated with buffer control, a low concentration of ACh (3 μM) in the presence or absence of LY2033298 for 10 min at 37°C. Positive control was determined by stimulating cells with 100 μM of ACh. Cells were dissociated and membranes were prepared using homogeniser as described in materials and methods. Membrane pellets were resuspended in TE buffer and protein concentrations in the membrane were determined by Bradford reagent. Membranes were mixed with 2x SDS-PAGE loading buffer and resolved on 8% gels. Resolved proteins were transferred onto nitrocellulose membrane and subjected to western blot analysis using pS379 antibody (A). Phosphorylation intensity was quantified using ImageQuant and AlphaEase FC softwares and presented as increase over basal phosphorylation (B). Data represent three independent experiments performed in singlicate. Bar graph represents the mean ± S.E.M of the phosphorylation bands. \*\*P<0.01; as measured using a one-way ANOVA with Bonferonni's post-hoc test.

## 6.4. Discussion

The M<sub>4</sub> mAChR is abundantly expressed in the central nervous system and has been implicated in a number of disorders including schizophrenia and neuropathic pain (Martino *et al.*, 2011; Tzavara *et al.*, 2004). Studies using knockout animals have shown that the receptor plays an important role in regulating pain sensation and dopaminergic neurotransmission, with the latter process being clinically relevant for the pathophysiology of schizophrenia (Tzavara *et al.*, 2003; Wess, 2004; Wess *et al.*, 2003a; Wess *et al.*, 2003b).

The signalling pathways linked to the M<sub>4</sub> mAChR have been extensively studied and it has been established that the receptor preferentially couple to G<sub>i</sub> family of G proteins to inhibit adenylate cyclase and regulate ion channels (GIRK and Ca<sup>2+</sup>) opening (Caulfield *et al.*, 1998; Clapham *et al.*, 1997). The receptor has also been shown to activate ERK1/2 in heterologous expression systems (Leach *et al.*, 2010).

An important feature of GPCR functions is that they are highly regulated. At the receptor level, this regulation has been primarily mediated by post-translational modification involving phosphorylation (Moore *et al.*, 2007; Pitcher *et al.*, 1998; Premont *et al.*, 2007; Tobin, 2008; Tobin *et al.*, 2008). This process leads to desensitisation, primes receptor for internalisation and promotes alternative signalling pathways (DeWire *et al.*, 2007; McDonald *et al.*, 2001; Pierce *et al.*, 2001). While this mechanism has been established for the M<sub>1</sub>-M<sub>3</sub> mAChRs, the role of phosphorylation in the regulation of M<sub>4</sub> mAChR functions is less well known (van Koppen *et al.*, 2003). A recent study using site directed mutagenesis and phosphorylation specific antibody has indicated that Thr145 was phosphorylated in a Ca<sup>2+</sup> and calmodullin-dependent manner by CaM kinase II (Guo *et al.*, 2010). This phosphorylation event was shown to increase the coupling efficiency of the receptor to the

inhibition of cAMP formation, thus providing a feedback mechanism for the signalling of the receptor to G<sub>i</sub> G proteins.

In addition to mutagenesis, mass spectrometry has emerged as a valuable analytical tool for studying protein phosphorylation as the method allows the identification of the exact locations of phosphorylation. Because phosphorylation adds ~80 daltons (Da) to the molecular mass of a peptide, peptides with changes of 80 Da (or multiple of it) from the theoretical mass can be identified. These peptides would then be trapped and fragmented by mass analysers to reveal the amino acid sequence and the sites of phosphorylation. A number of phosphorylation sites for some family A GPCRs, including the M<sub>1</sub> and M<sub>3</sub> mAChRs, chemokine CXCR4, β<sub>2</sub>-adrenergic and μ-opioid receptors (Busillo *et al.*, 2010; Butcher *et al.*, 2011; Chen *et al.*, 2013; Lau *et al.*, 2011; Nobles *et al.*, 2011) has been determined via this method and confirmed by phosphorylation specific antibodies. Furthermore the patterns of phosphorylation for some of these receptors appear to be distinct depending on the ligands that are used to stimulate the receptor (Butcher *et al.*, 2011; Nobles *et al.*, 2011). Hence the use of mass spectrometry and phosphorylation specific antibodies may provide a viable approach to dissect the pharmacology of biased ligands.

In this study we further investigated the phosphorylation profile of the M<sub>4</sub> mAChR expressed in CHO cells by employing <sup>32</sup>P-labelling, tandem mass spectrometry and phosphorylation specific antibodies. We chose CHO cells because they do not express M<sub>4</sub> mAChR endogenously.

Initial <sup>32</sup>P-labelling experiments have shown that the M<sub>4</sub> mAChR is phosphorylated under basal conditions and in response to agonist stimulation. Purification and subsequent mass spectrometric analysis of tryptic digested M<sub>4</sub> mAChR resulted in ~ 20% recovery of amino acid sequence. This low coverage appeared to be due to the transmembrane regions not being

resolved and the M<sub>4</sub> mAChR having unfavourable amino acid sequence. Very few arginines and lysines at which trypsin cuts were found which led to the generation of large peptides that are difficult to ionise and detect by mass spectrometry. Other methods of digestion to improve peptide coverage have been sought including the use of chymotrypsin and Lys-C. However, this did not improve peptides generation as predicted from in silico digest.

The nominal molecular mass of the M<sub>4</sub> mAChR is 53 kDa and in this study, the receptor runs at ~75 kDa on 8% SDS-PAGE gels. This indicates that in addition to phosphorylation, the receptor may also be modified by other mechanisms such as glycosylation or palmitoylation.

The application of collision induced dissociation to fragment the tryptic peptides resulted in the identification of two phosphopeptides with Ser247 and Ser379 being phosphorylated on each peptide. This approach also identified a phosphopeptide but the location of phosphorylation could not be determined confidently due to poor quality of spectra. To resolve the site(s) of phosphorylation we reanalysed the peptide using electron transfer dissociation and showed that Ser314 was the site of agonist-promoted phosphorylation (see **Figure 6.4.1** for summary of phosphorylation sites). We could not detect phosphorylation of T145 which was previously shown to be phosphorylated by CaMKII (Guo *et al.*, 2010) because the peptide containing this residue was not resolved. However, we consistently detected CaMKII in our mass spectrometry results indicating this protein interacted and co-purified with the M<sub>4</sub> mAChR.

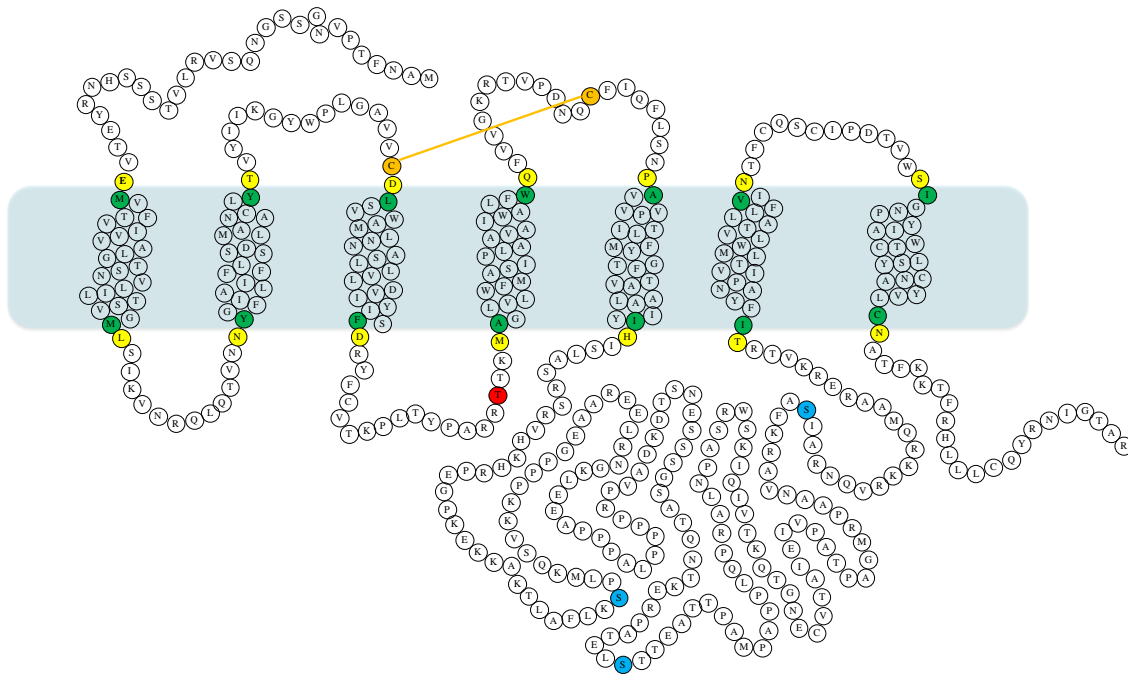


**Figure 6.4.1: Topography of M4 mAChR amino acid sequence indicating the putative phosphorylation sites.** The junctions between the TM and loop regions as determined by protein knowledgebase sequence alignment ([www.uniprot.org](http://www.uniprot.org), chrn4, accession number: P08173) are shown by residues in green and yellow. The phospho-serines identified in this study are highlighted in blue and phospho-threonine identified by Guo *et al.* is shown in red.

To confirm that Ser247, Ser314 and Ser379 are indeed phosphorylated, phosphospecific antibody against these residues was raised. While Ser379 was confirmed to be phosphorylated Ser247 and Ser314 could not be confirmed due to the antibodies not showing positive reactivity. These negative results could be due to the low antibody titre or the phosphopeptides used to generate the antibodies were insufficiently immunogenic.

The antibody directed against Ser379 was tested in CHO-hM<sub>4</sub>R membrane preparations and whole cell lysates. Interestingly, Ser379 was phosphorylated in an agonist dependent manner in membrane preparations but basally phosphorylated in whole cell lysates. These results suggest that intracellular M<sub>4</sub> mAChR may exist in a phosphorylated state (at least at Ser379).

Drug discovery efforts at GPCRs have increasingly been focused on targeting allosteric sites on the receptor (Burford *et al.*, 2011). Ligands that target these sites are presumed to be more selective because these sites are less evolutionarily conserved (Conn *et al.*, 2009a; Kenakin, 2010; Keov *et al.*, 2011; Melancon *et al.*, 2012; Wang *et al.*, 2009). At the M<sub>4</sub> mAChR LY2033298 was shown to be a selective allosteric modulator and the compound enhances the affinity and efficacy of ACh at the receptor. The compound also has an intrinsic efficacy in its own right suggesting ago-allosteric properties (Leach *et al.*, 2010; Nawaratne *et al.*, 2010; Nawaratne *et al.*, 2008). Interestingly, in this study LY2033298 did not significantly enhance phosphorylation of Ser379 following stimulation with a sub-maximal concentration of ACh. This suggests that the compound does not promote a receptor conformation that increases the accessibility of Ser379 to protein kinases.

In summary, this study revealed that the M<sub>4</sub> mAChR is regulated by phosphorylation and three serine residues (Ser247, Ser314 and Ser379) were reported to be phosphorylated in response to agonist stimulation. Ser379 was confirmed by phosphospecific antibody.

Additionally the antibody revealed that LY2033298 a positive allosteric modulator at the M<sub>4</sub> mAChR did not enhance phosphorylation of Ser379.

## Chapter 7: General discussion

GPCR represents one of the largest families of cell surface proteins in mammals (Kristiansen, 2004). These receptors mediate the action of diverse kinds of natural ligand, ranging from photons of light to ions, neurotransmitters, biogenic amines, peptides and large glycoproteins (Bockaert *et al.*, 1999; Gether, 2000; Lefkowitz, 2007a; Lefkowitz, 2007b; Pierce *et al.*, 2002). Recent breakthroughs in protein engineering and crystallographic methods have enabled the elucidation of the structures of the majority of family A GPCRs (Katritch *et al.*, 2013; Lebon *et al.*, 2012; Zhao *et al.*, 2012). These studies, together with pharmacological and biophysical data have revealed that GPCRs are structurally dynamic and able to adopt multiple conformations (Kobilka *et al.*, 2007). This conformational heterogeneity allows agonists to select or stabilise distinct receptor states that leads to the activation of a subset of signalling pathways available to the receptor (Caramellini *et al.*, 1998; Violin *et al.*, 2007). Such biased agonism offers an opportunity for developing novel therapeutics with greater safety profiles, by virtue of activating therapeutically beneficial signalling pathway(s) while negating the pathways that give rise adverse effects (Boerrigter *et al.*, 2011; Boerrigter *et al.*, 2012). Indeed, many compounds have been shown to display biased agonism in many different GPCRs (Rajagopal *et al.*, 2010; Reiter *et al.*, 2012). However, compelling evidence that ligands at the mAChRs behave in a similar manner is limited (Challiss *et al.*, 2009). Hence one of the aims of this study was to search for biased agonism at the mAChRs.

There are five subtypes of mAChR that have been cloned which represent a prototypical family A GPCRs (Hulme *et al.*, 1990). Among these subtypes, the M<sub>1</sub>, M<sub>3</sub> and M<sub>4</sub> mAChRs are considered important targets for the pharmaceutical industry for disease indications such as Alzheimer's disease, COPD and schizophrenia (Eglen *et al.*, 1999; Felder *et al.*, 2000; Langmead *et al.*, 2008b; Zhang *et al.*, 2007). These receptors signal via heterotrimeric G

proteins and other signalling proteins to various downstream effector molecules including phospholipase enzymes, adenylate cyclase and ion channels. The clearest indication that ligands may differentially modulate mAChR-mediated signalling pathways was reported by Akam *et al* (Akam *et al.*, 2001) who demonstrated that Pilo was more effective in activating  $G_{\alpha i}$  than  $G_{\alpha q}$  when compared to MCh at the  $M_3$  mAChR.

We extended this study in the first results chapter by investigating the effects of Pilo on various  $M_3$  mAChR mediated processes such as receptor phosphorylation, inositol phosphates accumulation and ERK1/2 activation. Using the operational model of agonism as a method of data analysis and MCh as a reference agonist, our data indicated that Pilo was more effective in promoting inositol phosphates accumulation than global receptor phosphorylation. Furthermore, the compound was able to fully drive phosphorylation of Ser412 (a potential GRK2/GRK6 site) and partially promote phosphorylation of Ser577 (a PKC site). These results also indicated that the compound was also showing preferential phosphorylation for one site (Ser412) compared to another (Ser577). The results also highlighted the need to investigate phosphorylation at individual sites when studying biased agonism (i.e. most studies focus mainly on signalling and global receptor phosphorylation).

Other studies have shown that Pilo activated ERK via a different mechanism in endogenously expressed  $M_3$  mAChR (Lin *et al.*, 2008) and that the compound also causes seizure when administered in rodents (Wess *et al.*, 2003a; Wess *et al.*, 2003b). These data indicate that Pilo also has unique pharmacological properties in native or physiological settings.

We would have liked to compare agonists to the endogenous ligand of the mAChRs (ACh) as biased factors may change depending on reference agonist. Therefore in the subsequent chapters we used ACh as the agonist comparator. It would also be interesting to extend this study to include a larger set of compounds to see if these “other” ligands display biased

agonism. However, there is a paucity of novel selective agonists acting at the M<sub>3</sub> mAChR and as such this idea was not pursued.

A great deal of knowledge into the physiological roles of the mAChRs has been gained through the study on genetically modified animals lacking each of the mAChR subtypes. In the case of the M<sub>3</sub> mAChR, it was shown that the receptor plays an important role in regulating smooth muscle contraction, learning and memory and insulin secretion and glucose homeostasis (Duttaroy *et al.*, 2004; Gautam *et al.*, 2007; Gautam *et al.*, 2006; Kong *et al.*, 2010; Poulin *et al.*, 2010; Wess, 2004). An emerging method to study the physiological roles of the mAChRs has been the use of a chemical genetic approach to create mutant receptors that are insensitive to the endogenous ligand but can be activated by an otherwise inert compound (Alexander *et al.*, 2009; Armbruster *et al.*, 2007; Dong *et al.*, 2010a; Guettier *et al.*, 2009). At the M<sub>3</sub> mAChR, two mutations at the orthosteric binding pocket was shown to significantly reduce the affinity and potency of ACh and confer activity to clozapine-N-oxide (CNO). While these *in vitro* studies are interesting, we would like extend the use of the technology to *in vivo*. Given that ligands acting at the same receptor can promote differential receptor signalling and gives rise to biased agonism (Galandrin *et al.*, 2007; Kenakin, 2011; Urban *et al.*, 2007), it has been necessary to thoroughly profile the signalling and regulation of such mutant receptor in response to CNO prior to *in vivo* studies. In the second results chapter of this thesis, we investigated the phosphorylation profiles of the M<sub>3</sub> RASSL receptor in response to CNO and compared the profiles to the WT M<sub>3</sub> mAChR responding to ACh stimulation. This study showed that the M<sub>3</sub> RASSL receptor was phosphorylated in response to CNO stimulation in a similar as the M<sub>3</sub> WT receptor responding to ACh. As such CNO is less likely to promote biased signalling at the M<sub>3</sub> RASSL receptor. Indeed, our collaborators have shown that the receptor signals in a similar manner as the WT receptor, hence replicating the WT receptor functionality (Alvarez-Curto *et al.*, 2011). Since then the M<sub>3</sub>

RASSL has been expressed in a number cells/tissues including the pancreatic  $\beta$ -cells and hippocampus where it was shown to modulate insulin secretion and neuronal firing, respectively, processes that are known to be mediated by the WT  $M_3$  mAChR (Alexander *et al.*, 2009; Guettier *et al.*, 2009). Recently a  $\beta$ -arrestin biased  $M_3$  RASSL has also been developed which provided powerful tool for studying the physiological role of arrestin dependent signalling in vivo (Nakajima *et al.*, 2012). Other RASSLs have also been created based on different GPCRs (including  $MC_4$ ,  $5HT_4$ , and  $M_1$  and  $M_4$  mAChRs) which provide valuable tools for the pharmaceutical industry to validate these receptors as drug targets.

A potential caveat in the use of the RASSL technology is that in vivo, the mutant receptor might not fully replicate the pattern of the endogenous receptor activation. In the case of the mAChRs, ACh is released from the presynaptic neurons and then rapidly degraded following interaction with the postsynaptic mAChRs (Sarter *et al.*, 2005; Teles-Grilo Ruivo *et al.*, 2013). This cycle of release and degradation results in pulsatile neurotransmission. In contrast, CNO is metabolically stable and is less likely to be degraded in the synaptic cleft. As such the compound may produce sustained receptor activation and continuous neurotransmission.

Among the five mAChR subtypes, the  $M_1$  mAChR has been considered an attractive drug target for the treatment of cognitive deficits associated with Alzheimer's disease and schizophrenia (Eglen *et al.*, 2001; Felder *et al.*, 2000; Langmead *et al.*, 2008b). Many of the drugs that act at the  $M_1$  mAChR interact with the same binding site as the endogenous ligand, ACh. Because this site is highly conserved among the five mAChRs, these ligands often produced unwanted side effects due to activation of other mAChR subtypes. As such these compounds have failed in late stage clinical studies.

In addition to the binding site used by ACh, the mAChRs have also been recognised to contain a secondary allosteric binding site that is unique for each receptor subtype (Christopoulos, 2002; Gregory *et al.*, 2007; Keov *et al.*, 2011). Ligands that act at this site often display superior subtype selectivity and may provide important lead compounds for clinical development. Such allosterically acting ligands include BQCA and VU0357017 (Lebois *et al.*, 2010; Ma *et al.*, 2009). BQCA was shown to be a positive allosteric modulator and the compound increases the affinity and potency of ACh at the M<sub>1</sub> mAChR. VU0357017 behaved as an allosteric agonist and the compound was shown to activate the M<sub>1</sub> mAChR in the absence of ACh. In the third chapter of this thesis, the pharmacology of these compounds was further investigated using a number of assay readouts. Our data showed BQCA acts as an ago-allosteric modulator. The compound increases the affinity and potency of ACh at the receptor and it has intrinsic efficacy in its own right when tested in a highly coupled system (i.e. ERK1/2 phosphorylation). Interestingly the degree of modulation by BQCA was probe dependent such that the affinity of partial agonist Pilo was increased to a lesser extent than the affinity of full agonists, MCh and ACh. BQCA also did not differentially modulate the signalling and phosphorylation of the M<sub>1</sub> mAChR in response to ACh suggesting that the compound is non-biased. This is consistent with the previously reported data (Canals *et al.*, 2012). Interestingly BQCA only partially potentiates phosphorylation of Ser228, but as an agonist, the compound caused greater phosphorylation than ACh at equivalent receptor occupancy. The former may reflect the difficulty in quantitatively measuring the change in phosphorylation because this site is only weakly phosphorylated and the latter may indicate that BQCA is biased toward phosphorylation of Ser228 or that the compound has lesser tendency to cause desensitisation. The difficulty in performing agonist concentration series for phosphorylation of Ser228 has hampered the dissection of whether BQCA is biased or less able to cause desensitisation. Biased agonists at the M<sub>1</sub> mAChRs may be useful for

developing pro-cognitive drugs, particularly ones that produce prolonged receptor stimulation without causing desensitisation.

In radioligand binding experiments, VU0357017 appeared to bind allosterically at the M<sub>1</sub> mAChR and the compound does not significantly inhibit the binding of <sup>3</sup>H-NMS. However, in ERK1/2 phosphorylation assays, the compound behaved in a manner consistent with a partial orthosteric agonist. Further investigation is needed to uncover the mode of action of VU0357017, in particular elucidating where the compound is binding by using site directed mutagenesis of allosteric/orthosteric residues. Interestingly, VU0357017 modulated the M<sub>1</sub> functions selectively in the cortex whereas BQCA modulated M<sub>1</sub> mAChR activity in the hippocampus (Digby *et al.*, 2012). These data may indicate differences in pharmacokinetic properties of these two allosteric ligands as the M<sub>1</sub> mAChR is expressed at similar levels in the cortex and hippocampus (Wall *et al.*, 1991).

The M<sub>4</sub> mAChR plays an important role in maintaining a proper balance between cholinergic and dopaminergic neurotransmissions in the striatum (Atzori *et al.*, 2007; Barch, 2010; Dencker *et al.*, 2012; Fink-Jensen *et al.*, 2011; Gomeza *et al.*, 1999). Studies have implicated that the receptor may be regulated by phosphorylation and that GRKs and CaMKII mediates this process (Guo *et al.*, 2010; Holroyd *et al.*, 1999; Tsuga *et al.*, 1998). However, very little information is available on the locations of this post-translational modification. In the results chapter four, we employed mass spectrometry to identify the sites of phosphorylation of the M<sub>4</sub> mAChR and generated antibodies to these sites. We identified three potential phosphorylation sites, one of which (pS379) was confirmed by the antibody. Interestingly, LY2033298, a positive allosteric modulator, did not potentiate the phosphorylation of this site when co administered with a low concentration of ACh. These results suggest that LY2033298 do not promote a receptor conformation that increases the accessibility of Ser379 to protein kinases.

Overall, this thesis provides further evidence that Pilo displays unique pharmacological properties at the M<sub>3</sub> mAChR and that the mutant M<sub>3</sub> mAChR (M<sub>3</sub> RASSL) is behaving in a similar manner as the WT receptor. This mutant receptor provides a valuable research tool to study the in vivo functions of M<sub>3</sub> mAChR.

Furthermore, we confirmed that BQCA is a positive allosteric modulator at the M<sub>1</sub> mAChR and the compound also has intrinsic efficacy in its own right when tested in a well coupled system (such as phosphorylation of ERK 1/2). The degree of allosteric potentiation by BQCA is probe dependent and that BQCA is non-biased as a positive allosteric modulator. We also confirmed that VU0357017 is a partial agonist, but the mode of action of this ligand is unclear.

We also provided novel evidence that the M<sub>4</sub> mAChR is phosphorylated at Ser379 which was confirmed by phosphorylation specific antibody.

## Chapter 8: Critical evaluation and future directions

Although we have shown that Pilo preferentially activate the inositol phosphates pathway compared to global M<sub>3</sub> mAChR phosphorylation, this comparison was made against MCh. Given the importance of probe dependency in GPCR pharmacology, it might also be interesting to test whether Pilo still displays preferential receptor activation when compared to ACh, the endogenous ligand of mAChRs. We have also shown that the M<sub>3</sub> mAChR became dephosphorylated at Ser384 upon stimulation by an agonist. It is possible that this may be due to phosphorylation of an adjacent site which causes the antibody not being able to recognise Ser384. To test this, site directed mutagenesis can be used to replace Ser385 to alanine and determine if ser384 is still dephosphorylated upon agonist application.

Allosteric modulators have been considered an attractive chemotype for developing novel therapeutics targeting GPCRs due to their superior subtype selectivity and saturable effects. Although VU0357017 was originally reported to be an allosteric agonist at the M<sub>1</sub> mAChR, data obtained from this study suggests that the compound may also act orthosterically. In order to establish the mode of interaction of this compound, site directed mutagenesis studies could be applied to generate mutations at the known allosteric residues (such as W101) and residues making up the orthosteric binding pocket (Asp<sup>3.32</sup>) to see the effects of these mutations on the affinity and signalling efficacy of the compound. It may also be interesting to determine if BQCA and VU0357017 share a common binding site using this approach.

Phosphorylation has been established as a key regulatory process that controls the signalling properties of GPCRs. Using a mass spectrometric approach we found that the M<sub>4</sub> mAChR was phosphorylated at three sites upon agonist stimulation. However we did not detect phosphorylation at T145 which was previously determined by (Guo et al., 2010a) et al. Therefore a more comprehensive analysis of M<sub>4</sub> mAChR phosphorylation is required. In so

doing, a different cell line expressing higher levels of receptor and phosphopeptide enrichment method (such as IMAC) could be used to improve phosphopeptide coverage and subsequent identification of phosphorylation sites.

## References

- Abdul-Ridha A, Lane JR, Sexton PM, Canals M, Christopoulos A (2013). Allosteric modulation of a chemogenetically modified G protein-coupled receptor. *Molecular Pharmacology* **83**(2): 521-530.
- Ahn S, Shenoy SK, Wei H, Lefkowitz RJ (2004). Differential kinetic and spatial patterns of beta-arrestin and G protein-mediated ERK activation by the angiotensin II receptor. *Journal of Biological Chemistry* **279**: 35518–35525.
- Ahuja S, Smith SO (2009). Multiple switches in G protein-coupled receptor activation. *Trends in Pharmacological Sciences* **30**(9): 494-502.
- Akam EC, Challiss RA, Nahorski SR (2001). G(q/11) and G(i/o) activation profiles in CHO cells expressing human muscarinic acetylcholine receptors: dependence on agonist as well as receptor-subtype. *British Journal of Pharmacology* **132**(4): 950-958.
- Alexander GM, Rogan SC, Abbas AI, Armbruster BN, Pei Y, Allen JA, *et al.* (2009). Remote control of neuronal activity in transgenic mice expressing evolved G protein-coupled receptors. *Neuron* **63**(1): 27-39.
- Alvarez-Curto E, Prihandoko R, Tautermann CS, Zwier JM, Pediani JD, Lohse MJ, *et al.* (2011). Developing chemical genetic approaches to explore G protein-coupled receptor function: validation of the use of a receptor activated solely by synthetic ligand (RASSL). *Molecular Pharmacology* **80**(6): 1033-1046.
- Alvarez-Curto E, Ward RJ, Pediani JD, Milligan G (2010). Ligand regulation of the quaternary organization of cell surface M3 muscarinic acetylcholine receptors analyzed by fluorescence resonance energy transfer (FRET) imaging and homogeneous time-resolved FRET. *Journal of Biological Chemistry* **285**(30): 23318-23330.
- Anagnostaras SG, Murphy GG, Hamilton SE, Mitchell SL, Rahnema NP, Nathanson NM, *et al.* (2003). Selective cognitive dysfunction in acetylcholine M1 muscarinic receptor mutant mice. *Nature Neuroscience* **6**(1): 51-58.
- Armbruster BN, Li X, Pausch MH, Herlitze S, Roth BL (2007). Evolving the lock to fit the key to create a family of G protein-coupled receptors potently activated by an inert ligand. *Proceedings of the National Academy of Sciences of the United States of America* **104**(12): 5163-5168.
- Atzori M, Paz RD (2007). Interplay Between Dopamine and Acetylcholine in the Modulation of Attention. In: Tseng K-Y, Atzori M (ed) (eds). *Monoaminergic Modulation of Cortical Excitability*, edn: Springer US. p<sup>pp</sup> 283-297.
- Avlani VA, Langmead CJ, Guida E, Wood MD, Tehan BG, Herdon HJ, *et al.* (2010). Orthosteric and allosteric modes of interaction of novel selective agonists of the M1 muscarinic acetylcholine receptor. *Molecular Pharmacology* **78**(1): 94-104.

Azzi M, Charest PG, Angers S, Rousseau G, Kohout T, Bouvier M, *et al.* (2003). Beta-arrestin-mediated activation of MAPK by inverse agonists reveals distinct active conformations for G protein-coupled receptors. *Proceedings of the National Academy of Sciences of the United States of America* **100**(20): 11406-11411.

Baker JG, Hall IP, Hill SJ (2003). Agonist and inverse agonist actions of beta-blockers at the human beta 2-adrenoceptor provide evidence for agonist-directed signaling. *Molecular Pharmacology* **64**(6): 1357-1369.

Ballesteros JA, Weinstein H (1995). Integrated methods for the construction of three-dimensional models and computational probing of structure-function relations in G protein-coupled receptors. In: Stuart CS (ed)^(eds). *Methods in Neurosciences*, edn, Vol. Volume 25: Academic Press. p^pp 366-428.

Barch DM (2010). Pharmacological Strategies for Enhancing Cognition in Schizophrenia. In: Swerdlow NR (ed)^(eds). *Behavioral Neurobiology of Schizophrenia and Its Treatment*, edn, Vol. 4: Springer Berlin Heidelberg. p^pp 43-96.

Bender D, Holschbach M, Stocklin G (1994). Synthesis of n.c.a. carbon-11 labelled clozapine and its major metabolite clozapine-N-oxide and comparison of their biodistribution in mice. *Nuclear Medicine and Biology* **21**(7): 921-925.

Benovic JL, DeBlasi A, Stone WC, Caron MG, Lefkowitz RJ (1989). Beta-adrenergic receptor kinase: primary structure delineates a multigene family. *Science* **246**: 235–240.

Benovic JL, Regan JW, Matsui H, Mayor Jr. F, Cotecchia S, Leeb-Lundberg LM, *et al.* (1987). Agonist-dependent phosphorylation of the alpha 2-adrenergic receptor by the beta-adrenergic receptor kinase. *Journal of Biological Chemistry* **262**: 17251–17253.

Berg KA, Maayani S, Goldfarb J, Scaramellini C, Leff P, Clarke WP (1998). Effector pathway-dependent relative efficacy at serotonin type 2A and 2C receptors: evidence for agonist-directed trafficking of receptor stimulus. *Molecular Pharmacology* **54**(1): 94-104.

Berkeley JL, Gomeza J, Wess J, Hamilton SE, Nathanson NM, Levey AI (2001). M1 muscarinic acetylcholine receptors activate extracellular signal-regulated kinase in CA1 pyramidal neurons in mouse hippocampal slices. *Molecular and Cellular Neuroscience* **18**(5): 512-524.

Bessis AS, Rondard P, Gaven F, Brabet I, Triballeau N, Prezeau L, *et al.* (2002). Closure of the Venus flytrap module of mGlu8 receptor and the activation process: Insights from mutations converting antagonists into agonists. *Proceedings of the National Academy of Sciences of the United States of America* **99**(17): 11097-11102.

Black J (1996). A personal view of pharmacology. *Annual Review of Pharmacology and Toxicology* **36**: 1-33.

Black JW, Leff P (1983). Operational models of pharmacological agonism. *Proceedings of the Royal Society of London. Series B, Biological Sciences* **220**(1219): 141-162.

- Bockaert J, Pin JP (1999). Molecular tinkering of G protein-coupled receptors: an evolutionary success. *Embo Journal* **18**(7): 1723-1729.
- Boerrigter G, Lark MW, Whalen EJ, Soergel DG, Violin JD, Burnett JC, Jr. (2011). Cardiorenal actions of TRV120027, a novel ss-arrestin-biased ligand at the angiotensin II type I receptor, in healthy and heart failure canines: a novel therapeutic strategy for acute heart failure. *Circulation: Heart Failure* **4**(6): 770-778.
- Boerrigter G, Soergel DG, Violin JD, Lark MW, Burnett JC, Jr. (2012). TRV120027, a novel beta-arrestin biased ligand at the angiotensin II type I receptor, unloads the heart and maintains renal function when added to furosemide in experimental heart failure. *Circulation: Heart Failure* **5**(5): 627-634.
- Bonner TI, Buckley NJ, Young AC, Brann MR (1987). Identification of a family of muscarinic acetylcholine receptor genes. *Science* **237**(4814): 527-532.
- Bonner TI, Young AC, Brann MR, Buckley NJ (1988). Cloning and expression of the human and rat m5 muscarinic acetylcholine receptor genes. *Neuron* **1**(5): 403-410.
- Bradley KN (2000). Muscarinic toxins from the green mamba. *Pharmacology & Therapeutics* **85**(2): 87-109.
- Brady AE, Jones CK, Bridges TM, Kennedy JP, Thompson AD, Heiman JU, *et al.* (2008). Centrally active allosteric potentiators of the M4 muscarinic acetylcholine receptor reverse amphetamine-induced hyperlocomotor activity in rats. *Journal of Pharmacology and Experimental Therapeutics* **327**(3): 941-953.
- Brann MR, JØrgensen HB, Burstein ES, Spalding TA, Ellis J, Jones SVP, *et al.* (1993). Studies of the Pharmacology, Localization, and Structure of Muscarinic Acetylcholine Receptors. *Annals of the New York Academy of Sciences* **707**(1): 225-236.
- Bruysters M, Jongejan A, Akdemir A, Bakker RA, Leurs R (2005). A G(q/11)-coupled mutant histamine H(1) receptor F435A activated solely by synthetic ligands (RASSL). *Journal of Biological Chemistry* **280**(41): 34741-34746.
- Budd DC, McDonald JE, Tobin AB (2000). Phosphorylation and regulation of a Gq/11-coupled receptor by casein kinase 1alpha. *Journal of Biological Chemistry* **275**(26): 19667-19675.
- Budd DC, Willars GB, McDonald JE, Tobin AB (2001). Phosphorylation of the Gq/11-coupled m3-muscarinic receptor is involved in receptor activation of the ERK-1/2 mitogen-activated protein kinase pathway. *Journal of Biological Chemistry* **276**(7): 4581-4587.
- Burford NT, Watson J, Bertekap R, Alt A (2011). Strategies for the identification of allosteric modulators of G-protein-coupled receptors. *Biochemical Pharmacology* **81**(6): 691-702.
- Busillo JM, Armando S, Sengupta R, Meucci O, Bouvier M, Benovic JL (2010). Site-specific phosphorylation of CXCR4 is dynamically regulated by multiple kinases and results in differential modulation of CXCR4 signaling. *Journal of Biological Chemistry* **285**(10): 7805-7817.

- Butcher AJ, Prihandoko R, Kong KC, McWilliams P, Edwards JM, Bottrill A, *et al.* (2011). Differential G-protein-coupled receptor phosphorylation provides evidence for a signaling bar code. *Journal of Biological Chemistry* **286**(13): 11506-11518.
- Bymaster FP, McKinzie DL, Felder CC, Wess J (2003). Use of M1-M5 muscarinic receptor knockout mice as novel tools to delineate the physiological roles of the muscarinic cholinergic system. *Neurochemical Research* **28**(3-4): 437-442.
- Cabrera-Vera TM, Vanhauwe J, Thomas TO, Medkova M, Preininger A, Mazzoni MR, *et al.* (2003). Insights into G protein structure, function, and regulation. *Endocrine Reviews* **24**(6): 765-781.
- Canals M, Lane JR, Wen A, Scammells PJ, Sexton PM, Christopoulos A (2012). A Monod-Wyman-Changeux mechanism can explain G protein-coupled receptor (GPCR) allosteric modulation. *Journal of Biological Chemistry* **287**(1): 650-659.
- Caramellini C, Leff P (1998). A Three-State Receptor Model: Predictions of Multiple Agonist Pharmacology for the Same Receptor Types. *Annals of the New York Academy of Sciences* **861**(1): 97-103.
- Carsi JM, Valentine HH, Potter LT (1999). m2-toxin: A selective ligand for M2 muscarinic receptors. *Molecular Pharmacology* **56**(5): 933-937.
- Caulfield MP, Birdsall NJ (1998). International Union of Pharmacology. XVII. Classification of muscarinic acetylcholine receptors. *Pharmacological Reviews* **50**(2): 279-290.
- Cavanaugh A, Huang Y, Breitwieser GE (2012). Behind the curtain: cellular mechanisms for allosteric modulation of calcium-sensing receptors. *British Journal of Pharmacology* **165**(6): 1670-1677.
- Cescato R, Loesch KA, Waser B, Macke HR, Rivier JE, Reubi JC, *et al.* (2010). Agonist-biased signaling at the sst2A receptor: the multi-somatostatin analogs KE108 and SOM230 activate and antagonize distinct signaling pathways. *Molecular Endocrinology* **24**(1): 240-249.
- Challiss RAJ, Thomas RL (2009). Signaling Diversity Mediated by Muscarinic Acetylcholine Receptor Subtypes and Evidence for Functional Selectivity. In: Neve K (ed) (eds). *Functional Selectivity of G Protein-Coupled Receptor Ligands*, edn: Humana Press. pp 125-153.
- Chan WY, McKinzie DL, Bose S, Mitchell SN, Witkin JM, Thompson RC, *et al.* (2008). Allosteric modulation of the muscarinic M4 receptor as an approach to treating schizophrenia. *Proceedings of the National Academy of Sciences of the United States of America* **105**(31): 10978-10983.
- Chang WC, Ng JK, Nguyen T, Pellissier L, Claeysen S, Hsiao EC, *et al.* (2007). Modifying ligand-induced and constitutive signaling of the human 5-HT4 receptor. *PLoS One* **2**(12): 0001317.

- Chapman KL, Vaswani D, Hendry N, Langmead CJ, Kew JN, Watson JM (2011). The muscarinic M(4) receptor is the functionally predominant subtype in rat and mouse striatum as demonstrated using [(35)S] GTPgammaS binding. *European Journal of Pharmacology* **652**(1-3): 1-6.
- Chen YJ, Oldfield S, Butcher AJ, Tobin AB, Saxena K, Gurevich VV, *et al.* (2013). Identification of phosphorylation sites in the COOH-terminal tail of the mu-opioid receptor. *Journal of Neurochemistry* **124**(2): 189-199.
- Chien EY, Liu W, Zhao Q, Katritch V, Han GW, Hanson MA, *et al.* (2010). Structure of the human dopamine D3 receptor in complex with a D2/D3 selective antagonist. *Science* **330**(6007): 1091-1095.
- Choe HW, Kim YJ, Park JH, Morizumi T, Pai EF, Krauss N, *et al.* (2011). Crystal structure of metarhodopsin II. *Nature* **471**(7340): 651-655.
- Christopoulos A (2002). Allosteric binding sites on cell-surface receptors: novel targets for drug discovery. *Nature Reviews Drug Discovery* **1**(3): 198-210.
- Christopoulos A (2007). Muscarinic Acetylcholine Receptors in the Central Nervous System: Structure, Function, and Pharmacology. In: Karczmar A (ed)^(eds). *Exploring the Vertebrate Central Cholinergic Nervous System*, edn: Springer US. p^pp 163-208.
- Christopoulos A, Kenakin T (2002). G protein-coupled receptor allosterism and complexing. *Pharmacological Reviews* **54**(2): 323-374.
- Christopoulos A, May LT, Avlani VA, Sexton PM (2004). G-protein-coupled receptor allosterism: the promise and the problem(s). *Biochemical Society Transactions* **32**(Pt 5): 873-877.
- Claing A, Laporte SA, Caron MG, Lefkowitz RJ (2002). Endocytosis of G protein-coupled receptors: roles of G protein-coupled receptor kinases and beta-arrestin proteins. *Progress in Neurobiology* **66**(2): 61-79.
- Clapham DE, Neer EJ (1997). G protein beta gamma subunits. *Annual review of pharmacology and toxicology* **37**: 167-203.
- Coffa S, Breitman M, Hanson SM, Callaway K, Kook S, Dalby KN, *et al.* (2011). The effect of arrestin conformation on the recruitment of c-Raf1, MEK1, and ERK1/2 activation. *PLoS One* **6**(12): 12.
- Conklin BR (2007). New tools to build synthetic hormonal pathways. *Proceedings of the National Academy of Sciences of the United States of America* **104**(12): 4777-4778.
- Conklin BR, Brann MR, Buckley NJ, Ma AL, Bonner TI, Axelrod J (1988). Stimulation of arachidonic acid release and inhibition of mitogenesis by cloned genes for muscarinic receptor subtypes stably expressed in A9 L cells. *Proceedings of the National Academy of Sciences of the United States of America* **85**(22): 8698-8702.

- Conklin BR, Farfel Z, Lustig KD, Julius D, Bourne HR (1993). Substitution of three amino acids switches receptor specificity of Gq alpha to that of Gi alpha. *Nature* **363**(6426): 274-276.
- Conklin BR, Hsiao EC, Claeysen S, Dumuis A, Srinivasan S, Forsayeth JR, *et al.* (2008). Engineering GPCR signaling pathways with RASSLs. *Nature Methods* **5**(8): 673-678.
- Conn PJ, Christopoulos A, Lindsley CW (2009a). Allosteric modulators of GPCRs: a novel approach for the treatment of CNS disorders. *Nature Reviews Drug Discovery* **8**(1): 41-54.
- Conn PJ, Jones CK, Lindsley CW (2009b). Subtype-selective allosteric modulators of muscarinic receptors for the treatment of CNS disorders. *Trends in Pharmacological Sciences* **30**(3): 148-155.
- Corrigan MH, Gallen CC, Bonura ML, Merchant KM (2004). Effectiveness of the selective D4 antagonist sonepiprazole in schizophrenia: a placebo-controlled trial. *Biological Psychiatry* **55**(5): 445-451.
- Coward P, Wada HG, Falk MS, Chan SD, Meng F, Akil H, *et al.* (1998). Controlling signaling with a specifically designed Gi-coupled receptor. *Proceedings of the National Academy of Sciences of the United States of America* **95**(1): 352-357.
- Daaka Y, Luttrell LM, Lefkowitz RJ (1997). Switching of the coupling of the beta2-adrenergic receptor to different G proteins by protein kinase A. *Nature* **390**(6655): 88-91.
- Davis AA, Fritz JJ, Wess J, Lah JJ, Levey AI (2010). Deletion of M1 muscarinic acetylcholine receptors increases amyloid pathology in vitro and in vivo. *Journal of Neuroscience* **30**(12): 4190-4196.
- Delmas P, Brown DA (2005). Pathways modulating neural KCNQ/M (Kv7) potassium channels. *Nature Reviews Neuroscience* **6**: 850-862.
- Dencker D, Weikop P, Sorensen G, Woldbye DP, Wortwein G, Wess J, *et al.* (2012). An allosteric enhancer of M(4) muscarinic acetylcholine receptor function inhibits behavioral and neurochemical effects of cocaine. *Psychopharmacology* **224**(2): 277-287.
- Dentone C, Fraccaro P, Fenoglio D, Firpo E, Cenderello G, Piscopo R, *et al.* (2012). Use of maraviroc in clinical practice: a multicenter observational study. *Journal of the International AIDS Society* **15**(6): 18265.
- DeWire SM, Ahn S, Lefkowitz RJ, Shenoy SK (2007). Beta-arrestins and cell signaling. *Annual Review of Physiology* **69**: 483-510.
- Digby GJ, Noetzel MJ, Bubser M, Utley TJ, Walker AG, Byun NE, *et al.* (2012). Novel allosteric agonists of M1 muscarinic acetylcholine receptors induce brain region-specific responses that correspond with behavioral effects in animal models. *Journal of Neuroscience* **32**(25): 8532-8544.
- Digby GJ, Shirey JK, Conn PJ (2010). Allosteric activators of muscarinic receptors as novel approaches for treatment of CNS disorders. *Molecular Biosystems* **6**(8): 1345-1354.

- Dong S, Allen JA, Farrell M, Roth BL (2010a). A chemical-genetic approach for precise spatio-temporal control of cellular signaling. *Molecular Biosystems* **6**(8): 1376-1380.
- Dong S, Rogan SC, Roth BL (2010b). Directed molecular evolution of DREADDs: a generic approach to creating next-generation RASSLs. *Nature Protocols* **5**(3): 561-573.
- Doré Andrew S, Robertson N, Errey James C, Ng I, Hollenstein K, Tehan B, *et al.* (2011). Structure of the Adenosine A2A Receptor in Complex with ZM241385 and the Xanthines XAC and Caffeine. *Structure* **19**(9): 1283-1293.
- Duttaroy A, Zimlikli CL, Gautam D, Cui Y, Mears D, Wess J (2004). Muscarinic stimulation of pancreatic insulin and glucagon release is abolished in m3 muscarinic acetylcholine receptor-deficient mice. *Diabetes* **53**(7): 1714-1720.
- Eglen RM, Choppin A, Dillon MP, Hegde S (1999). Muscarinic receptor ligands and their therapeutic potential. *Current Opinion in Chemical Biology* **3**(4): 426-432.
- Eglen RM, Choppin A, Watson N (2001). Therapeutic opportunities from muscarinic receptor research. *Trends in Pharmacological Sciences* **22**(8): 409-414.
- Ehlert FJ (2005). Analysis of Allosterism in Functional Assays. *Journal of Pharmacology and Experimental Therapeutics* **315**(2): 740-754.
- Ehlert FJ (1988). Estimation of the affinities of allosteric ligands using radioligand binding and pharmacological null methods. *Molecular Pharmacology* **33**(2): 187-194.
- Evans BA, Broxton N, Merlin J, Sato M, Hutchinson DS, Christopoulos A, *et al.* (2011). Quantification of Functional Selectivity at the Human  $\alpha$ 1A-Adrenoceptor. *Molecular Pharmacology* **79**(2): 298-307.
- Felder CC, Bymaster FP, Ward J, DeLapp N (2000). Therapeutic Opportunities for Muscarinic Receptors in the Central Nervous System. *Journal of Medicinal Chemistry* **43**(23): 4333-4353.
- Ferguson SM, Eskenazi D, Ishikawa M, Wanat MJ, Phillips PE, Dong Y, *et al.* (2011). Transient neuronal inhibition reveals opposing roles of indirect and direct pathways in sensitization. *Nature Neuroscience* **14**(1): 22-24.
- Figuroa KW, Ehlert FJ (2007). Use of Intrinsic Relative Activity to determine agonist dependent G-protein signaling at the M4 muscarinic receptor. *Faseb Journal* **21**(5): A424-A424.
- Figuroa KW, Griffin MT, Ehlert FJ (2009). Selectivity of agonists for the active state of M1 to M4 muscarinic receptor subtypes. *Journal of Pharmacology and Experimental Therapeutics* **328**(1): 331-342.
- Fink-Jensen A, Schmidt LS, Dencker D, Schulein C, Wess J, Wortwein G, *et al.* (2011). Antipsychotic-induced catalepsy is attenuated in mice lacking the M4 muscarinic acetylcholine receptor. *European Journal of Pharmacology* **656**(1-3): 39-44.

Fredriksson R, Lagerstrom MC, Lundin LG, Schioth HB (2003). The G-protein-coupled receptors in the human genome form five main families. Phylogenetic analysis, paralogon groups, and fingerprints. *Molecular Pharmacology* **63**(6): 1256-1272.

Galandrin S, Oligny-Longpré G, Bouvier M (2007). The evasive nature of drug efficacy: implications for drug discovery. *Trends in Pharmacological Sciences* **28**(8): 423-430.

Gautam D, Han SJ, Duttaroy A, Mears D, Hamdan FF, Li JH, *et al.* (2007). Role of the M3 muscarinic acetylcholine receptor in beta-cell function and glucose homeostasis. *Diabetes, Obesity and Metabolism* **2**: 158-169.

Gautam D, Han SJ, Hamdan FF, Jeon J, Li B, Li JH, *et al.* (2006). A critical role for beta cell M3 muscarinic acetylcholine receptors in regulating insulin release and blood glucose homeostasis in vivo. *Cell Metabolism* **3**(6): 449-461.

Gether U (2000). Uncovering molecular mechanisms involved in activation of G protein-coupled receptors. *Endocrine Reviews* **21**(1): 90-113.

Gomez J, Zhang L, Kostenis E, Felder C, Bymaster F, Brodtkin J, *et al.* (1999). Enhancement of D1 dopamine receptor-mediated locomotor stimulation in M(4) muscarinic acetylcholine receptor knockout mice. *Proceedings of the National Academy of Sciences of the United States of America* **96**(18): 10483-10488.

Goudet C, Gaven F, Kniazeff J, Vol C, Liu J, Cohen-Gonsaud M, *et al.* (2004). Heptahelical domain of metabotropic glutamate receptor 5 behaves like rhodopsin-like receptors. *Proceedings of the National Academy of Sciences of the United States of America* **101**(1): 378-383.

Granier S, Manglik A, Kruse AC, Kobilka TS, Thian FS, Weis WI, *et al.* (2012). Structure of the delta-opioid receptor bound to naltrindole. *Nature* **485**(7398): 400-404.

Granzin J, Wilden U, Choe HW, Labahn J, Krafft B, Buldt G (1998). X-ray crystal structure of arrestin from bovine rod outer segments. *Nature* **391**(6670): 918-921.

Gregory KJ, Hall NE, Tobin AB, Sexton PM, Christopoulos A (2010). Identification of orthosteric and allosteric site mutations in M2 muscarinic acetylcholine receptors that contribute to ligand-selective signaling bias. *Journal of Biological Chemistry* **285**(10): 7459-7474.

Gregory KJ, Sexton PM, Christopoulos A (2007). Allosteric modulation of muscarinic acetylcholine receptors. *Current Neuropharmacology* **5**(3): 157-167.

Grinshpoon A, Moskowitz M, Valevski A, Kreizman A, Palei L, Mar M, *et al.* (1998). Zuclopenthixol, D1/D2 antagonist, for treatment of chronic aggressive schizophrenia and psychotic oligophrenic patients. *European Psychiatry* **13**(5): 273-275.

Gudermann T, Kalkbrenner F, Schultz G (1996). Diversity and selectivity of receptor-G protein interaction. *Annual Review of Pharmacology and Toxicology* **36**: 429-459.

Gudermann T, Schoneberg T, Schultz G (1997). Functional and structural complexity of signal transduction via G-protein-coupled receptors. *Annual Review of Neuroscience* **20**: 399-427.

Guettier JM, Gautam D, Scarselli M, Ruiz de Azua I, Li JH, Rosemond E, *et al.* (2009). A chemical-genetic approach to study G protein regulation of beta cell function in vivo. *Proceedings of the National Academy of Sciences of the United States of America* **106**(45): 19197-19202.

Guo ML, Fibuch EE, Liu XY, Choe ES, Buch S, Mao LM, *et al.* (2010). CaMKIIalpha interacts with M4 muscarinic receptors to control receptor and psychomotor function. *Embo Journal* **29**(12): 2070-2081.

Gurevich EV, Gurevich VV (2006). Arrestins: ubiquitous regulators of cellular signaling pathways. *Genome Biology* **7**(9): 236.

Haga K, Kruse AC, Asada H, Yurugi-Kobayashi T, Shiroishi M, Zhang C, *et al.* (2012). Structure of the human M2 muscarinic acetylcholine receptor bound to an antagonist. *Nature* **482**(7386): 547-U147.

Hammer R, Berrie CP, Birdsall NJM, Burgen ASV, Hulme EC (1980). Pirenzepine distinguishes between different subclasses of muscarinic receptors. *Nature* **283**(5742): 90-92.

Han M, Gurevich VV, Vishnivetskiy SA, Sigler PB, Schubert C (2001). Crystal structure of beta-arrestin at 1.9 Å: possible mechanism of receptor binding and membrane Translocation. *Structure* **9**(9): 869-880.

Hanson MA, Roth CB, Jo EJ, Griffith MT, Scott FL, Reinhart G, *et al.* (2012). Crystal Structure of a Lipid G Protein-Coupled Receptor. *Science* **335**(6070): 851-855.

Hanyaloglu AC, von Zastrow M (2008). Regulation of GPCRs by endocytic membrane trafficking and its potential implications. *Annual Review of Pharmacology and Toxicology* **48**: 537-568.

Henrich TJ, Kuritzkes DR (2013). HIV-1 entry inhibitors: recent development and clinical use. *Current Opinion in Virology* **2**(12): 00190-00193.

Hermans E (2003). Biochemical and pharmacological control of the multiplicity of coupling at G-protein-coupled receptors. *Pharmacology & Therapeutics* **99**(1): 25-44.

Hirsch JA, Schubert C, Gurevich VV, Sigler PB (1999). The 2.8 Å crystal structure of visual arrestin: a model for arrestin's regulation. *Cell* **97**(2): 257-269.

Holroyd EW, Szekeres PG, Whittaker RD, Kelly E, Edwardson JM (1999). Effect of G protein-coupled receptor kinase 2 on the sensitivity of M4 muscarinic acetylcholine receptors to agonist-induced internalization and desensitization in NG108-15 cells. *Journal of Neurochemistry* **73**(3): 1236-1245.

Hosey MM, Pals-Rylaarsdam R, Lee KB, Roseberry AG, Benovic JL, Gurevich VV, *et al.* (1999). Molecular events associated with the regulation of signaling by M2 muscarinic receptors. *Life Sciences* **64**(6-7): 363-368.

Huang XP, Prilla S, Mohr K, Ellis J (2005). Critical amino acid residues of the common allosteric site on the M2 muscarinic acetylcholine receptor: more similarities than differences between the structurally divergent agents gallamine and bis(ammonio)alkane-type hexamethylene-bis-[dimethyl-(3-phthalimidopropyl)ammonium]dibromide. *Molecular Pharmacology* **68**(3): 769-778.

Hulme EC, Birdsall NJ, Buckley NJ (1990). Muscarinic receptor subtypes. *Annual Review of Pharmacology and Toxicology* **30**: 633-673.

Ibrahim IA, Kurose H (2012). beta-Arrestin-mediated signaling improves the efficacy of therapeutics. *Journal of Pharmacological Sciences* **118**(4): 408-412.

Jaakola VP, Griffith MT, Hanson MA, Cherezov V, Chien EYT, Lane JR, *et al.* (2008). The 2.6 Angstrom Crystal Structure of a Human A(2A) Adenosine Receptor Bound to an Antagonist. *Science* **322**(5905): 1211-1217.

Jaakola VP, Ijzerman AP (2010). The crystallographic structure of the human adenosine A(2A) receptor in a high-affinity antagonist-bound state: implications for GPCR drug screening and design. *Current Opinion in Structural Biology* **20**(4): 401-414.

Jacobson MA, Kreatsoulas C, Pascarella DM, O'Brien JA, Sur C (2010). The M1 muscarinic receptor allosteric agonists AC-42 and 1-[1'-(2-methylbenzyl)-1,4'-bipiperidin-4-yl]-1,3-dihydro-2H-benzimidazol-2-one bind to a unique site distinct from the acetylcholine orthosteric site. *Molecular Pharmacology* **78**(4): 648-657.

Jager D, Schmalenbach C, Prilla S, Schrobang J, Kebig A, Sennwitz M, *et al.* (2007). Allosteric small molecules unveil a role of an extracellular E2/transmembrane helix 7 junction for G protein-coupled receptor activation. *Journal of Biological Chemistry* **282**(48): 34968-34976.

Jeon J, Dencker D, Wortwein G, Woldbye DP, Cui Y, Davis AA, *et al.* (2010). A subpopulation of neuronal M4 muscarinic acetylcholine receptors plays a critical role in modulating dopamine-dependent behaviors. *Journal of Neuroscience* **30**(6): 2396-2405.

Johnston CA, Siderovski DP (2007). Receptor-mediated activation of heterotrimeric G-proteins: current structural insights. *Molecular Pharmacology* **72**(2): 219-230.

Jolkkonen M, van Giersbergen PL, Hellman U, Wernstedt C, Karlsson E (1994). A toxin from the green mamba *Dendroaspis angusticeps*: amino acid sequence and selectivity for muscarinic m4 receptors. *FEBS Letters* **352**(1): 91-94.

Kao YJ, Ghosh M, Schonbrunn A (2011). Ligand-dependent mechanisms of sst2A receptor trafficking: role of site-specific phosphorylation and receptor activation in the actions of biased somatostatin agonists. *Molecular Endocrinology* **25**(6): 1040-1054.

- Karin M, Greten FR (2005). NF- $\kappa$ B: linking inflammation and immunity to cancer development and progression. *Nature Reviews Immunology* **5**: 749–759.
- Katritch V, Cherezov V, Stevens RC (2012). Diversity and modularity of G protein-coupled receptor structures. *Trends in Pharmacological Sciences* **33**(1): 17-27.
- Katritch V, Cherezov V, Stevens RC (2013). Structure-function of the G protein-coupled receptor superfamily. *Annual Review of Pharmacology and Toxicology* **53**: 531-556.
- Kenakin TP (2009).  $\gamma$ TM Receptor Allostery: Putting Numbers to Shapeshifting Proteins. *Trends in Pharmacological Sciences* **30**(9): 460-469.
- Kenakin TP (2012). Biased signalling and allosteric machines: new vistas and challenges for drug discovery. *British Journal of Pharmacology* **165**(6): 1659-1669.
- Kenakin TP (2011). Functional Selectivity and Biased Receptor Signaling. *Journal of Pharmacology and Experimental Therapeutics* **336**(2): 296-302.
- Kenakin TP (2010). Ligand Detection in the Allosteric World. *Journal of Biomolecular Screening* **15**(2): 119-130.
- Kendall RT, Luttrell LM (2009). Diversity in arrestin function. *Cellular and Molecular Life Sciences* **66**(18): 2953-2973.
- Keov P, Sexton PM, Christopoulos A (2011). Allosteric modulation of G protein-coupled receptors: a pharmacological perspective. *Neuropharmacology* **60**(1): 24-35.
- Kim J, Ahn S, Ren XR, Whalen EJ, Reiter E, Wei HJ, *et al.* (2005). Functional antagonism of different G protein-coupled receptor kinases for beta-arrestin-mediated angiotensin II receptor signaling. *Proceedings of the National Academy of Sciences of the United States of America* **102**(5): 1442-1447.
- Kim KS, Abraham D, Williams B, Violin JD, Mao L, Rockman HA (2012). beta-Arrestin-biased AT1R stimulation promotes cell survival during acute cardiac injury. *American Journal of Physiology. Heart and Circulatory Physiology* **303**(8): 10.
- Kobilka BK, Deupi X (2007). Conformational complexity of G-protein-coupled receptors. *Trends in Pharmacological Sciences* **28**(8): 397-406.
- Kong KC, Butcher AJ, McWilliams P, Jones D, Wess J, Hamdan FF, *et al.* (2010). M3-muscarinic receptor promotes insulin release via receptor phosphorylation/arrestin-dependent activation of protein kinase D1. *Proceedings of the National Academy of Sciences of the United States of America* **107**(49): 21181-21186.
- Kong KC, Tobin AB (2011). The role of M(3)-muscarinic receptor signaling in insulin secretion. *Communicative & Integrative Biology* **4**(4): 489-491.
- Kristiansen K (2004). Molecular mechanisms of ligand binding, signaling, and regulation within the superfamily of G-protein-coupled receptors: molecular modeling and mutagenesis approaches to receptor structure and function. *Pharmacology & Therapeutics* **103**(1): 21-80.

- Kruse AC, Hu J, Pan AC, Arlow DH, Rosenbaum DM, Rosemond E, *et al.* (2012). Structure and dynamics of the M3 muscarinic acetylcholine receptor. *Nature* **482**(7386): 552-556.
- Kubo T, Fukuda K, Mikami A, Maeda A, Takahashi H, Mishina M, *et al.* (1986). Cloning, sequencing and expression of complementary DNA encoding the muscarinic acetylcholine receptor. *Nature* **323**(6087): 411-416.
- Kubo TAI (1993). Molecular Basis of the Muscarinic Acetylcholine Receptors. *Annals of the New York Academy of Sciences* **707**(1): 210-224.
- Kuhn H, Dreyer WJ (1972). Light dependent phosphorylation of rhodopsin by ATP. *FEBS Letters* **20**: 1-6.
- Kunishima N, Shimada Y, Tsuji Y, Sato T, Yamamoto M, Kumasaka T, *et al.* (2000). Structural basis of glutamate recognition by a dimeric metabotropic glutamate receptor. *Nature* **407**(6807): 971-977.
- Lagerstrom MC, Schioth HB (2008). Structural diversity of G protein-coupled receptors and significance for drug discovery. *Nature Reviews Drug Discovery* **7**(4): 339-357.
- Lambright DG, Sondek J, Bohm A, Skiba NP, Hamm HE, Sigler PB (1996). The 2.0 Å crystal structure of a heterotrimeric G protein. *Nature* **379**(6563): 311-319.
- Lameh J, Cone RI, Maeda S, Philip M, Corbani M, Nadasdi L, *et al.* (1990). STRUCTURE AND FUNCTION OF G-PROTEIN COUPLED RECEPTORS. *Pharmaceutical Research* **7**(12): 1213-1221.
- Lameh J, Philip M, Sharma YK, Moro O, Ramachandran J, Sadee W (1992). Hm1 muscarinic cholinergic receptor internalization requires a domain in the third cytoplasmic loop. *Journal of Biological Chemistry* **267**(19): 13406-13412.
- Lane JR, Sexton PM, Christopoulos A (2013). Bridging the gap: bitopic ligands of G-protein-coupled receptors. *Trends in Pharmacological Sciences* **34**(1): 59-66.
- Langmead CJ (2011). Determining allosteric modulator mechanism of action: integration of radioligand binding and functional assay data. *Methods in Molecular Biology* **746**: 195-209.
- Langmead CJ, Austin NE, Branch CL, Brown JT, Buchanan KA, Davies CH, *et al.* (2008a). Characterization of a CNS penetrant, selective M1 muscarinic receptor agonist, 77-LH-28-1. *British Journal of Pharmacology* **154**(5): 1104-1115.
- Langmead CJ, Christopoulos A (2006a). Allosteric agonists of 7TM receptors: expanding the pharmacological toolbox. *Trends in Pharmacological Sciences* **27**(9): 475-481.
- Langmead CJ, Fry VAH, Forbes IT, Branch CL, Christopoulos A, Wood MD, *et al.* (2006b). Probing the Molecular Mechanism of Interaction between 4-n-Butyl-1-[4-(2-methylphenyl)-4-oxo-1-butyl]-piperidine (AC-42) and the Muscarinic M1 Receptor: Direct Pharmacological Evidence That AC-42 Is an Allosteric Agonist. *Molecular Pharmacology* **69**(1): 236-246.

Langmead CJ, Watson J, Reavill C (2008b). Muscarinic acetylcholine receptors as CNS drug targets. *Pharmacology & Therapeutics* **117**(2): 232-243.

Lau EK, Trester-Zedlitz M, Trinidad JC, Kotowski SJ, Krutchinsky AN, Burlingame AL, *et al.* (2011). Quantitative encoding of the effect of a partial agonist on individual opioid receptors by multisite phosphorylation and threshold detection. *Science Signaling* **4**(185).

Lazareno S, Farries T, Gharagozloo P, Kuonen D, Popham A, Birdsall NJ (1997). Allosteric actions of brucine analogs at muscarinic receptor subtypes. *Life Sciences* **60**: 1169.

Leach K, Loiacono RE, Felder CC, McKinzie DL, Mogg A, Shaw DB, *et al.* (2010). Molecular mechanisms of action and in vivo validation of an M4 muscarinic acetylcholine receptor allosteric modulator with potential antipsychotic properties. *Neuropsychopharmacology* **35**(4): 855-869.

Leach K, Sexton PM, Christopoulos A (2007). Allosteric GPCR modulators: taking advantage of permissive receptor pharmacology. *Trends in Pharmacological Sciences* **28**(8): 382-389.

Lebois EP, Bridges TM, Lewis LM, Dawson ES, Kane AS, Xiang Z, *et al.* (2010). Discovery and characterization of novel subtype-selective allosteric agonists for the investigation of M(1) receptor function in the central nervous system. *ACS Chemical Neuroscience* **1**(2): 104-121.

Lebon G, Langmead CJ, Tehan BG, Hulme EC (2009). Mutagenic mapping suggests a novel binding mode for selective agonists of M1 muscarinic acetylcholine receptors. *Molecular Pharmacology* **75**(2): 331-341.

Lebon G, Warne T, Tate CG (2012). Agonist-bound structures of G protein-coupled receptors. *Current Opinion in Structural Biology* **22**(4): 482-490.

Lefkowitz RJ (1993). G protein-coupled receptor kinases. *Cell* **74**(3): 409-412.

Lefkowitz RJ (2004). Historical review: a brief history and personal retrospective of seven-transmembrane receptors. *Trends in Pharmacological Sciences* **25**(8): 413-422.

Lefkowitz RJ (2007a). Seven transmembrane receptors: a brief personal retrospective. *Biochimica et Biophysica Acta* **4**: 748-755.

Lefkowitz RJ (2007b). Seven transmembrane receptors: something old, something new. *Acta Physiologica* **190**(1): 9-19.

Lefkowitz RJ (2000). The superfamily of heptahelical receptors. *Nature Cell Biology* **2**(7): E133-136.

Lefkowitz RJ, Shenoy SK (2005). Transduction of receptor signals by beta-arrestins. *Science* **308**(5721): 512-517.

Lefkowitz RJ, Whalen EJ (2004). beta-arrestins: traffic cops of cell signaling. *Current Opinion in Cell Biology* **16**(2): 162-168.

Leppik RA, Miller RC, Eck M, Paquet JL (1994). Role of acidic amino acids in the allosteric modulation by gallamine of antagonist binding at the m2 muscarinic acetylcholine receptor. *Molecular Pharmacology* **45**(5): 983-990.

Liggett SB (2011). Phosphorylation barcoding as a mechanism of directing GPCR signaling. *Science Signaling* **4**(185): 2002331.

Lin AL, Zhu B, Zhang W, Dang H, Zhang BX, Katz MS, *et al.* (2008). Distinct pathways of ERK activation by the muscarinic agonists pilocarpine and carbachol in a human salivary cell line. *American Journal of Physiology. Cell Physiology* **294**(6): 2.

Liu Q, Dewi DA, Liu W, Bee MS, Schonbrunn A (2008). Distinct phosphorylation sites in the SST2A somatostatin receptor control internalization, desensitization, and arrestin binding. *Molecular Pharmacology* **73**(2): 292-304.

Liu QS, Bee MS, Schonbrunn A (2009). Site Specificity of Agonist and Second Messenger-Activated Kinases for Somatostatin Receptor Subtype 2A (Sst2A) Phosphorylation. *Molecular Pharmacology* **76**(1): 68-80.

Luo JS, Busillo JM, Benovic JL (2008). M-3 muscarinic acetylcholine receptor-mediated signaling is regulated by distinct mechanisms. *Molecular Pharmacology* **74**(2): 338-347.

Luttrell LM, Gesty-Palmer D (2010). Beyond desensitization: physiological relevance of arrestin-dependent signaling. *Pharmacological Reviews* **62**(2): 305-330.

Luttrell LM, Kenakin TP (2011). Refining efficacy: allosterism and bias in G protein-coupled receptor signaling. *Methods in Molecular Biology* **756**: 3-35.

Ma L, Seager MA, Wittmann M, Jacobson M, Bickel D, Burno M, *et al.* (2009). Selective activation of the M1 muscarinic acetylcholine receptor achieved by allosteric potentiation. *Proceedings of the National Academy of Sciences of the United States of America* **106**(37): 15950-15955.

Maeda S, Lameh J, Mallet WG, Philip M, Ramachandran J, Sadee W (1990). Internalization of the Hm1 muscarinic cholinergic receptor involves the third cytoplasmic loop. *FEBS Letters* **269**(2): 386-388.

Maeda T, Imanishi Y, Palczewski K (2003). Rhodopsin phosphorylation: 30 years later. *Progress in Retinal and Eye Research* **22**(4): 417-434.

Manglik A, Kruse AC, Kobilka TS, Thian FS, Mathiesen JM, Sunahara RK, *et al.* (2012). Crystal structure of the  $\mu$ -opioid receptor bound to a morphinan antagonist. *Nature* **485**(7398): 321-326.

Marcocci C, Cetani F (2012). Update on the use of cinacalcet in the management of primary hyperparathyroidism. *Journal of Endocrinological Investigation* **35**(1): 90-95.

Marinissen MJ, Gutkind JS (2001). G-protein-coupled receptors and signaling networks: emerging paradigms. *Trends in Pharmacological Sciences* **22**(7): 368-376.

- Martin NP, Whalen EJ, Zamah MA, Pierce KL, Lefkowitz RJ (2004). PKA-mediated phosphorylation of the beta1-adrenergic receptor promotes Gs/Gi switching. *Cellular Signalling* **16**(12): 1397-1403.
- Martino G, Puma C, Yu XH, Gilbert AK, Coupal M, Markoglou N, *et al.* (2011). The M1/M4 preferring agonist xanomeline is analgesic in rodent models of chronic inflammatory and neuropathic pain via central site of action. *Pain* **152**(12): 2852-2860.
- Max SI, Liang JS, Potter LT (1993). Purification and properties of m1-toxin, a specific antagonist of m1 muscarinic receptors. *Journal of Neuroscience* **13**(10): 4293-4300.
- May LT, Avlani VA, Langmead CJ, Herdon HJ, Wood MD, Sexton PM, *et al.* (2007a). Structure-function studies of allosteric agonism at M2 muscarinic acetylcholine receptors. *Molecular Pharmacology* **72**(2): 463-476.
- May LT, Christopoulos A (2003). Allosteric modulators of G-protein-coupled receptors. *Current Opinion in Pharmacology* **3**(5): 551-556.
- May LT, Holliday ND, Hill SJ (2010). The Evolving Pharmacology of GPCRs. *GPCR Molecular Pharmacology and Drug Targeting; Shifting Paradigms and New Directions*: 34-35.
- May LT, Leach K, Sexton PM, Christopoulos A (2007b). Allosteric modulation of G protein-coupled receptors. *Annual Review of Pharmacology and Toxicology* **47**: 1-51.
- McCudden CR, Hains MD, Kimple RJ, Siderovski DP, Willard FS (2005). G-protein signaling: back to the future. *Cellular and Molecular Life Sciences* **62**(5): 551-577.
- McDonald PH, Lefkowitz RJ (2001). Beta-Arrestins: new roles in regulating heptahelical receptors' functions. *Cellular Signalling* **13**(10): 683-689.
- Melancon BJ, Hopkins CR, Wood MR, Emmitte KA, Niswender CM, Christopoulos A, *et al.* (2012). Allosteric modulation of seven transmembrane spanning receptors: theory, practice, and opportunities for central nervous system drug discovery. *Journal of Medicinal Chemistry* **55**(4): 1445-1464.
- Melchiorre C, Cassinelli A, Quaglia W (1987). Differential blockade of muscarinic receptor subtypes by polymethylene tetraamines. Novel class of selective antagonists of cardiac M-2 muscarinic receptors. *Journal of Medicinal Chemistry* **30**(1): 201-204.
- Milligan G, Kostenis E (2006). Heterotrimeric G-proteins: a short history. *British Journal of Pharmacology* **147**(1): S46-55.
- Monod J, Changeux JP, Jacob F (1963). Allosteric proteins and cellular control systems. *Journal of Molecular Biology* **6**: 306-329.
- Monod J, Wyman J, Changeux JP (1965). On the nature of allosteric transitions: a plausible model. *Journal of Molecular Biology* **12**: 88-118.

Moore CAC, Milano SK, Benovic JL (2007). Regulation of receptor trafficking by GRKs and arrestins. *Annual Review of Physiology* **69**: 451-482.

Mora-Peris B, Croucher A, Else L, Khoo S, Vera J, Back D, *et al.* (2012). Pharmacokinetic profile of maraviroc 150 mg dosed with darunavir/ritonavir once daily, with and without nucleoside analogues, in HIV-infected subjects. *Journal of the International AIDS Society* **15**(6): 18332.

Moro O, Lameh J, Sadee W (1993). Serine- and threonine-rich domain regulates internalization of muscarinic cholinergic receptors. *Journal of Biological Chemistry* **268**(10): 6862-6865.

Nahorski SR, Tobin AB, Willars GB (1997). Muscarinic M3 receptor coupling and regulation. *Life Sciences* **60**(13-14): 1039-1045.

Nakajima K, Wess J (2012). Design and functional characterization of a novel, arrestin-biased designer G protein-coupled receptor. *Molecular Pharmacology* **82**(4): 575-582.

Nawaratne V, Leach K, Felder CC, Sexton PM, Christopoulos A (2010). Structural determinants of allosteric agonism and modulation at the M4 muscarinic acetylcholine receptor: identification of ligand-specific and global activation mechanisms. *Journal of Biological Chemistry* **285**(25): 19012-19021.

Nawaratne V, Leach K, Suratman N, Loiacono RE, Felder CC, Armbruster BN, *et al.* (2008). New Insights into the Function of M4 Muscarinic Acetylcholine Receptors Gained Using a Novel Allosteric Modulator and a DREADD (Designer Receptor Exclusively Activated by a Designer Drug). *Molecular Pharmacology* **74**(4): 1119-1131.

Nichols CD, Roth BL (2009). Engineered G-protein Coupled Receptors are Powerful Tools to Investigate Biological Processes and Behaviors. *Frontiers in Molecular Neuroscience* **2**(16): 23.

Nobles KN, Xiao K, Ahn S, Shukla AK, Lam CM, Rajagopal S, *et al.* (2011). Distinct phosphorylation sites on the beta(2)-adrenergic receptor establish a barcode that encodes differential functions of beta-arrestin. *Science Signaling* **4**(185).

Nozza S, Galli L, Chiappetta S, Antinori A, Tommasi C, Di Pietro M, *et al.* (2012). Maraviroc 150 mg QD plus lopinavir/ritonavir, a NRTI-sparing regimen for HIV-infected naive patients: 48-weeks final results. *Journal of the International AIDS Society* **15**(6): 18232.

O'Hara PJ, Sheppard PO, Thogersen H, Venezia D, Haldeman BA, McGrane V, *et al.* (1993). The ligand-binding domain in metabotropic glutamate receptors is related to bacterial periplasmic binding proteins. *Neuron* **11**(1): 41-52.

Oakley RH, Laporte SA, Holt JA, Caron MG, Barak LS (2000). Differential affinities of visual arrestin, beta arrestin1, and beta arrestin2 for G protein-coupled receptors delineate two major classes of receptors. *Journal of Biological Chemistry* **275**(22): 17201-17210.

- Offermanns S (2003). G-proteins as transducers in transmembrane signalling. *Progress in Biophysics & Molecular Biology* **83**(2): 101-130.
- Oldham WM, Hamm HE (2008). Heterotrimeric G protein activation by G-protein-coupled receptors. *Nature Reviews Molecular Cell Biology* **9**(1): 60-71.
- Oldham WM, Hamm HE (2006). Structural basis of function in heterotrimeric G proteins. *Quarterly Reviews of Biophysics* **39**(2): 117-166.
- Oppermann M, Mack M, Proudfoot AEI, Olbrich H (1999). Differential effects of CC chemokines on CC chemokine receptor 5 (CCR5) phosphorylation and identification of phosphorylation sites on the CCR5 carboxyl terminus. *Journal of Biological Chemistry* **274**(13): 8875-8885.
- Pagano A, Ruegg D, Litschig S, Stoehr N, Stierlin C, Heinrich M, *et al.* (2000). The non-competitive antagonists 2-methyl-6-(phenylethynyl)pyridine and 7-hydroxyiminocyclopropan[b]chromen-1a-carboxylic acid ethyl ester interact with overlapping binding pockets in the transmembrane region of group I metabotropic glutamate receptors. *Journal of Biological Chemistry* **275**(43): 33750-33758.
- Pal K, Melcher K, Xu HE (2012). Structure and mechanism for recognition of peptide hormones by Class B G-protein-coupled receptors. *Acta Pharmacologica Sinica* **33**(3): 300-311.
- Palczewski K (2000). Crystal structure of rhodopsin: a G protein-coupled receptor. *Science* **289**: 739-745.
- Pals-Rylaarsdam R, Gurevich VV, Lee KB, Ptasienski JA, Benovic JL, Hosey MM (1997a). Internalization of the m2 muscarinic acetylcholine receptor. Arrestin-independent and -dependent pathways. *Journal of Biological Chemistry* **272**(38): 23682-23689.
- Pals-Rylaarsdam R, Hosey MM (1997b). Two homologous phosphorylation domains differentially contribute to desensitization and internalization of the m2 muscarinic acetylcholine receptor. *Journal of Biological Chemistry* **272**(22): 14152-14158.
- Park JH, Scheerer P, Hofmann KP, Choe H-W, Ernst OP (2008). Crystal structure of the ligand-free G-protein-coupled receptor opsin. *Nature* **454**(7201): 183-187.
- Patterson P, Magneres C, Sued O, Fink V, Figueroa M, Cesar C, *et al.* (2012). A phase 4, single-arm, open-label, pilot study of maraviroc, raltegravir and darunavir/r in HIV-1 adults with triple class failure: TERCETO study. *Journal of the International AIDS Society* **15**(6): 18268.
- Pei Y, Rogan SC, Yan F, Roth BL (2008). Engineered GPCRs as tools to modulate signal transduction. *Physiology* **23**: 313-321.
- Pierce KL, Lefkowitz RJ (2001). Classical and new roles of beta-arrestins in the regulation of G-protein-coupled receptors. *Nature Reviews Neuroscience* **2**(10): 727-733.

- Pierce KL, Premont RT, Lefkowitz RJ (2002). Seven-transmembrane receptors. *Nature Reviews Molecular Cell Biology* **3**(9): 639-650.
- Pitcher JA, Freedman NJ, Lefkowitz RJ (1998). G protein-coupled receptor kinases. *Annual Review of Biochemistry* **67**: 653-692.
- Poll F, Lehmann D, Illing S, Ginja M, Jacobs S, Lupp A, *et al.* (2010). Pasireotide and octreotide stimulate distinct patterns of sst2A somatostatin receptor phosphorylation. *Molecular Endocrinology* **24**(2): 436-446.
- Portsmouth S, Valluri S, Craig C, Lewis M, Pokrovsky V, Gartland M, *et al.* (2012). Open-label study of maraviroc+lamivudine/zidovudine in treatment-naive adults infected with HIV-1, predominantly subtype A, by population genotyping. *Journal of the International AIDS Society* **15**(6): 18261.
- Poulin B, Butcher A, McWilliams P, Bourgoignon JM, Pawlak R, Kong KC, *et al.* (2010). The M3-muscarinic receptor regulates learning and memory in a receptor phosphorylation/arrestin-dependent manner. *Proceedings of the National Academy of Sciences of the United States of America* **107**(20): 9440-9445.
- Premont RT, Gainetdinov RR (2007). Physiological roles of G protein-coupled receptor kinases and arrestins. *Annual Review of Physiology* **69**: 511-534.
- Price MR, Baillie GL, Thomas A, Stevenson LA, Easson M, Goodwin R, *et al.* (2005). Allosteric Modulation of the Cannabinoid CB1 Receptor. *Molecular Pharmacology* **68**(5): 1484-1495.
- Prilla S, Schrobang J, Ellis J, Holtje HD, Mohr K (2006). Allosteric interactions with muscarinic acetylcholine receptors: complex role of the conserved tryptophan M2422Trp in a critical cluster of amino acids for baseline affinity, subtype selectivity, and cooperativity. *Molecular Pharmacology* **70**(1): 181-193.
- Puthenveedu MA, Yudowski GA, von Zastrow M (2007). Endocytosis of neurotransmitter receptors: location matters. *Cell* **130**(6): 988-989.
- Rajagopal S, Ahn S, Rominger DH, Gowen-MacDonald W, Lam CM, DeWire SM, *et al.* (2011). Quantifying Ligand Bias at Seven-Transmembrane Receptors. *Molecular Pharmacology* **80**(3): 367-377.
- Rajagopal S, Rajagopal K, Lefkowitz RJ (2010). Teaching old receptors new tricks: biasing seven-transmembrane receptors. *Nature Reviews Drug Discovery* **9**(5): 373-386.
- Rana BK, Shiina T, Insel PA (2001). Genetic variations and polymorphisms of G protein-coupled receptors: functional and therapeutic implications. *Annual Review of Pharmacology and Toxicology* **41**: 593-624.
- Rasmussen SG, Choi HJ, Fung JJ, Pardon E, Casarosa P, Chae PS, *et al.* (2011a). Structure of a nanobody-stabilized active state of the beta(2) adrenoceptor. *Nature* **469**(7329): 175-180.

Rasmussen SG, Choi HJ, Rosenbaum DM, Kobilka TS, Thian FS, Edwards PC, *et al.* (2007). Crystal structure of the human beta2 adrenergic G-protein-coupled receptor. *Nature* **450**(7168): 383-387.

Rasmussen SG, DeVree BT, Zou Y, Kruse AC, Chung KY, Kobilka TS, *et al.* (2011b). Crystal structure of the beta2 adrenergic receptor-Gs protein complex. *Nature* **477**(7366): 549-555.

Rebholz H, Nishi A, Liebscher S, Nairn AC, Flajolet M, Greengard P (2009). CK2 negatively regulates G alpha(s) signaling. *Proceedings of the National Academy of Sciences of the United States of America* **106**(33): 14096-14101.

Redfern CH, Coward P, Degtyarev MY, Lee EK, Kwa AT, Hennighausen L, *et al.* (1999). Conditional expression and signaling of a specifically designed Gi-coupled receptor in transgenic mice. *Nature Biotechnology* **17**(2): 165-169.

Reiter E, Ahn S, Shukla AK, Lefkowitz RJ (2012). Molecular mechanism of beta-arrestin-biased agonism at seven-transmembrane receptors. *Annual Review of Pharmacology and Toxicology* **52**: 179-197.

Reiter E, Lefkowitz RJ (2006). GRKs and beta-arrestins: roles in receptor silencing, trafficking and signaling. *Trends in Endocrinology & Metabolism* **17**(4): 159-165.

Remington G (2008). Alterations of dopamine and serotonin transmission in schizophrenia. In: Giuseppe Di Giovanni VDM, Ennio E (ed)^(eds). *Progress in Brain Research*, edn, Vol. Volume 172: Elsevier. p^pp 117-140.

Ren XR, Reiter E, Ahn S, Kim J, Chen W, Lefkowitz RJ (2005). Different G protein-coupled receptor kinases govern G protein and beta-arrestin-mediated signaling of V2 vasopressin receptor. *Proceedings of the National Academy of Sciences of the United States of America* **102**(5): 1448-1453.

Rosenbaum DM, Cherezov V, Hanson MA, Rasmussen SGF, Thian FS, Kobilka TS, *et al.* (2007). GPCR Engineering Yields High-Resolution Structural Insights into  $\beta$ 2-Adrenergic Receptor Function. *Science* **318**(5854): 1266-1273.

Rosenbaum DM, Rasmussen SGF, Kobilka BK (2009). The structure and function of G-protein-coupled receptors. *Nature* **459**(7245): 356-363.

Rosenbaum DM, Zhang C, Lyons JA, Holl R, Aragao D, Arlow DH, *et al.* (2011). Structure and function of an irreversible agonist-beta(2) adrenoceptor complex. *Nature* **469**(7329): 236-240.

Rosethorne EM, Charlton SJ (2011). Agonist-biased signaling at the histamine H4 receptor: JNJ7777120 recruits beta-arrestin without activating G proteins. *Molecular Pharmacology* **79**(4): 749-757.

Rumenapp U, Asmus M, Schablowski H, Woznicki M, Han L, Jakobs KH, *et al.* (2001). The M3 muscarinic acetylcholine receptor expressed in HEK-293 cells signals to phospholipase D via G12 but not Gq-type G proteins: regulators of G proteins as tools to dissect pertussis

toxin-resistant G proteins in receptor-effector coupling. *Journal of Biological Chemistry* **276**(4): 2474-2479.

Sarter M, Parikh V (2005). Choline transporters, cholinergic transmission and cognition. *Nature Reviews Neuroscience* **6**(1): 48-56.

Scearce-Levie K, Coward P, Redfern CH, Conklin BR (2001). Engineering receptors activated solely by synthetic ligands (RASSLs). *Trends in Pharmacological Sciences* **22**(8): 414-420.

Scearce-Levie K, Coward P, Redfern CH, Conklin BR (2002). Tools for dissecting signaling pathways in vivo: receptors activated solely by synthetic ligands. *Methods in Enzymology* **343**: 232-248.

Scheerer P, Park JH, Hildebrand PW, Kim YJ, Krauss N, Choe HW, *et al.* (2008). Crystal structure of opsin in its G-protein-interacting conformation. *Nature* **455**(7212): 497-502.

Schmidt M, Huwe SM, Fasselt B, Homann D, Rumenapp U, Sandmann J, *et al.* (1994). Mechanisms of phospholipase D stimulation by m3 muscarinic acetylcholine receptors. Evidence for involvement of tyrosine phosphorylation. *European Journal of Pharmacology* **225**(2): 667-675.

Schmidt ME, Kent JM, Daly E, Janssens L, Van Osselaer N, Hüsken G, *et al.* (2012). A double-blind, randomized, placebo-controlled study with JNJ-37822681, a novel, highly selective, fast dissociating D2 receptor antagonist in the treatment of acute exacerbation of schizophrenia. *European Neuropsychopharmacology* **22**(10): 721-733.

Schulte G (2010). International Union of Basic and Clinical Pharmacology. LXXX. The class Frizzled receptors. *Pharmacological Reviews* **62**(4): 632-667.

Shenoy SK, Lefkowitz RJ (2005). Seven-transmembrane receptor signaling through beta-arrestin. *Science Signal Transduction Knowledge Environment* **1**(308).

Shimamura T, Shiroishi M, Weyand S, Tsujimoto H, Winter G, Katritch V, *et al.* (2011). Structure of the human histamine H(1) receptor complex with doxepin. *Nature* **475**(7354): 65-U82.

Shirey JK, Brady AE, Jones PJ, Davis AA, Bridges TM, Kennedy JP, *et al.* (2009). A Selective Allosteric Potentiator of the M1 Muscarinic Acetylcholine Receptor Increases Activity of Medial Prefrontal Cortical Neurons and Restores Impairments in Reversal Learning. *Journal of Neuroscience* **29**(45): 14271-14286.

Shirey JK, Xiang Z, Orton D, Brady AE, Johnson KA, Williams R, *et al.* (2008). An allosteric potentiator of M4 mAChR modulates hippocampal synaptic transmission. *Nature Chemical Biology* **4**(1): 42-50.

Shockley MS, Tolbert LM, Tobin AB, Nahorski SR, Sadee W, Lameh J (1999). Differential regulation of muscarinic M1 and M3 receptors by a putative phosphorylation domain. *European Journal of Pharmacology* **377**(1): 137-146.

- Shukla AK, Xiao K, Lefkowitz RJ (2011). Emerging paradigms of beta-arrestin-dependent seven transmembrane receptor signaling. *Trends in Biochemical Sciences* **36**(9): 457-469.
- Slesinger PA, Reuveny E, Jan YN, Jan LY (1995). Identification of structural elements involved in G protein gating of the GIRK1 potassium channel. *Neuron* **15**: 1145-1156.
- Sondek J, Bohm A, Lambright DG, Hamm HE, Sigler PB (1996). Crystal structure of a G-protein beta gamma dimer at 2.1A resolution. *Nature* **379**(6563): 369-374.
- Sondek J, Lambright DG, Noel JP, Hamm HE, Sigler PB (1994). GTPase mechanism of Gproteins from the 1.7-A crystal structure of transducin alpha-GDP-AIF-4. *Nature* **372**(6503): 276-279.
- Sorkin A, von Zastrow M (2009). Endocytosis and signalling: intertwining molecular networks. *Nature Reviews Molecular Cell Biology* **10**(9): 609-622.
- Soudijn W, Van Wijngaarden I, AP IJ (2004). Allosteric modulation of G protein-coupled receptors: perspectives and recent developments. *Drug Discovery Today* **9**(17): 752-758.
- Spalding TA, Trotter C, Skjærbæk N, Messier TL, Currier EA, Burstein ES, *et al.* (2002). Discovery of an Ectopic Activation Site on the M1 Muscarinic Receptor. *Molecular Pharmacology* **61**(6): 1297-1302.
- Srinivasan S, Santiago P, Lubrano C, Vaisse C, Conklin BR (2007). Engineering the melanocortin-4 receptor to control constitutive and ligand-mediated G(S) signaling in vivo. *PLoS One* **2**(7).
- Srinivasan S, Vaisse C, Conklin BR (2003). Engineering the melanocortin-4 receptor to control G(s) signaling in vivo. *Annals of the New York Academy of Sciences* **994**: 225-232.
- Strader CD, Gaffney T, Sugg EE, Candelore MR, Keys R, Patchett AA, *et al.* (1991). Allele-specific activation of genetically engineered receptors. *Journal of Biological Chemistry* **266**(1): 5-8.
- Strange PG (2008). Agonist binding, agonist affinity and agonist efficacy at G protein-coupled receptors. *British Journal of Pharmacology* **153**(7): 1353-1363.
- Strange PG (2007). Mechanisms underlying agonist efficacy. *Biochemical Society Transactions* **35**(Pt 4): 733-736.
- Suratman S, Leach K, Sexton P, Felder C, Loiacono R, Christopoulos A (2011). Impact of species variability and 'probe-dependence' on the detection and in vivo validation of allosteric modulation at the M4 muscarinic acetylcholine receptor. *British Journal of Pharmacology* **162**(7): 1659-1670.
- Sutton RB, Vishnivetskiy SA, Robert J, Hanson SM, Raman D, Knox BE, *et al.* (2005). Crystal structure of cone arrestin at 2.3A: evolution of receptor specificity. *Journal of Molecular Biology* **354**(5): 1069-1080.

- Swaminath G, Xiang Y, Lee TW, Steenhuis J, Parnot C, Kobilka BK (2004). Sequential binding of agonists to the beta(2) adrenoceptor - Kinetic evidence for intermediate conformational states. *Journal of Biological Chemistry*(279): 686-691.
- Sykes DA, Dowling MR, Charlton SJ (2009). Exploring the mechanism of agonist efficacy: a relationship between efficacy and agonist dissociation rate at the muscarinic M3 receptor. *Molecular Pharmacology* **76**(3): 543-551.
- Teles-Grilo Ruivo L, Mellor J (2013). Cholinergic modulation of hippocampal network function. *Frontiers in Synaptic Neuroscience* **5**.
- Thomas RL, Langmead CJ, Wood MD, Challiss RA (2009). Contrasting effects of allosteric and orthosteric agonists on m1 muscarinic acetylcholine receptor internalization and down-regulation. *Journal of Pharmacology and Experimental Therapeutics* **331**(3): 1086-1095.
- Thomas RL, Mistry R, Langmead CJ, Wood MD, Challiss RA (2008). G protein coupling and signaling pathway activation by m1 muscarinic acetylcholine receptor orthosteric and allosteric agonists. *Journal of Pharmacology and Experimental Therapeutics* **327**(2): 365-374.
- Thompson AA, Liu W, Chun E, Katritch V, Wu H, Vardy E, *et al.* (2012). Structure of the nociceptin/orphanin FQ receptor in complex with a peptide mimetic. *Nature* **485**(7398): 395-399.
- Thomsen M, Lindsley CW, Conn PJ, Wessell JE, Fulton BS, Wess J, *et al.* (2012). Contribution of both M(1) and M(4) receptors to muscarinic agonist-mediated attenuation of the cocaine discriminative stimulus in mice. *Psychopharmacology* **220**(4): 673-685.
- Tobin AB (2002). Are we beta-ARKing up the wrong tree? Casein kinase 1 alpha provides an additional pathway for GPCR phosphorylation. *Trends in Pharmacological Sciences* **23**(7): 337-343.
- Tobin AB (2008). G-protein-coupled receptor phosphorylation: where, when and by whom. *British Journal of Pharmacology* **153**(1): 14.
- Tobin AB, Butcher AJ, Kong KC (2008). Location, location, location...site-specific GPCR phosphorylation offers a mechanism for cell-type-specific signalling. *Trends in Pharmacological Sciences* **29**(8): 413-420.
- Tobin AB, Lambert DG, Nahorski SR (1992). Rapid desensitization of muscarinic m3 receptor-stimulated polyphosphoinositide responses. *Molecular Pharmacology* **42**(6): 1042-1048.
- Tobin AB, Nahorski SR (1993). Rapid agonist-mediated phosphorylation of m3-muscarinic receptors revealed by immunoprecipitation. *Journal of Biological Chemistry* **268**(13): 9817-9823.
- Torrecilla I, Spragg EJ, Poulin B, McWilliams PJ, Mistry SC, Blaukat A, *et al.* (2007). Phosphorylation and regulation of a G protein-coupled receptor by protein kinase CK2. *Journal of Cell Biology* **177**(1): 127-137.

- Tran TM, Friedman J, Qunaibi E, Baameur F, Moore RH, Clark RB (2004). Characterization of agonist stimulation of cAMP-dependent protein kinase and G protein-coupled receptor kinase phosphorylation of the beta2-adrenergic receptor using phosphoserine-specific antibodies. *Molecular Pharmacology* **65**(1): 196-206.
- Tsuga H, Okuno E, Kameyama K, Haga T (1998). Sequestration of human muscarinic acetylcholine receptor hm1-hm5 subtypes: effect of G protein-coupled receptor kinases GRK2, GRK4, GRK5 and GRK6. *Journal of Pharmacology and Experimental Therapeutics* **284**(3): 1218-1226.
- Tzavara ET, Bymaster FP, Davis RJ, Wade MR, Perry KW, Wess J, *et al.* (2004). M4 muscarinic receptors regulate the dynamics of cholinergic and dopaminergic neurotransmission: relevance to the pathophysiology and treatment of related CNS pathologies. *Faseb Journal* **18**(12): 1410-1412.
- Tzavara ET, Bymaster FP, Felder CC, Wade M, Gomeza J, Wess J, *et al.* (2003). Dysregulated hippocampal acetylcholine neurotransmission and impaired cognition in M2, M4 and M2/M4 muscarinic receptor knockout mice. *Molecular Psychiatry* **8**(7): 673-679.
- Urban JD, Clarke WP, von Zastrow M, Nichols DE, Kobilka B, Weinstein H, *et al.* (2007). Functional selectivity and classical concepts of quantitative pharmacology. *Journal of Pharmacology and Experimental Therapeutics* **320**(1): 1-13.
- Urwyler S (2011). Allosteric modulation of family C G-protein-coupled receptors: from molecular insights to therapeutic perspectives. *Pharmacological Reviews* **63**(1): 59-126.
- Valant C, Felder CC, Sexton PM, Christopoulos A (2012a). Probe Dependence in the Allosteric Modulation of a G Protein-Coupled Receptor: Implications for Detection and Validation of Allosteric Ligand Effects. *Molecular Pharmacology* **81**(1): 41-52.
- Valant C, Robert Lane J, Sexton PM, Christopoulos A (2012b). The best of both worlds? Bitopic orthosteric/allosteric ligands of g protein-coupled receptors. *Annual Review of Pharmacology and Toxicology* **52**: 153-178.
- Valant C, Sexton PM, Christopoulos A (2009). Orthosteric/allosteric bitopic ligands: going hybrid at GPCRs. *Molecular Interventions* **9**(3): 125-135.
- van Koppen CJ, Kaiser B (2003). Regulation of muscarinic acetylcholine receptor signaling. *Pharmacology & Therapeutics* **98**(2): 197-220.
- Van Koppen CJ, Lenz W, Nunes JP, Zhang C, Schmidt M, Jakobs KH (1995). The role of membrane proximal threonine residues conserved among guanine-nucleotide-binding-protein-coupled receptors in internalization of the m4 muscarinic acetylcholine receptor. *European Journal of Pharmacology* **234**(2): 536-541.
- Venter JC, Adams MD, Myers EW, Li PW, Mural RJ, Sutton GG, *et al.* (2001). The sequence of the human genome. *Science* **291**(5507): 1304-1351.

- Violin JD, Lefkowitz RJ (2007). beta-arrestin-biased ligands at seven-transmembrane receptors. *Trends in Pharmacological Sciences* **28**(8): 416-422.
- Wall SJ, Yasuda RP, Hory F, Flagg S, Martin BM, Ginns EI, *et al.* (1991). Production of antisera selective for m1 muscarinic receptors using fusion proteins: distribution of m1 receptors in rat brain. *Molecular Pharmacology* **39**(5): 643-649.
- Wang L, Martin B, Brennehan R, Luttrell LM, Maudsley S (2009). Allosteric modulators of G protein-coupled receptors: future therapeutics for complex physiological disorders. *Journal of Pharmacology and Experimental Therapeutics* **331**(2): 340-348.
- Ward DT, Riccardi D (2012). New concepts in calcium-sensing receptor pharmacology and signalling. *British Journal of Pharmacology* **165**(1): 35-48.
- Warne T, Edwards PC, Leslie AG, Tate CG (2012). Crystal structures of a stabilized beta1-adrenoceptor bound to the biased agonists bucindolol and carvedilol. *Structure* **20**(5): 841-849.
- Warne T, Moukhametzianov R, Baker JG, Nehme R, Edwards PC, Leslie AG, *et al.* (2011). The structural basis for agonist and partial agonist action on a beta(1)-adrenergic receptor. *Nature* **469**(7329): 241-244.
- Warne T, Serrano-Vega MJ, Baker JG, Moukhametzianov R, Edwards PC, Henderson R, *et al.* (2008). Structure of a beta1-adrenergic G-protein-coupled receptor. *Nature* **454**(7203): 486-491.
- Waugh MG, Challiss RA, Berstein G, Nahorski SR, Tobin AB (1999). Agonist-induced desensitization and phosphorylation of m1-muscarinic receptors. *Biochemical Journal* **15**(338): 175-183.
- Wess J (2004). Muscarinic acetylcholine receptor knockout mice: novel phenotypes and clinical implications. *Annual Review of Pharmacology and Toxicology* **44**: 423-450.
- Wess J, Duttaroy A, Gomeza J, Zhang W, Yamada M, Felder CC, *et al.* (2003a). Muscarinic receptor subtypes mediating central and peripheral antinociception studied with muscarinic receptor knockout mice: a review. *Life Sciences* **72**(18-19): 2047-2054.
- Wess J, Duttaroy A, Zhang W, Gomeza J, Cui Y, Miyakawa T, *et al.* (2003b). M1-M5 muscarinic receptor knockout mice as novel tools to study the physiological roles of the muscarinic cholinergic system. *Receptors & Channels* **9**(4): 279-290.
- Wess J, Eglén RM, Gautam D (2007). Muscarinic acetylcholine receptors: mutant mice provide new insights for drug development. *Nature Reviews Drug Discovery* **6**(9): 721-733.
- Whalen EJ, Rajagopal S, Lefkowitz RJ (2011). Therapeutic potential of beta-arrestin- and G protein-biased agonists. *Trends in Molecular Medicine* **17**(3): 126-139.
- Willars GB (2006). Mammalian RGS proteins: Multifunctional regulators of cellular signalling. *Seminars in Cell & Developmental Biology* **17**(3): 363-376.

Willems JM, Challiss RAJ, Kelly E, Nahorski SR (2001). G protein-coupled receptor kinases 3 and 6 use different pathways to desensitize the endogenous M-3 muscarinic acetylcholine receptor in human SH-SY5Y cells. *Molecular Pharmacology* **60**(2): 321-330.

Willems JM, Challiss RAJ, Nahorski SR (2002). Endogenous G protein-coupled receptor kinase 6 regulates M-3 muscarinic acetylcholine receptor phosphorylation and desensitization in human SH-SY5Y neuroblastoma cells. *Journal of Biological Chemistry* **277**(18): 15523-15529.

Willems JM, Challiss RAJ, Nahorski SR (2003). Non-visual GRKs: are we seeing the whole picture? *Trends in Pharmacological Sciences* **24**(12): 626-633.

Witherow DS, Garrison TR, Miller WE, Lefkowitz RJ (2004).  $\beta$ -Arrestin inhibits NF- $\kappa$ B activity by means of its interaction with the NF- $\kappa$ B inhibitor I $\kappa$ B $\alpha$ . *Proceedings of the National Academy of Sciences of the United States of America* **101**: 8603–8607.

Woolley ML, Carter HJ, Gartlon JE, Watson JM, Dawson LA (2009). Attenuation of amphetamine-induced activity by the non-selective muscarinic receptor agonist, xanomeline, is absent in muscarinic M4 receptor knockout mice and attenuated in muscarinic M1 receptor knockout mice. *European Journal of Pharmacology* **603**(1-3): 147-149.

Wu G, Krupnick JG, Benovic JL, Lanier SM (1997). Interaction of arrestins with intracellular domains of muscarinic and alpha2-adrenergic receptors. *Journal of Biological Chemistry* **272**(28): 17836-17842.

Wu H, Wacker D, Mileni M, Katritch V, Han GW, Vardy E, *et al.* (2012). Structure of the human kappa-opioid receptor in complex with JDTic. *Nature* **485**(7398): 327-332.

Xu F, Wu HX, Katritch V, Han GW, Jacobson KA, Gao ZG, *et al.* (2011). Structure of an Agonist-Bound Human A(2A) Adenosine Receptor. *Science* **332**(6027): 322-327.

Yamada M, Basile AS, Fedorova I, Zhang WL, Duttaroy A, Cui YH, *et al.* (2003). Novel insights into M-5 muscarinic acetylcholine receptor function by the use of gene targeting technology. *Life Sciences* **74**(2-3): 345-353.

Yamada M, Miyakawa T, Duttaroy A, Yamanaka A, Moriguchi T, Makita R, *et al.* (2001). Mice lacking the M3 muscarinic acetylcholine receptor are hypophagic and lean. *Nature* **410**(6825): 207-212.

Yang J, Williams JA, Yule DI, Logsdon CD (1995). Mutation of carboxyl-terminal threonine residues in human m3 muscarinic acetylcholine receptor modulates the extent of sequestration and desensitization. *Molecular Pharmacology* **48**(3): 477-485.

Zhan X, Gimenez LE, Gurevich VV, Spiller BW (2011). Crystal structure of arrestin-3 reveals the basis of the difference in receptor binding between two non-visual subtypes. *Journal of Molecular Biology* **406**(3): 467-478.

Zhang HM, Zhou HY, Chen SR, Gautam D, Wess J, Pan HL (2007). Control of glycinergic input to spinal dorsal horn neurons by distinct muscarinic receptor subtypes revealed using knockout mice. *Journal of Pharmacology and Experimental Therapeutics* **323**(3): 963-971.

Zhao GQ, Zhang Y, Hoon MA, Chandrashekar J, Erlenbach I, Ryba NJ, *et al.* (2003). The receptors for mammalian sweet and umami taste. *Cell* **115**(3): 255-266.

Zhao Q, Wu BL (2012). Ice breaking in GPCR structural biology. *Acta Pharmacologica Sinica* **33**(3): 324-334.

Zidar DA, Violin JD, Whalen EJ, Lefkowitz RJ (2009). Selective engagement of G protein coupled receptor kinases (GRKs) encodes distinct functions of biased ligands. *Proceedings of the National Academy of Sciences of the United States of America* **106**(24): 9649-9654.